EFFECT OF ENHANCED LEACHATE RECIRCULATED (ELR) LANDFILL OPERATION AND GAS EXTRACTION ON GREENHOUSE GAS EMISSIONS

by

SONIA SAMIR

Presented to the Faculty of the Graduate School of

The University of Texas at Arlington in Partial Fulfillment

of the Requirements

for the Degree of

DOCTOR OF PHILOSOPHY

THE UNIVERSITY OF TEXAS AT ARLINGTON

May 2014

Acknowledgements

I would like to express my sincere gratitude to my advisor, Dr. Sahadat Hossain, for the motivation and support he provided me throughout this work. Dr. Hossain has been a true mentor, and his patience and constructive comments have helped me become a better researcher. The completion of this work would not have been possible without his continuous guidance, valuable suggestions and ever present encouragement.

Dr. Melanie Sattler's exceptional ideas and guidance were vital to the research, as was the opportunity she provided me to work in her laboratory to enhance my learning opportunities. She is a professor and mentor extraordinaire. I would like to express my appreciation to Dr. Han for his assistance with the statistical modelling work and to Dr. Laureano R. Hoyos and Dr. Stefan A. Romanoschi for agreeing to serve on my committee.

I wish to acknowledge the City of Denton, Texas Municipal Solid Waste (MSW) Landfill authority for their financial support throughout this project. Special appreciation goes to Mr. Vance Kemler, Mr. David Dugger, Mr. Mike Foggle and Ms. Ami Reeder for their readily available help during the field investigation and data collection. I also wish to acknowledge the Air and Waste Management Association (A&WMA), Solid Waste Association of North America-Lone Star Chapter (TXSWANA) and the National Science Foundation (NSF) for their support via multiple scholarships and student grants.

I would further like to extend my sincere appreciation to my colleagues and friends for their constant cooperation and assistance throughout my graduate studies. Special thanks to Mohammad Sadik Khan, Golam Kibria, Richa Karanjekar, Jahangir Alam, Md. Faysal, Dipta M. Joy and Ishti Shama.

Infinite gratitude goes to my family - my parents, siblings, and in-laws, for their endless support and encouragement. My father has been a constant source of inspiration

to me; everything I am today, I owe it to him. Special thanks to my husband, Ziaur Rahman, for his constant encouragement that motivated me to accomplish my goal. It would not have been possible to finish this work without his patience, and understanding. Finally, I would like to thank Almighty Allah for giving me the strength and patience to overcome every difficulty in my life.

April 17, 2014

Abstract

EFFECT OF ENHANCED LEACHATE RECIRCULATED (ELR) LANDFILL OPERATION AND GAS EXTRACTION ON GREENHOUSE GAS EMISSIONS

Sonia Samir, PhD

The University of Texas at Arlington, 2014

Supervising Professor: MD. Sahadat Hossain

The bioreactor/ enhanced leachate recirculated (ELR) landfill operation, with the addition of moisture/ leachate to the landfill accelerates the process of landfill waste decomposition and, over a short period of time, increases the generation of landfill gas (LFG). Since emissions from the landfills are directly related to the generation of gas, the increase in gas generation might also increase the emissions from the landfill. The presence of gas extraction is suggested to mitigate the fugitive emissions from the landfills. Therefore, the motivation of the current study was to evaluate the effect of an ELR operation, as well as the gas extraction, on the greenhouse gas emissions from the landfill. The current study was conducted in the City of Denton Landfill, Texas. Methane emissions were investigated using a portable flame ionization detector (FID) and static flux chamber technique at the landfill surface. Emissions were measured from an ELR-operated cell (cell 2), as well as a conventional cell (cell 0), in the City of Denton Landfill. Methane emissions for cell 2 varied from 9544.3 ppm to 0 ppm, while for cell 0, they varied from 0 ppm to 47 ppm. High spatial variations were observed during monitoring from both cells 0 and cell 2, which could be recognized as the variation of gas generation

below the cover soil. The comparison between emissions from the slope and surface of the landfill showed that more methane emissions occurred from the slopes than from the top surface. In addition, the average landfill emissions showed an increasing trend with an increase in temperature and decreasing trend with increasing precipitation.

The effect of the ELR operation near the recirculation pipes showed a lag period between the recirculation and the maximum emissions near the pipe. The emissions near the pipe decreased after 1 day of recirculation, and after the initial decrease, the emissions started to increase and continued to increase up to 7 days after the recirculation. However, after approximately 10 days of recirculation, the emissions resumed their original state (before the recirculation). It should be noted that the change in emissions was only near the pipe. No overall change in emissions was observed from the cell due to the recirculation. The comparison between the emissions from the conventional and ELR cells showed overall higher emissions from the ELR cell, which could be attributed to the overall higher gas generation from the ELR cell. The gas extraction had a direct impact on emissions; the emissions dropped substantially right after the gas extraction from the landfill. However, the gas was extracted once in a month, and comparison with the amount of gas extraction and emissions showed that the emissions decreased as the gas extraction increased.

A multiple linear regression (MLR) model was developed to incorporate the effect of the ELR operation and the gas extraction in the estimating the methane emissions from the landfill, using the statistical tool SAS. The model was validated and showed an excellent agreement between the predicted emissions and the measured emissions from the landfills (average variation 9.6%).

Table of Contents

List of Illustrations

List of Tables

Chapter 1

Introduction

1.1 Background

Atmospheric gases absorb solar radiation and convert the solar energy to thermal energy. However, if the concentration of greenhouse gases increases in the atmosphere, the solar radiation gets entrapped and increases the thermal energy in the atmosphere. Consequently, this increase in thermal energy plays a significant role in climate change. Methane, one of the primary greenhouse gases, has been increasing at a rate of 1% per year and has doubled from 0.8 ppm to 1.7 ppm since 1800 (Humer and Lechner, 1999). Current studies have reported that methane has 25 times higher greenhouse gas potential than carbon dioxide on a 100-year time horizon. Therefore, methane emissions to the atmosphere from the anthropogenic sources are considered to be of great concern.

Landfills have been identified as one of the largest anthropogenic sources of methane and contribute 15% of total annual greenhouse gas emissions (IPCC, 1996; USEPA, 2005). The USEPA (1990-2011) stated that landfills are the third largest source of methane emissions in the United States, with 17% of total methane emissions originating from landfills (Figure 1.1). Landfill gas (LFG), which is the natural by-product of the anaerobic decomposition of biodegradable waste in landfills, is a complex mixture of methane (CH_4), carbon dioxide (CO_2), and trace constituents of volatile organic compounds (VOC). Typically, LFG is comprised of approximately 40%-60% of methane (Yesiller et al., 2008).

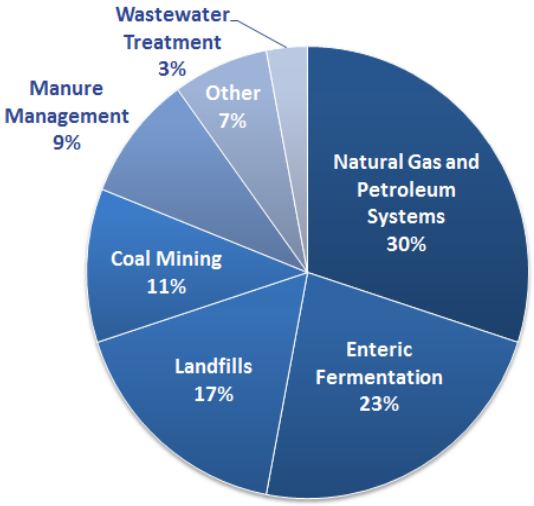

Figure 1.1 U.S. Methane Emissions, By Sources (U.S. EPA Inventory of U.S. Greenhouse Gas Emissions and Sinks: 1990-2011)

The generation of LFG is highly variable with the heterogeneity of wastes and site-specific climatological conditions, i.e. precipitation, temperature, humidity, atmospheric pressure, and seasonal variation of waste composition (Yesiller et al., 2008). In addition, LFG generation also depends on site-specific operational conditions (i.e. waste placement, density, cover materials, and water addition). Generated methane from the landfills might migrate to the atmosphere mostly due to dispersion of the cover, or through the fissures/cracks present on the cover. Methane migration from the landfill is a function of the landfill's internal pressure, as well as permeability of the surrounding media (USEPA, 1997a). A fraction of this migrating methane gets oxidized by the methanotrophs in the cover in the appropriate range of temperature and moisture, and the rest is released in the atmosphere until equilibrium is achieved (Chanton et al., 2009; Chanton et al., 2011). Several mechanisms have been proposed over the years to mitigate methane emission from the landfills; however, the presence of a gas recovery or gas extraction system is most frequently mentioned in the literature (Bogner et al., 1997;

Scheutz et al., 2009; Bogner et al., 2011; Jung et al., 2011).Conversely, an ineffective gas collection system or low gas collection efficiency of the installed system in the landfill might also lead to methane migration.

Current guidelines assume a typical gas collection efficiency of 75% that indirectly indicates that the remaining 25% of generated gas is emitted to the atmosphere. However, the collection efficiency achieved by LFG systems is widely debated by the landfill researchers and practitioners. The methane collection efficiency is the ratio of the amount of methane recovered to the amount of methane generated in the landfill (Barlaz et al., 2009) as presented in equation 1.

Collection Efficiency = Σ Methane (CH_4) recovered/ Σ Methane (CH_4) produced * 100%

…….. (1)

Where,

ΣCH_4 produced = $\Sigma(CH_4$ recovered + CH_4 emitted + CH_4 oxidized)

Typically, a high gas generation rate implies higher surface emissions due to higher pressure gradients in the waste (Czpiel et al., 2003). Summer collection efficiencies are often found to be lower than the winter since more gases are generated in summer due to increased microbial activity. Soil moisture content near the surface significantly affects landfill gas emissions. Landfill emissions increase with moisture content up to a point, but then decrease with increasing moisture content due to reduction in gas-filled pore volumes (Christophersen et al., 2001). In addition to temperature and moisture, barometric pressure and humidity might also play a substantial role in landfill gas emission. Therefore, accurate estimation is required to quantify the methane emissions from the landfills.

1.2 Problem Statement

A bioreactor/ ELR landfill operation, as first proposed by Pohland (1975), accelerates the process of landfill waste decomposition by water/ leachate addition to the landfill and increases the generation of LFG over a short period of time. Gas migration from the landfills is influenced by the generation of gas from the wastes underneath the cover, as well as the gas permeability of the cover soil (Gebert et al., 2010; Chanton et al., 2010; Scheutz et al., 2010). Consequently, higher gas generation during ELR operation might have a significant effect on emissions and gas collection efficiency.

There have been numerous studies on landfill gas emissions to date (Bogner and Spokas, 1993; Czepiel, et al., 1996; Börjesson, et al., 1997; Borjesson and Svensson, 1997; Abichou et al., 2006; Spokas et al., 2006; Stern et al., 2007; Albanna et al., 2007; Huitric et al., 2007; Yesiller et al., 2008; Chanton et al., 2009; Scheutz et al., 2009; Gebert et al., 2010; Reichenauer, et al., 2011; Scheutz et al., 2011; Bogner et al., 2011; Chanton et al., 2011). However, no systematic study has been conducted to evaluate the effect of the leachate recirculation and gas collection/ extraction/ recovery on greenhouse gas emissions from the landfills. Therefore, with an increasing concern of greenhouse gases' contribution to the global warming, it is important to assess the influence of ELR operation and gas collection/ recovery on greenhouse gas emissions from landfills.

1.3 Objective of the Study

The primary objective of this research was to develop an understanding of greenhouse gas emissions and to evaluate them in relation to ELR operation and gas collection from the landfills. Methane emissions were monitored in the field using a portable flame ionization detector (FID) and static flux chamber, and a correlation was

developed to express the portable FID results in conventional flux measurements for emissions.

The study investigated the changes in greenhouse gas emissions due to the addition of water/ leachate through the horizontal recirculation pipes in the ELR landfill cell and also compared the average emissions from an ELR landfill to a conventional landfill cell. Furthermore, the effect of gas recovery on greenhouse gas emissions was evaluated from the ELR and conventional landfill cell. Finally, a methane emission model was developed addressing the effect of gas recovery and ELR operation.

The specific objectives of the current study are outlined as:

1. to monitor methane emissions using a portable flame ionization detector (FID) and static flux chamber;
2. to evaluate the effects of spatial and temporal variations of methane emissions from the landfill;
3. to investigate the effects of meteorological and operational parameters on methane emissions from the landfill;
4. to evaluate the methane oxidation capacity of the cover, based on laboratory and field measurements;
5. to develop a methane emission model based on methane emission measurements from the landfill.

1.4 Dissertation Outline

The current study is reported into six chapters as summarized below:

- Chapter 1 provides an introduction and presents the problem and objective of the study;

- Chapter 2 presents the literature review on landfill gas, methane migration, methane emission measurements, and the controlling factors of methane emission from landfills, and generation-based emission models;
- Chapter 3 describes the experimental program, methane emission measurement using portable FID and flux chamber, and field and laboratory measurements of methane oxidation rate of the cover soil;
- Chapter 4 presents the experimental results, analysis and discussions of results and comparison with existing literature;
- Chapter 5 provides a step-by-step statistical modelling procedure using multiple linear regression based on methane emission measurements from the landfill;
- Chapter 6 summarizes the conclusions from the current study and provides recommendations for future work.

Chapter 2

Literature Review

2.1 Landfill and Landfill Gas (LFG)

2.1.1 Landfills

Landfilling remains the most dominant waste management practice in the United States, even though the recycling rate has increased from 5.6% to 34.7% over the years (USEPA, 2011). A landfill is a disposal site for solid waste burial that receives hazardous and non-hazardous wastes. A modern landfill must comply with the regulatory guidelines to inhibit groundwater pollution, monitor landfill gas and leachate and allow for gas collection/ venting. The typical components of a municipal solid waste (MSW) landfill are liner system, leachate collection system, gas collection/ venting system and the final cover.

Based on the current regulatory practices of the US EPA, landfills can be operated as a traditional landfill or as a bioreactor landfill. Traditional or conventional landfills, built in accordance with the Resource Conversion and Recovery Act (RCRA) Subtitle D, restrict the addition or intrusion of moisture in order to minimize the generation of leachate and reduce the groundwater pollution risk. The absence of moisture within the landfill prolongs the decomposition of waste and increases the period of post-closure monitoring of the landfill. Conversely, in a bioreactor landfill, controlled addition of liquid to the landfill rapidly accelerates the biological stabilization of landfilled waste.

Bioreactor landfills, first proposed by Pohland (1975), enhance waste decomposition, accelerate gas generation, attain rapid settlement, and provide in-situ treatment of generated leachate. The additional moisture stimulates the decomposition of biodegradable fractions via a series of complex microbial reactions while solid waste is

buried in a landfill (Bogner and Spokas, 1993). Moisture enhances the microbial activities within the MSW by providing better contact between insoluble substrates, soluble nutrients, and microorganisms, and reduces the total time of MSW decomposition to years, as compared to decades for traditional landfills (Barlaz, 1996). The bioreactor landfills are equipped with liners and leachate collection systems to keep the generated leachate from polluting the soil and groundwater.

Figure 2.1 presents a schematic of a bioreactor landfill.

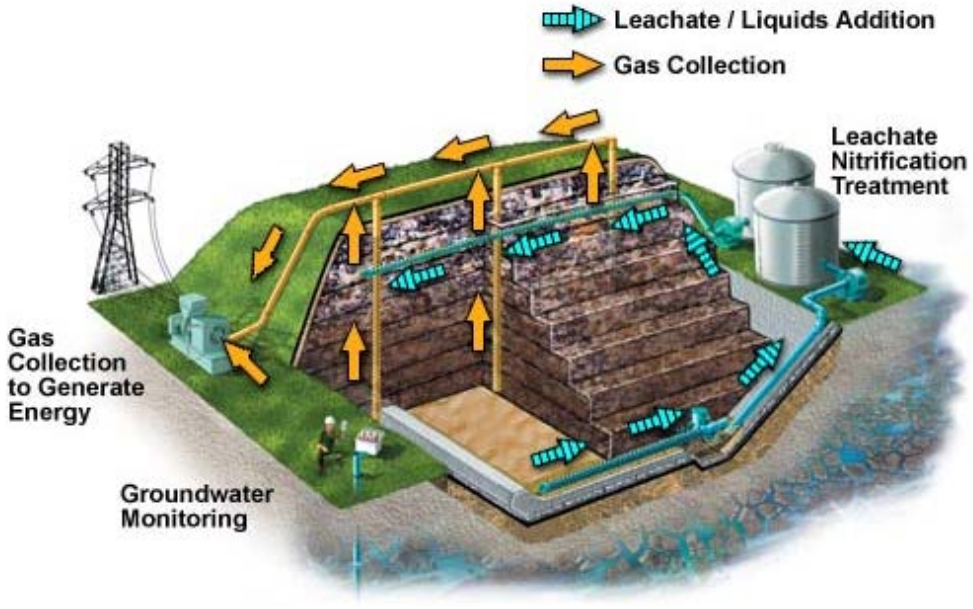

Figure 2.1 Schematic of a Bio-reactor Landfill Operation

The moisture content for maximum degradation is between 40%-55%, and, according to USEPA, the allowable moisture content for a bioreactor operation is 40%. However, under the current regulations, municipal solid waste (MSW) landfills are only allowed to operate as enhanced leachate recirculated (ELR) landfills in Texas. ELR

landfills are similar to bioreactor landfills, but the average moisture content in ELR landfills must be less than 36±3.9% (TCEQ).

2.1.2 Landfill Gas (LFG)

Gas generation in municipal solid waste (MSW) landfills is attributed to the natural decomposition process of the organic components by micro-organisms. MSW decomposition and gas generation from landfills occur in five different stages as shown in Figure 2.2. Stage one is the aerobic decomposition phase and begins as soon as the wastes are placed in the landfill. No methane is generated in phase I, and decomposition continues until all the available oxygen is consumed. Stage II is the acid formation phase in which organic components present in the waste are fermented. In stage II, both methane and carbon dioxide are generated and reach their maximum in stage IV. Gas composition is divided almost equally for both methane and carbon dioxide at stage IV. Stage V is the final phase of decomposition when degradation is stopped and most of what is present in the landfill is just air.

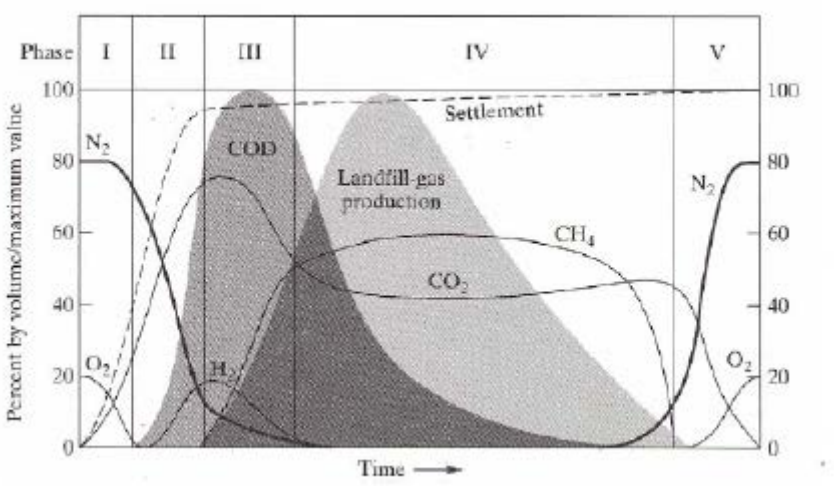

Figure 2.2 Five Phases of Landfill Gas Production (UKDOE, 1993)

Generation of LFG is highly variable due to heterogeneity of wastes, site specific operational conditions (waste placement, density, cover materials) and site-specific climatological conditions (i.e. precipitation, temperature, humidity, atmospheric pressure, and seasonal variation of waste composition) (Yesiller et al., 2008). The primary constituents of landfill gases are methane and carbon dioxide (see Table 2.1).

Table 2.1 Typical Composition of LFG (El-Fadel et al., 1997)

Component	**Concentration Range (volume basis)%**
Methane	40-70
Carbon dioxide	30-60
Carbon Monoxide	0-3
Nitrogen	3-5
Oxygen	0-3
Hydrogen	0-5
Hydrogen Sulfide	0-2
Trace compounds	0-1

Very few landfills have a gas collection system in their facility, thus allowing free movement of methane from the landfill envelope to the surface. However, even with the gas collection system present in a landfill, the efficiency of the landfill gas recovery remains uncertain and the uncollected LFG might still migrate from the landfill envelope. A major part of escaping LFG travels upward; however, only a fraction the migrating gas is oxidized in the cover and the rest is emitted to the atmosphere. These emitting gases

increase the global warming potential by entrapping the heat in the atmosphere. Therefore, the presence of an efficient gas recovery system might substantially assist in reducing the emissions from landfills.

2.2 Methane as a Greenhouse Gas (GHG)

Methane has become a target for emissions reduction due to its higher effectiveness as a greenhouse gas (Rodhe, 1990; WMO, 1998; IPCC, 2001). Landfills have been reported to be a major source of greenhouse gas emissions (U.S. EPA, 2005). According to USEPA (2011), landfills contribute 17% of total annual greenhouse gas emissions globally, as presented in Figure 2.3.

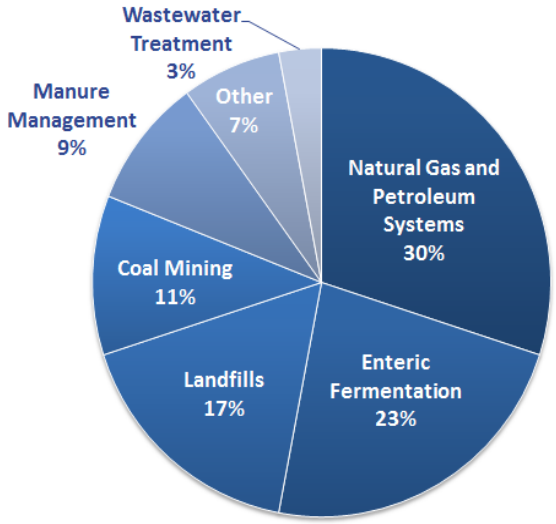

Figure 2.3 U.S. Methane Emissions by Source (U.S. EPA Inventory of U.S. Greenhouse Gas Emissions and Sinks: 1990-2011)

Hummer and Lechner (1999) reported that methane concentrations within the atmosphere have increased at a rate of about 1% per year since 1978 and have doubled since the last century. Methane has 20 to 30 times (on mass basis) higher global warming potential than carbon dioxide because of its ability to retain infrared radiation

(Ramanathan et al., 1985; Dickinson & Cicerone, 1986; Le Mer and Roger, 2001). Although methane has a short decay time in the atmosphere (9-10 years), it has higher effectiveness as a greenhouse gas (Rodhe, 1990; WMO, 1998; IPCC, 2001). Stern and Kaufmann (1996) stated that approximately 12% of worldwide methane emissions are caused by the decomposition of waste within landfills. Therefore, reducing methane emission from landfills might be a plausible way to control the greenhouse gas emissions from the atmosphere.

2.3 Methane Migration and Methane Collection

2.3.1 Methane Migration

Uncollected methane gases form the landfill attempt to migrate from the landfill envelope to the atmosphere. These migrations mostly occur by diffusion, dispersion, and advection. Diffusion is caused by the random movement of the methane molecules from the higher concentration zone to the lower concentration zone, and dispersion is caused by tortuous and variable flow paths in porous media (i.e. soil layers, garbage). However, the major transportation technique for gas migration from the landfills is advection. This advective flow is caused by the pressure difference from the high pressure zone within the landfill to the low pressure zone in the atmosphere. Several factors influence the direction of gas migration from the landfill, i.e. nutrient availability for bacteria, waste composition, moisture content, landfill age, temperature, pH, O_2 availability and the presence of a gas collection system. Depending on these factors, methane could migrate vertically and/or horizontally. The total generated methane from landfills can be partitioned into recovery, emissions, oxidation, lateral migration, and internal storage (Bogner and Spokas, 1993; Chanton et al., 2012), as presented in Figure 2.4. Migrating methane gases from the landfills might be responsible for possible explosion hazards for

the surrounding community or locality. Therefore, it is important to install methane collection or recovery systems.

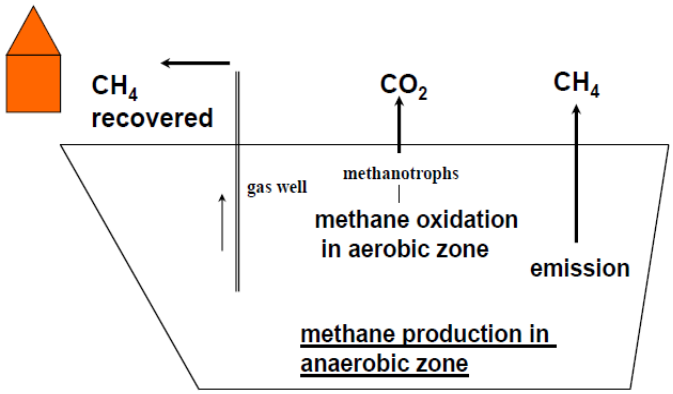

Figure 2.4 Methane Mass Balance (Chanton et al., 2012)

2.3.2 Methane Collection

A methane collection system is provided primarily to collect the migrating gases from the landfill and reduce the emissions to the atmosphere. If the methane gases are not collected properly, they might migrate laterally for a while and escape near the localities. In contrast, according to the regulatory agencies, generated methane gases from landfills are not allowed to travel outside the landfill properties. Similarly, stored gases might build up excessive pressure within the landfill envelope. Active or passive venting systems are required to reduce the emission from the landfill to the atmosphere and reduce these excessive pressure build-up within the landfill envelope.

2.3.2.1 Passive Gas Recovery

Passive gas recovery systems do not have a pump to apply suction to pull out the landfill gas. Instead of relying on any power driven force, the passive gas collection system relies on an advection mechanism to transport the landfill gases from the landfill envelope. As discussed earlier, advective flow is caused by the difference of pressure from the inside the landfill to the outside venting/ gas collection system. A passive gas

collection system is typically found in landfills with relatively smaller gas production, or in old landfills (Bagchi, 1994).

Figure 2.5 presents a typical passive vent system.

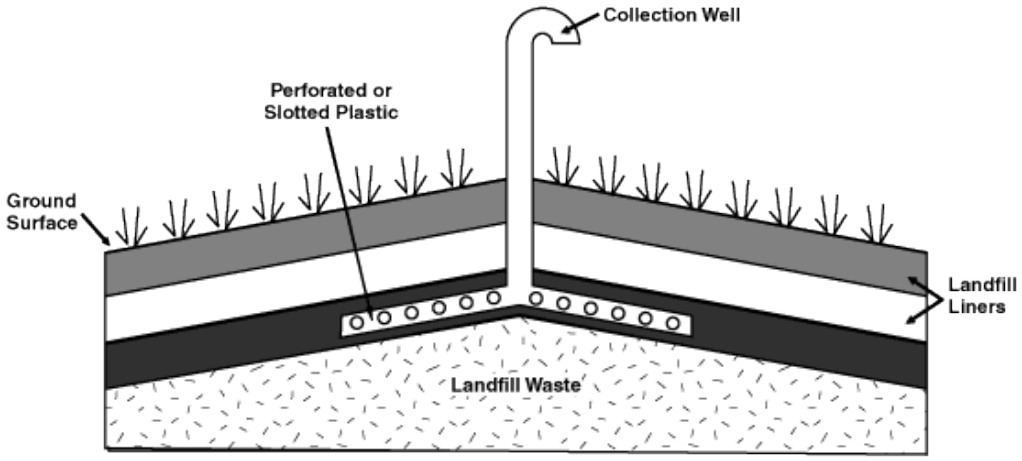

Figure 2.5 A Typical Passive Gas Vent (USEPA, 1994)

According to Reinhart (1997), passive wells can be of two types: cap vents or trench design. Cap vents are designed to penetrate the waste layer below the hydraulic barrier or final cover system. The trench is installed around the landfill perimeter and filled with high permeability material such as gravel. Perforated pipes are placed in these trenches and are connected to gas vents to escape the gas in the atmosphere. Trench designs are the most commonly used passive venting system. These gases from the passive vents can be flared, although they are generally emitted to the atmosphere.

2.3.2.2 Active Gas Recovery

According to current regulations by USEPA (2005), the new landfills are designed to accept large amount of MSW and are expected to generate relatively high amount of gas. Accordingly, these landfills are designed with active gas collection

systems in the field with mechanical gas pumps or fans/blowers. However, most of the closed landfills are not required to have an active gas collection system, assuming the gas generation is small and can be flared through passive gas vents.

A typical active gas collection system is presented in Figure 2.6.

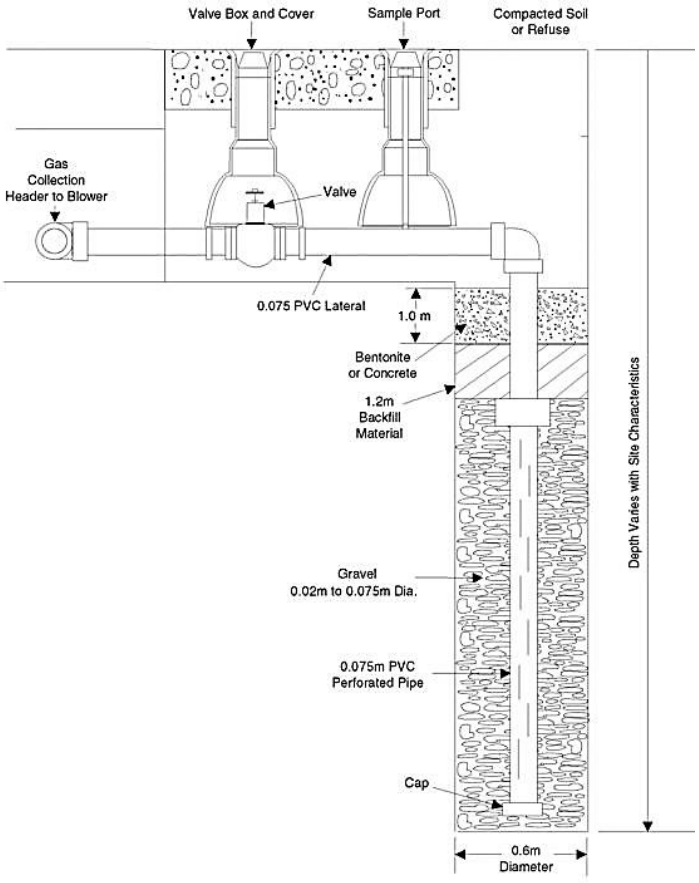

Figure 2.6 A Typical Active Gas Vent (USEPA, 2005)

Design of the active gas collection system is critical in terms of deciding on the number of gas wells, spacing of the wells and maximum amount of vacuum that might be applied for the gas collection. The spacing of the wells is designed based on the radius of influence of the gas wells, which is typically assumed to be 1.5 times the thickness of the

waste (Oweis and Khera, 1998). However, application of excessive vacuum might cause the intrusion of atmospheric gases, including oxygen, into the landfill envelope and could lead to combustion.

Active gas collection systems may include horizontal or vertical gas wells along with trenches or horizontal collection systems. Vertical wells are drilled from the top of the landfill surface and are backfilled with a high permeability layer, i.e. gravel, around the wells. A geo-membrane is placed at the top to avoid the escape of the gas. The gas wells are capped with well heads and gas control valves. These well heads are connected to a header pipe, and the header is connected to a pump or blower. The pump or blower provides the vacuum system to recover the generated gases from the gas wells. These recovered gases could be flared or utilized for energy.

2.4 Methane Emission Measurements

Methane emissions from landfills are reported to vary from 0.0004 to 4000 g-CH_4/m^2/day (Bogner et al., 1997b). Although several measurement techniques are available for measurement of methane emissions, there is uncertainty associated with the measurement of present landfill methane emissions in the USA as well as other parts of the world (Houghton, 1992). This uncertainty is mostly due to the limited availability of actual field measurements for landfill emissions.

Landfill emissions can be measured directly using a static flux chamber, dynamic flux chamber, micrometeorological methods, tracer method, vertical plumes and flame ionization techniques (Scheutz, C., Fredenslund, A. M., Nedenskov, J., Samuelsson, J., & Kjeldsen, P., 2009).

Among all the methods, the flux chamber method is most widely used for methane emissions measurement from landfills reported, based on studies in Europe,

U.S.A, and South Africa (Nozhevnikova, A. N., Nekrasova, V. K., Lebedev, V. S., and Lifshit, A. B., 1993; Czepiel, P. M., Mosher, B., Crill, P. M., & Harriss, R. C., 1996; Börjesson, 1997; Mosher et al., 1999; Morris, 2001; Borjesson, G., Sundh, I., and Svensson, B., 2004).

Figure 2.7 presents the global emission measurements techniques.

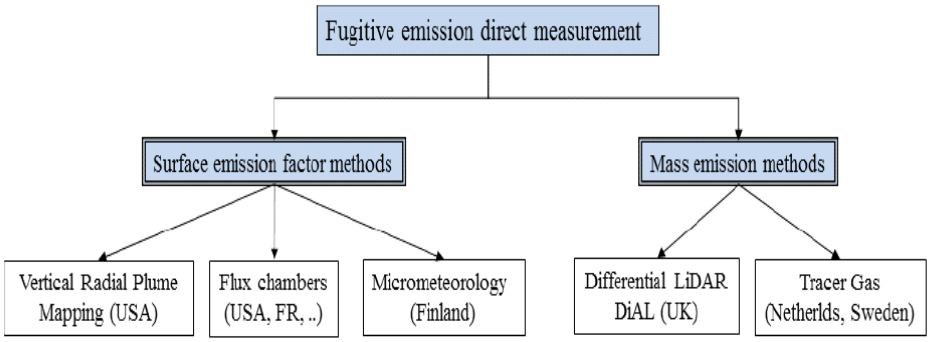

Figure 2.7 Global Schemes for Emission Measurement Technique (EREF, 2011)

2.4.1 Flux Chamber

A flux chamber is commonly used to take field emission measurements of area sources. Emission flux measurements provide an estimate of the amount of gas emitted from a specific surface area enclosed by the flux chamber per time. This data can be used to develop emission rates for a given source, necessary for dispersion modeling of off-site impacts, and to develop emission factors for remedial actions. The flux chamber measurement could be both static or dynamic, depending on the measurement technique. The most conventional dynamic flux chamber technique has an enclosed chamber, and clean sweep air is supplied to the chamber at a constant rate, determined by site conditions (i.e. 0.005 m^3/min) (Ekuland, 1992; Reinhart and Cooper, 1992). At the entry of the flux chamber, the volumetric flow rate of the sweep air is recorded, and at the exit, the concentration of the methane or any other gas of interest is measured. Figure

2.8 presents the schematic diagram of a dynamic flux chamber system; the emission flux is calculated based on equation 2.1.

$EF_i = (C_i)\ (Q)/\ A$ …… (2.1)

Where,

EF_i = Emission rate of gas i ($\mu g/m^2/min$)

C_i= Measured concentration of gas i (ppmv converted to $\mu g/m^3$)

Q = Sweep air flow rate (m^3/min)

A = Enclosed surface area (m^2)

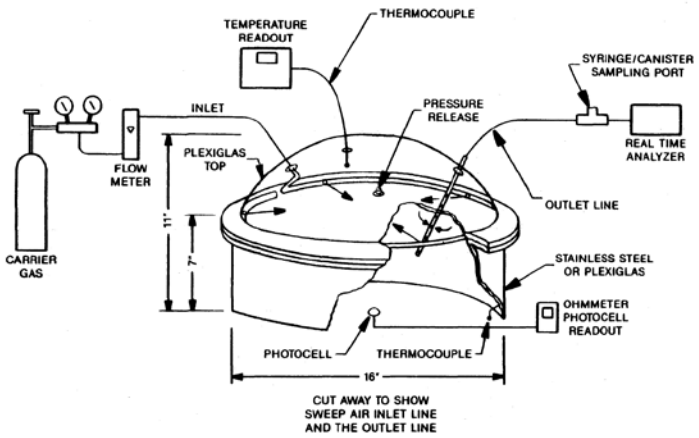

Figure 2.8 Schematic Diagram of Dynamic Flux Chamber and Support Equipment (Eklund, 1992)

Livingston and Hutchinson (2005) proposed a modified technique of emission flux measurement using a static flux chamber technique. This method is low cost, easy to operate and addresses the spatial and temporal variability to some extent. The principal purpose of a static flux chamber is to seal the area above a gas emitting surface to measure the volume of emitted gas. Chambers are typically sealed by firming soil around

the chamber on the ground or by clamping them to pre-installed collars. A series of air samples is collected from each chamber placed at grid points (maximum 100 ft apart according to USEPA, 2005) as illustrated in Figure 2.9.

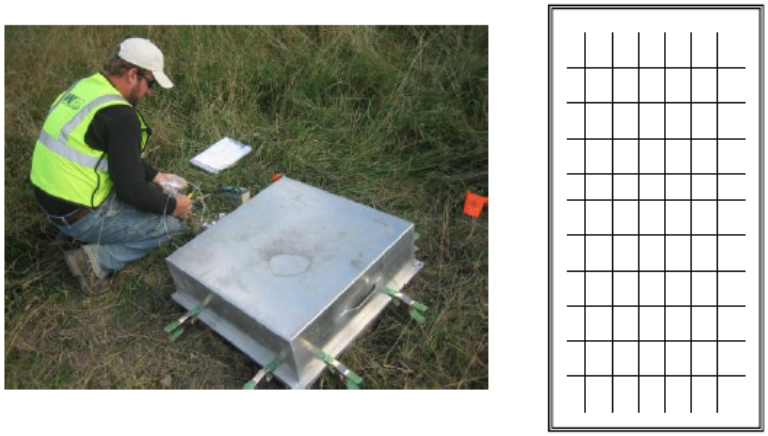

Figure 2.9 Flux Chamber Method General Configuration (EREF, 2011)

Methane samples are collected from a chamber immediately after sealing (time = 0 min) and after 2, 5, 10, and 15 min using 60-mL plastic syringes fitted with plastic plungers. Samples are analyzed using a gas chromatograph equipped with a flame ionization detector within 24 hours of collection (Abichou et al., 2005; 2008; Chanton et al., 2009; 2011). Methane flux is determined from concentration data (C in ppmv) plotted versus elapsed time (t in minutes).The data generally fit a linear relationship, in which case dC/dt is the slope of the fitted line. The methane flux, F ($g/m^2/day$), is then calculated as follows (Abichou et al., 2005):

$$F= (PVMU (dc/dt))/ (ATR) \quad (2.2)$$

Where, P is pressure (atm), V is chamber volume (80 L, plus collar volume), the molar mass of methane (16 g/mol), U is the units conversion factor (0.00144 L.min/(μLd)), A is the area covered by the chamber (0.4 m^2), T is chamber temperature

(K), and R is the gas constant (0.08205 L atm/(Kmol)). The slope of the line, dC/dt, is determined by linear regression between methane concentration and elapsed time. A non-zero flux is reported when $p < 0.1$ (90% confidence) in the correlation between methane concentration and time; otherwise, a zero-flux is reported (Barlaz et al., 2004).

A large number of chamber measurements are needed to quantify whole-site emissions due to the spatial variability in emissions. Therefore, the flux chamber method is time and labor-intensive and requires applying appropriate geo-statistical techniques for accurate determination of whole-landfill emissions (Börjesson et al., 2000; Spokas et al., 2003). Accordingly, chamber measurements might not be well suited for whole-site emissions measurements; however, the flux chamber method could be very useful for certain localized studies (Scheutz et al., 2009). An alternative method for quantification of landfill emissions is downwind plume concentration measurements (dynamic or stationary). When combined with meteorological data and atmospheric dispersion modeling, this can provide an integrated measure of whole landfill fluxes (Scharff et al., 2003). However, if a reference release system (tracer release) is in place, the need for both meteorological data and modeling can be avoided (Czepiel et al., 1996; Tregoures et al., 1999; Galle et al., 2001). A limitation of the plume measurement method, as currently applied, is that it does not quantify emissions from individual areas of the landfill or various on-site emissions point sources, such as leaks in gas collection systems and leachate collection systems. Similarly, flux chamber methods are not appropriate for quantification of emissions from point sources. For landfill operators, there is a need for development of measurement techniques that both quantify whole-site emissions as well as emissions from on-site sources, to be able to identify emission hot-spots and on-site sources, implement emission mitigation actions, and verify improvement in landfill management operation.

2.4.2 VRPM

ARCADIS developed the vertical radial plume mapping (VPRM) technique that records the direct measurement of pollutant mass emission flux from an area source using ground base optical remote sensing (ORS). This method uses a spectroscopic instrument to measure pollutant concentration along multiple optical paths. Wind vector information is processed with a plane integrating a computer algorithm to obtain pollutant emission flux. Figure 2.10 presents a typical VPRM measurement configuration.

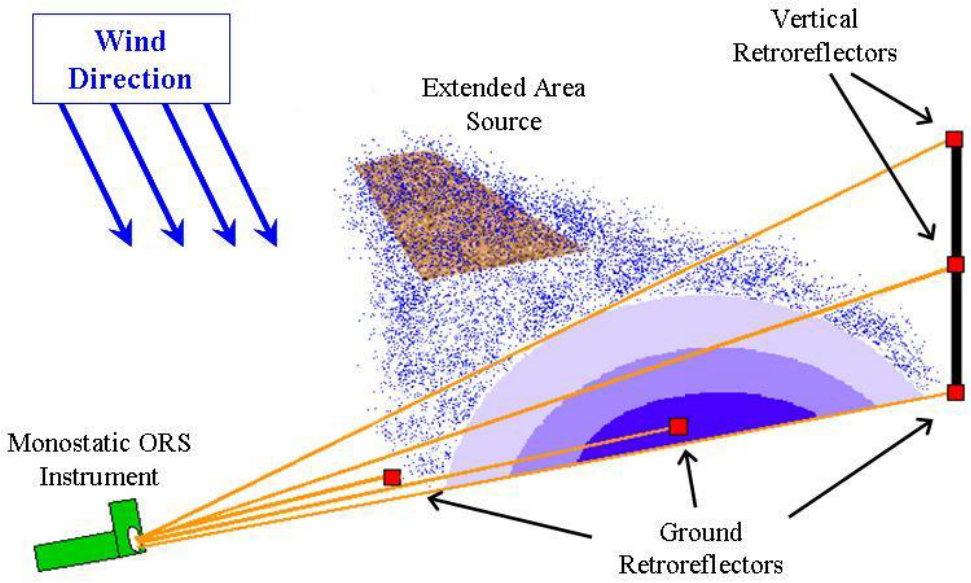

Figure 2.10 Typical Configuration of VPRM Method (EREF, 2011)

2.4.3 Tracer Gas

Tracer gas or Fourier transform infrared spectroscopy FTIR method measures the gas concentration based on tracer gas release in combination with downwind plume and tracer gas concentration. The FTIR system, with a multi pass cell, is mounted to a

van that collects continuous concentrations of methane and nitrous oxide, as presented in Figure 2.11.

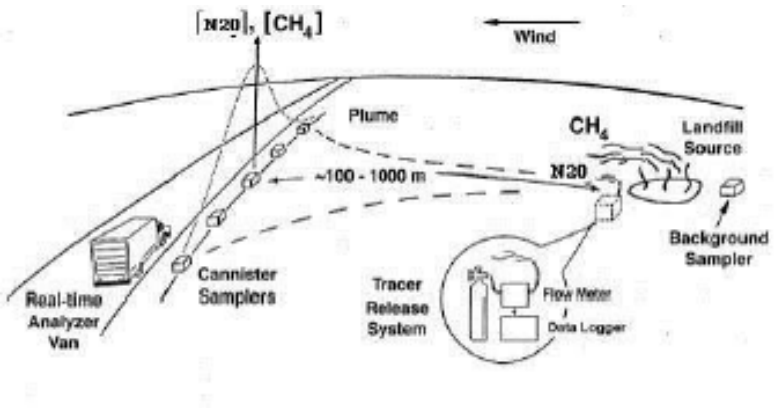

Figure 2.11 General Configuration of Tracer Gas Method (EREF, 2011)

Equation 2.3 is used to estimate the methane emission rate from the downwind of landfill site by integrating methane and nitrous oxide plumes.

$$\text{Emission}_{CH4} = Q_{N2O} \times (C_{CH4})/(C_{N2O}) \times (M_{CH4})/(M_{N2O}) \quad \ldots\ldots\ldots\ldots\ldots\ldots\ldots\ldots\ldots\ldots\ldots\ldots (2.3)$$

Where, Q_{N2O} is the release rate of tracer gas (nitrous oxide), C is the cross plume integrated concentrations above background and M values are the molar masses.

However, for tracer gas method, repeated estimation is required to overcome source variability and uncertainties. The average methane flux is estimated based on the concentrations recorded during the measurement period for this method.

2.4.4 Differential Absorption LIDAR Method-Dial

The Dial method measures methane emissions from the atmosphere using pulses of tunable laser radiation. Laser radiation is launched to the atmosphere over the monitoring area, and a fraction of energy scattered from the atmosphere comes back toward the laser source. These return signals are collected by a telescope close to the

source and measured by a LIDAR detection system, as presented in Figure 2.12. The atmosphere acts as an extended reflector for this method and produces backscattered radiation from the source. The time of arrival of the returning signals depends on the distance of the backscattered radiation from the source, and the amount of backscattered radiation is measured as a function of radiation travelling time. Moreover, the gas concentration can be measured depending on the wavelength and spectral absorption of the laser radiation. Integration of wind data and other meteorological data recorded concurrently with the radiation data estimates the methane emission flux value.

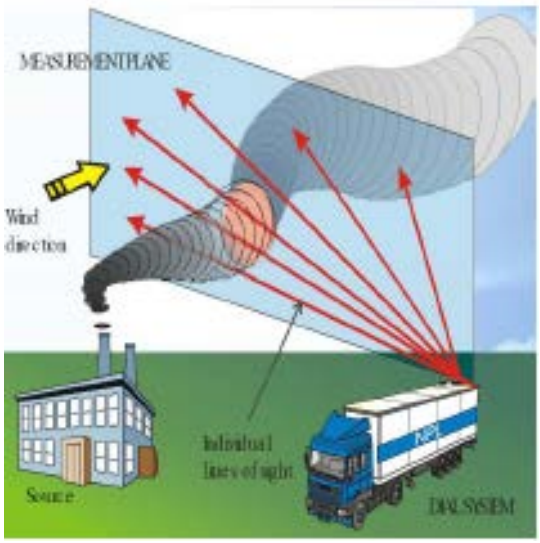

Figure 2.12 General Configuration of LIDAR-Dial Method (EREF, 2011)

2.4.5 Micrometeorological method

The micrometeorological method or eddy covariance method calculates average emission per unit area at an approximate height of 10 m. The emitted gas from the surface has higher gas concentration near the surface. Data is collected at a frequency of 10 Hz for methane concentration, carbon dioxide concentration, water vapor and

anemometer. Total emissions from landfills are calculated from average emissions per unit area multiplied by the total surface area of the landfill.

Figure 2.13 illustrates the micrometeorological method for emission measurements.

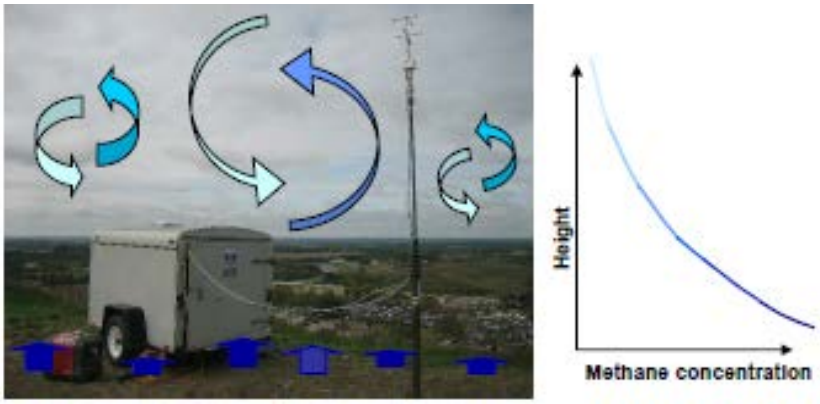

Figure 2.13 Micrometeorological Methods (EREF, 2011)

2.4.6 Flame Ionization Detector (FID)

Awono et al. (2005) first proposed a technique of methane emission measurement from the landfills with a portable flame ionization detector (FID). The FID (PortaFID M3K) was originally built for gas pipe detection with high accuracy and is resistant to interference as presented in Figure 2.14. Awono et al. (2005) used this PortaFID M3K in combination with kriging method for methane emission detection from landfill covers, which was later followed by few other researchers in UK (Awono et al., 2005; Leburn et al., 2007; Collart et al., 2008).

.

Figure 2.14 Flame Ionization Detectors (PORTAFID M3K)

The FID instrument is equipped with a microprocessor, integrated pump sample and hand held portable gas detector. The pump directly collects samples from the ground and analyzes the methane concentration using the same technique as a laboratory gas chromatograph (GC).

This method provides a semi-quantitative measurement of methane emissions, which is processed with linear kriging method to plot methane emission zones. This method is easy to implement, low cost, and can be useful for high methane concentration area detection from the landfills.

2.5 Controlling Factors for Methane Emissions

Although several methods are available to measure methane emissions, as discussed in previous section, the flux chamber method is most widely used for methane emissions measurement from landfills, based on studies in Europe, U.S.A, and South Africa (Nozhevnikova, A. N., Nekrasova, V. K., Lebedev, V. S., and Lifshit, A. B., 1993;

Czepiel, P. M., Mosher, B., Crill, P. M., & Harriss, R. C., 1996; Börjesson, 1997; Mosher et al., 1999; Morris, 2001; Borjesson, G., Sundh, I., and Svensson, B., 2004). Flux chamber measurements for methane emissions are reported to vary from <0.0001 to >1000 g CH_4 m^2 d^{-1} (Bogner et al., 1997b) from landfills. Furthermore, methane emission ''hot spots'' (the high concentration zones in the landfill surface) are very common in landfills, yielding emissions 2 to 3 orders of magnitude higher than the remainder of the landfill area (Bogner et al., 1997; Scheutz et al., 2009, 2011). These hot spots are often related to leakages from emissions at the edge of the landfill footprint, piping systems, or point sources, requiring cover maintenance. In addition, different micrometeorological conditions also play substantial roles in higher methane migration from the landfill cover systems.

The following sub-sections address the major controlling factors of methane emission from landfills.

2.5.1 Seasonal Variation

Seasonal variation might be one of major reasons for temporal variation of emission from landfill covers (Chanton and Liptay, 2000). The landfill gas migration is influenced by pressure, concentration and temperature that surround the landfill area (Wang-Yao et al., 2006). Methane emission measurements were conducted in seven different landfills in Thailand from September 2005 to February 2006, including four open dumps and three sanitary landfills. September to November was dry season and January to February was wet season (Wang-Yao et al., 2006).

Table 2.2 Methane Emissions at 7 Disposal Sites in Wet and Dry Seasons

Site	CH_4 emissions in wet season			CH_4 emissions in dry season			Emission ratio (wet season/dry season)
	Range	Number of test points	Average spatial emissions ($g/m^2/d$)	Range	Number of test points	Average spatial emissions ($g/m^2/d$)	
Pattaya	0.38 – 697.85	40	129.79	0.00 – 686.93	41	23.40	5.55
Cha-Am	0.00 – 58.24	30	5.45	0.00 – 8.45	31	1.00	5.45
Hua-Hin	0.00 – 295.82	30	51.79	0.00 – 117.00	40	10.31	5.02
Nakhon Pathom	0.00 – 825.79	30	7.89	0.00 – 38.09	32	4.17	1.89
Nonthaburi	0.00 – 358.22	20	3.94	0.00 – 19.94	20	1.64	2.40
Rayong	0.00 – 22.79	22	2.44	0.00 – 2.89	20	1.00	2.44
Samutprakan	0.00 – 724.09	16	12.21	0.00 – 14.28	16	4.82	2.53

Based on the flux chamber analysis, the authors concluded the average emissions in the wet season were 5 times higher than in the dry season. According to Wang-Yao et al. (2006), lower gas generation in the dry season might be the reason for the lower emissions in the dry season. In contrast, Bogner et al. (2011) suggested most of the variability in emissions can be attributed to variable methane oxidation rates at non-optimum temperatures and moisture of the cover soils.

The authors conducted a study with six different types of cover soil in two different landfills (Scholl Canyon landfill and Marina Landfill) in California, USA. The data was recorded twice a year - once in wet season and once in dry season - for over two years. According to the authors, the seasonal conditions cannot be directly characterized as dry or wet based on the average temperature or precipitation; they are more accurately characterized based on the optimum temperature and optimum moisture content. Figure 2.15 presents the wet and dry season methane fluxes for daily, intermediate and final covers at both landfill sites (Bogner et al., 2011). In the figure, positive and negative fluxes are plotted separately as they represent two different conditions of atmospheric emissions (positive flux) and atmospheric oxidation (negative flux).

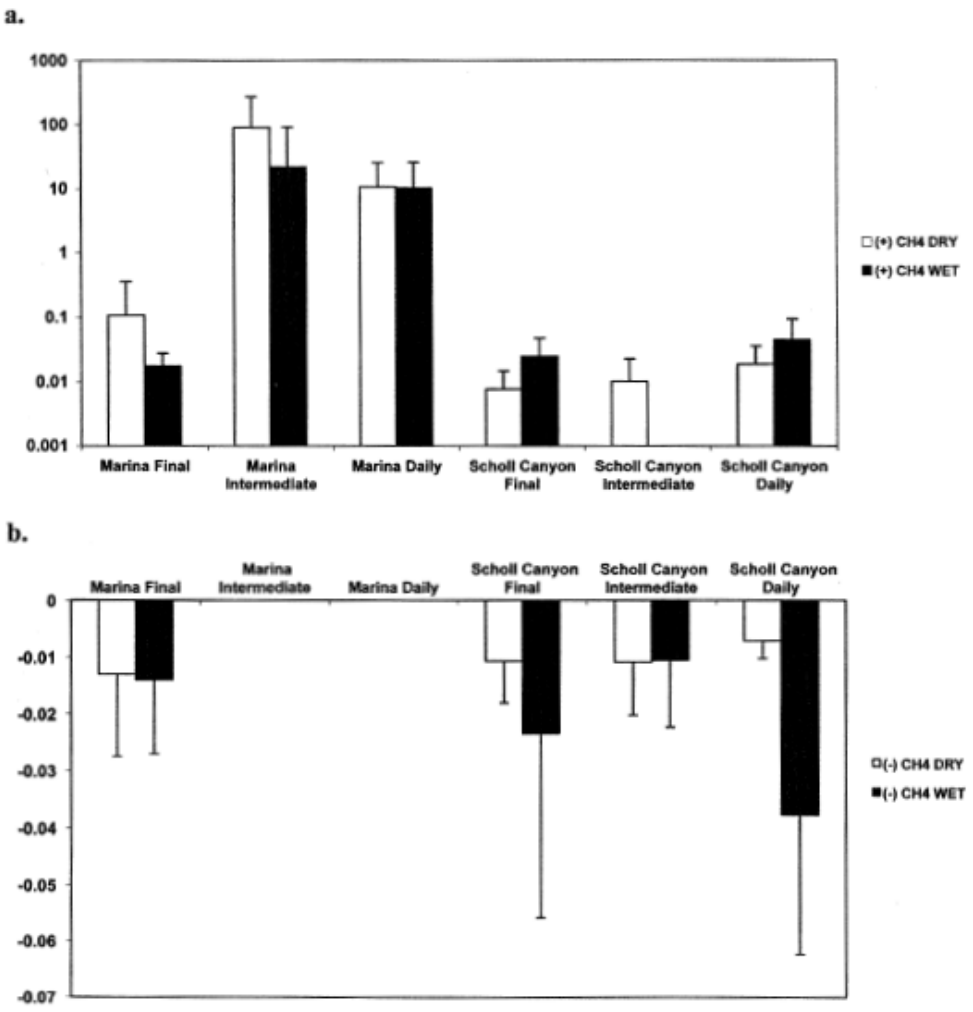

Figure 2.15 Dry and Wet Season Fluxes (a) Positive Methane Flux; (b) Negative Methane Fluxes (Bogner et al., 2011)

Maurice et al (2003) conducted an emission study for cold climatic conditions for three different sites and presented the seasonal variations of emissions based on the percent emissions of methane and carbon dioxide from the surface, as presented in Figure 2.16. The authors observed methane emissions from the sites in late summer and winter (when the soil was frozen due to snow). The landfill sites had little vegetation and very low soil organic content. Therefore, the authors concluded that the lower emissions

were mostly due to high oxidation of the cover soil. However, the landfill sites had a 3 m thick cover, which might be one of the reasons for lower migration of methane to the surface.

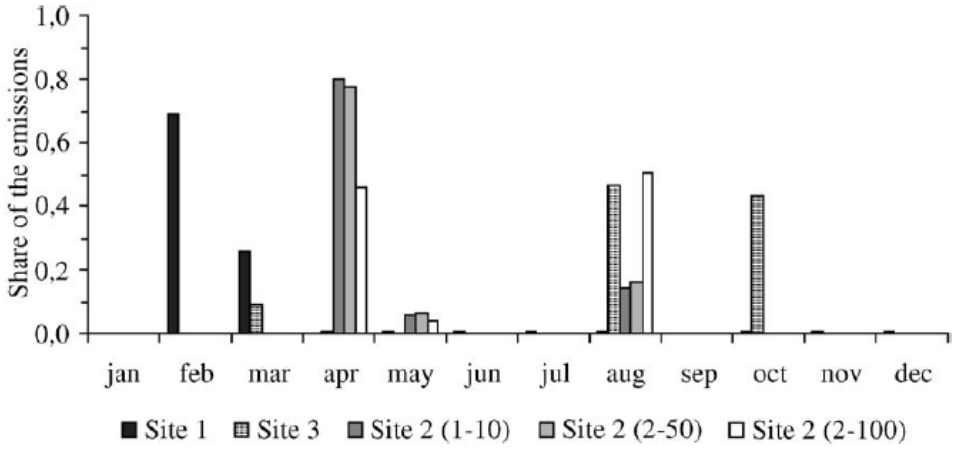

Figure 2.16 Seasonal Variation of Methane Emissions from Three Different Sites (Maurice et al., 2003)

Yuan (2006) presented a comparison of surface emissions for the presence of the mulch layer on top of the landfill. The study shows that a thick mulch cover effectively reduces the surface emission from the landfill, as presented in Figure 2.17.

A similar study was conducted by Fleiger (2006), comparing a control cell with a bio-cover cell as presented in Figure 2.18 and Figure 2.19. The study shows the bio cover helps reduce the surface emissions from the landfills, with a few exceptions. However, the authors did not identify the reasons for the high emissions from the bio-cells.

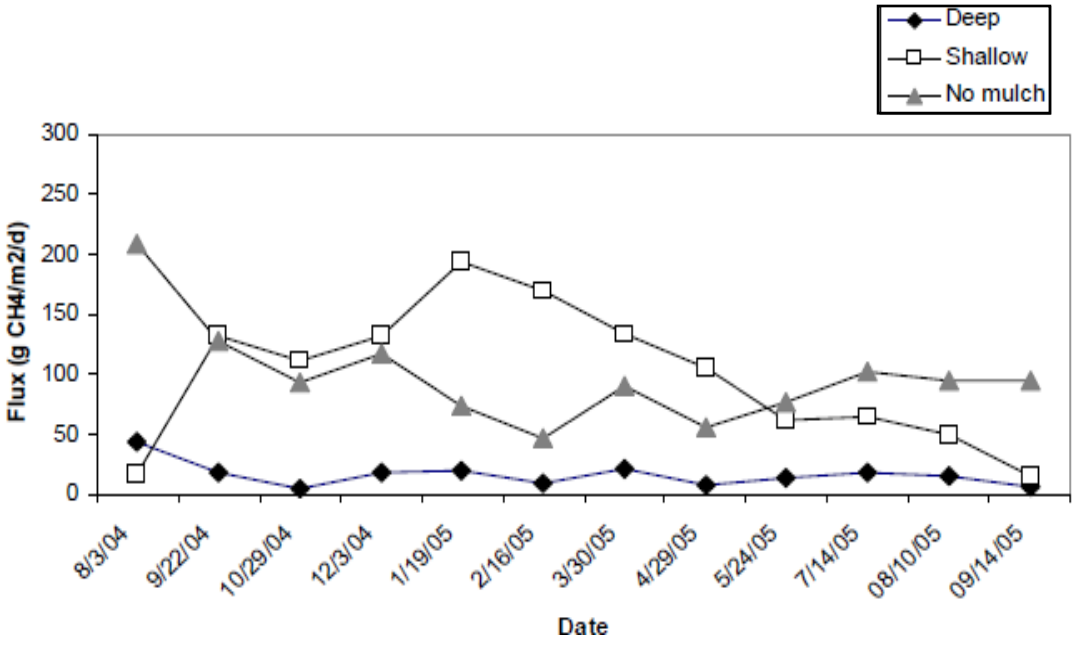

Figure 2.17 Effect of Mulch on Methane Emissions (Yuan, 2006)

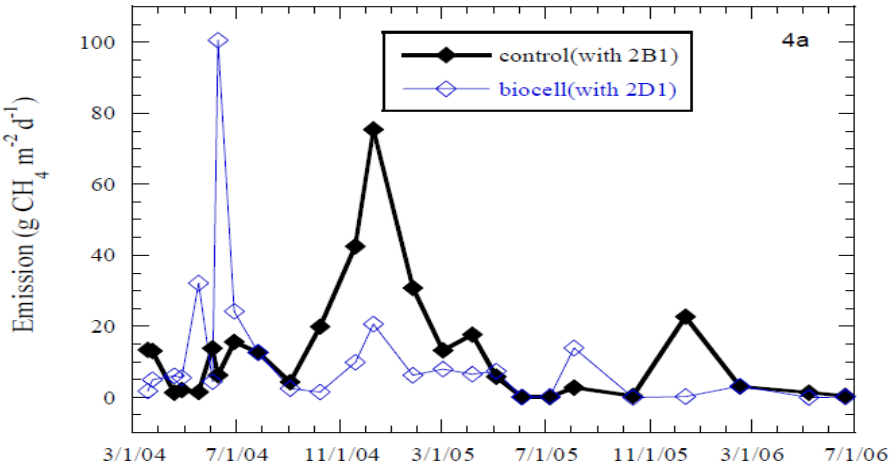

Figure 2.18 Comparison of Methane Emissions from Control Cell and Bio-Cover Cell (Including all the Data points) (Fleiger, 2006)

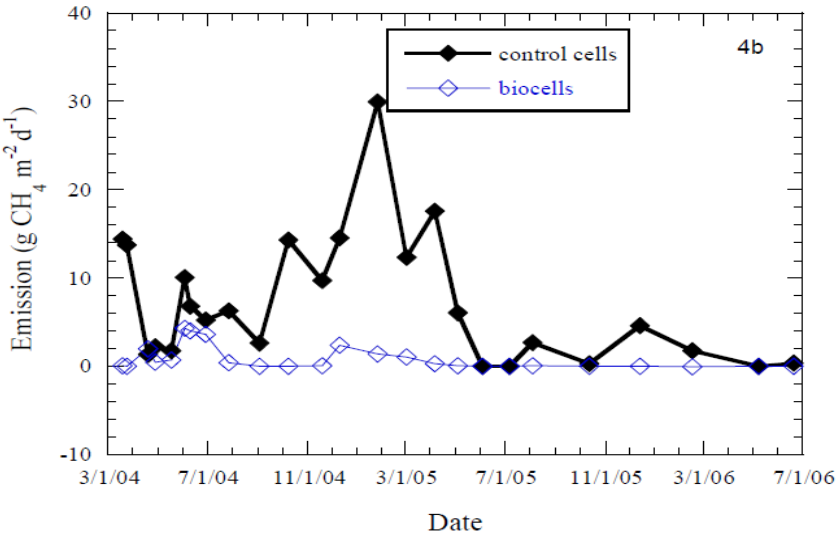

Figure 2.19 Comparison of Methane Emissions from Control Cell and Bio-cover Cell (Excluding the Outliers) (Fleiger, 2006)

2.5.2 Spatial Variation (Slope/ Flat)

One of the most challenging aspects of methane emission estimation is the integration of the isolated flux chamber measurements to assess the emissions from the whole landfill.

Methane fluxes from the landfills are spatially non-uniform, and previous studies reported more than four orders of variation in the magnitude of methane emissions from the landfills (Abichou et al., 2006; Bogner et al., 2011). In addition, methane emissions from the top flat surface of the landfill were found higher than landfill slopes (Abichou et al., 2006). The cover of the soil was observed to form cracks during the dry season and loose cohesion during the wet period. Both of these conditions might initiate conduits for gas migration from the landfill to the atmosphere. Furthermore, the differences in pressure may result in advective flow (Abichou et al., 2006).

Table 2.3 Methane Emissions from Four Sites with Different Spatial Conditions

Properties	Site 1	Site 2	Site 3	S1-grid	All sites
Age of latest waste (year)	7	14	1	7	1–14
Cover thickness (cm)	30–60	45	15–30	21–119	15–119
Slope aspect	Flat	Slope	Flat	Slope	
First sampling date	June 18, 2003	June 23, 2003	June 26, 2003	September 29, 2003	June 18, 2003
Last sampling date	September 22, 2003	July 16, 2003	November 26, 2003	February 16, 2004	February 16, 2004
Flux ($g\ m^{-2}\ day^{-1}$)					
n	62	18	28	112	220
Maximum	1,754.8	63.1	5,21.2	3,42.5	1,754.8
Median	24.0	2.1	32.7	0.72	4.8
Minimum	−13.6	−2.3	0	−6.1	−13.6
Mean	167.0	8.6	87.0	24.5	71.3
s	332.3	16.4	143.5	63.4	198.5
$Mean_g$[a]	43.8	3.4	24.9	6.5	18.6
s_g[a]	4.6	2.8	6.1	2.5	3.2

[a]Geometric mean ($mean_g$) and standard deviation (s_g) are defined in Eqs. (6)–(8).

32

2.5.3 Gas Generation

2.5.3.1 Waste Age

The spatial variability of methane fluxes was also reported to be a function of gas generation from wastes underlying the cover soil (Abichou et al., 2006). However, landfill generation is a function of MSW composition, age, climatological conditions, and operational practices in a landfill (Maciel et al., 2011). Seasonal conditions also play a significant role in volumes of landfill gas generation and collection efficiencies (Spokas et al., 2006; Barlaz et al., 2009). Summer collection efficiencies were found to be lower than winter values since more landfill gas is generated in the summer due to greater microbial activity (Spokas et al., 2006).

2.5.3.2 Operational Practices

EPA conducted a study on the effect of a bioreactor landfill operation on emissions in 2004, using FTIR at 10 m height. The study was conducted before and after the leachate recirculation in the landfill. The leachate was recirculated on January 21, and the study continued until right before the leachate injection on January 21 and the morning and afternoon of the next day, on January 22, 2004. The results are presented in the figure below. The red dot in the figure shows the location of the scanner. The results are plotted in ppm above the ambient background, and surface emissions higher than 23 ppm above ambient background was considered to be a possible emission zone.

Figure 2.20 through Figure 2.21 presents the result of the study.

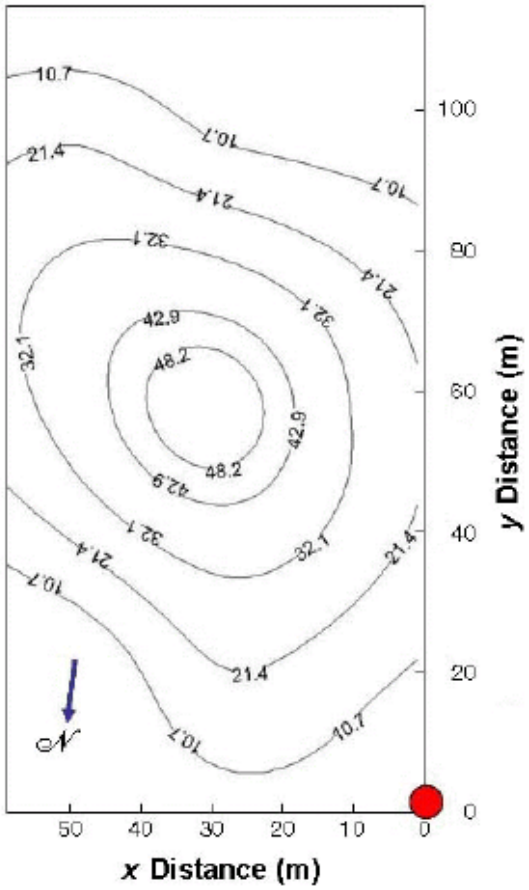

Before Injection

Figure 2.20 Average Surface Methane Concentration Contour Maps from the HRPM Survey of 01/21/04 (EPA, 2004)

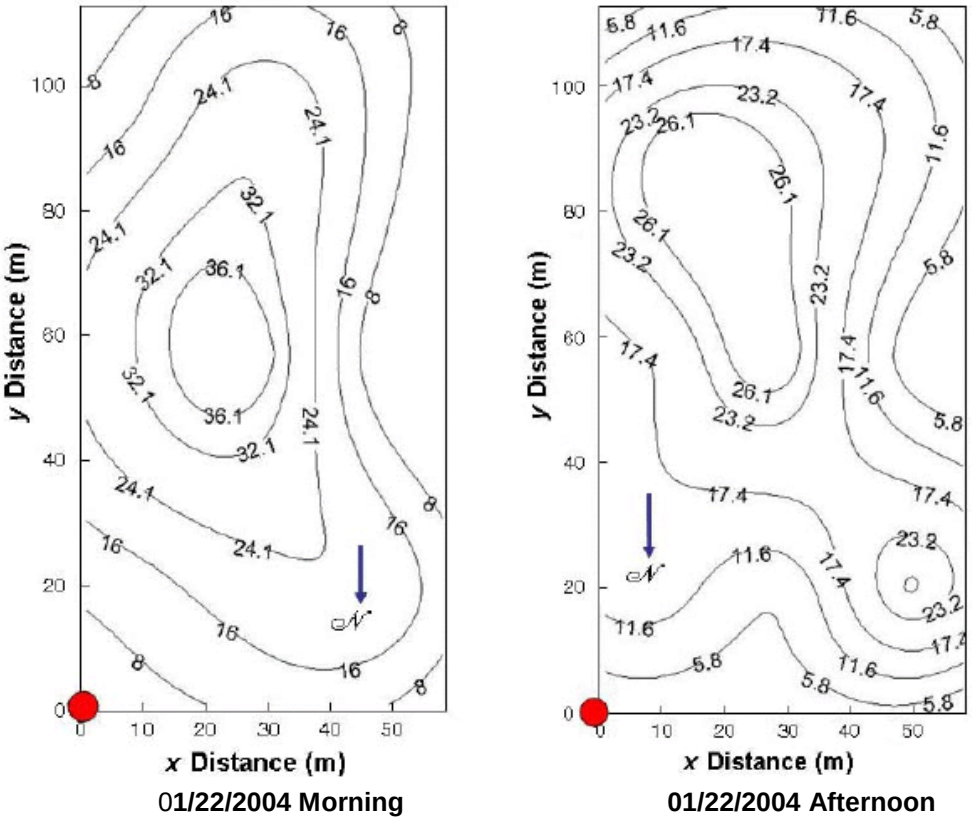

Figure 2.21 Average Surface Methane Concentration Contour Maps from the HRPM Survey of 01/22/04 (EPA, 2004)

Based on the before-and-after injection analysis, the report concluded that due to pumping, higher surface methane concentrations were observed at the northwest section of the landfill, near the location of the leachate pond at that corner.

2.5.4 Oxidation of Cover

In order to understand the methane emissions from the landfill cover system, it is important to understand the methane oxidation as well as methane generation from the landfills. One of the major mechanisms that has been proposed over the years to reduce methane emissions from landfills is the oxidation by methanotrophs in cover soils

(Bogner et al., 1997; Bogner et al., 2011; Scheutz et al., 2009; Jung et al., 2011). The importance of methanotrophs in the cover was first observed by Whalen et al. (1990) and estimated to oxidize approximately 50% of the migrating methane.

Methane oxidation can be defined as the fraction of methane oxidized in the cover soil on the landfill. Oxidation highly depends on the presence of oxygen in the cover, and from most of the field studies, it appears that the top 1 ft of the cover is found to be the most active zone for oxidation (Albanna et al., 2006). From previous studies, the oxidation has been reported to vary from 7% to 50% of methane emissions. However, methane oxidation increases with the increase in temperature; up to 100% of methane emissions can be oxidize (Kjeldsen et al., 1997; Czepiel et al.,1996). From different studies, negative fluxes of methane emissions were reported where methane is consumed in the cover instead of being emitted to the atmosphere (Bogner et al., 1995; Bogner et al., 1997a; Borjesson and Svensson, 1997; Borjesson et al., 1998; Abichou et al., 2006a and b). The ability to oxidize methane is also reported as methanotrophy (expressed in g-CH_4/m^2/day). The maximum methane oxidation rate was reported to be 45 g-CH_4/m^2/day, 100 g-CH_4/m^2/day and 170 g-CH_4/m^2/day, respectively, by Whalen et al. (1990), Visvanathan et al. (1999) and Kightley et al. (1995).

Table 2.4 shows the methanotrophy values listed for different soils.

Table 2.4 Methanotrophy (g-CH_4/m^2/day)of Different Soils (Yuan, 2006)

Soil Type	No. of Data	Minimum	Average	Maximum
Cultivated Soil	13	0	$5.5x10^{-4}$	$8.86x10^{-2}$
Grassland Soil	7	$1.75x10^{-4}$	$6.5x10^{-4}$	$4.85x10^{-2}$
Non-Cultivated Upland Soil	6	$1.0x10^{-5}$	$8.3x10^{-4}$	$2.28x10^{-2}$
Forest Soils	17	$1.6x10^{-5}$	$9.9x10^{-4}$	0.1659
Wetland Soils	9	0	$1.72x10^{-2}$	70
Upper Soil Layer in covered landfill	3	7	45	$1.7x10^{2}$

2.5.4.1 Oxidation Measurement

Oxidation capacity of the landfill covers can be measured from laboratory investigation (Boeckx et al., 1996; Czepiel et al., 1996; Borjesson et al., 1997; Chanton et al, 1999; Visscher et al., 1999; Abichou et al., 2006; Abichou et al., 2006; Stern et al., 2006; Albanna et al., 2007; Bohn et al, 2007; Abichou et al., 2008; Abichou et al., 2009; Chanton et al, 2010). Initially, incubated soil samples were used to analyze the oxidation capacity of the cover soil (Boeckx et al., 1996; Czepiel et al., 1996; Borjesson et al., 1997; Visscher et al., 1999; Bohn et al, 2007, Albanna et al., 2007). However, the more modern carbon isotoping technique analyzes the oxidation capacity of the soil based on the in situ soil gas samples (Chanton et al, 1999; Abichou et al., 2006; Abichou et al., 2006; Stern et al., 2006; Abichou et al., 2008; Abichou et al., 2009; Chanton et al, 2010). Soil gas samplings from different depths are also evaluated to identify the depth vs methane concentration profile in many studies. Although the depth vs concentration results provide a perception of the oxidation within the cover, no studies are reported to

estimate the oxidation capacity of the soil based on the soil gas behavior. Very few studies reported developing a statistical model for methane oxidation capacity measurement.

(i) Incubation or Batch Experiment

Although the oxidation capacity of the soil primarily depends on the type of the soil, the climatological conditions also have an effect on the oxidation. Several studies reported measuring the oxidation capacity of soil based on laboratory incubation of the cover soil (Boeckx et al., 1996; Czepiel et al., 1996; Borjesson et al., 1997; Visscher et al., 1999; Bohn et al, 2007, Albanna et al., 2007). Recently, a few researchers have reported measuring the methane oxidizing capacity of soil with the carbon isotoping technique (Chanton et al, 1999; Abichou et al., 2006; Abichou et al., 2006; Stern et al., 2006; Abichou et al., 2008; Abichou et al., 2009; Chanton et al, 2010). Although carbon isotoping provides more accurate results, it fails to address the climatological effects on the oxidation capacity. Besides, the carbon isotoping technique (GC-irms) is very sensitive and expensive, and very few laboratories have access to the equipment. Therefore, to evaluate the climatological and other operational effects, incubation or batch experiment techniques are more effectively used to date.

Several laboratory studies reported measuring methane oxidation in columns or batch experiments. These studies were conducted in different types of soil and under different methane injection rates (Boeckx et al., 1996; Czepiel et al., 1996; Borjesson et al., 1997; Visscher et al., 1999; Bohn et al, 2007, Albanna et al., 2007). Oxidation tests can be conducted either at in-situ moisture content or at any adjusted moisture content of the soil. The soil samples are air dried for 72 hours before adjusting the moisture of the soil samples (Czepiel et al., 1996). Once the moisture content is adjusted, the samples are incubated in air-tight jars for 12 to 48 hours at a specific temperature required for the

test (Boeckx et al., 1996; Czepiel et al., 1996; Borjesson et al., 1997; Visscher et al., 1999; Bohn et al, 2007, Albanna et al., 2007). Methane is then injected into the incubated soil samples, and headspace samples are tested with time. This change in concentration with time is known as the rate of oxidation. Methane oxidation rate can be measured from first-order kinetics, as proposed by Boeckx et al. (1996) and presented in equation 2.4.

$$\frac{d[CH_4]}{dt} = -K_1\,[CH_4] \quad \text{..... (2.4)}$$

Based on the methane consumption results, the oxidation efficiency can be calculated as

$$\textbf{CH4 oxidation efficiency} = \frac{(C_{CH_4})_{t,0} - (C_{CH_4})_{t,l}}{(C_{CH_4})_{t,0}} X100\% \quad \text{..... (2.5)}$$

(Albanna et al., 2007)

(ii) Carbon Isotope Analysis

Merrit et al. (1995) first proposed the stable isotope technique to determine the methane oxidation. Recently, this method has been employed in several studies (Chanton et al, 1999; Liptay et al., 1998; Chanton and Liptay, 2000; Borjesson et al., 2001; Christophersen et al., 2001; Abichou et al., 2006; Abichou et al., 2006; Stern et al., 2007; Abichou et al., 2008; Abichou et al., 2008; Chanton et al., 2010). Carbon has two isotopes- ^{12}C which comprises 99% and ^{13}C that is only 1% of the total carbon atoms. ^{12}C is lighter than ^{13}C and microbial culture studies have shown that the methanotropic bacteria preferably consume lighter isotopes i.e. $^{12}CH_4$ (Powelson et al., 2007). Therefore, the extent of methane oxidation can be estimated based on the isotopic difference between the unaffected and residual methane. The carbon isotope method can be applicable for landfill cover soils or bio-filters to identify their ability to oxidize methane

(Powelson et al., 2006; 2007). This method measures the difference in $\delta^{13}C$ in the anoxic zone where methane is unaffected and in the surface where methane is, by that time, subjected to oxidation. Chanton et al. (2008b) proposed to determine the quantitative estimation of oxidation based on the difference in $\delta^{13}C$ ratio, as presented in Figure 2.22.

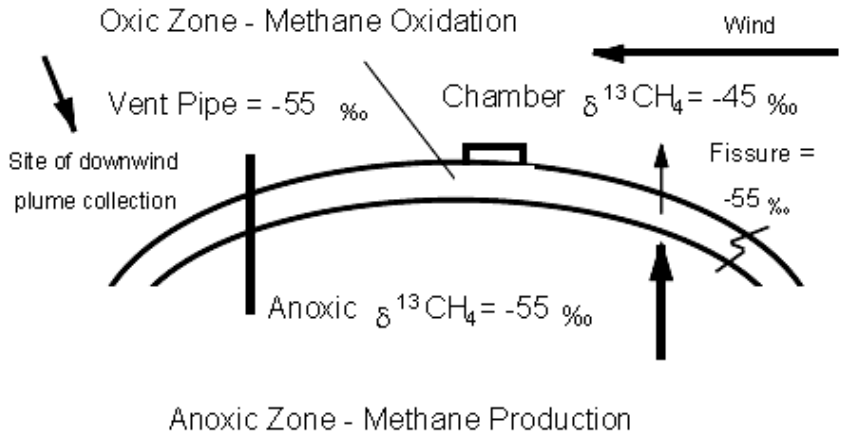

Figure 2.22 Diagram showing the main means of methane escape from landfills (Chanton et al., 1999)

Emitted methane can be captured from enclosed flux chambers or from the downwind plumes and integrated for the whole landfill from soil gas profiles for oxidation measurement (Liptay et al., 1998; Chanton et al., 1999; Chanton and Liptay, 2000; Borjesson et al., 2001; Christophersen et al., 2001). Furthermore, gas samples collected from different depths can also be used to quantify the methane oxidation within the landfill covers. Oxidation percentage is determined by the isotropic fraction as presented in equation 2.6 (Chanton et al., 1999).

$$f_0\% = \left[\frac{\delta E - \delta A}{\alpha_{ox} - \alpha_{trans}}\right] * 1000 * 100 \quad \ldots\ldots\ldots\ldots\ldots\ldots\ldots\ldots\ldots\ldots (2.6)$$

Where,

f_0= % of methane oxidized in transit through the cover soil

$\delta E = \delta^{13}C$ value of emitted methane

$\delta A = \delta^{13}C$ value of anoxic zone methane

α_{ox}= isotropic fractionation factor for bacterial oxidation

α_{trans}= isotropic fractionation factor for gas transport

(iii) Model

Visscher et al. (2003) proposed a simulation model based on mass balance across an infinitesimal soil layer. The model was developed to accurately estimate gas transport and methane oxidation from landfill covers, based on laboratory scale simulation. According to the model, the maximum influencing parameters for methane oxidation are soil temperature and soil moisture. Visscher et al. (2003) showed an excellent agreement between the proposed simulation model and actual field investigations. The simulation model leads to the following equation, as presented in equation 2.7.

$$\varepsilon\left(\frac{\partial y_i}{\partial t}\right)\left(\frac{P}{RT}\right) = \rho_{DB} r_i - \frac{\partial N_i}{\partial z} \qquad \ldots\ldots\ldots\ldots\ldots (2.7)$$

Where, ε= air filled pore space

Z= depth (where z=0 m means surface)

ρ_{DB}= dry bulk density of the soil (Kg soil $_{DW}$ m^{-3} soil)

r_i= reaction rate of compound i (mol $Kg^{-1}soil_{DW}$ s^{-1})

Ni= flux (N.B. flux chosen positive in the case of downward flux)

However, the proposed model is applicable for steady state conditions only and may not be representative of a real landfill. Therefore, this model will be best for estimating average yearly calculations, and further extended calculations will be required for specific conditions.

A Hydrus 1D gas transport model was used to simulate methane emission and oxidation for specific water content and temperature (Abichou et al., 2008). The gas flow within the porous media was expressed using mass balance and continuity equations.

$$\varepsilon \frac{dC_i}{dt} = -\frac{dJ_i}{dx} + r_i \quad \text{..... (2.8)}$$

Where,

ε= air filled pore space ($m^{-3}_{gas}\ m^{-3}_{soil}$)

C_i = molar gas concentration model

J_i = flux of the gas component I including the diffusive and advective flux (mol $m^{-2}\ s^{-1}$)

r_i= reaction rate of compound i (mol $Kg^{-1}_{dry\ soil}\ s^{-1}$)

dt= time (s)

dx= vertical distance (m)

$$J_i = -D_{soil,i} \frac{dC_i}{dx} - \frac{K}{\mu} \frac{dp}{dx} C_i \quad \text{..... (2.9)}$$

Where,

J_i = flux of the gas component i including the diffusive and advective flux governed by Fick's law and Darcy's law (mol $m^{-2}\ s^{-1}$)

$D_{soil,i}$= diffusion coefficient of gas component i ($m^{-2}\ s^{-1}$)

K= intrinsic permeability of soil (m^{-2})

μ= viscosity of gas mixture (Ns m^{-2})

P= pressure (Pa)

The flow chart of the model algorithm is presented in Figure 2.23.

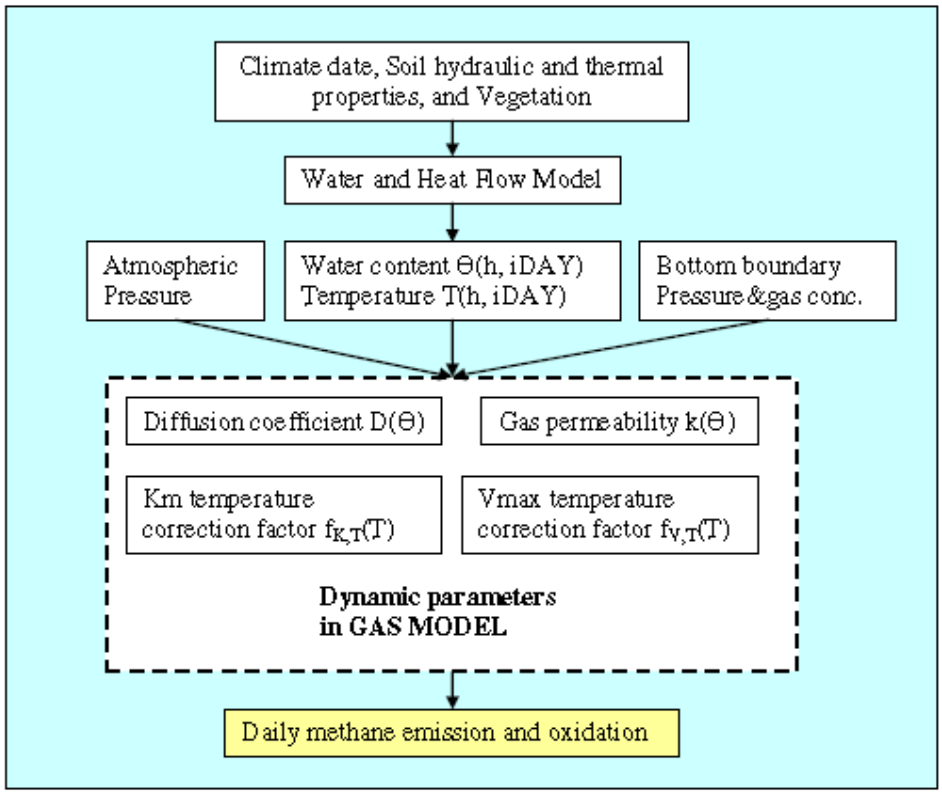

Figure 2.23 Flow Chart of Model Algorithm

Based on this algorithm, a CALMIM model was built that is the most updated model so far for emission and oxidation analysis. This is the first preliminary model that has a visual surface and estimates the methane emission and oxidation based on cover soil properties and climatological conditions. However, the model is specifically built only for California landfills, and there is a built-in data for the climatological conditions.

Consequently, the model cannot perform analysis for specific climatological conditions. Methane oxidation rate of the cover soil is a function of not only the soil properties, but also the climatological parameters, i.e. temperature, moisture, and barometric pressure. Therefore, specific information is required for the analysis or modelling of oxidation capacity of a soil cover system.

2.5.4.2 Controlling Factors for Methane Oxidation

(i) Temperature

The methane oxidation rate typically increases with the increase in temperature (De Visscher et al., 2001). Borjesson and Svensson (1997) reported that soil temperature is the only controlling factor of methane oxidation, and most variations of methane oxidation can be explained with the change of temperature alone.

Czepiel et al. (1996) reported that methanotrophic bacteria work in optimum range of temperatures, and oxidation rate increases as the temperature increases. They also reported that the oxidation increases until the temperature reaches 36°C and stops when the temperature reaches at 45°C. The optimum temperature range for the maximum oxidation is from 25°C to 35°C, as presented in Figure 2.24 (Borjesson and Svensson, 1997). Lower temperature ceases the bacterial activity and inhibits the CH_4 oxidation (Whalen et al. 1990; Borjesson and Svensson, 1997). However, methane oxidation is not controlled by temperature alone, and the optimum temperature range for methane oxidation decreases with increasing moisture content (Boeckx et al., 1996; Czepiel et al., 1996).

(ii) Moisture

Boeckx et al. (1996) conducted a multiple linear regression analysis under different incubation environments (i.e. temperature and moisture) and concluded that

moisture content of the cover soil has a bigger influence on methane oxidation than temperature.

Moisture content is a very important factor affecting CH_4 oxidation in landfill cover soils. It plays three important roles: 1) a certain moisture content is required for optimum methane oxidation; 2) oxygen (O_2), which is the most important parameter in oxidation, is affected by moisture content because diffusion of oxygen (O_2) is delayed as the moisture content increases; 3) water content affects the porosity of the soil and as water fills the pores in the soil, it blocks the upward flow of gas; however, at the same time, the blocking of flow might lead to higher methane emissions due to the excess pressure built-up in the cover soil (Boeckx et al., 1996).

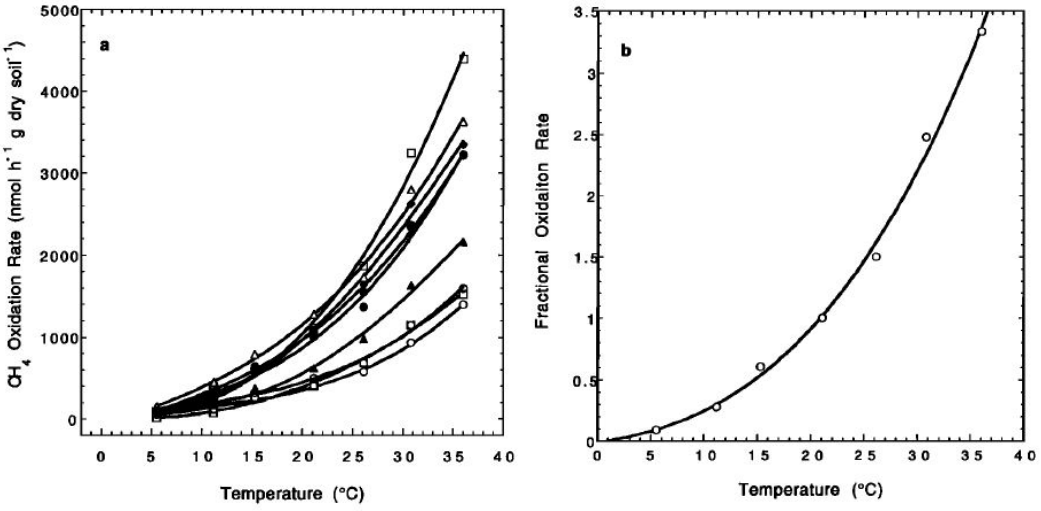

Figure 2.24 Effect of Temperature on Oxidation Rate: (a) Results from Nine Samples; (b) Average Results from Nine Samples

The low methane oxidation at the low range of soil water content may be caused by less methanotrophy activity. Oxidation peaks when the balance between optimum moisture content and temperature is achieved (Czepiel et al., 1996). The optimum oxidation soil water content will be different for each soil types and depends on

temperature and other environmental factors. Below the optimum water content, the oxidation rate will increase as the water content increases, and above the optimum water content, the oxidation rate will decrease as the water content increases, as presented in Figure 2.25 (Czepiel et al., 1996).

The optimal oxidation water content ranged between 15.6 and 18.8% for soils tested by Boeckx et al. (1996), and Czepiel et al. (1996) measured 15.7% as optimum moisture content for methane oxidation.

Methanotrophic microorganisms become inactive when the water content falls 13% below the maximum water holding capacity, and the oxidation becomes zero when moisture content is less than 6% (Bender and Conrad, 1992; Visvanathan et al., 1999; Christophersen et al., 2000). When the water content increases to saturation, the oxidation rate decreases because water fills all voids of soil and inhibits oxygen diffusion into the soil.

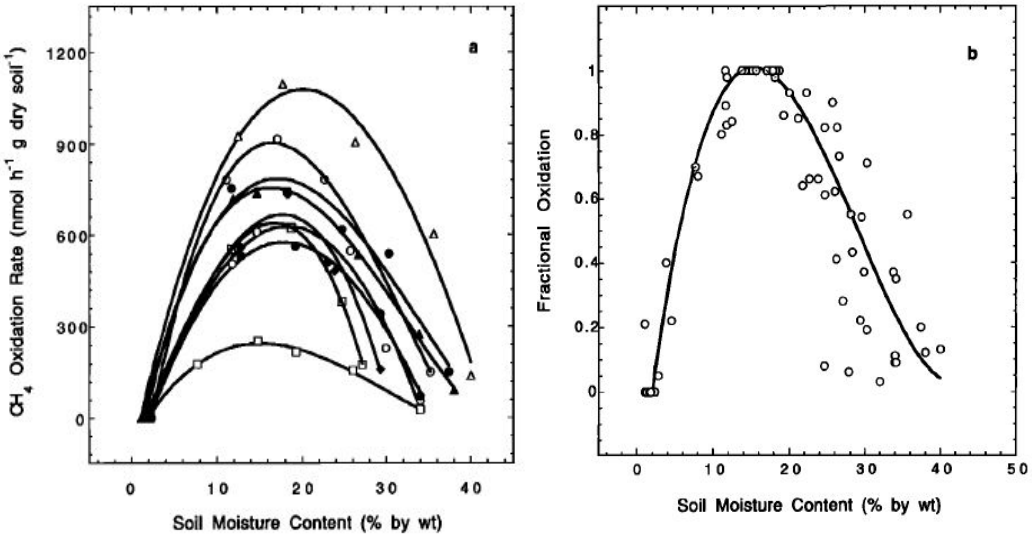

Figure 2.25 Effect of Moisture Content on Oxidation Rate: (a) Results from Nine Samples; (b) Average Results from Nine Samples

(iii) Barometric Pressure

Contradictory results are reported on the effect of barometric pressure on methane emission and oxidation. Although Borjesson and Svensson (1997) reported that there is no relationship between methane emission and air pressure or change in air pressure over the seasons, Czepiel et al. (2003) reported a very strong negative relationship between measured methane emissions and atmospheric air pressure. However, the effect of barometric pressure on methane emissions depends on the gas transport mechanism from the landfill through the cover soils. Although no strong evidence has been reported of diffusive flux being dependent on pressure difference, the pressure difference might be an influential factor for diffusive fluxes.

(iv) Organic Content of Soil

Christophersen et al. (2000) conducted an incubation test and concluded that the CH_4 oxidation rate increases with an increase in organic content. They also reported that there was a relationship between optimum moisture content and organic content.

Typically, the oxidation rate increases with increasing organic matter content in soils; hence, soils with high organic content soil may be used to reduce methane emission from the landfills (Borjession and Svensson, 1997; Christophersen et al., 2000).

The soils from old landfill covers, which have been exposed to CH_4 for a long period time, have higher oxidation rates than fresh soils (Nozhevnikova et al., 1993; Visvanathan et al., 1999). The optimum water content for oxidation increases with increasing organic content.

The compost covers enriched with organic matter were able to entirely oxidize all CH4 emitted from their landfill. Organic particles provide nutrients for methanotrophic

bacteria and have high porosity, allowing more O_2 penetration (Humer and Lechner, 2001).

2.5.5 Cover Vegetation

Vegetation aids in oxygen penetration into the soil and enhances methane oxidation in the cover soil. It influences the properties of soil, such as presence of nitrogen (N), pH, and moisture content. De Visscher et al. (1999) reported that vegetation on landfill covers may prevent the methane oxidation by uptake of N through the roots of the plants. However, the roots of the plants provide a suitable microbiological environmental for methane oxidation and in general may be used to enhance methane oxidation (Maurice et al., 1999).

2.5.6 Permeability of the Cover Soil

The landfill cover soil typically consists of locally available soil, bio-compost or mulch (Bogner et al., 2011). As soil properties determine gas flow patterns, it is hypothesized that the variability in soil gas composition and subsequent methanotrophic activity corresponds to the variability of soil properties. Methanotrophic activity is highly subjected to soil properties (soil type, soil vegetation, availability of nutrient, and cover thickness). Therefore, spatial variation in methane oxidation capacity is also observed, which eventually causes the spatial variation in methane emission from surface (Abichou et al., 2006; Albanna et al., 2007; Rower et al., 2011).

2.5.7 Gas Collection Efficiency

Unpublished data from California Department of Resources Recycling and Recovery indicates that the engineered gas collection system provides a primary control of methane emissions from landfills (Spokas et al., 2006). EPA (1997) suggests a default value of 75% collection efficiency, based upon different researchers and practitioners

reporting the gas collection efficiency to be in the range of 60% to 85%. However, Huitric and Kong (2007) reported the landfill collection efficiency to be 94%-96% based on surface methane monitoring techniques.

A more recent study by Barlaz et al. (2009) on lifetime performance of landfill gas collection efficiency suggested more than 90% efficiency with a final cover, and 50% to 90% efficiency with a temporary cover system.

Table 2.5 Collection Efficiency for Various Covers (Barlaz et al., 2009)

Cover Type	Equation 3 Collection Efficiency (%)	Equation 4 Collection Efficiency (%)
Final clay cover (1 m) with LFG recovery	91.5	92.6
Final geosynthetic clay with LFG recovery	51.5	53.0
Final clay cover (1 m) with LFG recovery—summer	90.7	92.9
Final clay cover (1 m) with LFG recovery—winter	97.8	98.6
Thin clay temporary cover (30 cm) with LFG recovery—summer	53.9	54.7
Thin clay temporary cover (30 cm) with LFG recovery—winter	93.2	95.1
Final clay cover (1 m) with LFG recovery	99.2	100
Final geomembrane with horizontal gas collection	98.1	99.2

Cover Type	Equation 4 Collection Efficiency (%)
Fiborna (wood chips and sludge)	68.4
Fiborna (wood chips and sludge)	65.0
Fiborna (wood chips and sludge)	70.0
Heljestorp (sewage sludge and soil)	57.8
Hogbytorp (sewage sludge and soil)	33.9
Hogbytorp (sewage sludge and soil)	43.2
Sundsvall (sewage sludge and soil)	63.3

2.6 Landfill Gas Generation/ Emission Models

LFG estimation is one of the major deciding factors for a landfill operator in determining whether or not to install a landfill gas collection system in a landfill. Moreover to consider the technical and economic feasibility of the landfill gas-to-energy (LFGE)

project, landfill owners or project operators have to estimate the total possible LFG generation.

Estimation of LFG generation is difficult due to heterogeneity of MSW composition, compaction and moisture content. In addition, there is no direct measurement method for the total generated gas. Several models have been developed to estimate the total generation of LFG, considering various orders of decay (zero, first, second, and multiphase).

The current landfill gas generation models are the United States Environmental Protection Energy (USEPA's) LANDfill gas GEneration Model (LandGEM), Intergovernmental Panel on Climate Change (IPCC's) landfill gas generation model, and UTA's Capturing Landfill Emissions for Energy Need (CLEEN) model (USEPA, 2005; IPCC 2006; Karanjekar, 2012).

Table 2.6 presents a brief review of different gas generation models based on different orders of decay rates.

Table 2.6 Landfill Gas Generation Models based on Different Orders of Decay Rate

Model	Equation
Zero-Order Decay Model Landfill gas generation in a certain amount of waste is assumed to be constant with time. Effect of waste age is not incorporated in the model.	$Q = \frac{M L_o}{(t_i - t_f)}$ for $t_i \le t \le t_f$ Where, Q= Methane generation rate (m^3/yr); M= Mass of solid waste in place (yr); L_o= Ultimate methane generation potential (m^3/yr); t = Time (yr); t_i = Lag time (time between waste placement and gas generation) (yr); t_f = Time to the end of gas generation (yr).
First-Order Decay (FOD) Model Landfill gas generation in a certain amount of waste is assumed to decrease exponentially. The first-order decay equation is used in US EPA's LandGEM.	$Q = M L_o k e^{-k(t-t_i)}$ Where, k = First-order decay rate constant (yr^{-1})
Modified First-Order Model This model assumes that methane generation from a certain amount of waste may be initially low (due to the "lag phase"). The generation then rises to a peak before declining exponentially, like in the first-order decay model.	$Q = M L_o \frac{k+s}{s} (1 - e^{-s(t-t_i)})(k e^{-k(t-t_i)})$ Where, k = First-order decay rate constant (yr^{-1}); s = First-order rise phase rate constant (yr^{-1})
First-Order Multi-Phase Decay Model The first-order multi-phase decay model assumes that different fractions of the waste decay at different rates. The waste is divided into three (or more) fractions, depending on the rate of their decay. E.g., food waste and grass are assumed to degrade faster than paper or certain types of textile waste. However, each fraction is assumed to follow first-order decay.	$Q = \sum_{i=0}^{n} M_i L_o [F_r (k_r e^{-k_r(t-t_i)}) + F_m (k_m e^{-k_m(t-t_i)} + F_s (k_s e^{-k_s(t-t_i)})$ Where, F_r, F_m, F_s= Fraction of rapidly, moderately or slowly decomposition wastes; k_r, k_m, k_s= First-order decay constants for rapidly, moderately, slowly degrading wastes (yr^{-1}); t_i = Age of i^{th} increment (yr).
Second-Order Decay Model The second-order model is considered better when a large number of reactions, all of a first-order but with differing reaction rates, occur in the system.	$Q = M k (\frac{L_o}{kL_o t+1})^2$ Where k = Second-order rate constant (m^3/kg/yr).

2.6.1 LandGEM Model

US EPA's LandGEM uses a simple first-order decay equation (Eq. 2.10) for predicting methane generation rate from landfills.

$$Q_{CH4} = \Sigma K L_0 M_i \ (e^{-kt}) \quad \text{(2.10)}$$

Where,

Q_{CH4}= methane generation (m^3/yr)

k = first-order degradation rate constant (yr^{-1})

L_0 = methane generation potential (m^3/Mg)

M_i= initial mass of degradable waste (Mg)

t = time elapsed (yr)

Critical input parameters in this model are ultimate methane generation potential (L_0) and the methane generation rate constant (k). According to LandGEM User's Guide (USEPA 2005), methane generation potential (L_0) depends on the waste composition and the first-order rate constant (k) depends on moisture content, pH, temperature of waste mass and availability of nutrients.

2.6.2 IPCC Model

IPCC guidelines (2006) recommended the use of a "multiphase first-order decay model" for estimation of methane emissions from landfills (Eggleston et al. 2006). A simplified version of the multiphase model is shown in Eq. 2.11. The landfilled waste is divided into categories: slowly degrading waste, moderately-degrading waste, and rapidly-degrading waste.

$Q_{CH4} = \Sigma M_i \, L_0 \, [F_r \, (k_r \, e^{-kr(t-ti)}) + F_m \, (k_m \, e^{-km(t-ti)}) + F_z \, (k_z \, e^{-kz(t-ti)})$……..…… (2.11)

Where,

Q_{CH4}= methane emission rate, m^3/yr

L_0 = methane generation potential, m^3 of CH_4/ Mg refuse

Mi = mass of waste in i^{th} section (annual increment), Mg

F_r, F_m ,F_s = fraction of rapidly, moderately or slowly decomposing wastes

k_r, k_m, k_s= first-order decay constants for rapidly-, moderately- or slowly-decomposing waste

t_i = age of i^{th} increment in years

These variables k_r, k_m and k_s are assumed to be dependent on waste composition and other environmental factors such as moisture, ambient temperature, and the depth of the landfill, while L_0 is assumed to be dependent of the waste composition. Although a multiphase model is challenging to work with, it has several advantages associated with it. Major advantages of multiphase modelling are to incorporate the degradability of waste components and waste composition while estimating the methane generation rate. Multiphase models help identifying the effect of recycling and different operational practices on landfill gas emissions.

2.6.3 CLEEN Model

Although the LandGEM model considers first-order decay constant and IPCC considers the multiphase first order, that is not the only difference between these two models. The initial lag time period before the methane generation begins is also different for these models. LandGEM assumes a lag period of 0-1 year; whereas, IPCC considers

0-6 months of initial delay before the methane generation starts. Moreover, LandGEM ignores the fugitive methane emissions, considering the efficiency of methane recovery system and methane oxidation in the landfill covers. These factors induce considerable uncertainty in landfill gas modeling. The efficiency of a model to predict methane generation from landfills depends on its input parameters (L_0 and k). Literature shows that k values depend on the waste composition, moisture and ambient temperature. However, the studies for finding k values based on waste composition, particularly with respect to moisture and ambient temperatures, have not yet been conducted. Therefore, the CLEEN model was developed considering first-order decay rate (k) constant with respect to waste composition, rainfall and temperature and also to study any interactions among these predictor variables.

$$Log_{10}k = -3.02658-0.0067282R2 + 0.069313R + 0.00172807(RxF) + 0.01046T – 0.01152F + 0.00418TX + 0.00598Y \quad \text{…….. (2.12)}$$

Where,

R = Annual Rainfall (mm/day)

T = Annual ambient temperature (K)

F = % Food in landfilled waste

TX = % Textile in landfilled waste

Y = % Yard in landfilled waste

The methane recovered from the gas collection system depends on several factors, i.e. landfill cover, permeability of cover soils, presence of preferential pathways and the operating parameters of landfill gas collection system. Therefore, the uncertainty in estimating total gas generation, gas recovery and fugitive emission still remains.

2.6.4 CALMIM Model

California Landfill Methane Inventory Model (CALMIM) model is a process-based site specific annual inventory model for methane emissions. While most methane emission models are focused on methane generation, CALMIM model is developed based on the effect of cover soil and oxidation. This model also addresses reduction in methane diffusion from the landfills and the effect of seasonal variation of moisture and temperature on methane oxidation of the cover soil.

The model was generated based on field studies from several landfills and lab scale oxidation study on different types of cover soil. It considers 1 dimensional diffusional transport of methane from the landfill surface where diffusion is dependent on concentration gradient. The model includes the weather based on solid waste information system (SWIS) database for the landfills, information on cover soil (type of cover, cover thickness, and soil type) and information on presence and efficiency of gas collection system. Finally, based on the information present the model predicts the methane emission with and without the oxidation at the cover soil.

The CALMIM model restricts the prediction of methane emission to California landfills. The model displays a warning box to the user if the landfill is not within California, showing the site was not found in the database as presented, in Figure 2.26.

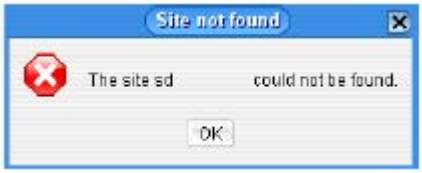

Figure 2.26 Error Message for Non-available Site in the CALMIM Database

The user is allowed to input the type of cover, thickness of soil cover and type of soil. The model also allows the user to input the qualitative coverage of vegetation and gas collection efficiency. The model auto generates the weather data based on the coordinates of the landfill location. The CALMIM input screen is presented in Figure 2.27.

Figure 2.27 CALMIM Input Screen

CALMIM is the first non-generation based landfill emission model. However, the model has several limitations as listed below:

- The model does not consider any gaseous transportation except the diffusion.
- It mainly considers the effect of cover soil or oxidation in cover on methane emissions.
- The weather input data for the model is auto-generated and is not site specific.

- The model estimates the emissions based on the user input of gas collection efficiency in the landfill, which introduces vast uncertainty in methane emissions.

2.7 Summary

The surface emission of methane gases from a landfill is considered to be a direct function of total gas generation; however, other meteorological parameters and gas recovery may also contribute to the surface emission of methane from landfills. Generated methane gases from landfills tend to migrate through the cover soils and emit to the atmosphere. While migrating through the cover, a fraction of the methane is oxidized, depending on the presence of oxygen in the cover. The oxidation reduces the emissions to the atmosphere and, for the landfills with no gas collection system, oxidation is the primary mechanism to minimize the surface methane emissions. Due to wide variation of landfill operation processes, heterogeneity of waste, and different gas transportation mechanisms, estimating the emissions from landfills is a complex process. For the past few years, there have been numerous studies on methane emission from landfills and oxidation from landfills, on effects of meteorological parameters on methane emission and oxidation and on effects of the presence of gas recovery system in the landfills. However, the major limitations of the previous studies are:

1. Several new and improved techniques were evolved in last few years to accurately estimate the methane emission from the landfills. However, flux chamber remains as the only direct estimation method of methane emissions from the landfills and has several limitations, i.e. point informative, cost-prohibitive, time consuming, and labor intensive.

2. Numerous studies were conducted on direct emission measurements from the landfill. However, most of the studies were conducted on conventional or traditional landfills without the presence of a gas collection/ recovery system.

3. Very few studies were reported in the literature on emissions from the bioreactor landfills, and none of them addressed the effect of water addition/ leachate recirculation on the methane emissions from the landfills.

4. No systematic study has been conducted to evaluate the effect of the leachate recirculation and gas collection/ extraction/ recovery on greenhouse gas emissions from the landfills.

5. Several generation-based emission models were present, and only one methane emission model was available to date, which was developed primarily for considering the soil oxidation behavior. However, the model auto-generates the weather data and is not site specific. Additionally the model estimates the emissions based on the user input of gas collection efficiency (between 0 to 100%), which introduces vast uncertainty in methane emission estimation. Consequently, estimating the collection efficiency based on the predicted methane emissions from this model would be misleading.

With an increasing concern of greenhouse gases' contribution to the global warming, it is of utmost importance to evaluate the effect of bioreactor/ ELR operation and gas collection/ recovery on greenhouse gas emissions from landfills.

Chapter 3

Methodology

3.1 Introduction

In this chapter, the experimental design of the study is presented at the beginning, followed by the selection of the study area. Brief descriptions are provided of the methane emission monitoring methodologies. A comparatively new method, portable flame ionization detector (FID), was used to determine the methane emissions from the field, accompanied by the traditional flux chamber method. Therefore, a detail description of the portable FID is presented in this chapter. Further descriptions are included on the cover soil properties and methane oxidation capacity of the cover soil. Methods of monitoring the climatological and operational parameters, i.e. the gas recovery and leachate recirculation monitoring details, are also presented in the subsections of 3.5. Finally, development of a MLR model is discussed for the methane emissions from the landfill.

3.2 Investigation Program Overview

The experimental program includes field and laboratory investigation on methane emissions, oxidation and gas recovery from the landfill.

The field investigation section consists of emissions monitoring, using portable FID and flux chamber, and the gas extraction from the gas wells installed in the landfill. During the field investigation, the temperature, wind speed and wind direction were also monitored in the landfill. The soil samples were collected from the cover of the landfill and tested in the laboratory to determine the soil properties and the moisture content of the cover. Three sets of oxidation pipes were installed in the landfill cover (each set includes two oxidation pipes, with one was installed at 2 ft depth and another at 1ft) to measure

the methane concentrations at different depths and to evaluate the methane oxidation in the cover. In addition, temperature probes were installed in the landfill cover to evaluate the soil temperature variations in the cover soil during the investigation.

The laboratory investigation section includes the batch experiments (laboratory incubation tests) for determining the oxidation capacity of collected cover soil from the landfill, as discussed in section 3.5.3. Tests were conducted in controlled temperatures and different moisture contents of the collected cover soil.

The experimental program also includes the gas extraction and leachate recirculation operations to address the effect of ELR operation and gas recovery in methane emission from landfills.

Table 3.1 presents an overview of the experimental program of study as below.

Table 3.1 Experimental Program

Test	Sample	Field/ Lab	Equipment Used	Remarks
Methane Emissions	Methane from Landfill Surface	Field	**Flux chamber, manufactured in the laboratory; portable FID (model: Trimble site FID, Manufactured by: Trimble)	**Flux chamber built in UTA following the EPA requirements
		Lab	Gas Chromatograph (model: SRI GC 8610c, manufactured by: SRI Inc.),	
Gas Recovery/ Extraction Data	Landfill Gas	Field	LandTEC GEM 2000 plus (manufactured by: LandTEC Inc.)	--
Water/Leachate addition	--	Field	--	Data Collected from landfill personnel
Temperature	--	Field	Digital Thermometer (model: 800061, 800023 , Manufactured by: Sper scientific)	--
Precipitation	--	Field	Rain Gauge	Data Collected from KDTO weather station
Soil Classifications	Cover Soil	Lab	Casagrande apparatus, US standard sieves	--
Methane Oxidation	Landfill Gas from different depths of Cover, Cover soil	Field		
		Lab	LandTEC GEM 2000 plus, manufactured by: LandTEC Inc.; Gas Chromatograph (model: SRI GC 8610c, manufactured by: SRI Inc.)	--

**The Flux chamber was designed and built in the University of Texas at Arlington. The design of the flux chamber followed the current EPA guidelines. However, the proposed flux chamber design in EPA was a dynamic flux chamber and the flux chamber for the study was designed for steady flux chamber operations without the flow of the carrier gas into the chamber.

61

3.3 Selection of Field Investigation Area

The City of Denton landfill is located on the southeast side of Denton, Texas. The aerial view of the city of Denton Landfill is presented in Figure 3.1.

Figure 3.1 City of Denton Landfill Layout

The landfill was built in 1983 and received its permit to begin accepting waste on March 7, 1983 (permit# 1590). Cell 1590 (also known as cell 0) was a pre subtitle D landfill which initially started with a 32 acre footprint. The landfill was extended in 1998 and the original permit was later modified to 1590 A. The extended landfill covers an area of 252 acres, with 152 acres for waste and 100 acres for offices, buffer zone, compost and some rented lands. The City of Denton landfill currently receives approximately 550 tons of municipal solid waste (MSW) a day, with 80% commercial waste and 20% residential waste. The landfill is a Type I landfill, which means that it is a standard landfill

for disposal of MSW. The landfill follows operational rules cited in the 30 TAC 330 Subchapter D, which is provided by the Texas Administrative Code.

At present, there are six cells (cell 1, cell 2, cell 3, cell 4, cell 5 and cell 6) in the landfill excluding the initial cell, cell 1590 A (cell 0). The landfill operators recently installed an intermediate cover on cell 3, and cell 4 is currently accepting the daily waste stream of the fresh MSW. The landfill modified its permit in May 2009 to operate as an enhanced leachate recirculated (ELR) landfill. ELR operation allows injecting water/ leachate to the landfill facility and converts it into an energy recovery facility. The injection of additional liquid enhances the degradation of the waste and generates a large amount of gas in short period of time. Although cell 0 and cell 1 are still operated as a traditional or conventional landfill, cell 2 has operated as an ELR landfill since 2009.The future cells (cell 3, 4, 5 and 6) will also be operated as ELR operated cells.

The Cell 2 (ELR-operated landfill cell) covers an approximate area of 2000 ft. x 700 ft. The approximate height of the cell is 60 ft., with 2 ft. of intermediate soil cover. Cell 2 accepted waste from 2001 to 2009, and the daily waste acceptance was approximately 500 tons.There are 36 horizontal pipes for leachate injection/ recirculation to the landfill cell. In addition, Cell 2 has both vertical (25) and horizontal (36) gas wells to collect the generated gas from the cell.

On the other hand, cell 0 (traditionally operated landfill cell) has an approximate area of 1000 ft. x 1400 ft. with an approximate height of 60 ft. Cell 0 was active from 1984 to 2001 and accepted 300 tons of waste daily for six days a week. Cell 0 has a 10 ft thick soil cover on its top, and near the surface, the thickness of cover soil varies up to 15 ft (Samir, 2011). A total of thirty vertical gas wells are installed in cell 0 for gas collection/ recovery.

The site information and layout for cell 0 and cell 2 are presented in Table 3.2 and Figure 3.2.

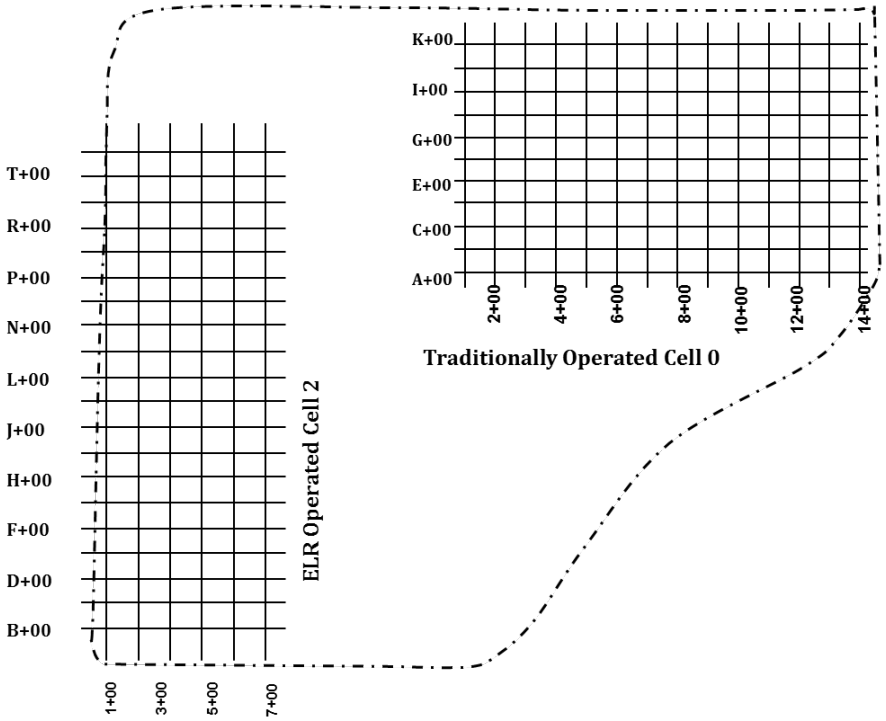

Figure 3.2 City of Denton Landfill Layouts and Area of Interest: Cell 2 and Cell 0

Table 3.2 Landfill Site Information

Location	**Cell 2**	**Cell 0**
Operational Practice	Bioreactor/ ELR	Traditional
Cover System	Intermediate	Intermediate
Cover Thickness	2 ft.	10 ft.
Cover Soil	CL	CL
Gas Collection System	Yes	Yes
No of Gas Wells	H: 35; V: 25	H: 0; V: 30
Total Area covered	2000 ft. x 700 ft.	1000 ft. x 1500 ft.
Data Collection Grids	100 ft. x 100 ft.	100 ft. x 100 ft.
Interval of Data Recording	50 ft.	50 ft.
Total No. of Data Points	560	600

3.4 Methane Emissions

Methane emissions were primarily measured using a portable flame ionization detector (FID) in the field. However, portable FID is an indirect method of measuring emissions and does not provide information on methane flux. Therefore, static flux chambers were also used in the landfill to supplement the portable FID results. The following sections present the flux chamber method and the portable method to measure methane emissions from the landfill.

3.4.1 Flux Chamber Method

A static flux chamber technique was used to measure methane fluxes. A total of four flux chambers were built in the UTA machine shop, using an acrylic dome and acrylic cylinder, in accordance with the EPA (2004) guidelines. During each measurement, the flux chamber was placed on the ground and a small amount of wet sand was applied at the soil-chamber interface to provide an adequate seal. Four locations were randomly selected from four different sections of the landfill cell. Three of the locations were from the flat surface of the three different zones (zone 1, zone 2 and zone 3 as presented in section 4.4.1.2) and one from the slope near pipe location O2 as presented in section 3.5.3.1. Samples were collected every month from these four locations for 14 months. The chamber surface area and volume were 0.13 m^2 and 30 L, respectively. Three to five headspace samples were collected from the enclosed static chamber at different times in 0.5 L teddlar bags through active sampling with a SKC grab air bag sampler pump (Cat. No.222-2301). Collected samples were analyzed within 48 hours of collection using a gas chromatograph (GC) (model: 8610 C, column: Haysep D, Temperature: 40°C) with flame ionization detector in the laboratory. Fluxes were calculated from change in concentration with time (dc/dt) and integrated in the following equation to estimate methane flux from

the location. The slope of the time vs. concentration is combined in the following equation (equation 3.1) to calculate the flux (Abichou et al., 2006).

$$F = PVMU\,(dc/dt)/\,(ATR) \quad (3.1)$$

Where,

F= Methane Flux ($g/m^2/day$)

P= Atmospheric Pressure =1 atm

V = Volume of the Flux Chamber = 30 L

M = Molecular Weight of Methane = 16 g/mol

U= Unit Conversion Factor = 0.001446 L/min/µLd

A= Area Covered by the Chamber = 0.13 m^2

T= Chamber Temperature = Air Temperature in Kelvin

R= Gas Constant = 0.08205 L.atm/(mol*K)

Figure 3.3 and Figure 3.4 presents sampling and analysis of surface methane gas using static flux chamber and a typical time vs. concentration plot.

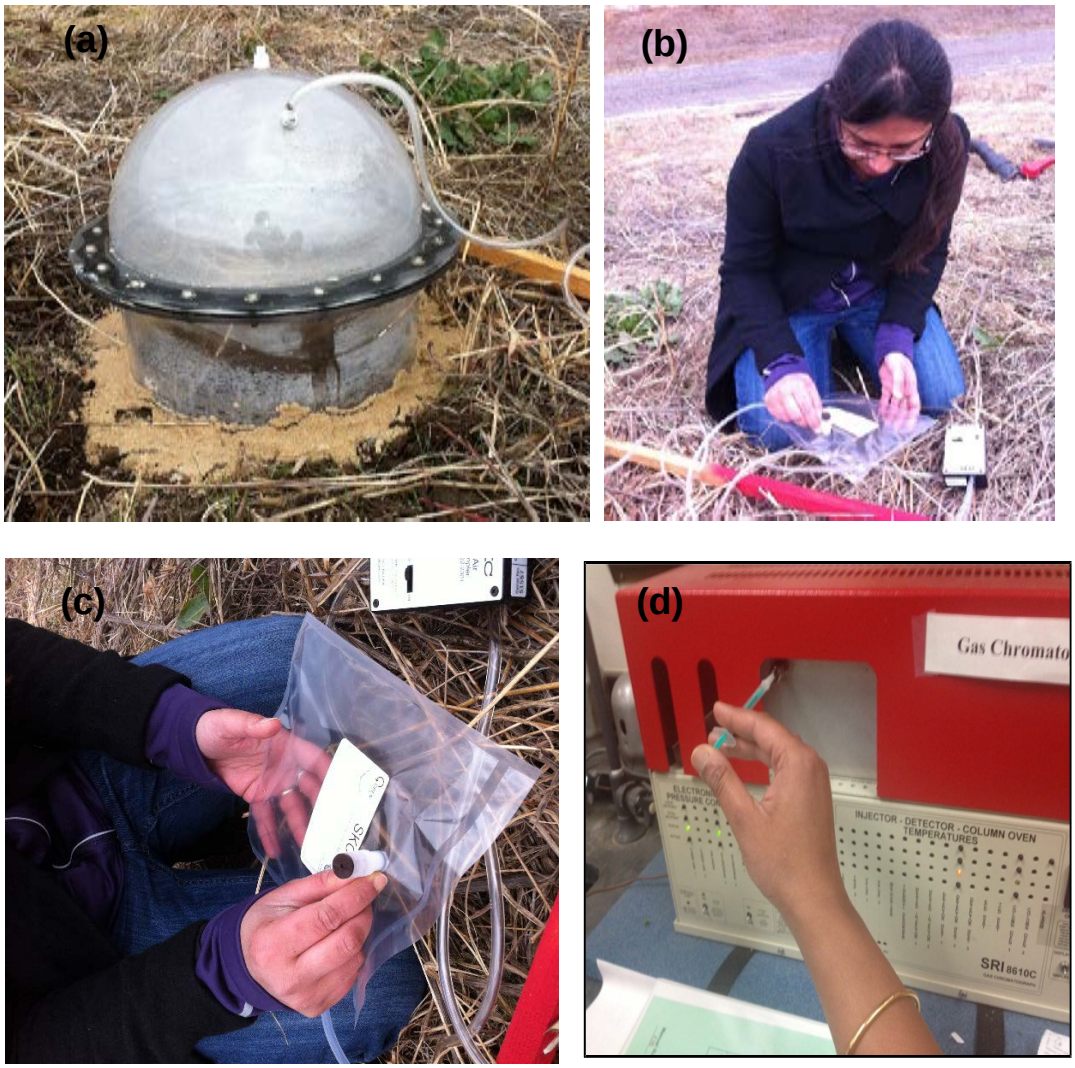

Figure 3.3 Flux Chamber Sampling and Determination of Concentration with G: (a) Flux Chamber Sealed with with Wet Sand, (b) Connecting Teddlar Bags to the Flux Chamber to Collect Samples, (c) Taking Sample from the Flux Chamber with a Suction Pump, (d) Testing the Collected Gas Sample in GC

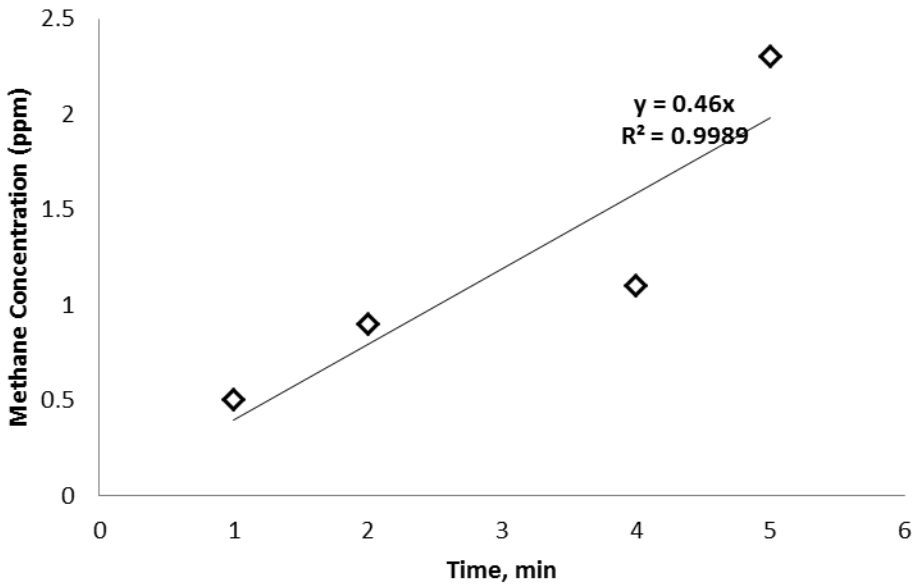

Figure 3.4 Typical Time vs. Concentration Plot

3.4.2 Flame Ionization Detector (FID)

Initially, a 100' x 100' sampling grid was established in the study area depending on the survey grid lines in the landfill. Surveying poles were used to maintain grid spacing, and the readings were taken at approximately 50 ft spacing. A portable flame ionization detector (Trimble site FID) was used to study the fugitive emission of methane from the landfill surface, as presented in Figure 3.5.

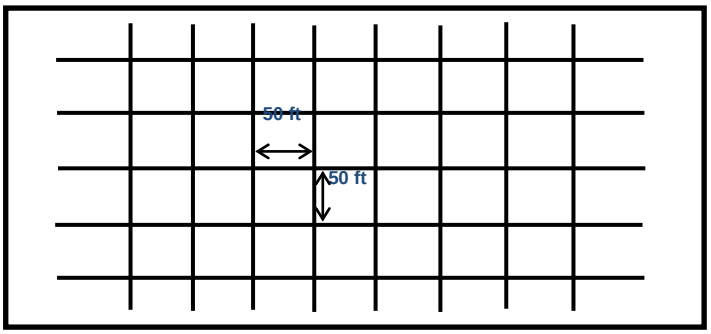

(a)

(b)

(c)

Figure 3.5 Surface Emission Measurements with Portable FID: (a) Data Collection Grids, (b) Portable FID, (c) Data Collection with the Portable FID

The detector is used to measure, display, and record the concentration of methane in the air that is ionized by the flame ionization detector at parts per million (ppm) or parts per billion (ppb) levels. When the site FID detector is in “flamed on” mode, the internal pump starts to draw air from the atmosphere to the detector inlet. With the presence of the correct ratio of hydrogen to air, the combustion chamber starts the “flame on” mode. The combustible organic compounds present in the sample are ionized by the flame while the air samples pass through the flame. The ionized particles are subjected to continuous electric field, and with the ions moving to the electric field, the ions start generating currents which are proportional to the concentration of the ionized molecules in the ionization chamber. An electrometer circuit converts the current to a voltage that is then fed to the microprocessor. The processor records the concentration with the geographical co-ordinate assessed from the built in GPS in the equipment. For the portable FID, the operating temperature ranges between 32°F (0°C) to 122°F (50°C) and operating concentration ranges between 0.1 to 50,000 ppm.

The equipment was calibrated with 0 ppm concentration of CH_4 and 500 ppm concentration CH_4 before taking the field measurements. The calibration procedure includes the precision measurement, as well as precision timing for calibration. Three (3) calibrations are required for precision in measurement, and two (2) calibrations are required for precision time measurement. The acceptable range of error for precision measurement is ±3% and for precision time less than or equal to three (3) seconds.

Emissions were recorded within 15 cm (5in) above the ground level with a handheld sensor, and data was recorded in a microprocessor connected with the portable FID via Bluetooth.

3.4.2.1 Plotting Emission Data with Surfer

The collected data was plotted with the mapping software Surfer by the linear Kriging method due to high variability in the study area and high sampling numbers. The general formula for the linear kriging method is formed as a weighted sum of the data, as presented in equation 3.2.

$$Z(s_0) = \sum \lambda_i Z(s_i) \quad \text{..... (3.2)}$$

Where,

$Z(s_i)$ = the measured value at the i^{th} location

λ_i = an unknown weight for the measured value at the i^{th} location

s_0 = the prediction location

N = the number of measured value

The weight, λ_i, depends solely on the distance to the predicted location. However, with the kriging method, the weights are not only based on the distance between the measured points and the predicted location but also on the overall spatial arrangement of the measured points. To use the spatial arrangement in the weights, the spatial autocorrelation must be quantified. Thus, in ordinary kriging, the weight, λi, depends on a fitted model to the measured points, the distance to the predicted location, and the spatial relationships among the measured values around the predicted location.

3.4.2.2 Validation of FID with Laboratory GC Analysis

The surface concentration of methane reported from the portable FID was validated using a laboratory gas chromatograph (GC) with flame ionization detector (SRI model 8610 C). Gas samples were collected in Tedlar bags using static flux chamber. The static flux chamber was placed in locations with known concentrations (known from

the FID results) for 30 minutes, and gas samples were collected using the active gas sampling method. These samples were tested using a GC within 24 hours to determine the concentration of methane in the laboratory, as presented in Figure 3.6.

(a) (b)

Figure 3.6 (a) Flux Chamber Sampling; (b) Determination of Concentration in the Laboratory with GC

The methane concentration results from laboratory GC and portable FID are summarized in Table 3.3 and Figure 3.7. Five gas samples were tested from different locations, and the concentrations were recorded from the portable FID in the field. The samples were then tested in the laboratory to determine the methane concentration using a gas chromatograph. Based on the results, the portable FID provides the methane concentrations in field within ±10% of GC.

3.5 Monitoring and Operational Parameters and their Impact on Emissions

This section describes the methods and equipment to measure the climatological and operational parameters that might affect the landfill gas emissions. The section is divided into three subsections: (1) the first subsection includes the climatological parameters; (2) second section covers operational parameters that were measured

during the investigation; and (3) the last subsection includes the laboratory investigation method for evaluating the maximum oxidation capacity of the cover soil present in the area of investigation.

Table 3.3 Portable FID Concentration Results Validation using Laboratory Gas Chromatograph

Sample	Concentration from GC (ppm)	Concentration from FID (ppm)
1	69.03	67.7
2	47.09	53.1
3	70.99	78.0
4	323.57	282.6
5	898.65	906.9

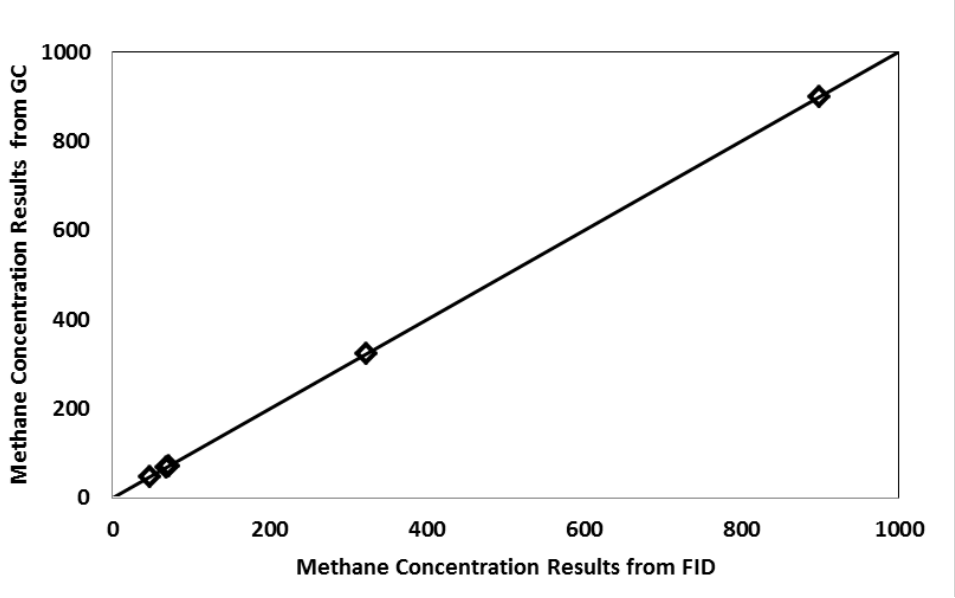

Figure 3.7 Methane Concentration Results from GC vs. Methane Concentration Results from FID

3.5.1 Climatological Parameters

Methane emission from the landfill surface is substantially affected by the climatological condition of the site. Emission has been reported to be affected by the air/ soil temperature, soil moisture, wind speed, barometric pressure and so on. Therefore, for the current study the climatological parameters specifically the air and soil temperature, and precipitation data were monitored throughout the study period.

3.5.1.1 Air Temperature

Air temperature was monitored using a portable weather station (WS-108) as illustrated in Figure 3.8. The portable weather station also measured the barometric pressure data.

3.5.1.2 Soil Temperature

Soil temperature was monitored using temperature probes (Sper scientific Type K thermocouple probe; model no. 800061) and a digital thermometer (Sper scientific 4 channel thermometer; model no. 800023) as shown in Figure 3.9 and Figure 3.10.

Temperature thermocouple probes were installed in three different locations at 1 ft. and 2 ft. depths, respectively, to monitor the soil temperature variation within the cover soil. The locations and installation of the temperature probes are illustrated in Figure 3.11.

Figure 3.8 Portable Weather Stations (WS-108) for Measuring Air Temperature and Barometric Pressure

Figure 3.9 Type K Thermocouple Probe for Temperature Monitoring

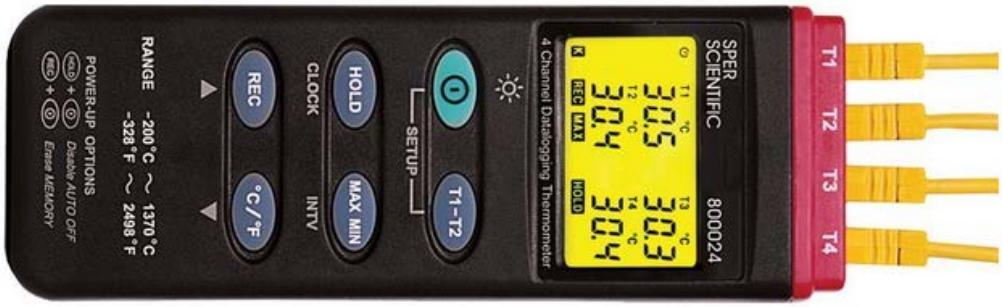

Figure 3.10 Four (4) Channel Digital Thermometer for Temperature Monitoring

Figure 3.11 Locations, Installation and Monitoring of Soil Temperature at the Cover

3.5.1.3 Precipitation

Precipitation data was obtained from the rain gauge readings of nearby KDTO weather stations of the selected study area.

3.5.1.4 Wind Speed and Direction

Wind Speed and direction were recorded during the emission monitoring in the field using an anemometer (WM-2) as illustrated in Figure 3.12.

Figure 3.12 Anemometer for Monitoring Wind Speed and Direction in the Landfill

3.5.2 Operational Parameters

Landfill cover system influences the growth of the microbes in the soil and consequently is anticipated to mitigate the migration of the generated landfill gas in some extent. The predominant measures to mitigate landfill emissions from the landfill also include the presence of gas extraction/ recovery in the landfill. On the contrary, the higher gas generation from the landfill due to ELR operation might also increase the emissions from the landfills. The objective of the current investigation is to address the effect of ELR operation and also the gas extraction from the landfills. The following subsections include the methods to measure the leachate recirculation and gas extraction in the landfill.

3.5.2.1 Landfill Cover System

The current study investigates the greenhouse gas emission from both cell 0 and cell 2, as discussed in the earlier sections. Cell 2, which was operated as an ELR cell, was a subtitle D landfill with 2 ft thick intermediate clay cover. On the other hand, cell 0, which is operated as a traditional landfill, had thick clay covers (10 ft to 15 ft) on top to minimize the infiltration from the rain. The cover soil properties for both cell 2 and cell 0 was similar since on-site soil was used as cover materials. However, mulch or compost cover was used on top of the landfill cover on both of the cells. Cell 2 had only 2 in mulch on top whereas cell 0 had a 1 foot thick mulch cover.

Figure 3.13 illustrates the cross section of the cover soil system for cell 2 (ELR landfill cell) and cell 0 (traditional landfill cell).

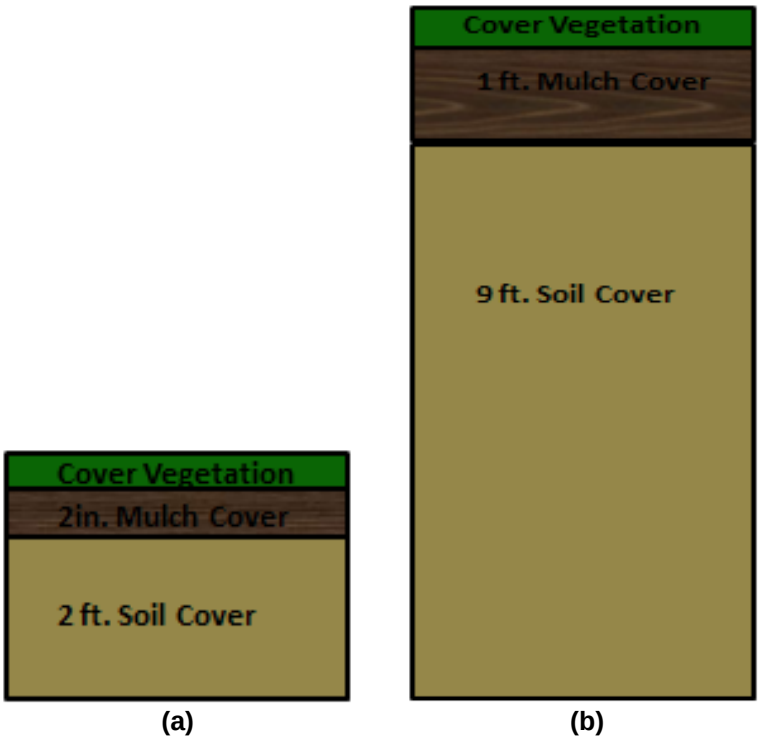

Figure 3.13 Cover Soil Systems for (a) Cell 2, and (b) Cell 0

A summary of laboratory tests for geotechnical properties of soil is presented in Table 3.4.

3.5.2.1.1 Cover Soil Properties

Soil test borings were conducted twice, using hand augers from three different locations in cell 2. Soil samples were collected from a total of six borings, two from each location at 1 ft and 2 ft depths. However, to monitor the moisture content, soil samples were collected twice more near the surface from 3 locations.

Table 3.4 Laboratory Testing for Geotechnical Properties of Soil

Test	Material	Frequency of Sample Collection	No of Sample each time	No. of Tests
Liquid Limit	Soil	2 times	3x2=6	6x2x3 = 24
Plastic Limit	Soil	2 times	3x2=6	6x2x3 = 24
Sieve Analysis	Soil	2 times	3x2=6	6x2 = 12
Organic Content	Soil	2 times	3x2=6	6x2 = 12
Moisture Content	Soil	2 times from Boring	3x2=6	6x2+3x2= 18
		3 times from surface	3x1=3	

(i) Sieve Analysis

Sieve analyses were conducted on the collected samples in the laboratory according to ASTM standard D422 for the current study. The tests were carried out using 300 gm of oven dried samples to determine the particle size distribution. The grain size distribution was conducted using a set of US standard sieves (No. 4, 8, 16, 30, 50, 100, 200 and pan). A lid was also placed at the top to provide cover of the sample. The weight of each sieve was determined individually, and the weight of the sieves was recorded before and after shaking. Wet washing was conducted to prevent aggregation of large clumps of fine particles in soil samples retained on sieve No. 200. A bowl was placed under the sieve. Washing of the sample was continued until clean water was coming out. The remaining sample was dried in the oven and its weight was measured.

(ii) Liquid Limit and Plastic Limit

To obtain Liquid limit and Plastic limit of the soil samples, ASTM standard D4318 method- A was adopted. Soil Samples passing through a No. 40 sieve were used in the test. Moisture cans were labeled, and their individual mass was recorded. Casagrande's

Liquid limit device and the grooving tool were cleaned, and the fall height (1 cm) of the cup was adjusted. Appropriately, 250 gm soil samples were put into a bowl and mixed with water. A water content of 25% was considered in the first trial. After addition of water, the soil sample was chopped, stirred and kneaded repeatedly. A portion of the soil was placed in the device. A groove was cut at the center of the placed soil in the device. The cup of the device was lifted and dropped by a rate of 2 drops/second. The process was continued until the groove was closed, around 13 mm. The test was repeated three times to plot the number of blow against moisture content. Liquid limit was the moisture content corresponding to 25 blows on the straight line. For Plastic limit, soil samples were separated in the plate. Ellipsoidal soil masses were formed by adding water. Soil masses were rolled in the glass plate until they became threads of about 3 mm. When the threads were broken at 3 mm diameter, they were put into the moisture cans. Samples were dried in the oven and moisture contents were determined.

(iii) Moisture Content

The moisture content of the soil is an indicator of the amount of water present in soil. Moisture content is the ratio of the mass of water in a sample to the mass of solids in that sample as expressed in equation 3.1:

$$w = M_w / M_s \times 100 \quad \text{(3.1)}$$

Where,

w= moisture content of soil (expressed as percentage)

M_w=mass of water in the soil sample

M_s=mass of soil solids present in soil sample

The moisture content of the soil samples was determined on a dry weight basis according to test method A of ASTM D2974-07a in Standard Methods (ASTM, 2007). Approximately 200 gm of soil was dried in an oven at 105 ºC for 24 hours until a constant weight was achieved.

(iv) Organic Content

Organic content of the soil is an indication of the presence of organic fractions in the soil. The percentage of organic content is important to classifying peat or other organic soil and for general classification purposes.

Organic content, also known as volatile solids (VS), was determined for the collected boring soil samples according to test method C of ASTM D2974-07a in Standard Methods (ASTM, 2007). Soil samples were initially dried at 105ºC before igniting the samples in a muffle furnace at a temperature of 550ºC. Approximately 50 grams of the dried sample was ignited for one hour until a constant weight was achieved. The percent of weight lost on ignition is the organic content.

3.5.2.2 Landfill Gas Collection/ Recovery

The City of Denton monitors the gas concentration data and gas flow data from the individual gas wells on a monthly basis. For the current research purpose, gas recovery or gas collection applied suction to recover gas and gas flow data was collected from City of Denton personnel. Gas recovery or gas collection data was monitored using a Landtec GEM 2000 plus that measures the percentage concentration of methane, carbon-dioxide, oxygen and NMOC in the collected gas and also records the gas flow. Figure 3.14 illustrates the monitoring of gas flow rate and composition measurement in the field.

Figure 3.14 Gas Collection Pipe, Flow Measurement and Landtec GEM

3.5.2.3 Monitor Leachate Recirculation

Leachate injection/ recirculation data was obtained from the City of Denton personnel. The information on leachate injection was provided based on total recirculation on individual wells in daily basis. Figure 3.15 presents the interconnected leachate recirculation pipes in the landfill.

Figure 3.15 Interconnected Leachate Recirculation Pipes in the City of Denton Landfill

Figure 3.16 and Figure 3.17 illustrate the leachate recirculation per year and total leachate recirculation in cell 2 through individual pipes.

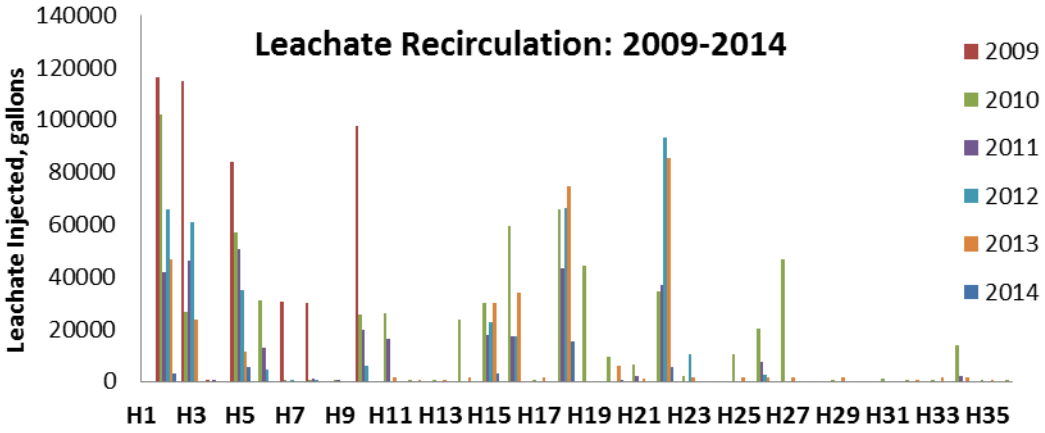

Figure 3.16 Leachate Recirculation through Individual Pipes from 2009-2014

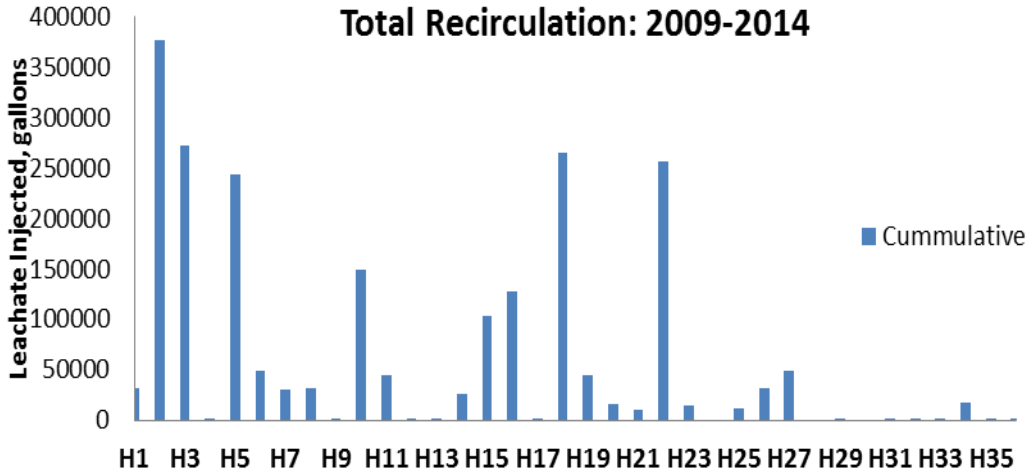

Figure 3.17 Total Leachate Recirculation through Individual Pipes

Table 3.5 Leachate Recirculation in Cell 2 through the Major Pipes (gallons)

	H2	H3	H5	H9	H16	H18	H22
May-09	7508	2387	-	-	-	-	-
Jun-09	-	-	-	-	-	-	-
Jul-09	14061	10145	16242	-	-	-	-
Aug-09	10154	10007	9903	-	-	-	-
Sep-09	10082	5518	5095	-	-	-	-
Oct-09	36204	34327	19114	-	-	-	-
Nov-09	20034	37417	27886	-	-	-	-
Dec-09	18247	14936	5678	-	-	-	-
Jan-10	1396	-	10752	567	-	-	-
Feb-10	22944	-	8505	-	34896	25978	-
Mar-10	24076	-	8944	-	16689	-	-
Apr-10	7846	9813	6995	-	2979	5149	-
May-10	11694	2498	2813	-	-	3012	-
Jun-10	8268	-	-	-	2705	2633	-
Jul-10	7553	2573	6440	-	2332	9006	15028
Aug-10	6149	-	-	-	-	-	-
Sep-10	-	2745	4102	-	-	14045	11210
Oct-10	5291	1990	-	-	-	6021	-
Nov-10	7003	7070	8640	-	-	-	-
Dec-10	-	-	-	-	-	-	8355
Jan-11	-	-	-	-	4450	8375	-
Feb-11	11007	-	-	-	-	-	-
Mar-11	-	9119	7762	-	-	-	-
Apr-11	-	-	-	-	-	-	8500
May-11	-	-	-	-	10660	7000	-
Jun-11	6700	9650	12642	-	-	-	7105
Jul-11	7010	-	-	-	-	5005	-
Aug-11	-	-	-	-	1735	-	-
Sep-11	-	9975	-	-	-	-	-
Oct-11	11761	-	9742	-	-	-	-
Nov-11	-	-	-	-	-	-	10507
Dec-11	5480	17442	20340	136	460	22864	10899
Jan-12	9155	15475	5660	-	-	22740	21045
Feb-12	16196	25578	-	-	3940	20365	20689
Mar-12	14739	12305	13588	-	-	7982	18389

Table 3.5-Continued

	H2	H3	H5	H9	H16	H18	H22
Apr-12	8590	-	-	-	6750	-	10405
May-12	-	-	-	-	-	-	10350
Jun-12	9030	1210	-	-	5440	6770	-
Jul-12	-	-	-	-	-	-	9610
Aug-12	3530	-	-	-	930	4960	2920
Sep-12	4590	6210	-	-	-	-	-
Oct-12	-	-		-	-	-	-
Nov-12	-	-	15888	-	-	-	10510
Dec-12	-	-	6642	-	-	3385	0
Jan-13	7235	4075	-	-	2755	7835	9690
Feb-13	5335	12130	-	-	-	10560	9330
Mar-13	15405	0	-	-	5560	9785	7635
Apr-13	13550	2935	-	-	-	6140	6730
May-13	-	-	-	-	5660	-	-
Jun-13	-	-	6840	-	5840	5930	0
Jul-13	-	-	-	-	-	-	9220
Aug-13	-	-	-	-	-	-	-
Sep-13	-	-	-	-	-	5213	6250
Oct-13	-	-	-	-	6010	6249	4275
Nov-13	-	-	-	-	-	7950	8790
Dec-13	5400	4500	8700	-	4372	15167	23418
Jan-14	2933	0	5310	-	2330	15226	14350
Cumulative	**376156**	**272030**	**254223**	**703**	**126493**	**265345**	**275210**

3.5.3 Methane Oxidation in Soil Cover

The methane oxidation rate was determined from laboratory incubation of the cover soil collected in the field. Moreover, soil gas measurements were taken from the gas probes installed in the cover of the study area at 1 ft and 2 ft depths from three individual locations.

3.5.3.1 Soil Gas Measurements

Three different locations were selected (based on the preliminary investigation conducted in Dec'12, cell 2 was divided into three different zones; zone 1, zone 2 and

zone 3 according to their variations in emissions) in which to install the gas probes at 1 ft. and 2 ft. depths of the cover, considering the intermediate cover thickness to be approximately 2 ft. The borings were conducted using a 2.5 inch diameter hand auger. The gas probes were 2 inch diameter PVC pipes with 6 inch bottom perforation. Soil gas concentration was measured from these installed gas probes using Landtec GEM 2000 plus in the field.

Figure 3.18 presents the locations and schematic of gas pipe.

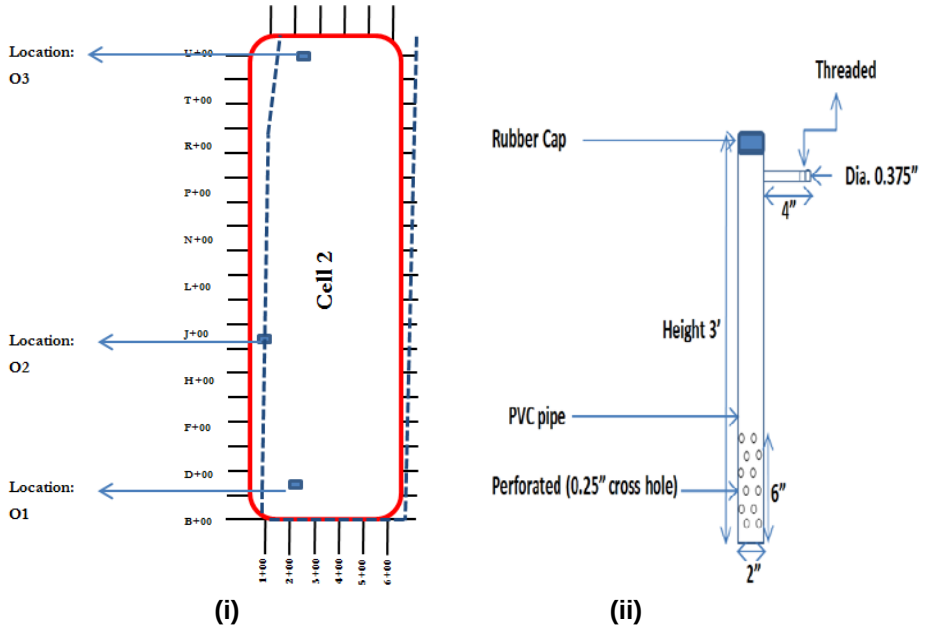

Figure 3.18 (i) Locations of Oxidation Pipes; (ii) Details of Gas Pipes

Figure 3.19 presents the installations and taking measurements in the field from the gas probes and temperature sensors.

Figure 3.19 Oxidation Pipe Installations

3.5.3.2 Batch Experiments

Methane oxidizing capacity of the cover soil was tested under controlled laboratory conditions. At one location on the landfill, a complete layer (±30cm) of the soil covering the landfill was collected. The collected soil sample was air dried, ground, mixed and sieved (200 mm) before use. In an initial experiment, the combined effect of soil temperature and moisture content on the methane oxidizing capacity was determined. In a second experiment, the effect of ammonium and moisture content was tested. Airtight bottles (180 ml), sealed with rubber septa for gas sampling, were filled with 30 gm of air dry soil and brought to moisture contents of 5, 10, 15, 20, 25 or 30% w/w (30% = WHC). To study the combined effect of temperature and water content, the soil was incubated at 5, 15, 20, 30 or 40°C temperature for all the specified moisture contents. 1 ml of methane was injected into the bottles where the soils were conditioned for 7 days at ambient methane concentrations. Gas samples were taken 0, 0.04, 0.08, 2, 4, and 6 h after methane injection. Each test was triplicated.

Figure 3.20 presents the sample preparation and test procedure for methane oxidation.

Figure 3.20 Batch Experiments/ Incubation in the Laboratory for Determining Methane Oxidation Capacity of the Soil

3.6 Developing Multiple Linear Regression Model

Using statistical software SAS, a comprehensive model was developed that incorporates abovementioned climatological and operational parameters (temperature, precipitation, leachate recirculation, gas recovery) in predicting the response variable (average methane emission from the landfill surface).

The multiple linear regression model was developed to predict methane emissions from the landfill as a function of temperature, precipitation, leachate injection and gas collection/ recovery as presented in Equation 3.3.

$$E = \beta_0 + \beta_1 T + \beta_2 W + \beta_3 G + \epsilon \qquad (3.3)$$

Where,

E = Average Methane Emission (ppm)

β_0, β_1, β_2, β_3, = Parameters to be determined through multiple linear regression, based on field data

T = Air Temperature (ºF)

W = Leachate Injected (in) + Precipitation (in)

G = Gas Collection/ Recovery (cfm)

Є = Error uncertainty, modeled as random variable.

B_s' were determined through multiple linear regressions, using data from the field measurements. Based on the data collection, the precipitation, leachate injection and the gas extraction data was available on monthly basis; whereas the temperature was recorded during the emission monitoring with the FID. However, for the model development, all the predictor variables are to be standardized. Therefore, for standardizing all the parameters for the model development, the average monthly temperature was also considered for the regression analysis.

Chapter 4

Results and Analysis

4.1 Introduction

This chapter includes the methane emission results from the field emission monitoring, using portable FID and static flux chambers. The portable FID results are measured and reported in parts per million (ppm), whereas the most conventional unit of reporting methane emissions from different sources is methane flux in $gCH_4/m^2/day$. Therefore, a correlation between the methane emission results in ppm and flux is also developed and presented in this chapter.

The methane emission results were analyzed for various spatial and temporal variations. Furthermore, the analysis was continued to determine the parameters that substantially affect the fugitive emissions from landfill surfaces. Finally, a statistical model was developed based on these parameters and is included at the end of this chapter.

4.2 Methane Emission Monitoring

Several methods are available for evaluating the methane emission monitoring from the landfill. However, most of these methods are time consuming, labor intensive and require extensive training. Therefore, a portable FID was used for the current study. The FID results were validated using a gas chromatograph in the laboratory, as discussed in section 3.4.2.2. The static flux chamber, which is the most commonly used existing method, was also used in the field, and a correlation was developed to express the FID results in terms of methane flux.

4.2.1 Emissions Using Portable FID

The baseline study for methane emissions was conducted in December 15, 2012 in cell 2. Based on the initial study conducted on the selected ELR-operated cell, designated as cell 2, the methane emissions mostly fell below 10 ppm. However, the measured methane concentration throughout the cell was highly variable and might be mostly attributed to non-homogeneity of waste and gas generation below the soil cover. Comparatively high methane concentrations were observed in a few locations designated as x, y, and z for the current study. Figure 4.1 illustrates the emission contour profile for the baseline study. The emissions are presented in ppm.

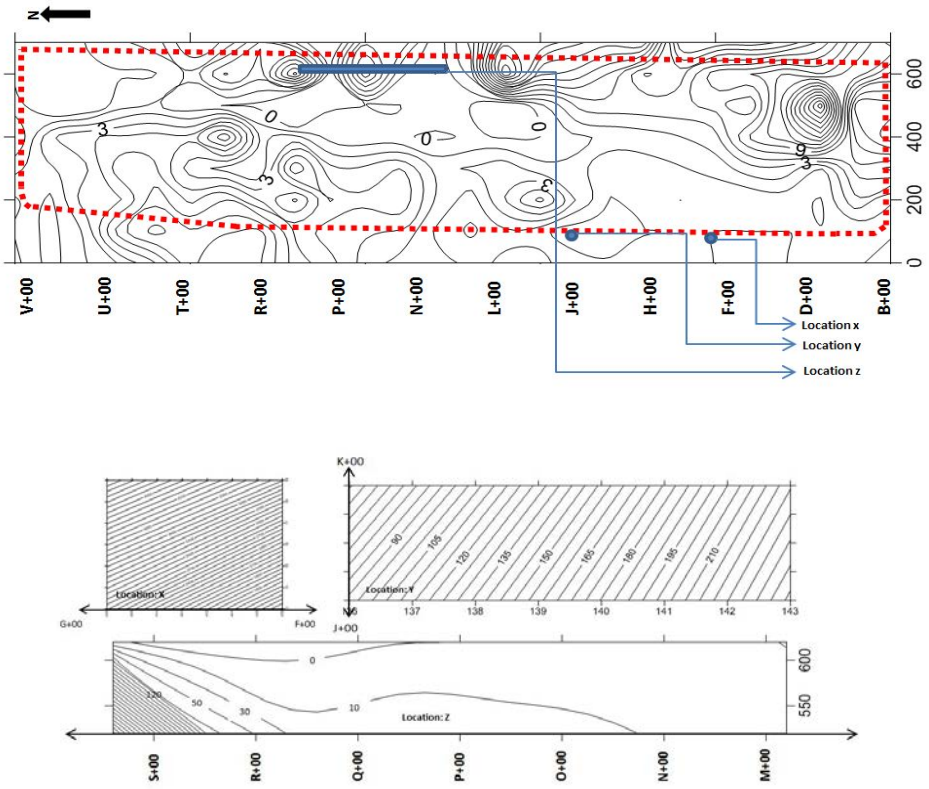

Figure 4.1 Baseline Emission Study of Cell 2 (ELR Operated Cell) Conducted in December 2012

Methane emissions at x, y and z locations were more than 50 ppm and in one of the locations it exceeded 1000 ppm of surface concentrations. Figure 4.2 presents the cross section profiles at x, y and z locations in cell 2.

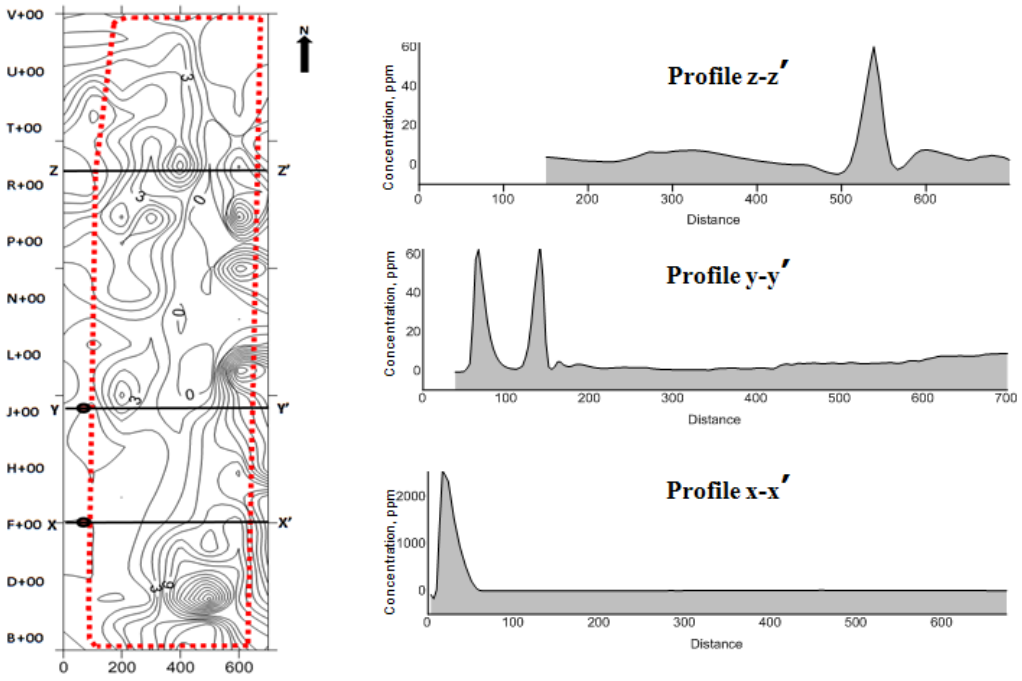

Figure 4.2 High Emission Zones ("Hot Spots") from Baseline Emission Study of Cell 2 Conducted in December 2012

Based on the figure, x-x' showed the maximum concentration of 2200 ppm, whereas the maximum emission from y-y' and z-z' was around 60 ppm. However, further monitoring of these locations in later months during the investigation period (location x, y and z) showed no signs of methane concentrations > 10 ppm, and the high methane concentrations during the baseline study can be established as a one-time event. The major difficulty with soil cover systems, as identified by Spokas et al. (2003), is that the variability of the methane emission rate cannot be captured by a single variable. Furthermore, it is highly unlikely that the exact same combination of soil temperature and

moisture will occur at the same locations of the landfill covers. The combination of soil temperature and moisture in the cover primarily influences the growth and activity of the microbial population, which is responsible for methane oxidation in the cover. The high surface methane concentrations in the baseline study might have occurred due to the lack oxidation in the soil during that specific time period. Therefore, these high concentration areas might be explained as being a result of unusual combinations of meteorological conditions at the landfill surface.

According to the U.S. EPA's (1996b) flow chart for surface emission monitoring, if a methane concentration of more than 500 ppm is observed in any location during field measurement, the concentration has to be checked again every 10 days for three consecutive months. If the same trend is observed again, then appropriate mitigating measures should be taken. If it does not reoccur, only quarterly monitoring of that location must be continued and the methane is not expected to pose any threat. At extremely high concentrations, methane is considered as an asphyxiant (a nontoxic or minimally toxic gas that displaces oxygen) and can displace oxygen in the blood. Although the Occupational Safety and Health Administration (OSHA) has no permissible exposure limit for methane, the National Institute for Occupational Safety and Health's (NIOSH) maximum recommended safe methane concentration for workers during an 8-hour period is 1,000 ppm (0.1 percent).

4.2.1.1 Emissions from Cell 2

Cell 2 was monitored for 14 months, from December 2012 to January 2014. During the investigation of cell 2, substantial variations in methane concentration were observed from the landfill cell. Figure 4.3 illustrates the variations in surface emissions.

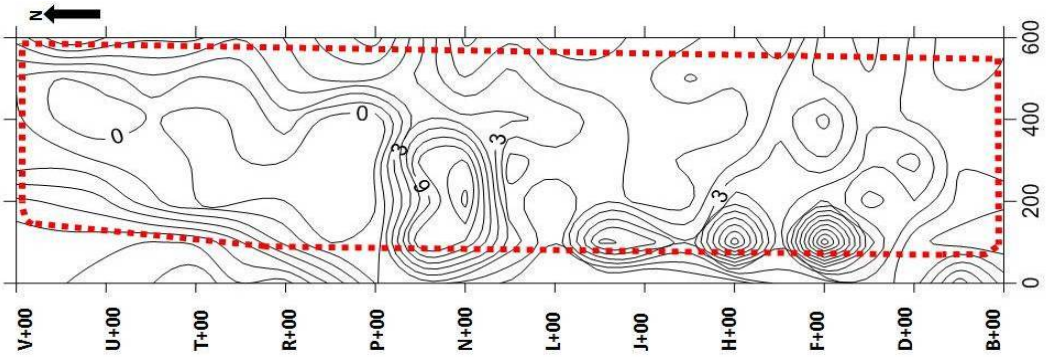

(i) Emission Contour of Cell 2 from February, 2013

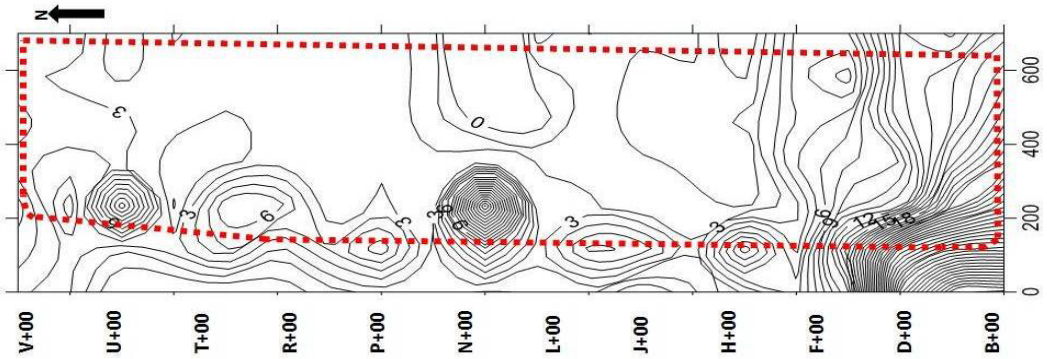

(ii) Emission Contour of Cell 2 from June, 2013

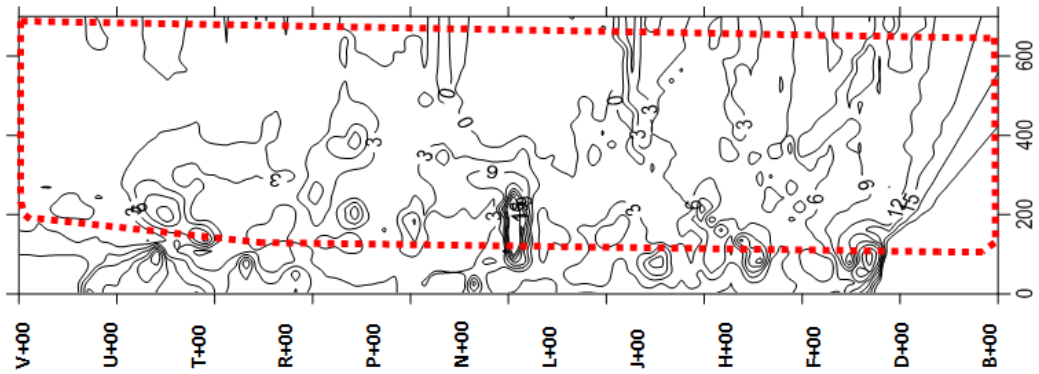

(iii) Change in Emission from February, 2013 to June, 2013

Figure 4.3 Emission Contour Profile of Cell 2 (i) from February 2013; (ii) from June 2013; and (iii) Change in Emissions from February 2013 to June 2013

Based on the figure presented above, the variation in emissions is non-uniform, and notable emissions occurred in some areas. As mentioned earlier, these spatial variations can be attributed to the variation of gas generations below the cover, which is a function of physical properties of the MSW in the landfill. However, based on the contour profiles presented, the notable emissions did not occur in the same areas during every investigation. It is to be noted that the presence of moisture influences the generation of gas underneath the intermediate cover, and due to the injection of leachate through the recirculation pipes, the moisture of the waste varies substantially in the landfill cell. In addition, the current investigation area, cell 2, had an active gas extraction system in the landfill, which may have influenced the spatial variation of emissions. Therefore, the changes in the surface methane concentration might be due to the operational practices of the landfill. The study was continued for 14 months and emissions were recorded from cell 2 once per month. The emission contours from cell 2 for the rest of the months during the investigation period are presented in Appendix A.

4.2.1.2 Emissions from Cell 0

Cell 0, which is operated as a traditional or conventional landfill cell from the City of Denton Landfill, was added to investigation plan from August, 2013. The surface emissions profiles of cell 0 for August 2013 and December 2013 are presented in Figure 4.4. The figure also includes the changes in concentration for cell 0 between August 2013 and December 2013.

The rest of emission contour profiles for cell 0 are included in Appendix B.

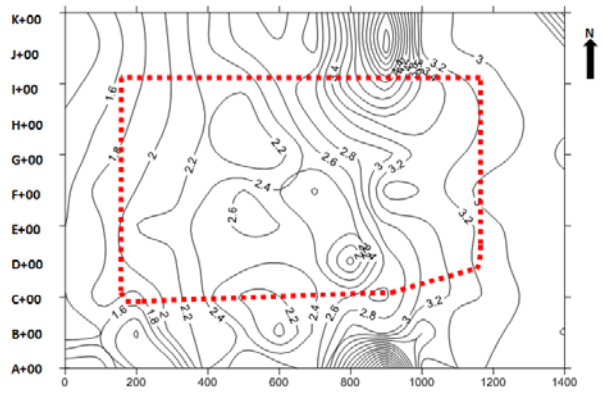

(i) Emission Contour of Cell 0 in August, 2013

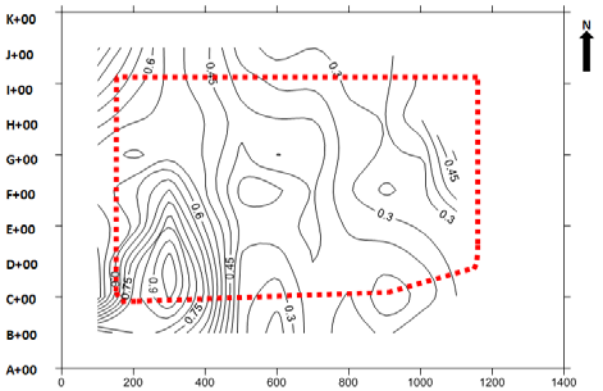

(ii) Emission Contour of Cell 0 in December, 2013

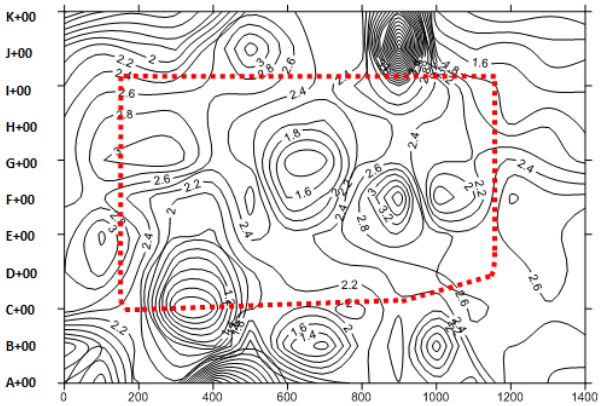

(iii) Change in Emission from August, 2013 to December, 2013

Figure 4.4 Emission Contour Profile of Cell 0 (i) from August, 2013; (ii) from December, 2013; and (iii) Change in Emission from August, 2013 to December, 2013

Based on the figure, the emission contours in cell 0 were very close. No substantial variation was observed throughout the cell. The change in concentration between August and December also reflected that the emission contours from cell 0 were fairly close. However, nominal spatial variations were observed throughout the landfill cell, which can be attributed to the non-homogeneity of the waste underneath the cover.

4.2.1.3 Comparison between the Emission Contours from Cell 2 and Cell 0

Figure 4.5 presents the emission contour profiles from cell 2 (ELR-operated cell) and cell 0 (conventional cell) for the month of August 2013.

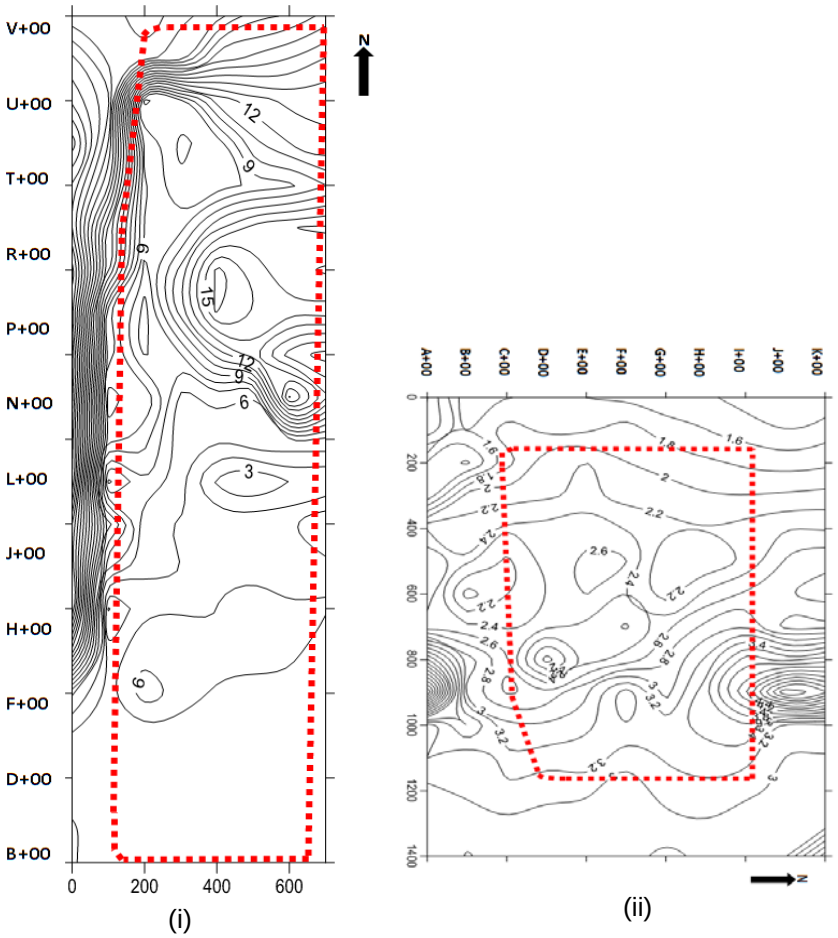

(i) (ii)

Figure 4.5 Emission Contour Profile in August (i) for Cell 2; (ii) for Cell 0

Based on the comparison from August 2013, the overall emissions from the ELR landfill cell (cell 2) were higher than the conventional cell (cell 0). This is to be expected, since cell 2 is operated as an ELR landfill, and since cell 2 received waste more recently than cell 0. In addition, higher spatial variations were observed from the ELR-operated landfill compared to the traditional landfill. It is to be noted that leachate is not added uniformly to the ELR cell; however, leachate is injected through only a few recirculation pipes in one month, and the influence of the recirculation is mostly limited to 50ft to 75 ft. around the pipe. Therefore, the higher variation throughout cell 2 might be attributed to the variations of moisture presence in the waste. In addition, the variations in emission concentrations contour in the conventional cell were very close, which substantiates the previous hypothesis.

4.2.2 Emissions using Flux Chamber

The flux chamber method is the most referred to method in literature for direct measurement of methane flux from the landfills (Abichou et al., 2006). Although the primary investigation was carried out using a portable FID, as discussed earlier, a set of static flux chambers (built in the UTA machine shop) were used to collect gas samples from the surface. Gas samples were collected from the four locations every month, as described in section 3.4.1.

The flux chamber method uses geo-statistical methods to predict the overall emissions from the landfill. Emission flux values (mass per area per time) are required for emission inventory and dispersion modeling purposes. However, the use of this geo-statistical method to predict the methane emissions is based on the point information obtained from the field measurements and can be misleading and increase the uncertainty of the emissions measurement. More recent or accurate methods have been developed for measuring the overall emission without doing point surveys. These

methods confirm that the emissions from the landfill surface are highly variable and geo-statistical methods might not be able to reflect unbiased results. The arithmetic mean estimated, based on the measured methane fluxes, may or may not be equal to the geometric mean based on the geo-statistical analysis. A dataset with high variability or without normal distribution might skew the average emission estimation from the landfill (Abichou et al., 2006).

The flux chamber samples were collected from only a few points in the landfill cell, and estimating the methane flux for overall landfill based on these limited observations would lead to non-representative or biased results. Therefore, no effort was made to estimate the overall emission based on the flux chamber results. However, the flux chamber results were used to correlate the methane concentrations obtained from the portable FID chamber results. A more in-depth discussion of the development of correlation is included in the following subsection.

4.2.3 Correlation between FID Results and Flux Chamber Results

Methane emissions from the landfill surface were measured using a portable FID and static flux chamber technique. The portable FID technique was more suitable for this research because it would provide more in-depth information than the point specific information on surface methane concentrations than the flux chamber method. However, the standard measurement of methane flux emission was also conducted and used to develop a correlation with the portable FID results. This correlation will help to express the measured methane concentration results in standard methane flux results and will result in better understanding of emissions.

The flux chamber measurements were recorded from four different locations from cell 2 in the landfill surface during each investigation. Consequently, the average

methane flux determined, based on these four locations, might be skewed; particularly, if the selected locations were emitting high methane concentrations compared to average emissions. Therefore, it was necessary to develop a correlation between the FID results and flux chamber results to determine the average methane flux measurement based on the average methane concentration (in ppm) of the whole landfill cell.

The developed correlations between FID results and flux chamber are presented in Figure 4.6.The correlations were developed based on 48 data points collected from landfill cell 2. Data was collected from flux chamber each month for 14 months. However, the dc/dt plots with less than r^2 less 0.75 were not included in the development of the correlation.

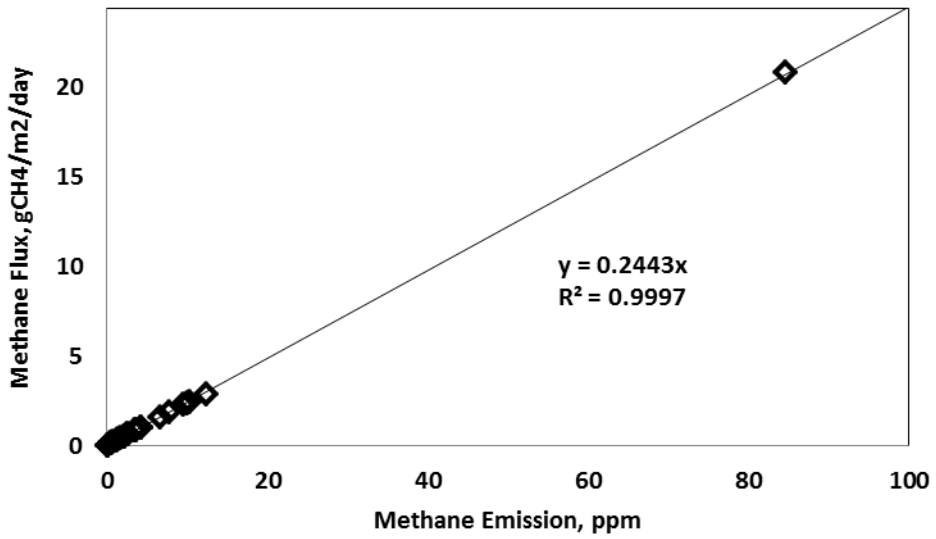

Figure 4.6 Correlations between Methane Emission Flux and Methane Concentration

Based on the correlations developed:

Methane Emission Flux ($gCH_4/m^2/day$) = 0.2443 x Methane Emission (ppm)

However, negative methane fluxes cannot be determined using the portable FID method, as the equipment does not record methane concentrations below 0 ppm. In addition, based on the correlation developed, for 0 ppm methane emissions measured using the portable FID, the methane flux will be 0 g.CH_4/m^2/day.

4.3 Spatial and Temporal Variations of Methane Emissions

Fugitive emissions were measured primarily using a portable FID from more than 1000 points on the landfill during each investigation. Methane emissions for cell 2 varied from 0 ppm to 9544.3 ppm and for cell 0 varied from 0 ppm to 47 ppm for the investigation period (from December 2012 to January 2014). The highest methane emission concentration was observed during the baseline study in cell 2 in December 2012, as previously described.

4.3.1 Slope and Surface Emission

Figure 4.7 presents the slope and surface concentrations from the ELR operated cell 2.

Based on the preliminary observations from the initial investigation conducted in December 2012, a higher methane concentration was emitted from the slopes than from the top surface of cell 2. It is to be noted that the cover soil thickness (2 ft.) for both the top surface and the slope for cell 2 was similar. On the contrary, the vegetation coverage in the top surface was sparse and discontinuous, while the vegetation throughout the slope was dense and more consistent. Vegetation in landfill covers aids in oxygen penetration into the cover soil and consequently increases the methane oxidation in the cover soil (Maurice et al., 1999).

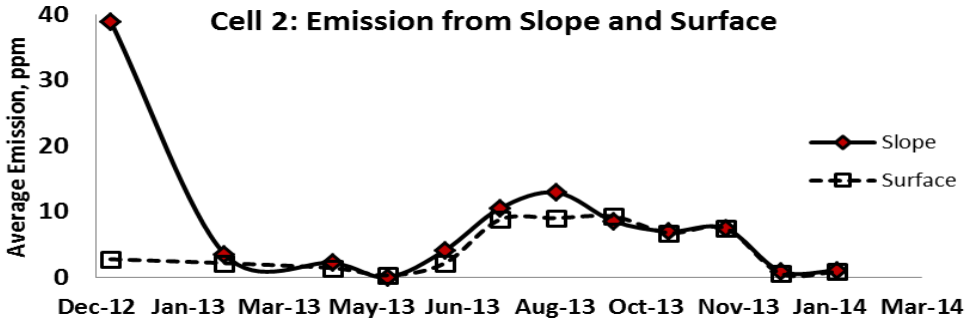

(a)

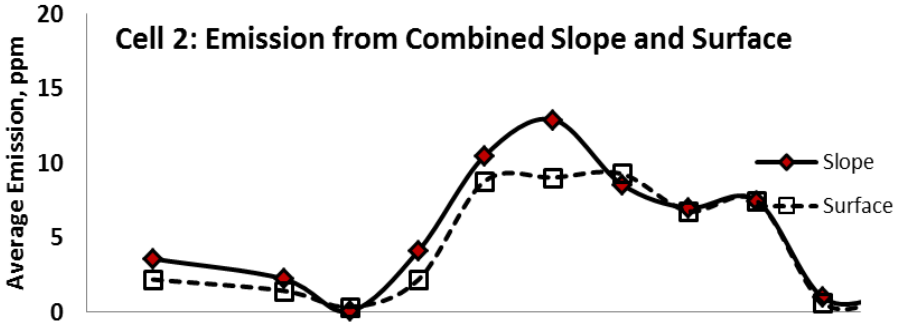

(b)

Figure 4.7 Average Methane Concentrations from the Slope and the Top Surface of Cell 2: (a) from Dec. ’12 to Jan. ’14; (b) from Feb. ’12 to Jan. ’14

Although the landfill slopes were covered with mulch and vegetation, consistently higher than average methane concentrations were observed from the slopes throughout the study except for the months of October and December in 2013. From the figure, the average concentration measured in October 2013 from the slope and the top surface of cell 2 was approximately same, and for December 2013, the average concentration from the slope was slightly less than the surface concentration. However, due to the fact that the mulch and vegetation reduce the surface concentration, the concentration from the slopes would still be higher if the cover soil vegetation was similar for the slope and the top surface.

Similarly, the average concentration from the landfill slope and top surface was compared from cell 0 which is being operated as a conventional landfill without any recirculation of water/ leachate in Figure 4.8.

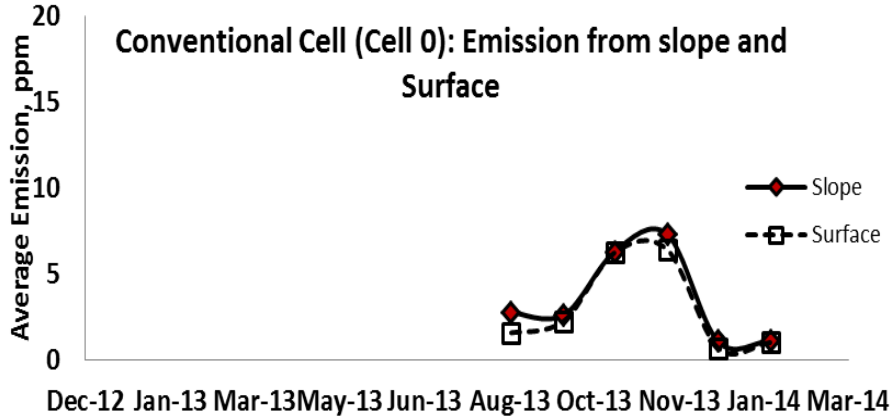

Figure 4.8 Average Methane Concentrations from the Slope and the Top Surface of Cell 2

Based on the preliminary observation, the variation between the slope and surface emission was not substantially different throughout the study period. However, the average concentrations for the slope were observed to be consistently lower than the top surface.

Figure 4.9 presents the combined comparison of slope and surface concentrations from cell 0 and cell2.

Based on the figure, the concentration from the slope was dominant for both cell 0 and cell 2. However, the difference between the slope and surface concentrations were not substantially different for cell 0.

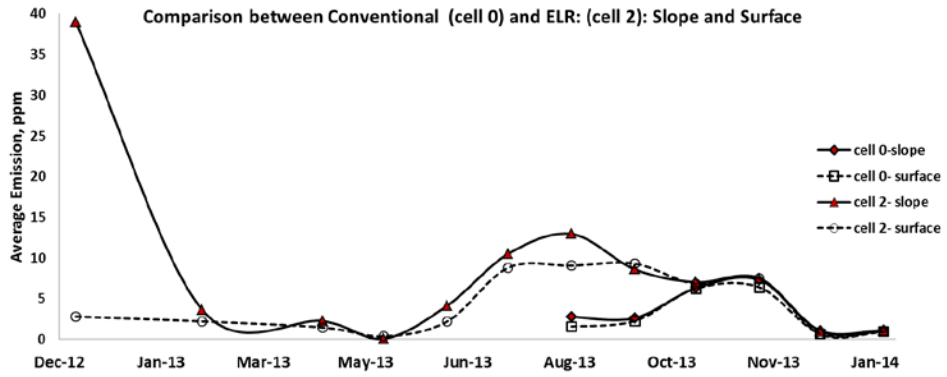

Figure 4.9 Comparisons between the Average Concentration from the Slope and Surface from Cell 0 and Cell 2

The results reported in literature on spatial variability, considering slope and flat surface were contradictory to the observations of the current study (Abichou et al., 2006). The current study concluded that methane concentration was typically lower at the side slopes compared to the flat surface on the top. However, Abichou et al. (2006) conducted the study with static flux chambers. Since this study measured a concentration and Abichou measured a flux, the difference in results is not surprising. Also, for Abichou's study, interpolation based on this point information might introduce high uncertainty to the results. In addition, based on the results reported, the results for the slope and flat areas are not compared from the same site or not recorded at the same day or time. Subsequently, several uncertainties might have been associated with the reported results, i.e. difference in waste age and comparison, difference in soil cover thickness, operational practice and climatological conditions. Therefore, the comparison based on the conducted study, the difference in site conditions and climatological conditions might have more impact on the results than the spatial variation, as reported by the authors (see Table 4.1).

Table 4.1 Comparison of Spatial Variation with Previous Study (Abichou et al., 2006)

Properties	Unit	Current Study				Previous Study (Abichou et al., 2006)			
		Cell 2		Cell 0		Site 1	Site 2	Site 3	SI-grid
Slope Aspect		Flat/ Top Surface	Slope	Flat/ Top Surface	Slope	Flat Surface	Slope	Flat Surface	Slope
Age of Waste	Year	11 to 13	11 to 13	28 to 30	28 to 30	7	14	1	7
Cover Thickness	cm	300	450	60	60	30 to 60	45	15 to 30	21 to 119
Operational Practice		ELR/ Bioreactor	ELR/ Bioreactor	Traditional	Traditional	Traditional	Traditional	Traditional	Traditional
Gas Collection System		Active Gas Collection	Active Gas Collection	Active Gas Collection	Active Gas Collection	No Gas Collection	No Gas Collection	No Gas Collection	No Gas Collection
Sampling Date		Dec'12 to Jan'14	Dec'12 to Jan'14	Aug'13 to Jan'14	Aug'13 to Jan'14	Jun'03 to Sept'03	Jun'03 to Jul'03	Jun'03 to Nov'03	Sept'03 to Feb'04
Total Number of Samples		11200	2800	2100	900	62	18	28	112
Maximum Emission	ppm	246.9	9544.3	39.0	47.0	--	--	--	--
	$g.CH_4 m^{-2} day^{-1}$	60.3	2332.9	9.5	11.5	1754.8	63.1	5212.2	342.5
Average Emission	ppm	4.3	8.1	3.0	3.5	--	--	--	--
	$g.CH_4 m^{-2} day^{-1}$	1.1	2.0	0.7	0.9	167.0	8.6	87.0	24.5

105

4.3.2 Diurnal Variation

The change in average methane concentration was measured hourly for one day, from 9.00 am to 4.00 pm. Since, the temperature rises as the day moves on, from morning until afternoon, it is anticipated that the average concentration will also increase. Figure 4.10 presents the variation of concentration with time.

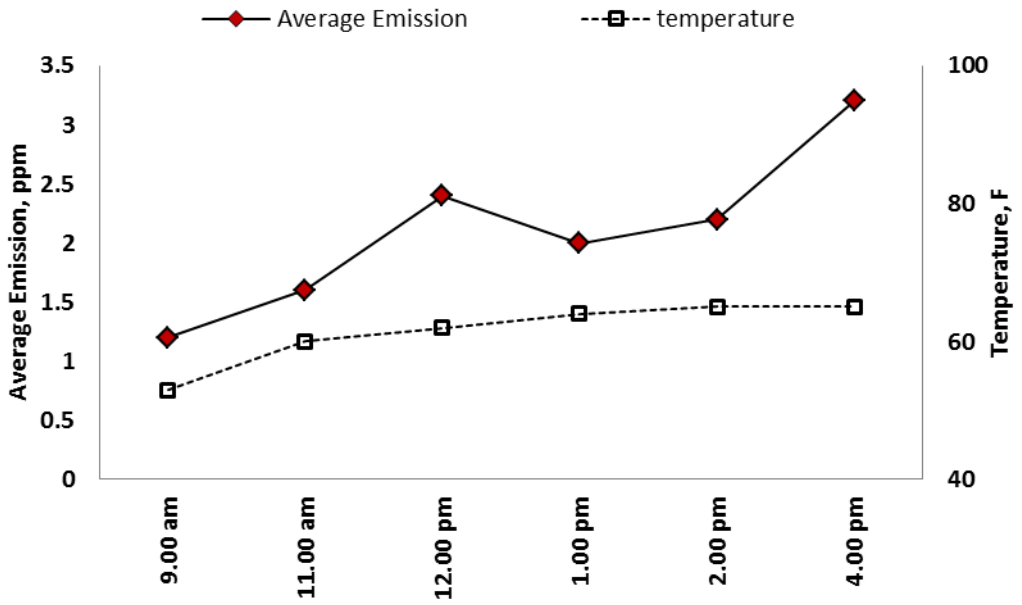

Figure 4.10 Studies on Diurnal Variation from Cell 2 at 02/21/2014

Based on the results, the average concentration from the landfill surface increased with an increase in temperature, which was anticipated from the study.

Considering the spatial variability of concentration from a landfill surface, the concentration was compared by averaging the surface concentrations measured from the total landfill cell. Therefore, to evaluate the diurnal variations from the landfill, six isolated points were selected on the landfill cell, cell 2, to monitor the variations caused by

continuous temperature variations in a day. Figure 4.11 and Figure 4.12 present the locations and results from these six points in cell 2 respectively.

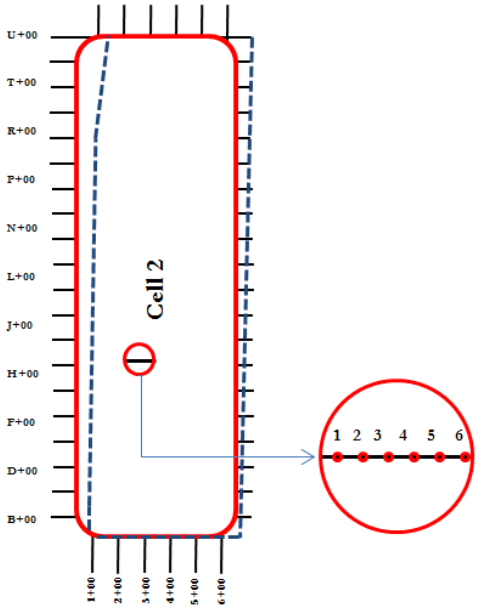

Figure 4.11 Locations of the Selected Points for Monitoring Diurnal Variations for Cell 2

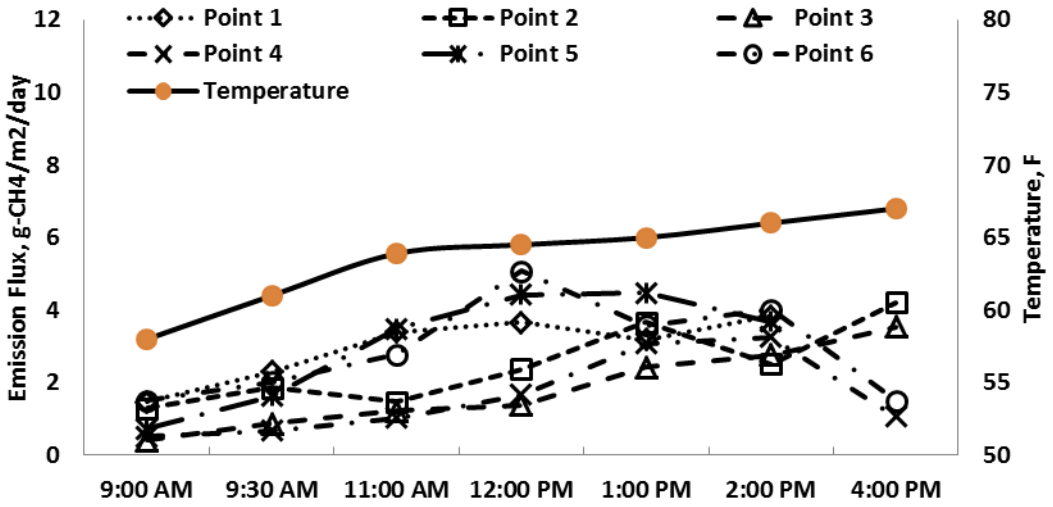

Figure 4.12 Diurnal Variations for Cell 2 from the Six Selected Points

Based on the figure, when the landfill surface temperature increased, from 9.00 am to 4.00 pm, the methane emission flux also increased. The results followed a trend similar to the study conducted in the total landfill cell during a 1-day period, as presented in Figure 4.10.

Park et al. (2001) conducted a methane emision study from the landfills to evaluate the effect of duiurnal and seasonal variations on methane emissions. They conducted the study at four hour internvals for one day, to monitor the diurnal variation of emisions from the landfills, as presented in Figure 4.13. Based on their results, they concluded that the emission from the landfills peak around 2 pm when the temperature is at its peak.They have also confirmed that higher methane emisions were observed in the summer, while lower emissions were measured during the winter period. Consequently, based on their observations, it was evident that the landfill emissions increase in direct relationship to increased increments in air and soil temperature. The current study was

conducted for 8 hours, from 9.00 am to 4.00 pm, and the results showed the similar increasing trend with increasing temperature of the day, as reported by Park et al. (2001).

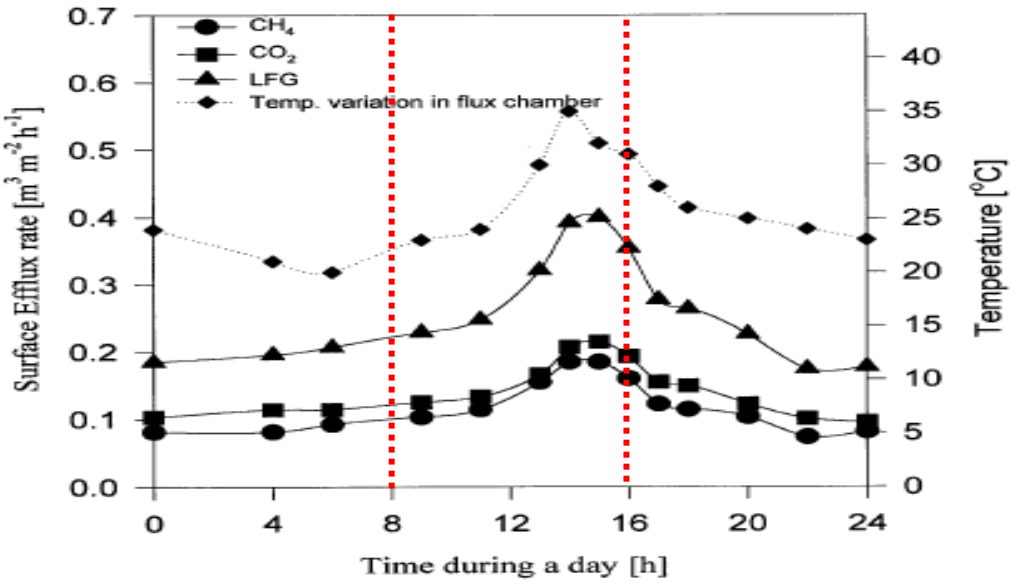

Figure 4.13 Diurnal Variations of Landfill Gas (Park et al., 2001)

The diurnal variations monitored from the selected points verify the previously presented hypothesis of higher temperatures resulting in higher emissions. Consequently, it is also important to monitor the direct effect of temperature/ seasonal variations on the methane concentrations.

4.3.3 Monthly/ Seasonal Variation

Seasonal variations were monitored from the City of the Denton Landfill on both cell 2 and cell 0. However, cell 0 was added to the monitoring plan in August 2013, which means that cell 0 has been monitored less than a year, while cell 2 was monitored for more than a year. Figure 4.14 and Figure 4.15 present the seasonal variation of emissions from cell 2 and cell 0, respectively. Figure 4.12 presents the seasonal variations of temperature, average monthly concentration measured (ppm) and average

monthly emission estimated in flux ($g/m^2/day$). Based on the figure presented below, the average emission from cell 2 was at the lower end from December 2012 to May 2013 and started to increase from June'13. The average emission from June 2013 to November 2013 was at the higher end for the current study. The highest temperatures were observed from May' 2013 to Oct 2013, which is basically the summer in Texas. Higher surface temperatures generally lead toward higher rates of emission from the landfill surface; however, a few anomalies were observed during the study. Although the temperature started to rise from May 2013, one of the lowest surface emissions was also observed in May 2013 (marked in green in the figure). Further analysis revealed that the gas was being extracted from cell 2 on the same day when the surface emission was being monitored in May 2013, which had substantially reduced the emission from the surface. Very low emissions were also measured from cell 2 in December 2013 and January 2014, due in large part to the effect of frequent precipitation and freezing on the soil. The effect of rainfall on the soil cover and the methane emission from soil cover will further be discussed in section 4.5.

Based on the results from cell 0, as presented in Figure 4.13, the methane emission does not follow the exact trend as the temperature. It is noteworthy that the highest emission for cell 0 was observed in November 2013 and December 2013 when winter was approaching and the temperature was decreasing. However, additional information on gas extraction or recovery data from cell 0 indicated that the gas extraction was lower in these two months (216 cfm and 281 cfm). Therefore, it again indicates that the gas extraction/ collection had a remarkable effect on landfill surface emission, reducing the landfill emission immediately after the gas extraction from the landfill.

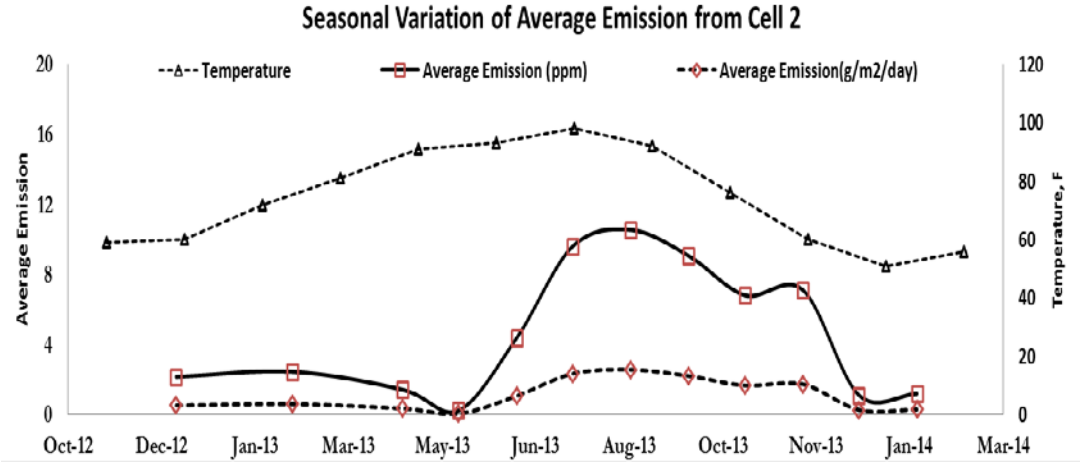

Figure 4.14 Seasonal Variations of Methane Emission from Cell 2

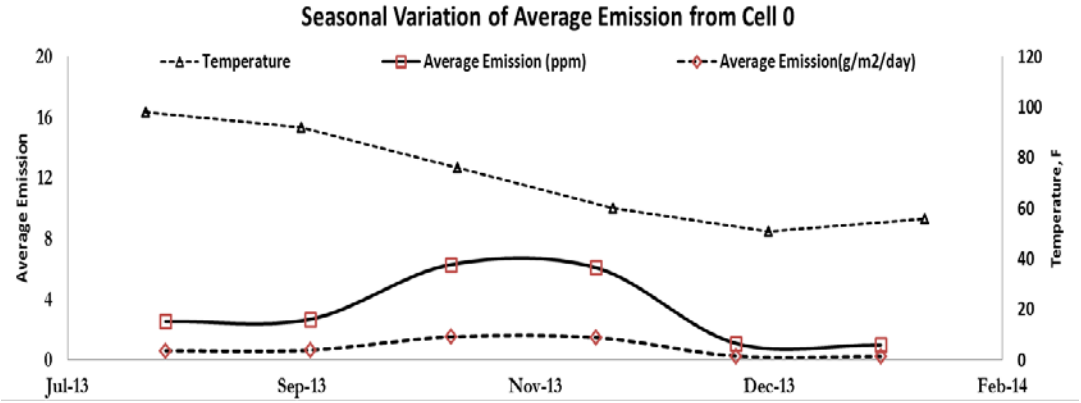

Figure 4.15 Seasonal Variations of Methane Emission from Cell 0

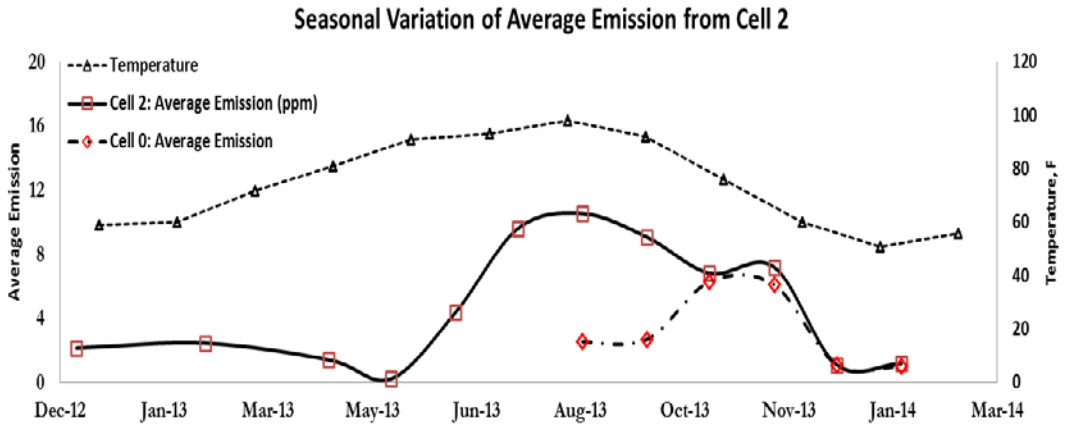

Figure 4.16 Comparisons of Seasonal Variations from Cell 2 and Cell 0

Seasonal variation was reported to be one of the major reasons for temporal variations of emissions in literature (Chanton and Liptay, 2000; Maurice et al., 2003; Wang-Yao et al., 2006; Yuan, L., 2006; Fleiger, J. E., 2006; Bogner et al., 2011). Table 4.2 compares the current emission study with a recent study by Bogner et al. (2011). Bogner et al. (2011) conducted the study over a period of two years in two landfills with different types of cover systems: daily cover, intermediate cover, and final cover. They measured the landfill emissions twice every year, once in summer and once in winter. The current study that was conducted on cell 2 and cell 0 of the City of Denton Landfill had intermediate covers on top. Therefore, the table compares the emission results obtained from the intermediate covers of the two landfills: Marina Landfill and Scholl Canyon Landfill, with the emissions from cell 2 and cell 0. According to the authors, the Marina landfill had higher emissions than the Scholl Canyon landfill, which was attributed to the different oxidation behaviors of the two landfill covers. The Scholl Canyon Landfill shows both positive and negative emission, where positive flux indicates emission of methane from the landfill surface and the negative flux indicates the uptake of methane due to negative pressure or suction of the cover soil. The current results were more

similar to the Scholl Canyon Landfill emissions. However, based on the results from Scholl Canyon, no comments could be made on seasonal variations of emissions. On the contrary, the Marina Landfill shows a consistently higher emission from the landfill in August (summer) than March (winter). Again, based on the results from the current study from cell 2, higher emissions were observed from June 2013 to November 2013, whereas lower emissions were observed from December 2012 to May 2013. The results showed higher emissions during the summer, when the temperatures were high. However, the results from cell 0, which was monitored from August 2013 to January 2014, showed higher emissions in October and November 2013, and were on the lower end for the rest of the monitoring period. Therefore, no strong conclusions could be made based on the results from cell 0. Although, low emissions in August 2013 and September 2013 could be attributed to high gas extraction from the gas recovery wells for these two months, no overall seasonal trend was observed from the cell 0 results that were similar to results from the School landfill, as reported by Bogner et al. (2011).

Table 4.2 Comparison Current Study to Previous Study for Seasonal Variations

Date	Current Study		Date	Previous Study (Bogner et al., 2011)	
	Cell 2	Cell 0		Marina Landfill	Scholl Canyon Landfill
**N.B. Unit for all emissions: $g/m^2/day$					
Dec'12	0.53	--			
Feb'13	0.60	--	Mar'07	0.03204	-0.00628
April'13	0.35	--			
May'13	0.06	--			
Jun'13	**1.07**	--	**Aug'07**	**53.2**	0.00226
Jul'13	**2.35**	--			
Aug'13	**2.58**	0.62			
Sep'13	**2.20**	0.70	Mar'08	34.2	0.01294
Oct'13	**1.70**	**1.50**			
Nov'13	**1.70**	**1.48**			
Dec'13	0.30	0.30	**Aug'08**	**238**	-0.00318
Jan'14	0.30	0.30			

4.4 Effect of Climatological Parameters

Several studies reported the effect of climatological conditions (i.e. temperature, moisture, wind speed, barometric pressure etc.) on surface emissions. However, the temperature and the moisture were identified to be the governing factors of emission. The landfill covers are typically constructed of the widely abundant on-site soil materials. The available cover soil for the current study was CL, and there was a 2 ft. thick cover on cell 2 and 10 ft. thick cover on cell 0. The behavior or oxidation of soil covers, especially the clay covers, are highly affected by the moisture content of soil, as the porosity or the voids within the soil cover changes with the presence of moisture. The higher the

moisture content, the more the voids are filled with water and less gas migration is possible. On the other hand, if more voids are available, higher gas diffusion will occur through the cover soils. The precipitation and the temperature are the two major controlling factors that impact the soil moisture content in the field, and hence, the gas migration through the cover.

4.4.1 Temperature

4.4.1.1 Air Temperature

Methane emissions were measured for the current study from the landfill, using a portable FID and static flux chambers, as discussed in the earlier sections of this report. The total duration for the emission monitoring in each cell was approximately two and one-half hours. During the time of emission monitoring in the field, the temperature was recorded at every hour and then averaged to obtain the representative average temperature during the data collection.

Based on the previous discussions on the effects of seasonal variations on methane emissions, it was apparent that methane emission is positively affected by the temperature. However, to evaluate the direct effect of temperature variations on methane emissions, the average emission results from cell 0 and cell 2 were plotted with the average temperatures during the methane emission monitoring from the landfill. Figure 4.17 illustrates the temperature vs average emission results from cell 2 and cell 0 of the City of Denton Landfill. Based on the figure presented below, the average emission shows an increasing trend with increase in emission. Three data points (plotted in red) were excluded while plotting the regression trend that was predicting a misleading correlation between the methane emissions and temperature. These three data points were: average emission of cell 2 in May 2013 and average emission from cell 0 in August 2013 and September 2013. These three data points were highly affected by the gas

extraction from the landfill cell. For the average emission from cell 2 in May 2013, the emission was monitored at the time of gas extraction from the landfill. The other two data points that were excluded were more affected by the higher gas extraction than by the temperature at the time of monitoring.

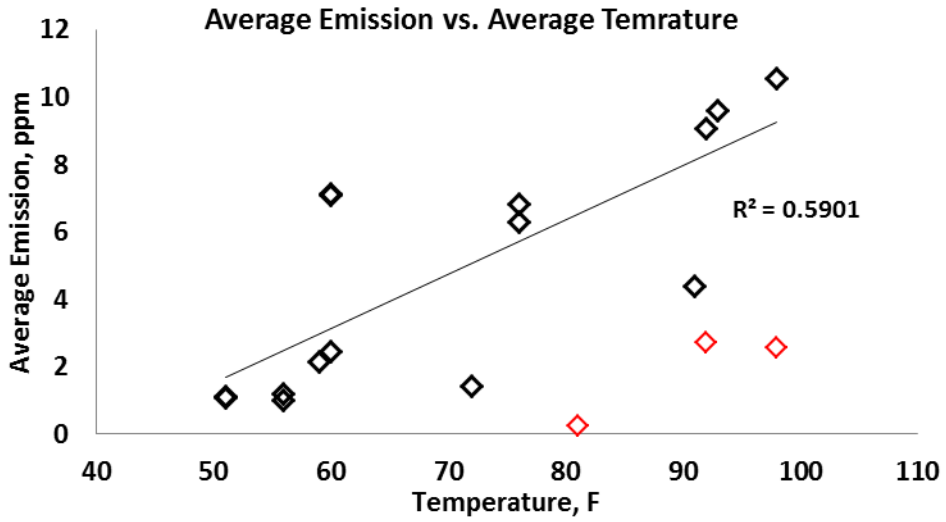

Figure 4.17 Effect of Temperature on Methane Concentration

Based on the trend line shown in the figure, methane concentration was directly proportional to the temperature of the landfill. It could be easily anticipated that the increase in temperature would aid in increasing the soil temperature adjacent to the waste. The increasing temperature in the waste would enhance the degradation process in the landfill and, as a result, the gas generation would also increase. On the other hand, the presence of an active collection system and the methane oxidation in the landfill cover is expected to prevent the increase in emissions from the surface. Yet, the changes in concentrations were observed due to change in temperature. Based on the results, the temperature change positively affected the average concentration from the landfill except in a few cases where gas extraction was the controlling factor in concentration. The

results verified that the seasonal variations in methane emissions were highly dependent on the changes in temperature with seasonal variations.

4.4.1.2 Soil Temperature

The soil temperature was measured using the temperature probes installed in the landfill in three different locations, as presented in the Figure 4.18. The temperature probes were installed at 1 ft. and 2 ft. depths to monitor the temperatures within the soil at locations O1, O2 and O3. In addition, the ambient temperature was also monitored at the surface for cell 2.

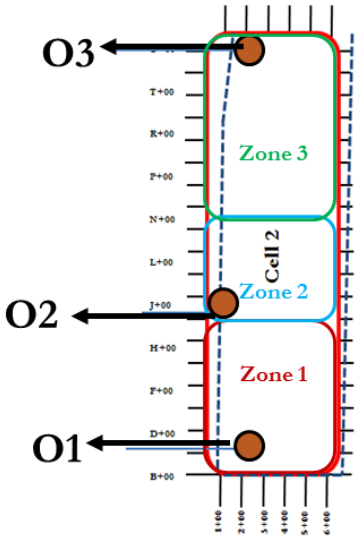

Figure 4.18 Locations of Soil Temperature Probes

Figure 4.19 presents the soil temperature and the ambient temperatures monitored in the locations O1, O2 and O3. From the figures, the soil temperatures from 1ft. and 2 ft. depths were observed to be very similar and close to the ambient temperature of the air.

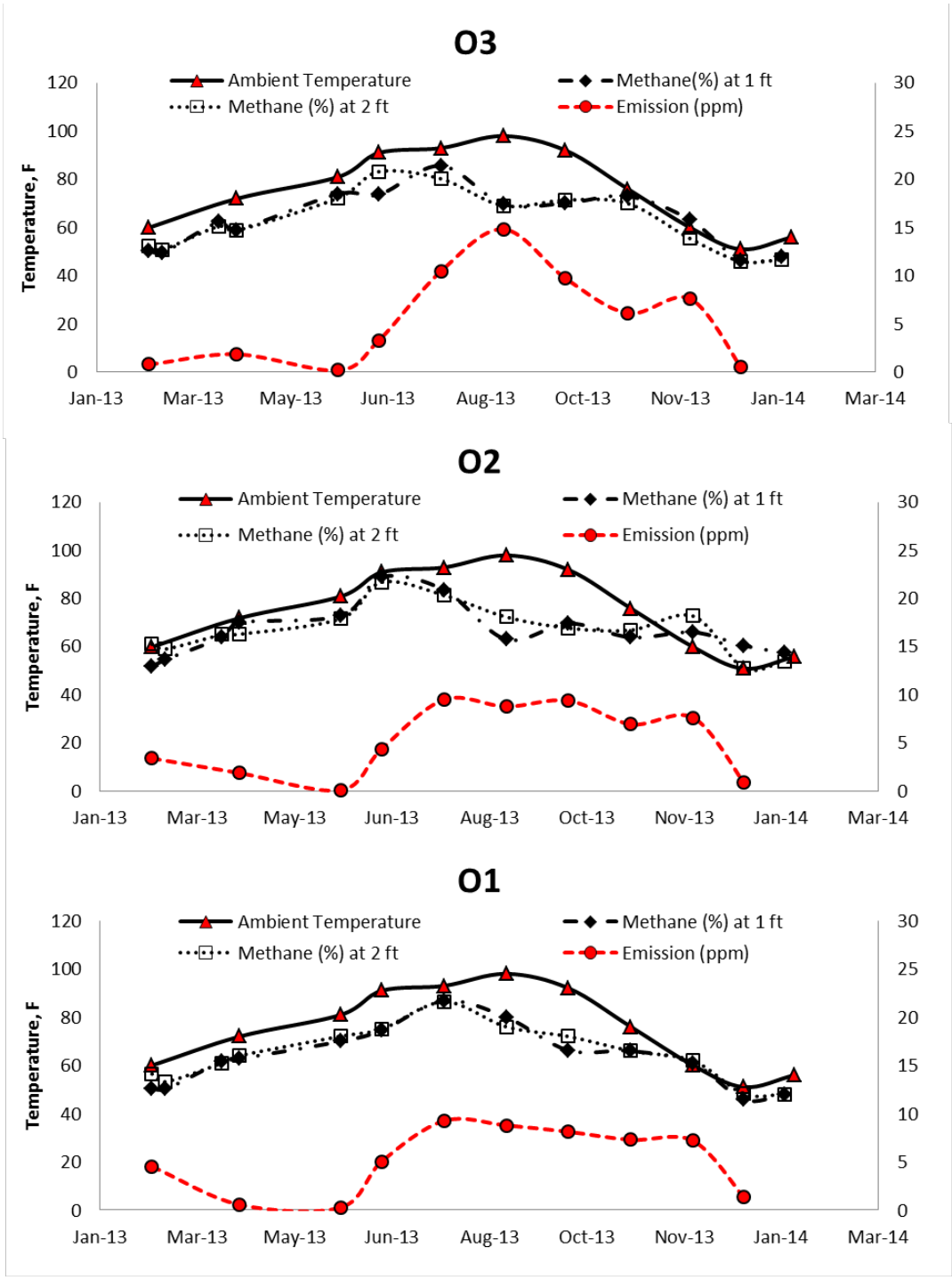

Figure 4.19 Ambient Air and Soil Temperature from locations O1, O2 and O3

However, for all three locations the soil temperatures dropped around the month of August and started to rise again in November. Maximum methane emissions were also observed during the same time period. The gas generation from the MSW is an endothermic process; hence, the heat is absorbed from the surrounding atmosphere to generate gas (U.S>EPA, 2012). Therefore, the higher gas generation in the corresponding time might have absorbed the heat from the surrounding atmosphere, and, as a result, the soil temperature might have dropped.

4.4.2 Precipitation

The landfills cells monitored during the study were operated as an ELR cell (cell 2) and a conventional cell (cell 0); and none of the cells were exposed to surface irrigation. Therefore, the rainfall events were the only media of adding moisture to the soil cover. However, high temperature helps in surface evaporation and increases the number of available voids and consequently the methane migration from the landfills. On the contrary, rainfalls or ice during the winter time while the overall surface temperature is on the lower end reduces the voids in the soil by remain filled with water/ moisture.

Figure 4.20 presents the average emission vs. average monthly precipitation from cell 0 and cell 2. Based on the results the average emission decreases with the increase in precipitation of the month. However, there were few results (the points plotted in red) that did not follow the decreasing trend with increasing moisture. As previously discussed, the moisture content of the cover is a combined effect of the climatological factors (i.e. temperature and precipitation) where higher temperature helps in drying the soil and reduces the moisture content of the soil cover.

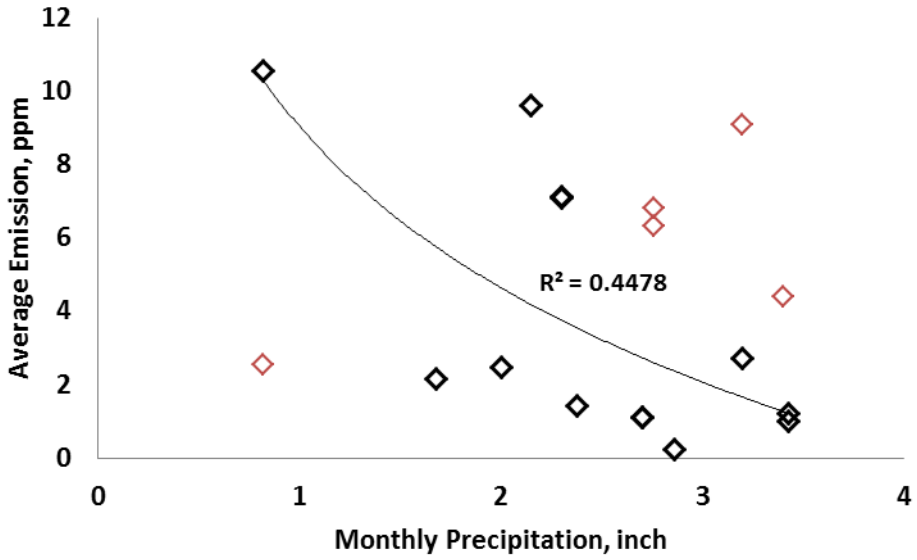

Figure 4.20 Effect of Temperature on Methane Emission

Decreasing emission with increasing precipitation is consistent with the previous studies conducted on emission and oxidation from the landfills. The soil moisture and temperature are vital in methane oxidation. The methanotropic bacteria present in the cover soil are most active in an optimal range of temperature and moisture, and very low temperature moisture reduces the oxidation capability of these bacteria. Methane emission substantially decreases while the methanotrophs are most active in the landfill cover. In addition, the methane oxidation was reported to increase with the duration of exposure to methane. Therefore, the longer the cover soils are exposed to the landfill methane, the higher will be the oxidation capacity of the cover. The effects of cover oxidation and the oxidation rate of the cover soil present in the study will be discussed in detail in the next section.

4.5 Effects of Operational Parameters on Methane Emissions

Gas extraction or collection from active or closed landfills has been suggested in different studies to mitigate the landfill emissions. Uncollected landfill gas travels through the landfill cover and escapes through possible cracks or pressure differences between the landfill cover and the atmosphere. Another highly recommended landfill gas mitigation method is providing soil covers with higher oxidation capacity that will minimize LFG emission through the cover. Previously landfills were operated as conventional landfills with restrictions in water addition and consequently the gas generation rate was also low from the landfills. However, advancement of technologies evolved the idea of faster degradation and higher gas generation in shorter period of time by introducing liquid/ moisture to the landfill. While this new technology is helping in higher gas generation and utilizing the collected gases in gas to energy projects, the effect of moisture/ liquid addition on emission is of great concern for the ELR/ bioreactor operation.

The following subsections discuss the effect of ELR/ bioreactor operation and also the presence of a gas extraction system in the landfill.

4.5.1 Effect of ELR Operation

Cell 2 was operated as an ELR cell where leachate was injected/ recirculated through the horizontal recirculation pipes (namely H1, H2, H3, H4, H5, H6..., and H36.). The added moisture to the landfill was expected to enhance the degradation around the perimeter of the recirculation pipes and therefore, was also anticipated to increase the emission through the landfill covers. The leachate was recirculated through few pipes in a month (sometimes in the same day or in different days in different amounts). Therefore,

increase in emission due to the addition of moisture was also anticipated to be near or around the recirculation pipes.

4.5.1.1 Variation of Emission with Time

For the current study in the ELR landfill cell, there was no fixed dosing plan. According to the permit, each pipe could accept less than 50,000 gallons of leachate/ day. However, the leachate generation from the landfill is very low and the fresh water collection in the sumps was not sufficient to add 50,000 gallon/ day. Consequently, the leachate was recirculated based on the gas generation trends of the gas collection pipes. Most of the time, leachate was recirculated through 2 to 6 pipes in a month. Also, the clogging or saturation in the pipes often hindered the leachate recirculation through many of the leachate recirculation pipes in the landfill. Currently, only few pipes would accept the recirculation in the cell 2. Therefore, the leachate is often recirculated with these specific pipes: H2, H3, H5, H16, H18 and H22 (as presented in chapter 3). Therefore, pipe H18 and pipe H22 were selected to monitor the effect of leachate recirculation in the landfill after 1 day, 4 days and 10 days of recirculation.

Figure 4.21 and Figure 4.22 presents the effect of leachate recirculation on methane emission at 50ft, 100ft and 200 extents on both sides of the pipe H18 and H22 respectively. The effect of emission was monitored with the time variation to evaluate the changes in emission with time after the leachate injection.

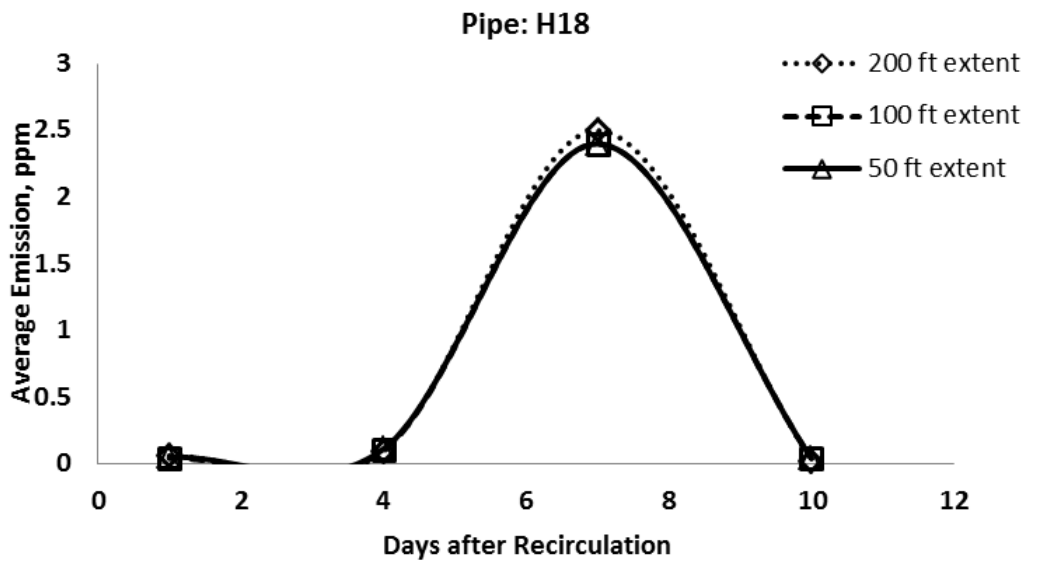

Figure 4.21 Effect of Leachate Recirculation on Methane Emission near the Recirculation Pipe H18 with Time

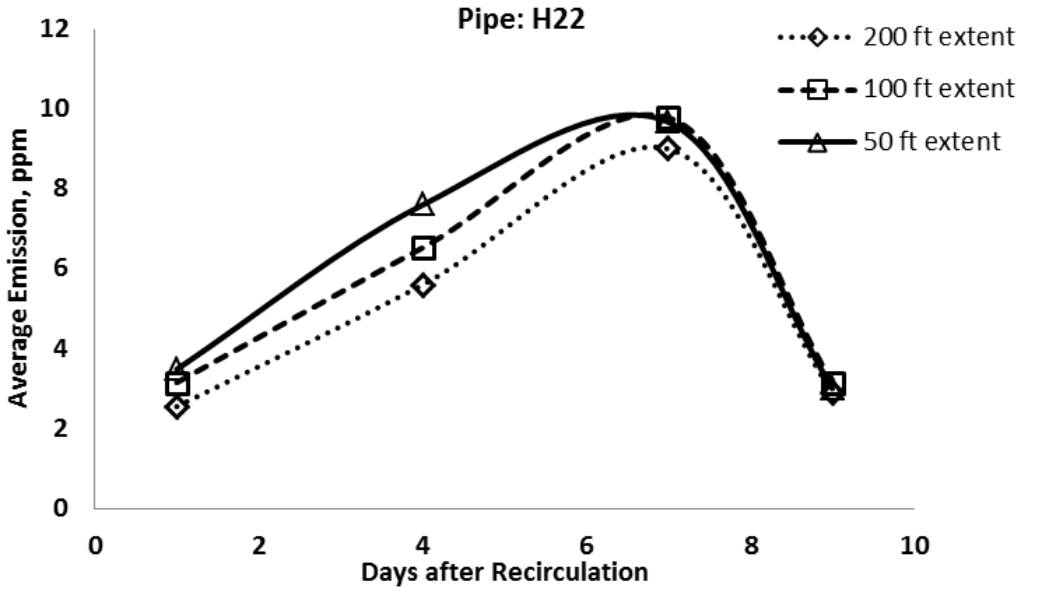

Figure 4.22 Effect of Leachate Recirculation on Methane Emission near the Recirculation Pipe H22 with Time

Based on the results presented in Figure 4.21, emission substantially decreased right after the recirculation through the pipes and started to increase after 4 days. Even 7 days after the leachate recirculation, the emission was observed to increase adjacent to the leachate injection pipe H18. The next measurement taken after the 10 days of leachate recirculation showed the emission near the pipe was similar to the emission right after the recirculation through the pipes. The addition of water in the waste would reduce the temperature in the waste due to differences in temperature between the landfill waste and recirculated water (Manzur et al., 2012). Subsequently, the gas generation would also decrease right after the recirculation; however, the gas generation would improve as soon as the temperature of the waste increased and the moisture was distributed around the waste. Then, when the added water was utilized for the gas generation, the gas generation would stop and would be back to the initial condition before the recirculation.

Figure 4.22 present the similar time sensitive analysis of the effect of leachate recirculation around the recirculation pipe H22. The study was conducted similar to the previous study near pipe H18. The emission was monitored around the pipe H18 after 1day, 4 day and 9 day after the leachate recirculation near pipe H22. The study illustrated an increasing trend of emission until 7 days of initial leachate recirculation/ injection through the pipe and a decreasing trend after 9 days which was similar to the emission after 2 days of recirculation. Since, for H22 the emission was not monitored until 2 days after the leachate recirculation, no initial drop in emission was observed similar to H18.

Therefore, based on the observations, the emissions showed a similar trend as the anticipated gas generation from the landfilled waste. The emission showed a sudden decrease right after the initial addition of moisture that could be attributed to the thermal changes within the landfilled waste and then started to increase up to 7 days after the

recirculation and finally after 10 days, the emission near the pipes decreased and came back to initial condition.

Based on the results presented in Figure 4.21 and Figure 4.22, the emission could be expected to increase after 2 days of recirculation until the first 7 days, and return to its initial or original condition after 10 days of recirculation when all the moisture would already have been used in the gas generation process.

However, no increase was observed in the overall emission from the landfill due to recirculation in the landfill cell. It should be noted that the leachate recirculation in a landfill cell through a recirculation pipe would be anticipated to affect only the adjacent landfilled solid waste. The comparison between the average emission between the ELR landfill cell (cell 2) and the tradition cell (cell 0) would be helpful in understanding the differences in landfill emission due to the operational practice.

4.5.1.2 Variation of Emission with the Amount of Recirculation

The variation of emission with the amount of recirculation is evaluated in this section. To evaluate the impact of the amount of water/ leachate added three pipes (namely H2, H16, and H22) were selected based on the frequency of the leachate addition. Table 4.3 presents the amount of leachate recirculated through pipes H2, H16 and H22 during the monitoring period from Dec'12 to Jan'14. Leachate/ water was recirculated through six times through H2, seven times through H16 and ten times through H22. However, due to unavailability of the portable FID no emission monitoring was conducted on cell 2 in Jan'13 and Mar'13. Therefore, the leachate recirculation in these two months (data points presented in grey) could not be taken into consideration for the variation of emission due to the change in amount of water/ leachate addition.

Table 4.3 Leachate Recirculation in Cell 2 through H2, H16, and H22 during the Monitoring Period of the Study

Month/ Pipe	H2	H16	H22
Dec'12	0	0	0
Jan'13	7235	2755	9690
Feb'13	5335	0	9330
Mar'13	15405	5560	7635
Apr'13	13550	0	6730
May'13	0	5660	0
Jun'13	0	5840	0
Jul'13	0	0	9220
Aug'13	0	0	0
Sep'13	0	0	6250
Oct'13	0	6010	4275
Nov'13	0	0	8790
Dec'13	5400	4372	23418
Jan'14	2933	2330	14350
Cumulative	**49858**	**32527**	**99688**

Figure 4.23 presents the total recirculation amount (in gallons) vs. the total average emission (in ppm) near the respective recirculation pipes. Based on the results, no direct correlation was obtained between the amount of leachate/ water recirculation and the emission near the pipes. Subsequently, individual analysis was carried out for the pipes H2, H16 and H22. Figure 4.24, Figure 4.25 and Figure 4.26 present the total recirculation and cumulative recirculation of water/ leachate through H2, H16 and H22 for the monitoring period from Dec'12 to Jan'14.

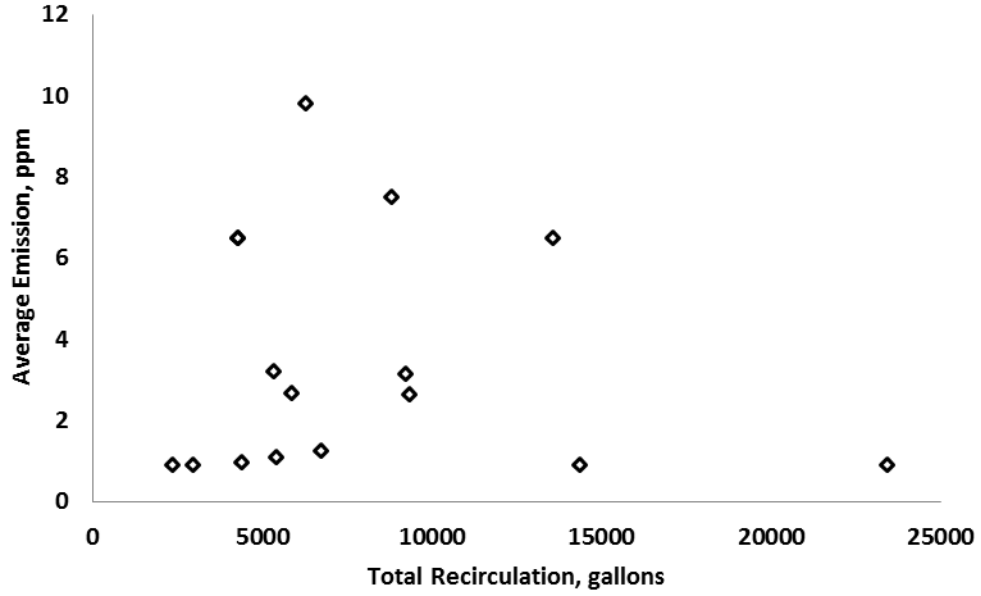

Figure 4.23 Leachate Recirculation Volumes and Cumulative Leachate Recirculation through H2

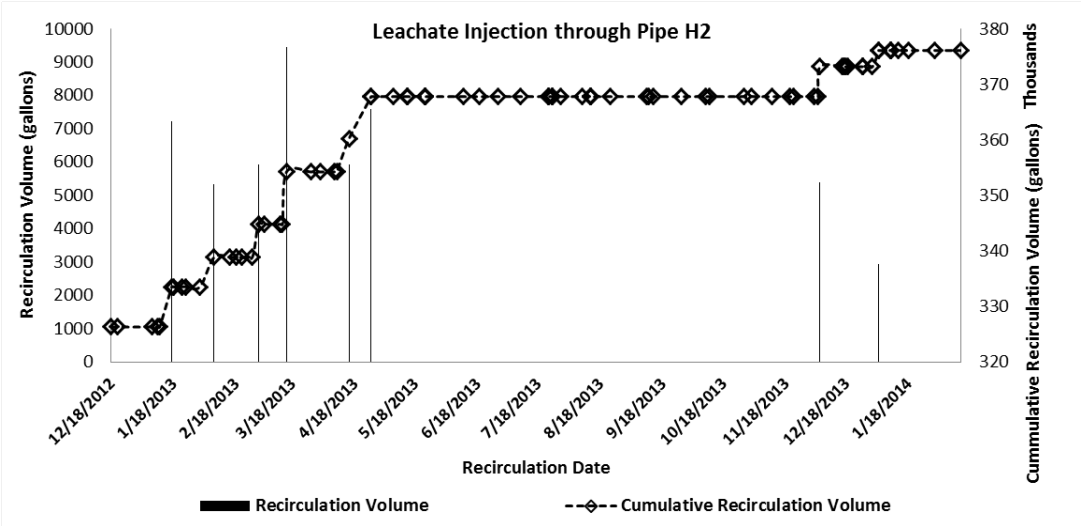

Figure 4.24 Leachate Recirculation Volumes and Cumulative Leachate Recirculation through H2

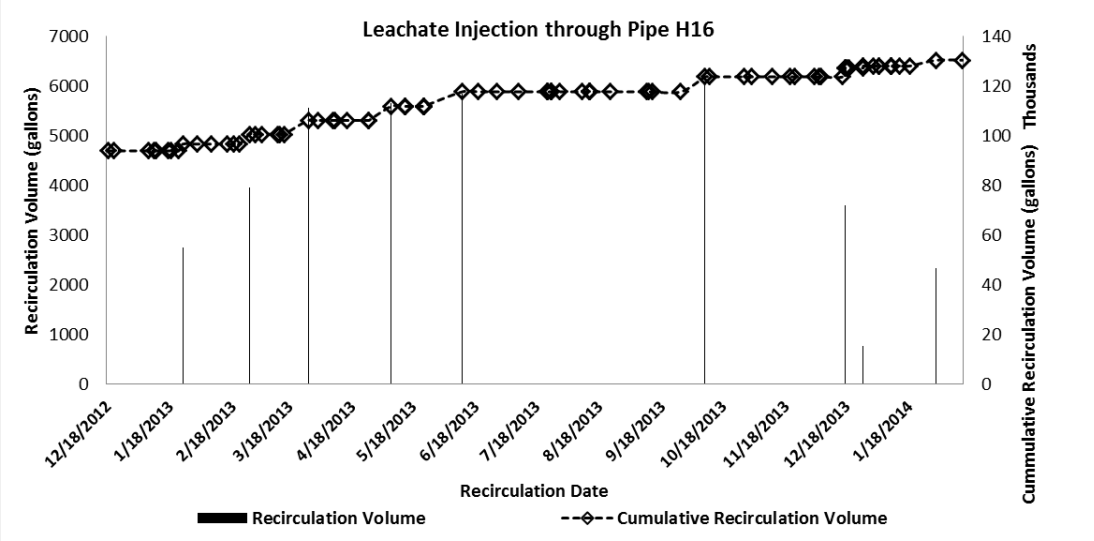

Figure 4.25 Leachate Recirculation Volumes and Cumulative Leachate Recirculation through H16

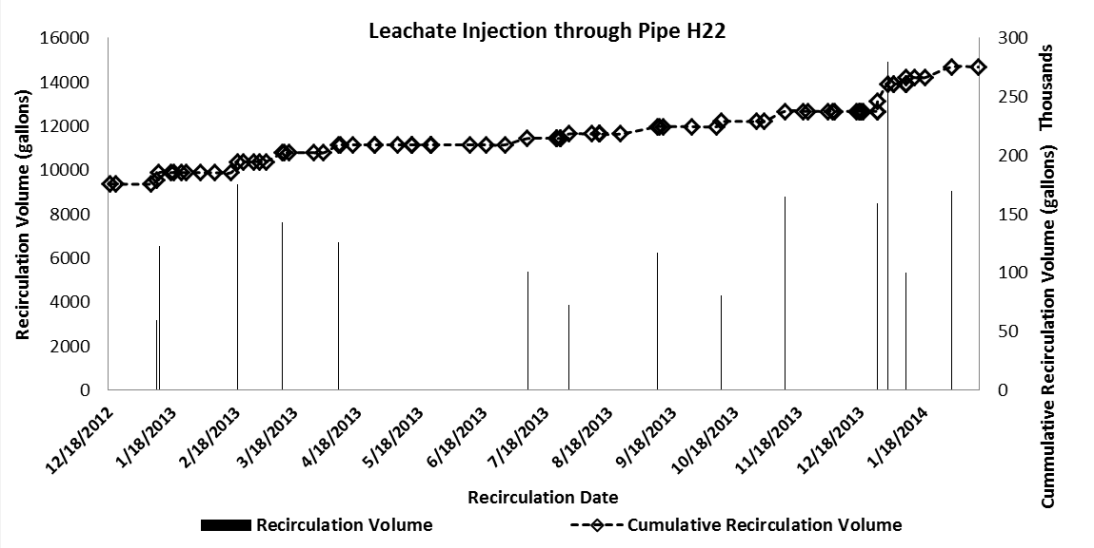

Figure 4.26 Leachate Recirculation Volumes and Cumulative Leachate Recirculation through H22

Figure 4.27, Figure 4.28, and Figure 4.29 present the leachate injection and corresponding emission respectively near the pipe H2, H16, and H22. Based on the

figures presented below, the methane emission typically increased near the corresponding recirculation pipes with the increasing leachate recirculation through pipes. However, the methane emission measured in Dec. '13 and Jan. '14 had overall low emission throughout the landfill and might be misleading for some of cases, especially from Figure 4.27.

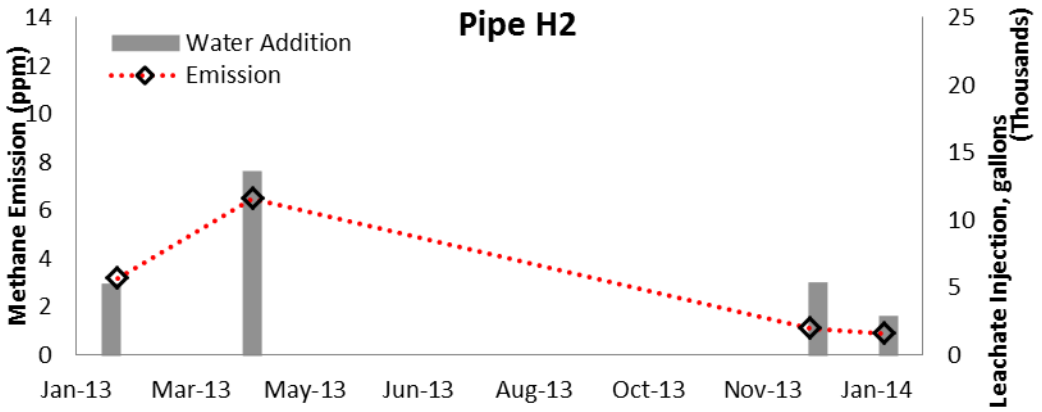

Figure 4.27 Leachate Recirculation Volumes and Methane Emission near H2

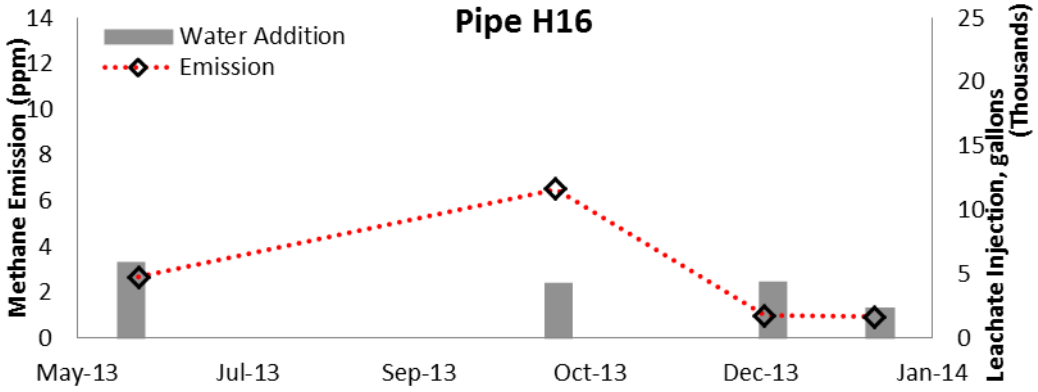

Figure 4.28 Leachate Recirculation Volumes and Methane Emission near H16

Figure 4.29 presents the leachate recirculation volumes and methane emission near pipe H22. Based on the figure, the methane emission typically increased with the

increased quantity of leachate recirculation. However, the results obtained from Dec'13 and Jan'14 showed very low emission near the pipe although a substantial amount of leachate was recirculated in Dec'13 through H22.The low emission during Dec'13 and Jan'14 could be mostly accredited to the frequent rainfall, freezing and consistent low temperature. During the time of emission monitoring in Dec'13 and Jan'14 the soil cover was very wet and also had stagnant water in few locations as illustrated in Figure 4.30.

The soil cover was possibly highly saturated during these time and the voids in the soil covers were mostly filled with water and consequently comparatively low methane migration was plausible during this time.

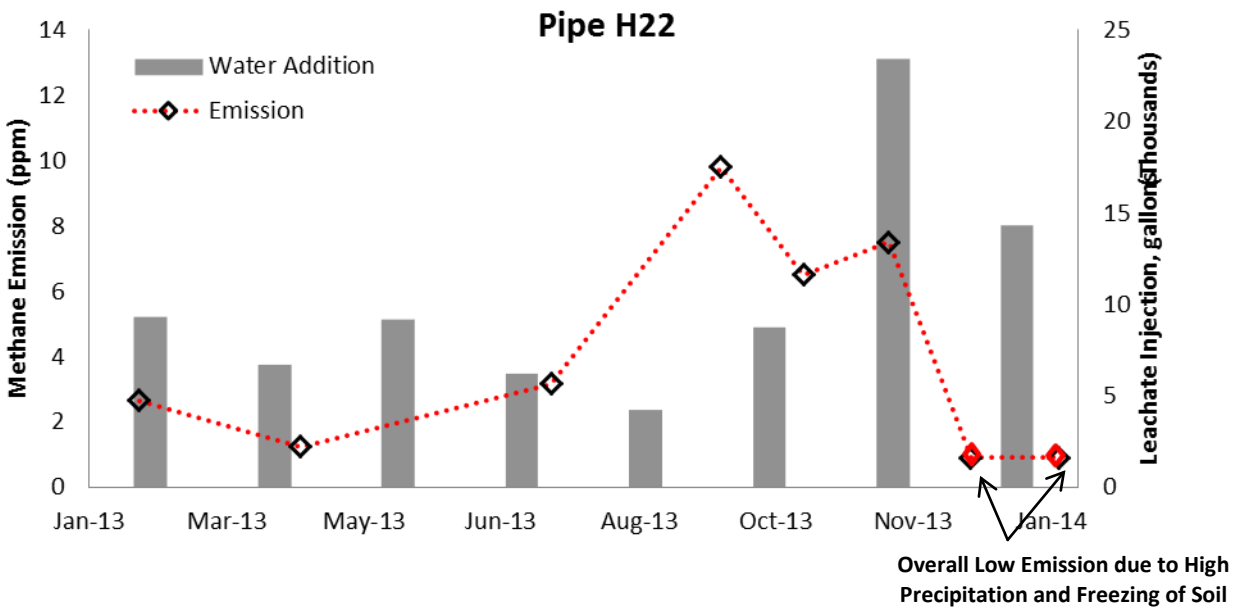

Figure 4.29 Leachate Recirculation Volumes and Methane Emission near H22

Figure 4.30 Cover Soil Condition during the Methane Emission Monitoring in Dec'13 and Jan'14

Therefore, based on the results presented above, the effect of ELR operation can be summarized as below:

- There was no direct correlation between the amounts of leachate injected to amount of surface emission measured;
- A quantitative analysis showed that the methane emission near the recirculation pipe increased with increasing leachate injection;
- Methane emission increased due to the ELR operation; however, the changes in emission was time variable. The emission decreased right after the leachate recirculation and then started to increase until 1 week after the recirculation. Approximately, 10 days after the recirculation the average emission adjacent to the pipe returned to its original/ initial condition before the recirculation;

- The leachate was recirculated through only few pipes each month and the influence of leachate injection was only limited near the 50 to 75 ft radius near the pipe. Therefore, no substantial change in overall emission was observed due to the ELR/ bioreactor operation in the landfill cell.

4.5.2 Comparison of Average Methane Emission from ELR and Conventional Landfill

The average emission based on the ELR operated landfill cell (cell 2) and conventional landfill cell (cell 0) were compared to evaluate the effect of leachate recirculation on overall emission from the landfills. Although, based on the prior discussion, the effect of leachate recirculation is more prominent near the adjacent recirculation pipe and reached at its peak after one week of recirculation. However, to evaluate the effect of operational practice on the emission a study was required to compare between two landfill cells with different landfill operation.

Figure 4.31 present the comparison between the average methane emission from cell 0 and cell 2. Emission from cell 0 and cell 2 was monitored in the same day to minimize the climatological variation during the monitoring. Cell 2 was added to monthly monitoring plan from August therefore the comparison between the two landfill cells were compared from Aug'13 to Mar'14. Based on the figure, the overall emission from cell 2 (ELR cell) was higher than the cell 0 (conventional cell). During the monitoring period the maximum temperature was observed in Aug'13 (98°F) and Sep'13 (92°F). Consequently, the highest emissions were also observed from cell 2 in these two months. However, the emission measured from the cell 0 was comparatively low in Aug'13 and Sep'13 and eventually increased in later months (Oct'13 and Nov'13). As presented in earlier section, the temperature had direct effect to the surface emission from landfills and hence the low emission from cell 0 during the hottest time of the year was not anticipated. Initially, the lower gas generation from the conventional cell (cell 0) compared to the ELR cell (cell 2)

was thought of the primary reason behind the lower emission. However, the increased emission in later months from the conventional cell (cell 0) declined the initial assumption of lower gas generation. On the contrary, the average temperature during Oct'13 and Nov'13 was not 76°F and 60°F respectively which were considerably low than the previous months. Therefore, it was evident that the temperature was not playing the governing role in the variation of emission from cell 0. The further analysis indicated that the lower gas extraction in Oct'13 and Nov'13 might have been the major reason for increased methane emission in lower temperature. In addition, the gas recovery data also showed higher gas extraction during Aug'13 and Sep'13 which also explained the lower emission during Aug'13 and Sep'13.

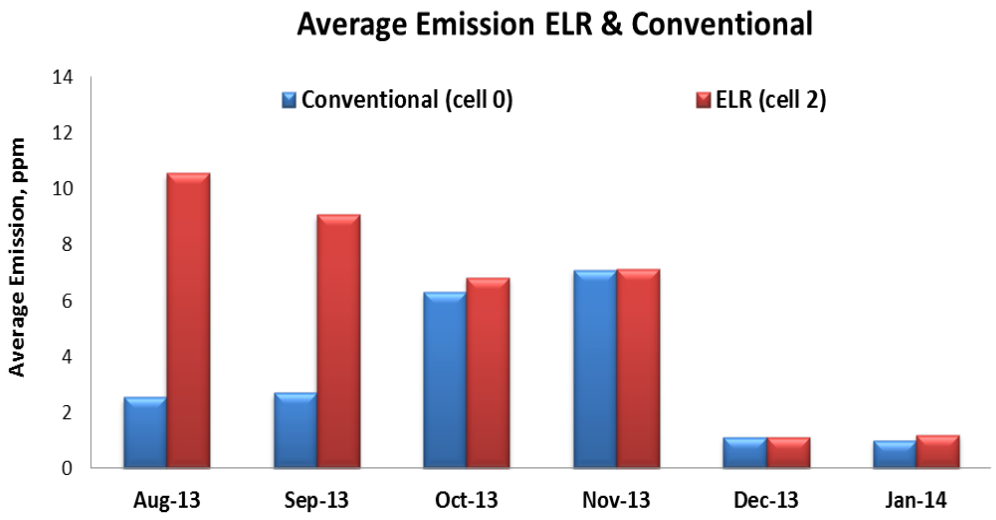

Figure 4.31 Comparison of Average Emission from ELR (cell 2) and Conventional (cell 0) Landfill Cell

Based on the overall comparison between the conventional and traditional cell it could be summarized that:

- ELR or bioreactor operation increased the overall emission from the ELR operated cell which could be attributed to the higher gas generation from the ELR landfill cell due to leachate/ moisture addition.
- However, the overall average emission from the traditional and ELR cell was similar except in Aug'13 and Sep'13. The substantially lower emission from the conventional cell during the hottest time of the year was explained as a result of higher gas extraction during those months. Consequently, the gas extraction from the landfill cell demonstrated higher impact on surface emission than the average temperature of the landfill cell.

4.5.3 Effect of Gas Collection

The study was conducted on 14th and 21st of February, 2014. However during the first study at 14th of February, the average emission decreased as the day proceeded from morning to afternoon as presented in Figure 4.7. On the other hand, it was a sunny day and the temperature also increased from 50°F to 70°F. Based on the preliminary investigation conducted on 14th of February, it was challenging to draw any strong conclusion on the diurnal variation on emission. Therefore, the study was repeated on 21st of February as presented in Figure 4.32.

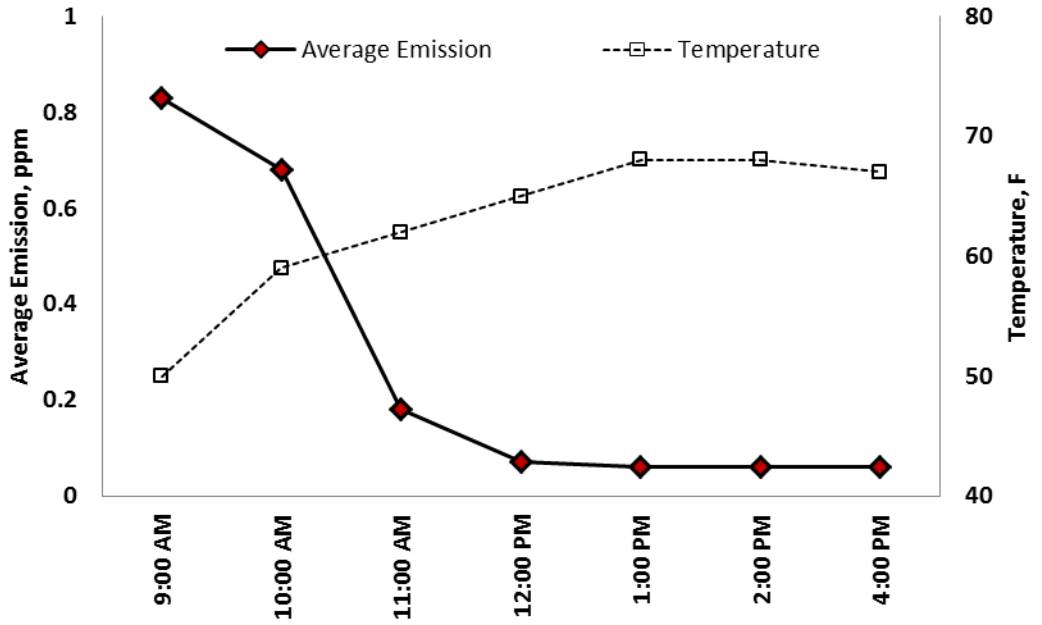

Figure 4.32 Initial Studies on Diurnal Variation from Cell 2 at 02/14/2014

Previous literatures have suggested the presence of gas collection or extraction system as a measure of methane emission reduction from the landfills. However, no systematic study was performed so far to evaluate the effect of gas recovery/ gas extraction on mitigation of emission from the landfill. The previous discussions on the effect of other climatological and operational parameters on the landfill emission measured from in the current study indicated that the higher gas extraction resulted in reduced methane emission from the landfill even in the hottest summer. In this section, the effect of gas collection will be evaluated more extensively.

Figure 4.33 and Figure 4.34 present the average emission and total gas extraction with time for cell 2 and cell 0 respectively. Cell 2 had both horizontal and vertical gas extraction and cell 0 had only vertical gas collection wells present. Gas extracted from both cell 0 and cell 2 was collected through a main header pipe and used

for the gas to energy project in the landfill site. Figure 4.33 presented the average emission and gas recovery with time from the ELR operated cell (cell 2). The figure showed a clear trend of increasing emission with reducing gas collection from the landfill. Based on the figure, the maximum gas extraction was in May'13 where the lowest emission from the cell was observed. It should also be noted that the methane emission in May'13 was monitored in the same as the gas extraction which might be the most plausible reason of the lowest methane emission in May'13. A diurnal study also confirmed that the methane emission reduced substantially after the gas extraction from the landfill (presented in Figure 4.32) that the methane emission reduced substantially after the gas extraction from the landfill.

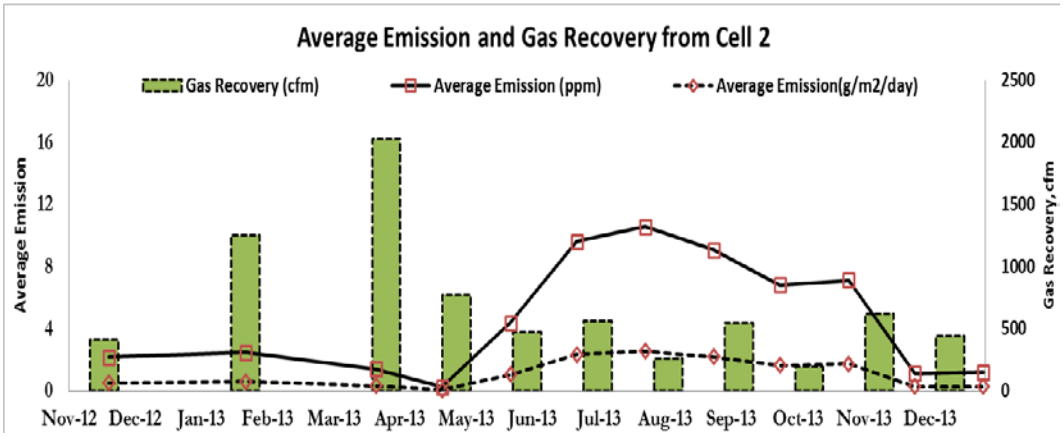

Figure 4.33 Average Emission and Gas Recovery from the ELR Cell (cell 2)

Figure 4.34 presents the similar comparison of average emission and gas extraction from the cell 0 (conventional landfill) in the City of Denton landfill. Based on the figure the emission was substantially increased while the gas extraction decreased from the landfill cell in Oct'13 and Nov'13. Although the gas extraction from cell 0 was also low in Dec'13, the methane emission did not increase in dec'13. During the time of emission monitoring in Dec'13 and Jan'14 the soil cover was very wet and also had stagnant water

in few locations as illustrated in Figure 4.30, the soil cover was possibly highly saturated during these time and the voids in the soil covers were mostly filled with water in Dec'13. Hence, comparatively low methane migration occurred during this time.

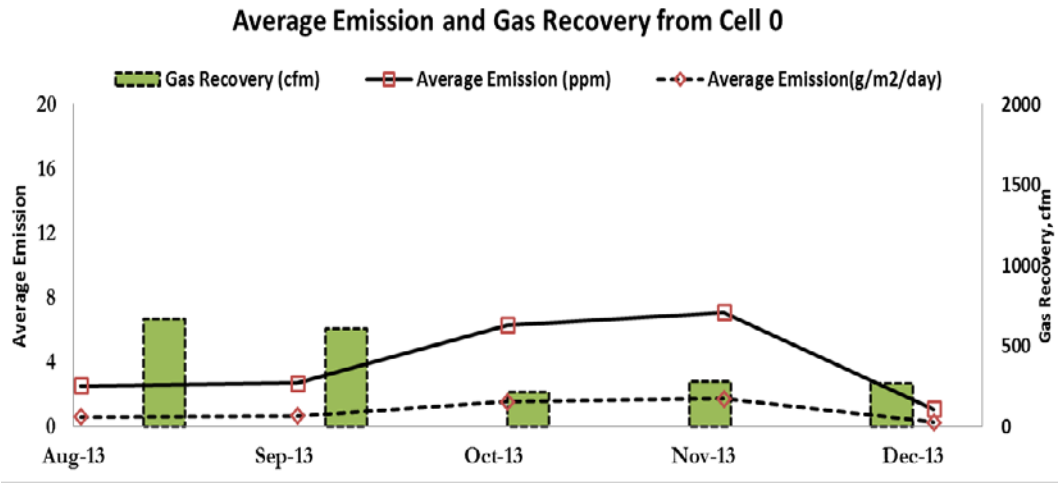

Figure 4.34 Average Emission and Gas Recovery from the Traditional Cell (cell 0)

Figure 4.35 present the average emission vs. the gas recovery or total gas extraction. A decreasing trend was observed from the figure with the increasing gas extraction from the landfill cell. The data points were based on all the average monthly emission from cell 0 and cell 2 with their corresponding total gas extraction from the respective cells. Few observations were excluded for the representative trend line. These excluded points were the data points measured in Dec'13 for both the landfill cell where the overall emission were substantially low due to the cover soil saturation. In addition, the point from May'13 for cell 2 was also excluded as it was measured right after the gas extraction and would represent a biased condition.

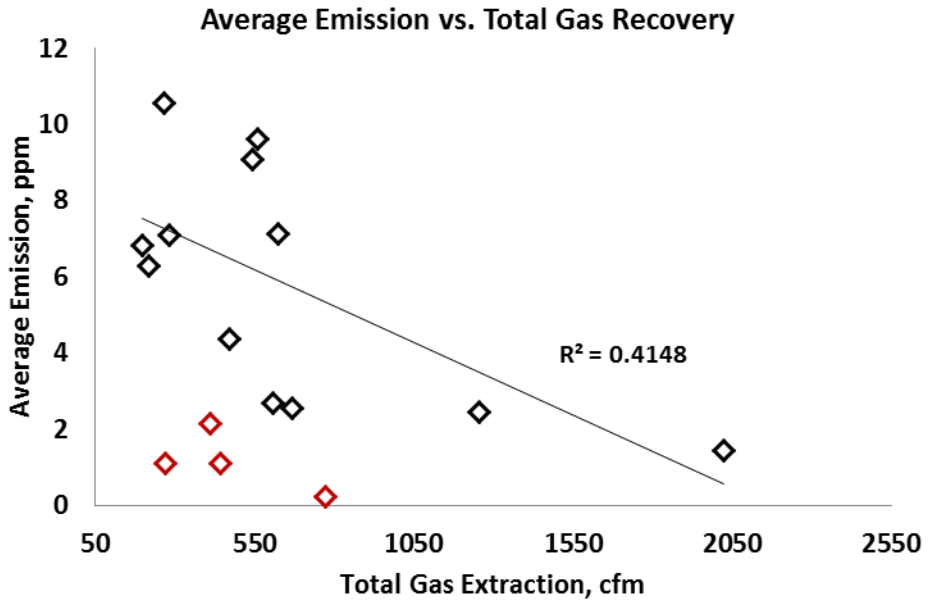

Figure 4.35 Average Emissions vs. Gas Recovery from Cell 2 and Cell 0

Based on the figures presenting the effect of gas extraction on methane emission from landfills it could be summarized as follows:

- The average emission showed an opposite trend with the gas extraction from the landfill cells;
- A considerable decrease in emission was noticed right after the gas extraction from the landfill
- The average emission showed a negative trend with gas recovery; the emission increased as the gas extraction decreased and vice versa.

4.5.4 Effect of Cover Soil

The cover soil used for the landfill cells were CL (LL: 33, PL: 17, PI: 16, Average Organic Content: 10.06% on top and 4.3% on the bottom). The thickness of the cover for cell 2 was 2ft and cell 0 was 10 ft. For the cells mulch was used on top of the soil covers.

For cell 2 the thickness of the mulch layer was 2 in and for cell 0, 1 ft (see Figure 3.12 for details). The overall emissions for the current study was comparatively lower than most of the previous studies on methane emission. The plausible reasons for the comparatively lower emissions could be accredited to: (1) the presence of gas collection system for both of the landfill cells or (2) the presence of mulch on the cover (as presented in Figure 4.36) which is also known as bio-cover system and reported to severely reduce the emission from the landfills.

Figure 4.36 Mulch Cover on the Slopes of the City of Denton Landfill

Yuan (2006) presented a comparison of surface emission for the presence of mulch layer on top of the landfill. The study shows thick mulch cover effectively reduces the surface emission from the landfill, as presented in Figure 4.37. For the current study, the methane emission measured from the landfill covers was comparatively lower than most of the studies have reported so far. The results obtained matches the methane emission results with emission from the deep mulch cover (<50 $g/m^2/day$).

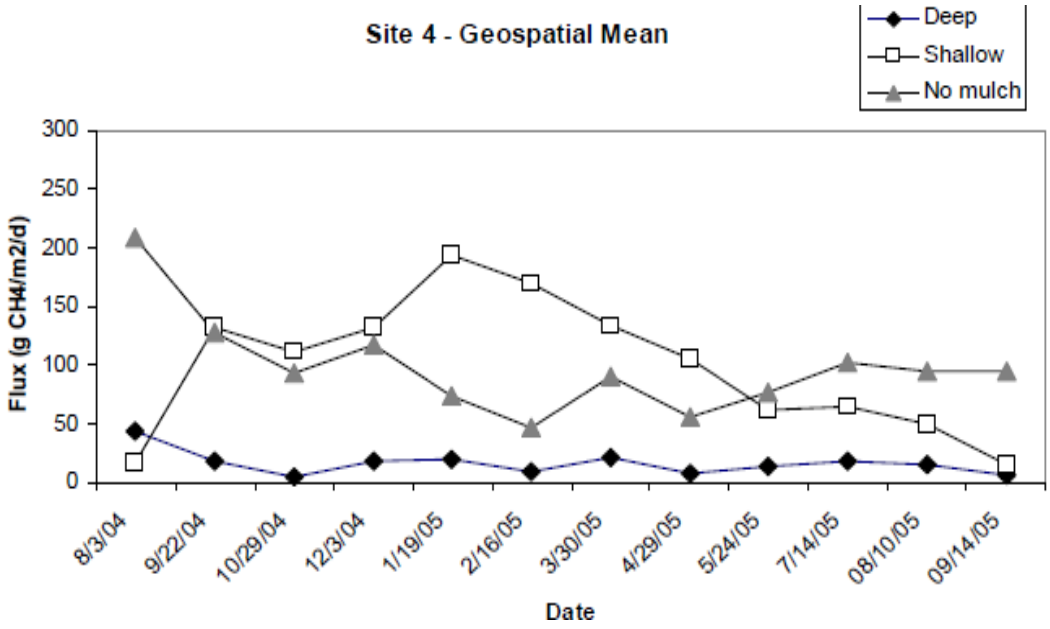

Figure 4.37 Effect of Mulch on Methane Emission (Yuan, 2006)

Similarly, Fleiger (2006) compared a control cell with a bio-cover cell as presented in Figure 4.38 and Figure 4.39. The study showed the bio cover helps reducing the surface emission from the landfills except few exceptions. However, the authors did not identify the reasons for the variability of emissions from the bio-cells and the sudden peaks in June/ July. The results obtained from the current study and the bio cover studies from Yuan (2006) and Fleiger (2006) showed similar methane flux from the landfills and based on the results it could be concluded that the overall low emission observed form the landfill study was due to the mulch or bio cover on the landfill cells. Bio cover or mulch increases the cover soil oxidation immensely and thus reduces the emission through the cover. Filed monitoring was continued to evaluate the soil gas profiles in the cover. In addition, to determine methane oxidation capacity of the cover soil an elaborate lab scale studies were undertaken and the results are presented in the following section.

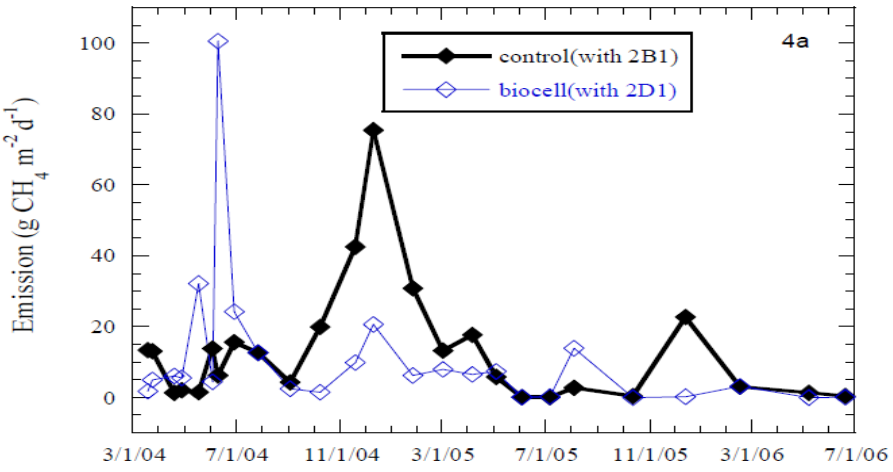

Figure 4.38 Comparison of Methane Emission from Control Cell and Bio-Cover Cell (Including all the Data points) (Fleiger 2006)

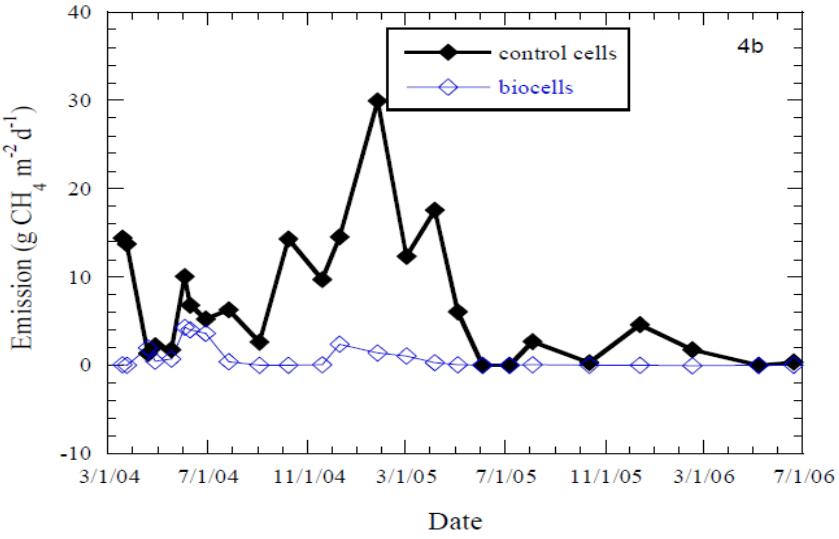

Figure 4.39 Comparison of Methane Emission from Control Cell and Bio-Cover Cell (Excluding the Outliers) (Fleiger 2006)

4.5.4.1 Soil Gas Profiles

Soil gas profiles provide an understanding of the methane generation and migration through the soil cover in the landfills. For the current study, three locations were selected to evaluate the soil gas behavior in cell 2. The study locations are included in chapter 3 as O1, O2 and O3. Figure 4.40 and Figure 4.41 present the methane concentrations at 1 ft and 2 ft depth for the three locations.

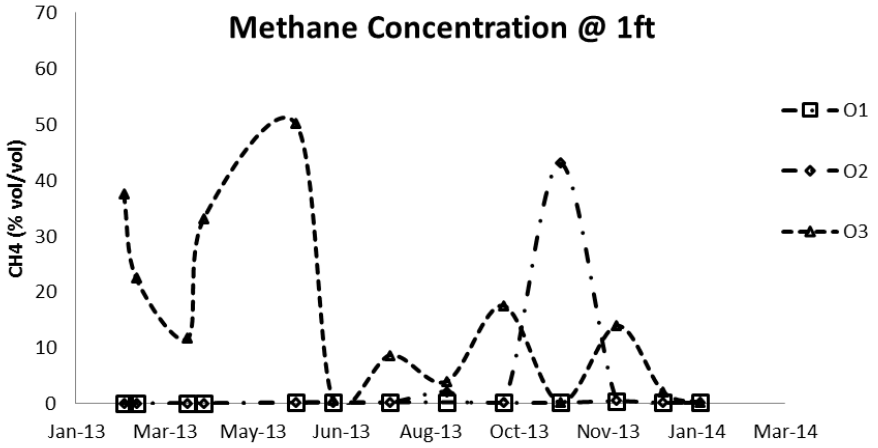

Figure 4.40 Methane Concentration at 1ft Depth for O1, O2 and O3 locations

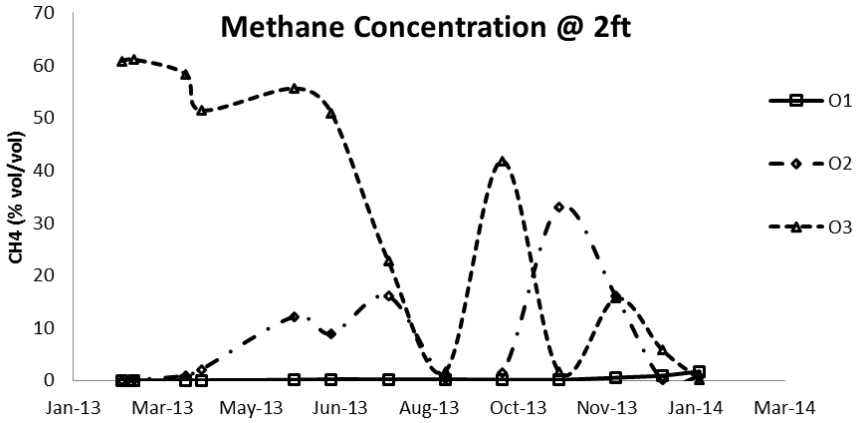

Figure 4.41 Methane Concentration at 2ft Depth for O1, O2 and O3 locations

Location O1 was near the recirculation pipe H2, the location O2 was in the crest of the slope near grid line K and the O3 was located near the grid line U and at the top surface. In all these three locations, a set of two pipes were installed respectively at 1 ft and 2 ft depth to monitor the variations in gas profile. The methane concentrations near 2 ft depth were anticipated to be the representation of generated gas below the soil cover (as the cover thickness of the intermediate cover was 2 ft). Consequently, higher gas concentrations from the 2 ft depth gas probes were expected. Due to the methane oxidation capacity of the cover soil, the methane concentration at the surface was lower than the 2 ft depth. On the other hand the O2 pipe was located near recirculating pipe H5 which was one of most recirculated pipe during the monitoring period. The consistent methane concentrations in 2 ft depth near O2 indicated a steady gas generation near that location. However, gas extraction rate this location was also very high which might have resulted into very low methane concentrations near the 1ft depth. It is to be noted the oxidation capacity of the cover might also have a substantial role in reducing the methane concentration from 2 ft to 1 ft depth. For the O3 pipe both 1 ft and 2 ft depth had very high methane concentrations and it is to be noted that no gas collection pipes were present adjacent to O3. The reasonable assumption behind the consistent high methane concentration in O3 might be lack of adequate gas extraction or suction present near the pipe.

From the figures, O3 showed consistently high methane emission at both 1 ft and 2 ft depth. For O2 a consistent concentration of methane was observed at 2 ft; however, at 1 ft depth most of the time no methane concentration was measured. And for o1 consistently less than 0.1 methane concentrations was observed at both 1 ft and 2 ft depth. Maximum water/ moisture were recirculated through the pipe H2 in the first few years and therefore; very high gas generation and consequently high gas concentrations

were expected from the O1 location. However, during the monitoring period leachate was recirculated through H2 only twice and amount of recirculation was not very high. In addition, the individual gas well data (the total gas recovery from H2 less than 30 cfm/ month) indicated very low gas generation near this pipe. Therefore, lower gas generation

Figure 4.42 presents the depth profile of methane concentration where methane concentration at the surface was measured using the portable FID and the gas concentration within the soil cover was measured from the gas pipes using the LandGEM 2000 plus.

Based on the concentration profiles presented in the figure higher methane concentrations were observed at the bottom of the intermediate cover, at 2 ft depth. And the methane concentration at the surface was very low compared to the methane concentration adjacent to waste in the landfill cell. The reduction in methane concentration from the bottom of the landfill cover to the surface indicated the oxidation within the cover soil. However, the rate or capacity of oxidation was unknown. The next section presents the oxidation capacity results conducted in the controlled temperature and moisture condition in the laboratory.

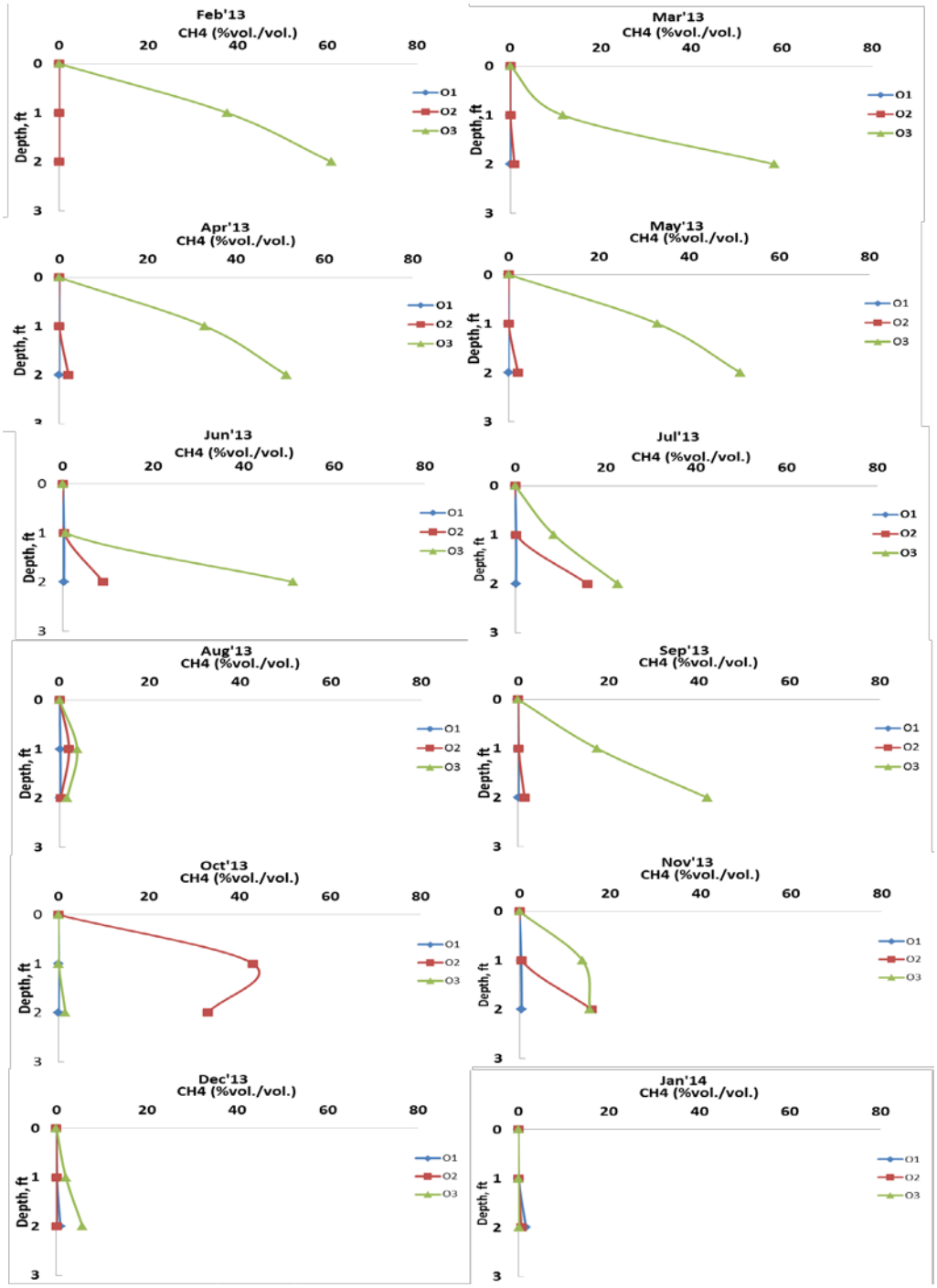

Figure 4.42 Depth Profile of Methane Concentration from O1, O2 and O3 locations

Based on the soil gas analysis from the probes the results could be summarized as:

- The methane concentration at the bottom of the cover was the maximum being adjacent to the waste layer. Therefore, the methane concentration at the bottom of the intermediate cover was representative of the corresponding gas generation of that location.
- The surface methane concentration substantially reduced from the bottom of the cover.
- The reduction in methane concentration from the bottom of the cover to the surface indicated the oxidation in the cover soil. However, based on the soil gas analysis the rate of oxidation could not be determined in the cover.

4.5.4.2 Methane Oxidation Results from Laboratory Tests

Methane oxidation capacity was determined using the batch experiments presented in the methodology section. The soil samples were retrieved from the cover of the landfill and were incubated in the required temperature, and moisture was adjusted to the dried soil samples by adding adequate water. Figure 4.43 presents the methane oxidation rate with varying moisture levels, and the tests were repeated with different temperatures. Based on the figure, the oxidation capacity showed a decreasing trend with increasing moisture content for all the temperatures of the samples that were tested. From the figure, the lowest oxidation rates were observed at 60°F and the maximum oxidation was observed at 70°F. The well-fitted trend of decreasing oxidation rate was observed for all the temperatures except 70°F. For 70°F, the methane oxidation rate was close to 500μmol CH_4/ gm dry soil/ day with varying moisture contents.

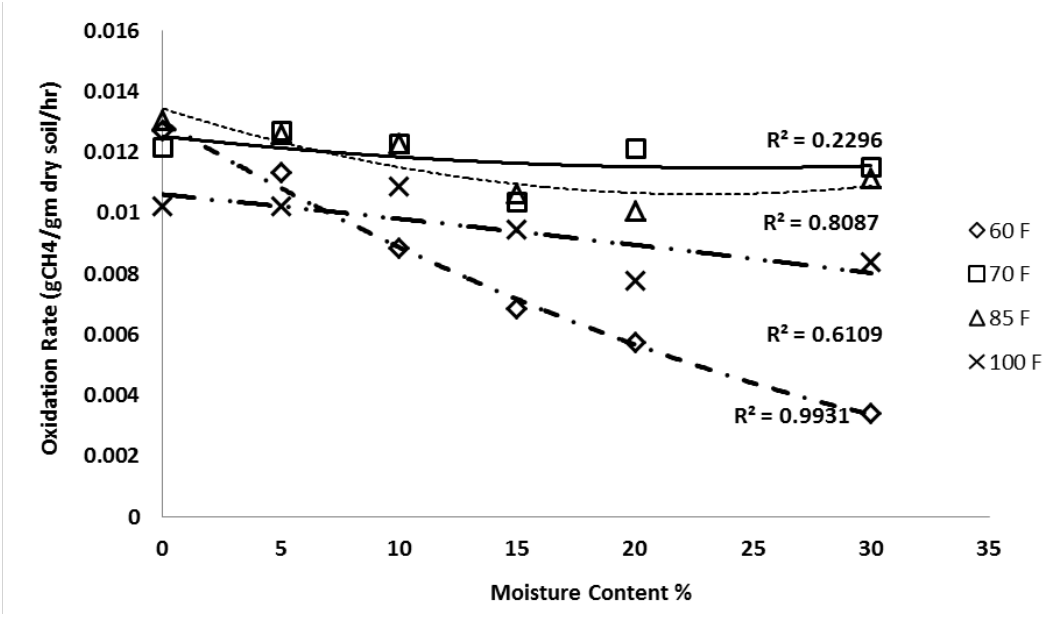

Figure 4.43 Methane Oxidation Results with Moisture Content

Figure 4.44 presents the study conducted by Borjesson et al. (1997) to evaluate the effect of moisture methane consumption or oxidation. However, the study was conducted on the collected sample without controlling the temperature. Based on the study, the oxidation or consumption rate was observed to decrease with increasing moisture, which was also similar to the current study.

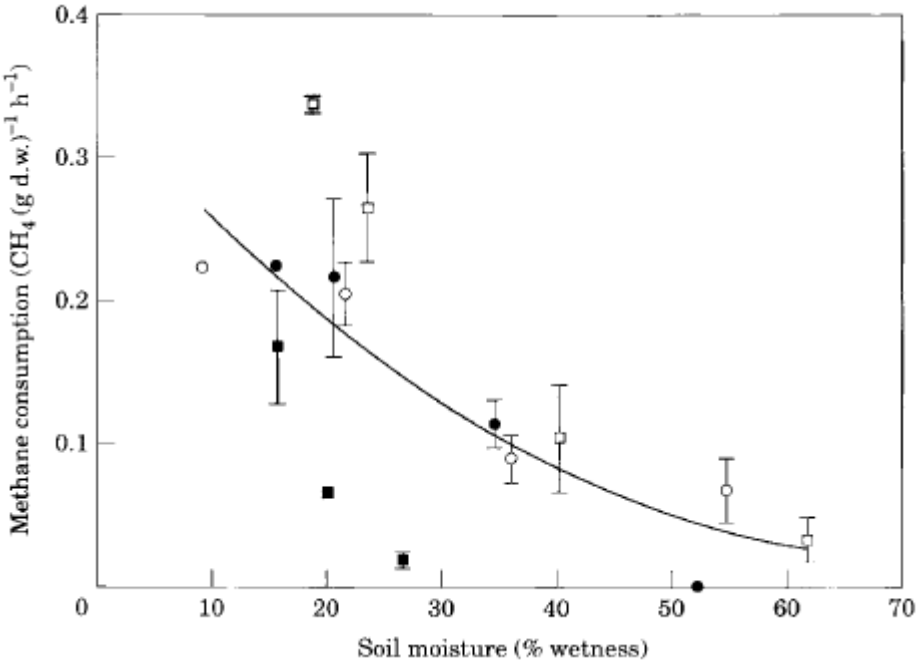

Figure 4.44 Methane Oxidation Results with Moisture Content (Borjesson et al., 1997)

Figure 4.45 presents the methane oxidation rate with varying temperatures. The methane oxidation was observed to reach the peak between 70°F and 85°F for different moisture contents of the soils. Initially, for all the soil samples, the oxidation rate increased with increasing temperature and started to decrease after the peak was reached.

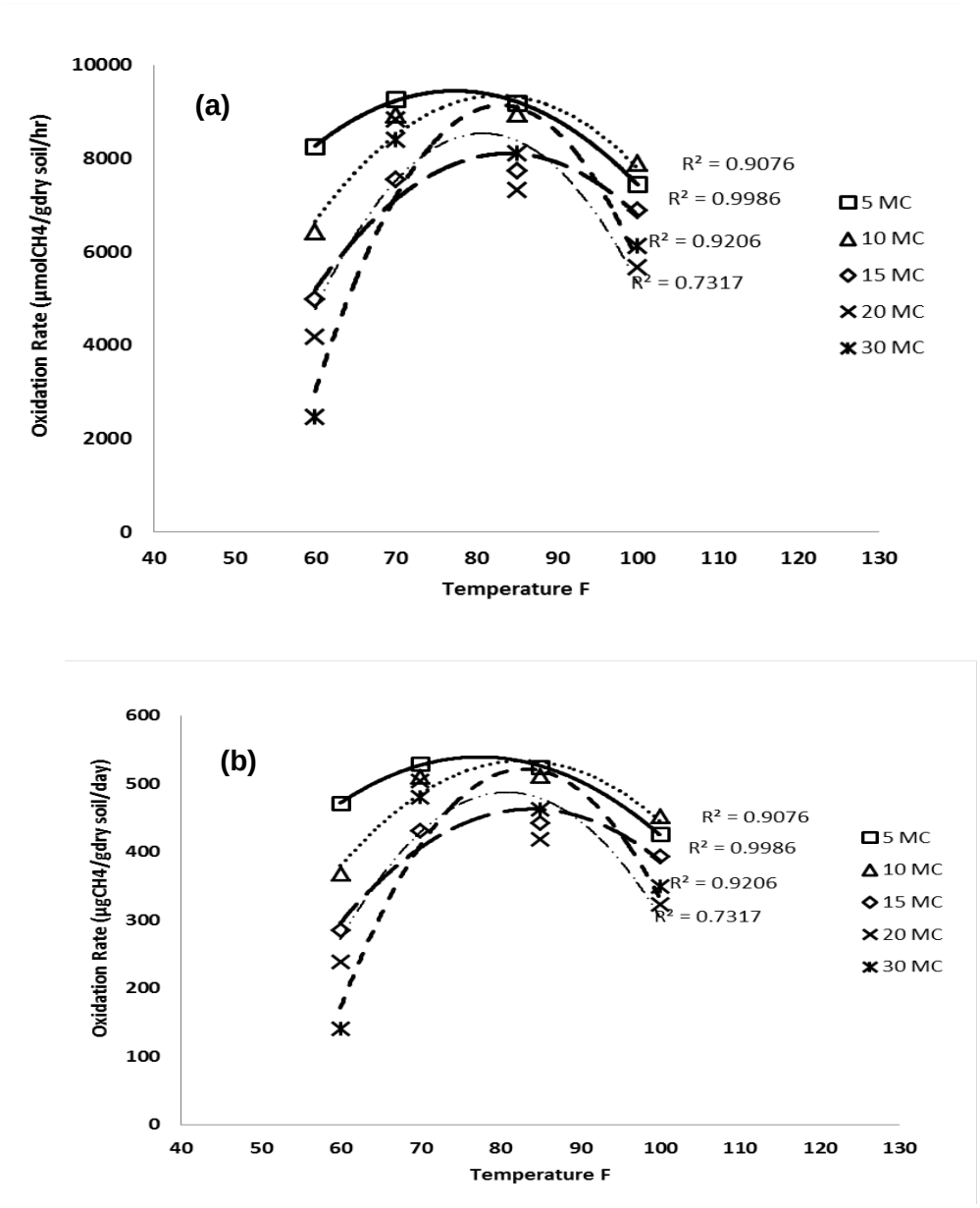

Figure 4.45 Methane Oxidation Results with Temperature (a) Oxidation Rate in nmol CH_4/g dry soil/day; (b) Oxidation Rate in µgCH_4/g dry soil/day

Figure 4.46 present the methane oxidation with change in temperature from a study conducted by Czpiel et al. (1996). Based on the study, the methane oxidation in the

cover increased with increase in temperature up to 36°C. Another study reported by Whalen et al. (1990) which showed an increasing trend in oxidation rate with temperature up to 32°C. The peak temperature reported by Czpiel et al. (1990) was less than the peak temperature reported by Whalen et al. (1990) which might be due to the variation in soil properties between the studies. According to the study, the oxidation rate decreased with increase in temperature after reaching the peak at 32°C.

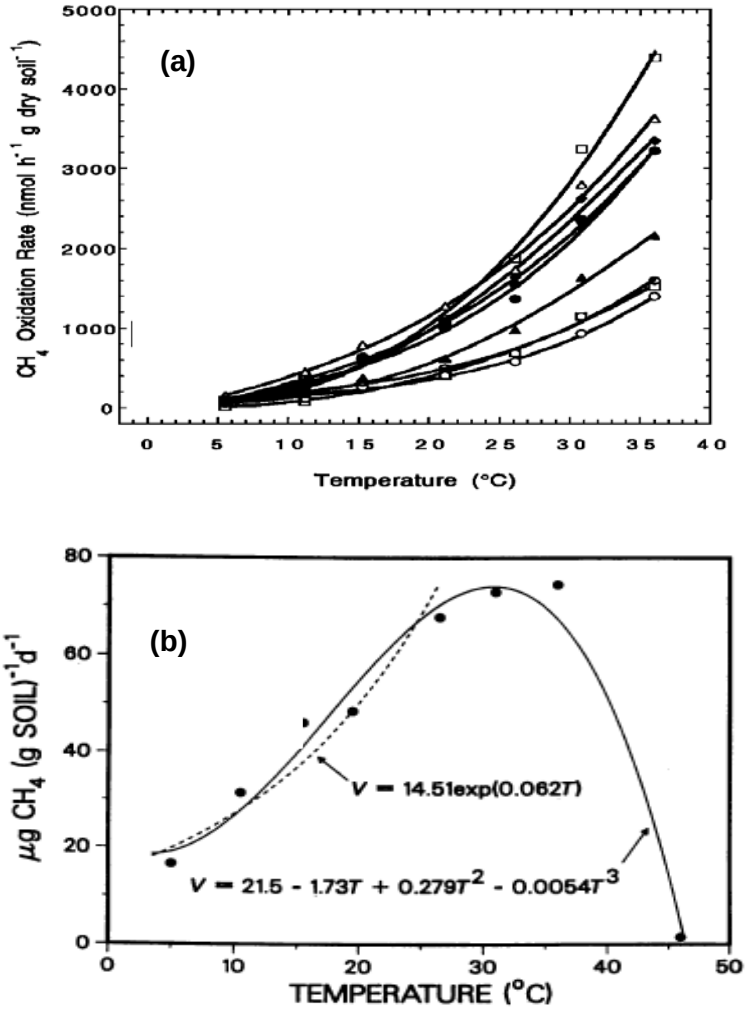

Figure 4.46 Methane Oxidation Results with Temperature (a) Study Conducted by Czpiel et al. (1996); (b) Study Conducted by Whalen et al. (1990)

The current investigation showed a similar trend and oxidation rate initially increased with temperature up to 75°F to 80°F (23°C to 27°C) and then decreased with increase in temperature. The peak temperature for the current study was observed to be less the previous studies reported which may be due to the different type of soil for cover.

4.5.4.3 Prediction of Methane Oxidation from the Laboratory Results

Based on the measured soil moisture content and soil temperature, methane oxidation rate for the landfill was predicted from the laboratory test results as presented in Table 4.4.

Table 4.4 Soil Temperatures, Moisture and Predicted Methane Oxidation for the Cover

Zone	Moisture Content of Soil (%)				
	February	April	August	October	December
1	18.12	9.88	8.30	7.35	18.29
2	18.02	17.21	16.50	11.58	18.89
3	13.52	14.02	11.20	8.56	17.54
Zone	Soil Temperature (°F)				
	February	April	August	October	December
1	53.5	63.4	62.7	65.0	47.0
2	56.5	67.7	62.8	68.5	55.9
3	51.5	58.9	69.4	70.0	46.2
Zone	Predicted Oxidation Rate (µgCH4/gm- dry soil/day)				
	February	April	August	October	December
1	116.98	422.60	414.17	505.25	284.73
2	193.16	386.71	332.98	473.44	179.96
3	157.89	281.05	481.15	485.49	49.69

Figure 4.48 presents the predicted methane oxidation, measured emission, and gas extraction results for the months of Feb'13, Apr'13, Aug'13, Oct'13 and Dec'13.

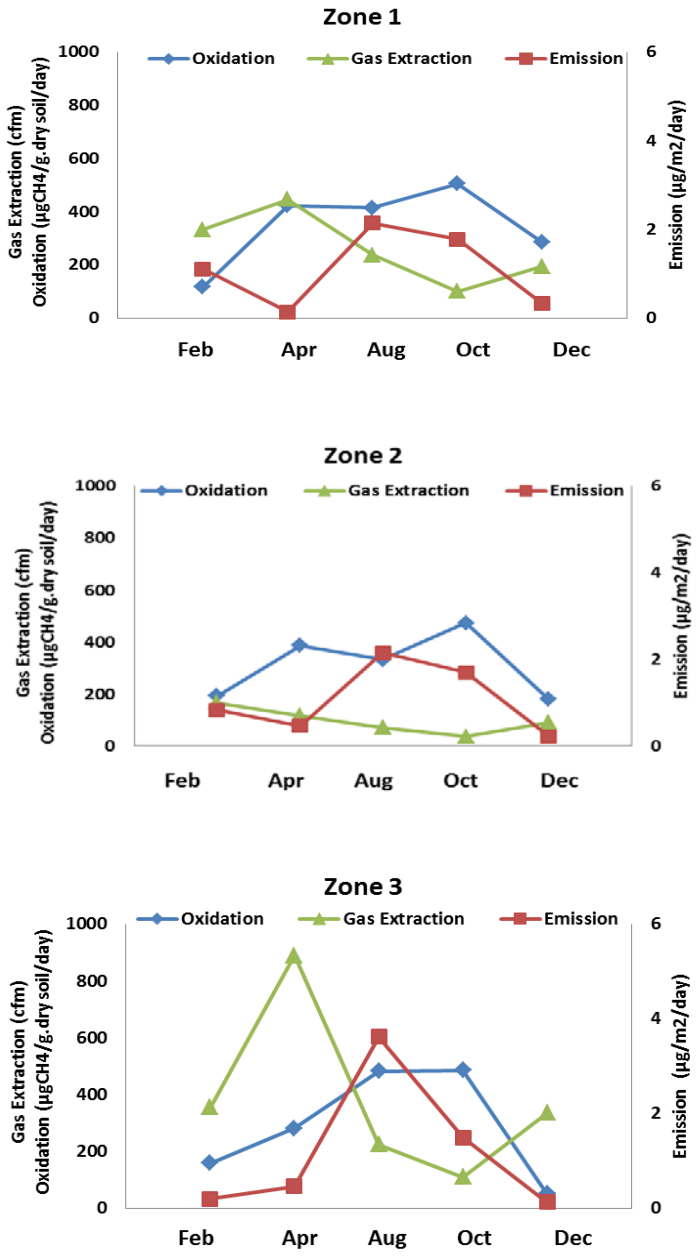

Figure 4.47 Predicted Oxidation, Emission and Gas Extraction

From the methane mass balance, when oxidation or gas recovery is low, the methane emission is expected to increase. For some of the cases, increase in oxidation

resulted in decrease in emission; however, the increase in oxidation did not always show decrease in emission from the landfill. It is to be mentioned that the compared oxidation rate estimated based on the laboratory test results were the maximum oxidation rate possible without the consideration of the gas extraction system for the cover soil present in the field. On other hand, the methane emission increased as gas extraction decreased and emission decreased as gas extraction increased from the landfill. Therefore, based on the results, emission was more governed by the gas extraction than oxidation.

Chapter 5

Methane Emission Model

5.1 Introduction

Methane emission is a complex process and depends on numerous variables, as reported previously. The non-homogeneity of the solid waste stream always creates uncertainty in predicting the gas generation, gas collection and emission from the landfills. The current available emission models are mostly gas generation-based models where the emissions from the landfills are anticipated to be directly correlated with the gas generation. The landfill cover system and the landfill gas collection system are proposed to mitigate the methane emission from the landfills; however, no systematic model has been developed considering the direct effect of gas extraction on the methane emission. In addition, no studies have evaluated the effect of leachate addition during landfill operation on emissions. Therefore, the objective of this chapter is to develop an emission model considering the effect of ELR operation and gas extraction in the landfill.

This chapter describes the procedure of developing the proposed methane emission model based on methane emission measurements from the City of Denton Landfill. This chapter is divided into two sections. The first section describes the assumptions made in development of the model, and the section includes the procedure for developing the multiple linear regression equation for predicting the methane emission depending on the temperature, precipitation, leachate recirculation and gas extraction data obtained during the field monitoring.

5.2 Model Development

Multiple linear regression (MLR) analysis was conducted using a statistical modelling tool SAS (2009), and the model assumptions were investigated to satisfy the model assumptions. The analysis steps followed to develop the MLR model on methane emissions are presented in Figure 5.1.

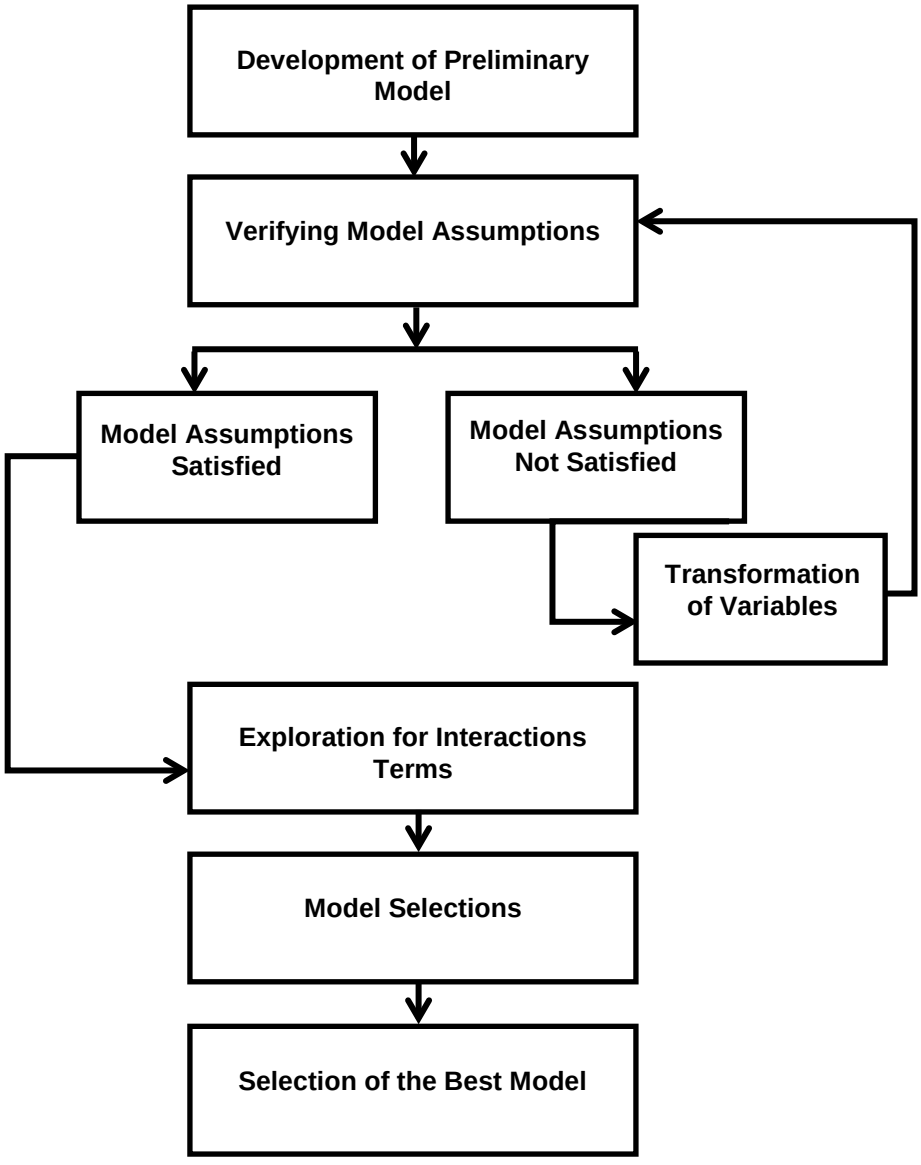

Figure 5.1 Flow Chart for MLR Model Development using SAS

5.2.1 Model Assumptions

(i) Parameters

The preliminary concern for the model development was to generate a methane emission model considering the effect of the ELR operation and the gas extraction. Therefore, only the ELR operated cell data were considered in the development of the emission model. The parameters considered to have effect on the methane emission were temperature, precipitation, water addition, gas extraction and oxidation in cover soil. Based on the mass balance equation, the total gas generation would be the summation of methane recovered/ extracted, methane emitted and methane oxidized (neglecting the methane storage in the waste).The predictor variables in the MLR model should not be correlated among themselves and the summation of the predictor variables cannot be 1 or 100% (Kutner et al., 2005). Therefore, both methane recovery and methane oxidation cannot be considered as predictor variables to develop the emission model. Since, the primary concern was to incorporate the effect of methane recovery on emission, the oxidation was not considered in the model development. Therefore, the predictor variables considered for the methane emission were:

- Temperature
- Precipitation + water addition
- Gas recovery/ extraction

(ii) Data Collection

The selected ELR-operated cell was monitored for a year for the current study. The methane emissions were monitored once a month around the middle of each month. The temperature was recorded during the emission monitoring from the field. However, the gas well data was collected from DTE and was only made available once in every

month. On the other hand, for the leachate recirculation in the landfill cell, there was no systematic plan for leachate injection in a month. Leachate was recirculated based on the gas extraction patterns and was injected to the corresponding location by the responsible person whenever they felt it necessary. Therefore, there was no standard injection plan for leachate recirculation in the landfill. The addition of leachate to the pipe was considered as monthly addition of leachate on that particular section. Based on the results presented in Chapter 4, it was observed that methane emission peaked around the recirculation pipes after 7 days of recirculation and ten returns to the previous condition. On the contrary, it was not possible to conduct methane emissions monitoring with a standard lag time between the leachate injection and monitoring methane emission, as the leachate injection plan was unknown. For the current model, total gas recovery and leachate recirculation were both monitored on a monthly basis. Therefore, to standardize all the predictor variables, the temperature and the precipitation were also considered from the monthly average. While the monitoring plan was observed monthly, 11 data sets were available from the current study for the EL- operated cell. However, the rule of thumb is to have at least 15 data points for the analysis. Therefore, the selected ELR-operated cell (cell 2) was divided into three different zones, depending on the operational practices (leachate recirculation frequency, and gas recovery). These zones were divided based on the leachate recirculation and are similar to the cells 2A, 2B and 2C for data collection. Zone 1 was considered from recirculation pipe H1 to H10, zone 2 from H11 to H20 and zone 3 from H21 to H36. During the first two years of recirculation, the largest amount of leachate was injected in zone 1. In more recent years, a larger amount of leachate was injected into zone 2 and zone 3. The highest amount of gas was recovered from zone 1, then from zone 2 and zone 3, respectively.

Figure 5.2 presents the layout of cell 2 with the boundaries of zone 1, zone 2 and zone 3.

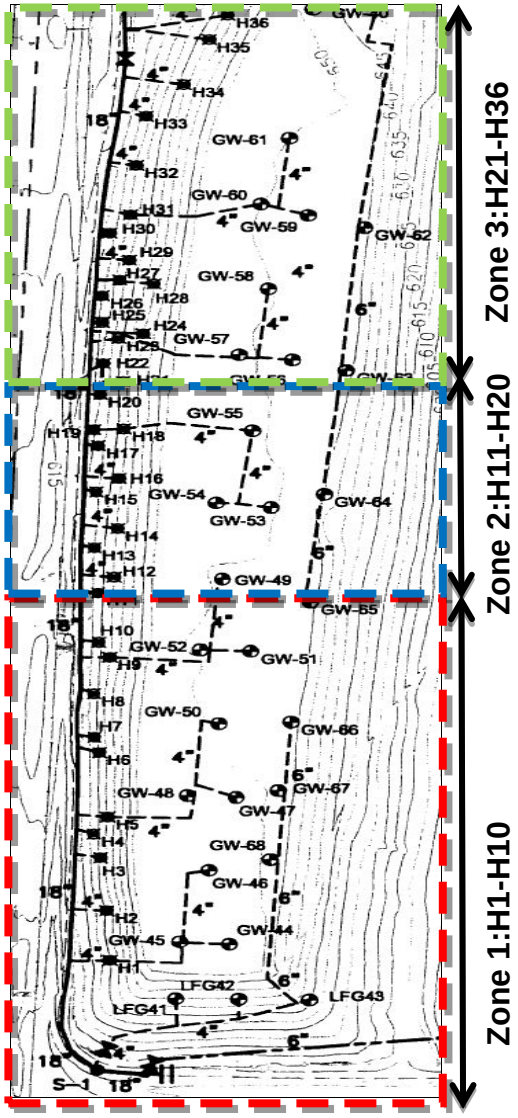

Figure 5.2 Locations of Zone 1, Zone 2 and Zone 3 in the ELR Operated Cell (Cell 2)

5.3 Multiple Linear Regression Analysis

This section includes a detailed description of the multiple linear regression analysis. Based on the field scale monitoring, a MLR equation was developed to predict the emission as a function of temperature, water addition (precipitation + leachate recirculation), gas recovery/ extraction.

5.3.1 Raw Data Plots and Correlation Analysis

5.3.1.1 Response Vs Predictor Plots

The response vs. predictor plots are used for studying whether a multiple linear regression form would be suitable for fitting the data. The response vs. predictor plots are presented in Figure 5.3.

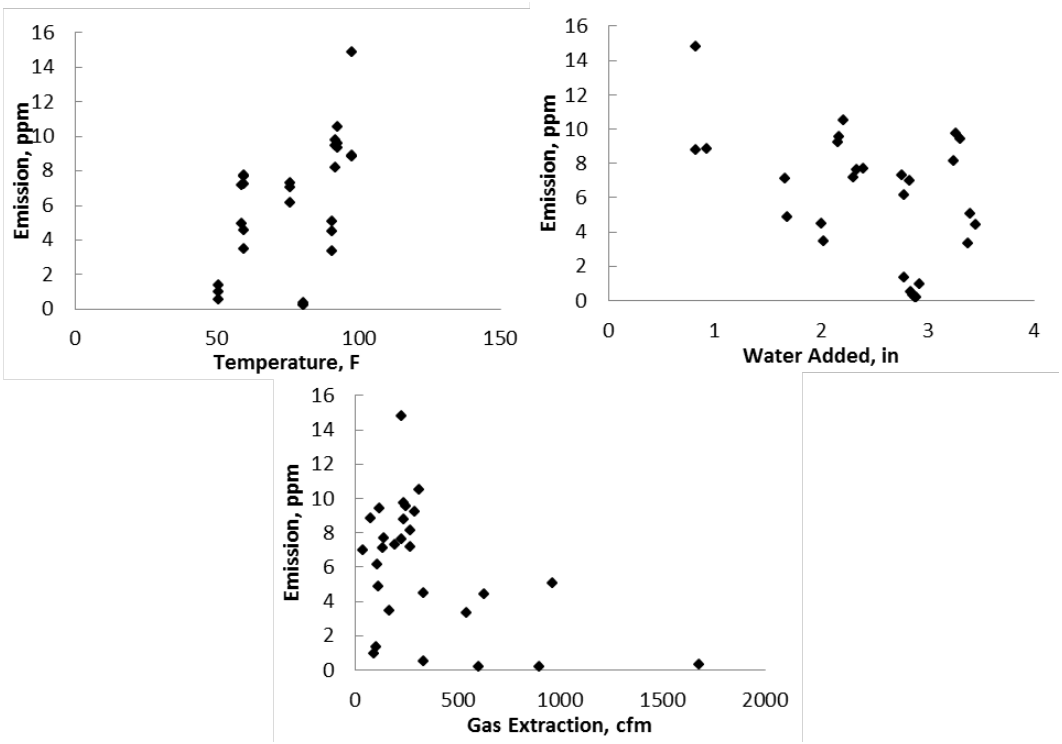

Figure 5.3 Response vs. Predictor Plots

It was observed that the emissions vs. temperature graph showed an increasing trend, while emissions vs. water addition showed an overall decreasing trend. Thus increase in temperature increased the surface methane concentrations, and increase in water addition decreased the surface methane concentrations. A decreasing was also observed in the emission vs. gas extraction plot, indicating the higher the gas recovery the lower the emissions would be.

5.3.1.2 Predictor Vs Predictor Plots

The predictor vs. predictor plot is presented in Figure 5.4.

The predictor vs. predictor plots help in exploring whether any predictors are linearly correlated with each other. The presence of any trends, upward or downward, in the plots indicates that the predictors are correlated to each other. Complications in the MLR analysis might occur if there is high multicolinearity between the predictor variables. Based on the plots, a slight upward trend was observed between water added and gas extraction. Hence, multicolinearity might be an issue for the present data set. The presence of extremely high multicolinearity indicates that two or more predictors are helping in explaining same variation in the response variable, leading to numerical issues in precisely predicting the appropriate estimated parameters. While multicolinearity is present in the data set, the variance of least square estimators are inflated and VIF values are high (<5).

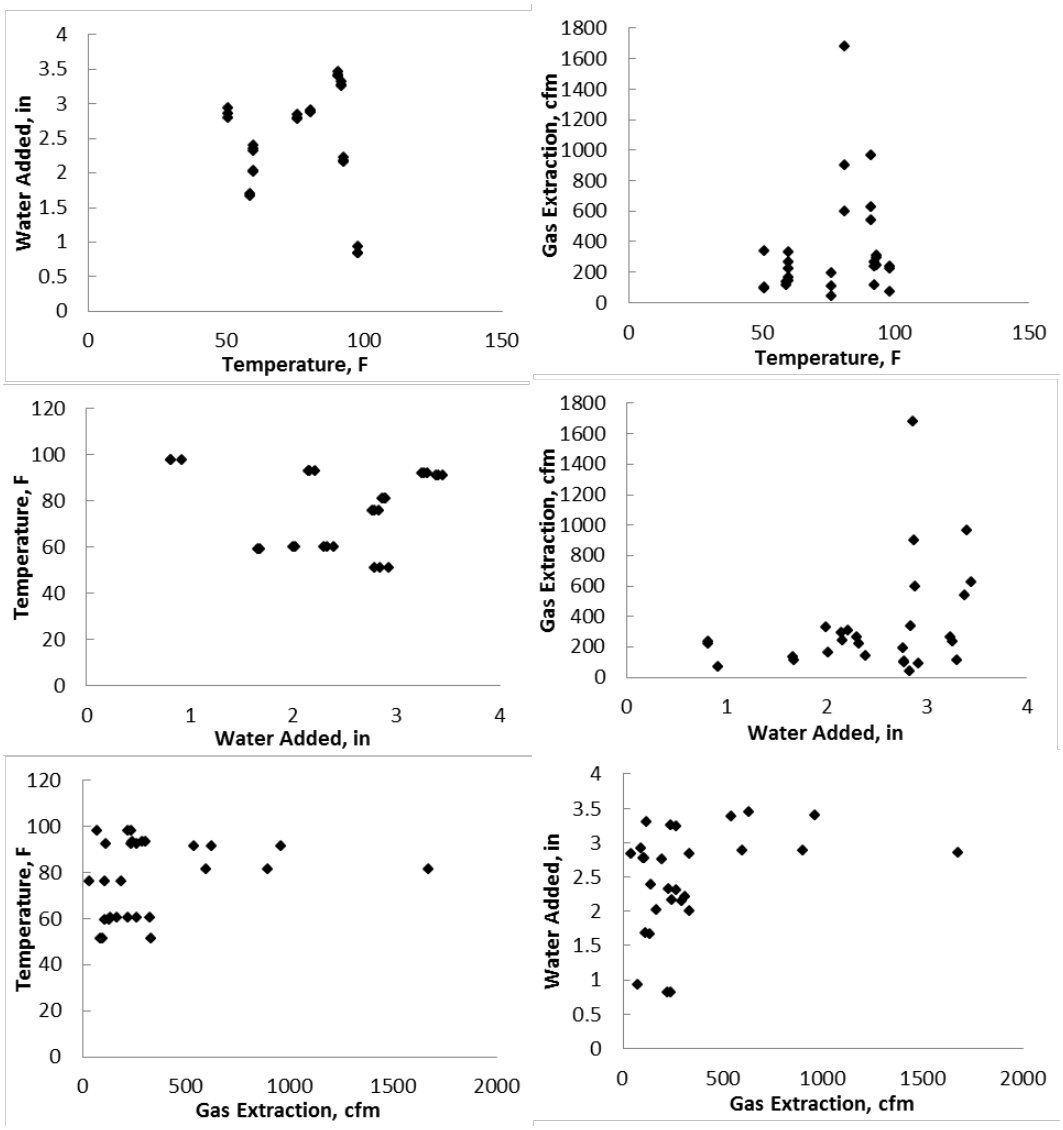

Figure 5.4 Predictor vs. Predictor Plots

5.3.1.3 Correlation Analysis

Correlation analysis helps in quantifying the liner association between two variables. Table 5.1 presents the Pearson's correlation coefficients computed for all response vs. predictor and predictor vs. predictor plots.

Pearson's correlation coefficient "r" ranges from -1 to +1, while -1 indicates strong negative correlation and the +1 indicates a strong positive correlation between the parameters. When r=0, little or no correlation is indicated between the parameters.

Table 5.1 Correlations Analysis for Raw Data

Pearson Correlation Coefficients, N = 28				
	Emission	**Temperature**	**Water Addition**	**Gas Extraction**
Emission	1.00000	0.51517	-0.45688	-0.45856
Temperature	0.51517	1.00000	-0.04401	0.22879
Water Addition	-0.45688	-0.04401	1.00000	**0.34242**
Gas Extraction	-0.45856	0.22879	**0.34242**	1.00000

From Table 5.2, the emissions are positively correlated with the temperature and negatively correlated with water addition and gas extraction. None of the r values were very high (r>0.7); however, the non- zero values indicated some correlations between the parameters. The r value between gas extraction and water addition was 0.34242, which indicated a possibility of multicolinearity between the parameters. However, if r<0.7 it could be assumed, then the multicolinearity would not be an issue for the data set.

5.3.2 Preliminary Multiple Linear Regression Equation

Initially an attempt was made to develop an MLR model as follows:

$$E = \beta_0 + \beta_1 T + \beta_2 W + \beta_3 G + \epsilon$$

Where,

E = Emissions (ppm)

T = Temperature (F)

W = Water Addition (in)

G = Gas Extraction or Recovery (cfm)

B_0, β_1, β_2, β_3 = correlation parameters to be determined from multiple regression. The preliminary model was developed using SAS, and the estimators for the model parameters are presented in Table 5.2.

Table 5.2 Parameter Estimates for the Preliminary MLR Model

Parameter Estimates						
Variable	**DF**	**Parameter Estimate**	**Standard Error**	**t Value**	**Pr > |t|**	**Variance Inflation**
Intercept	**1**	0.18926	2.63136	0.07	0.9433	0
Temperature	**1**	0.13905	0.02712	5.13	<.0001	1.07447
Water Addition	**1**	-1.24257	0.61559	-2.02	0.0548	1.15347
Gas Extraction	**1**	-0.00547	0.00137	-3.99	0.0005	1.21482

Based on the preliminary analysis, the fitted MLR equation is presented in equation 5.1.

E = 0.18926 + 0.13905T – 1.24257W – 0.00547G …….. (5.1)

Where,

E = Emissions (ppm)

T = Temperature (F)

W = Water Addition (in)

G = Gas Extraction or Recovery (cfm)

5.3.2.1 Checking Assumptions for the MLR Equation

The following assumptions have to satisfy any multiple linear regression (MLR) analysis to verify the model.

1. The model form is reasonable.

2. The residuals have constant variance.
3. The residuals are normally distributed.
4. The residuals are not auto correlated.

These assumptions can be verified by performing residual analysis. Residuals are the error terms or the difference between the predicted value and observed value for the response variable (emissions).

5.3.2.2 MLR Model Form is Reasonable

The MLR model form is assumed to be adequate when all the residuals versus predictor plots have no curvature in them. However, the plots are pretty scattered for the preliminary model, and no curvature was observed in the plots. Therefore, the model form was reasonable.

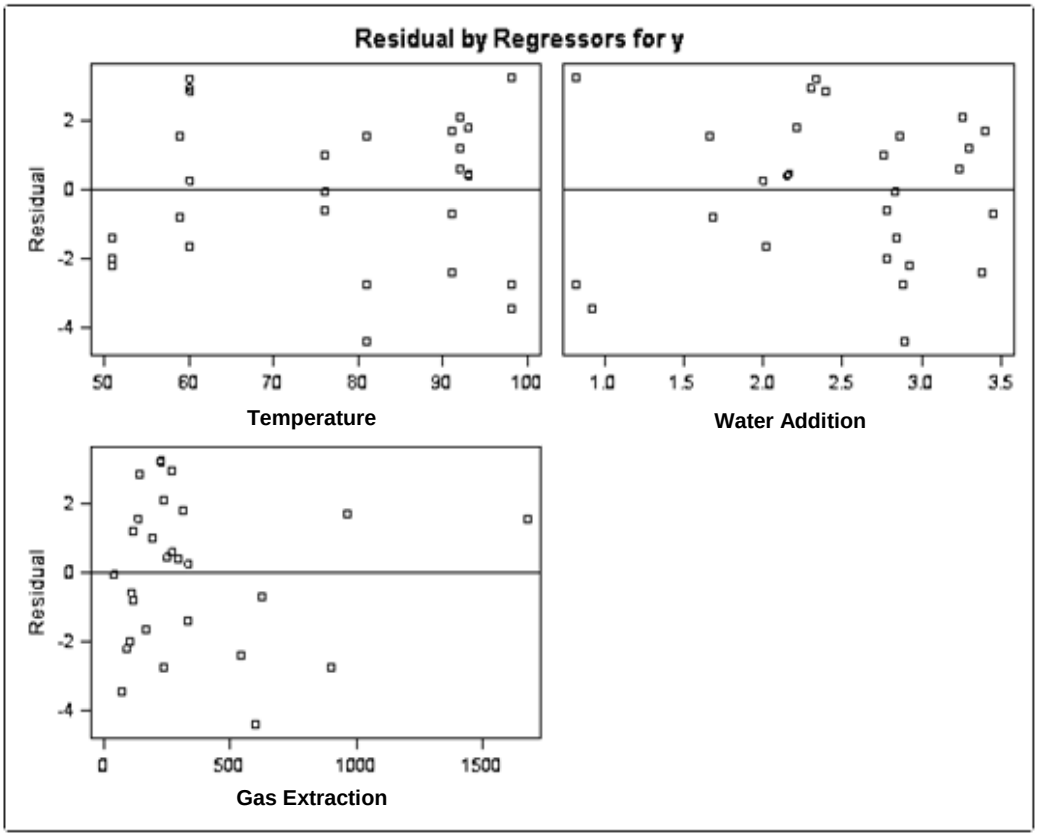

Figure 5.5 Residual vs. Predictor Plots for the Preliminary Model

5.3.2.3 Residuals have Constant Variance

The MLR model assumes that the errors have constant variance, which means when the residuals are plotted against the value of emission, they should be randomly scattered. The presence of a funnel shape indicates that variance is not constant and model form is not acceptable.

Figure 5.6 presents the residuals vs. predicted emission value for the preliminary model. Based on the plot, no funnel shape was observed which indicated that the residuals had a constant variance in the model. This assumption was further verified using the Modified-Levene test.

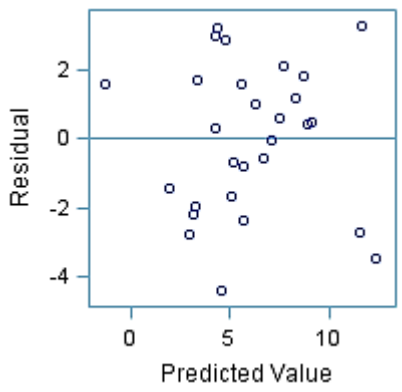

Figure 5.6 Residual vs. Predicted Emission Value for the Preliminary Model

5.3.2.4 Residuals are Normally Distributed

The MLR model assumes that the residuals are normally distributed. To check this assumption, residual vs. normal scores were plotted in Figure 5.7. A linear trend in residuals vs. the normal score plot indicates that the residuals are normally distributed. From the figure, the residuals displayed an S shaped, curved with shorter tails. Therefore, based on the plot it could be potentially concluded that the normality was violated.

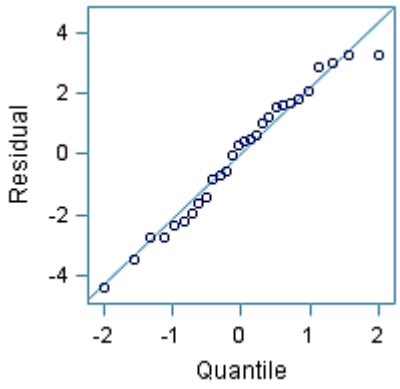

Figure 5.7 Normal Probability Plot for the Preliminary Model

However, the normality of the preliminary model was further verified using the normality test.

5.3.2.5 Modified-Levene Test for Checking Constant Variances

This test was performed to detect non-constant variance even when there is serious departure from normality. In order to conduct this test, the dataset was divided into two groups based on the fitted values, so that the number of observations in both the groups was approximately equal. In this case, the dividing point was chosen to be E = 5.6. This value was chosen as the dividing value because the number of observations in each group was equal to 14. The absolute division (d_{i1}, d_{i2}) of residuals around the medians was calculated for each group. The SAS output for conducting the Modified-Levene test, which uses two sample t-tests, is presented in Table 5.3.

The following hypotheses are considered for the Modified-Levene Test:

F-test Hypothesis:

H_0: Variances of the two populations (d_1, d_2) are equal.

H_1: Variances of the two populations (d_1, d_2) are not equal.

Considering $\alpha = 0.05$, from the table p value 0.5975> α. Hence, we fail to reject H_0, which means the variances of d_1 and d_2 are equal. Hence, the equal variance output from the t-test was referred for further analysis.

T-test Hypotheses:

H_0: Means of the two populations (d_1, d_2) are equal-hence the constant variance assumption is satisfied.

H_1: Means of the two populations (d_1, d_2) are not equal-hence the constant variance assumption is violated.

From the table p-value = 0.1509>α. Hence, we fail to reject H_0, and the constant variance assumption is satisfied.

Table 5.3 SAS Output for the Modified-Levene Tests for the Preliminary MLR Model

Obs	group	meand
1	1	2.08794
2	2	1.43008

The TTEST Procedure

Variable: d

group	N	Mean	Std Dev	Std Err	Minimum	Maximum
1	14	2.0879	1.0853	0.2901	0.4793	4.2034
2	14	1.4301	1.2604	0.3369	0.0253	3.8775
Diff (1-2)		0.6579	1.1761	0.4445		

group	Method	Mean	95% CL Mean		Std Dev	95% CL Std Dev	
1		2.0879	1.4613	2.7146	1.0853	0.7868	1.7485
2		1.4301	0.7023	2.1578	1.2604	0.9137	2.0306
Diff (1-2)	**Pooled**	0.6579	-0.2559	1.5716	1.1761	0.9262	1.6118
Diff (1-2)	**Satterthwaite**	0.6579	-0.2569	1.5726			

Method	Variances	DF	t Value	Pr > |t|
Pooled	Equal	26	1.48	0.1509
Satterthwaite	Unequal	25.439	1.48	0.1512

Equality of Variances				
Method	**Num DF**	**Den DF**	**F Value**	**Pr > F**
Folded F	13	13	1.35	0.5975

5.3.2.6 Test for Normality

For testing normality, the following hypotheses are considered.

H_0: Normality is satisfied.

H_1: Normality is violated.

The SAS output for correlation between residuals and normal scores is shown in Table 5.5. From the table, ρ (e, z) = 0.98807.

Considering α = 0.1, c(α, n) = c (0.1, 28) = 0.969

According to the decision rule, if ρ< c(α, n), then reject H_0.

From Table 5.4, ρ = 0.98807 > c(α, n) = 0.969 ; hence we fail to reject H_0. In this case, the test failed to conclude that the normality was violated. Hence, we conclude that the normality was satisfied for the preliminary model.

Table 5.4 SAS Output for Testing Normality for the Preliminary MLR Model

Pearson Correlation Coefficients, N = 28 Prob > |r| under H0: Rho=0		
	e	**enrm**
e Residual	1.00000	0.98807 <.0001
enrm Normal Scores	0.98807 <.0001	1.00000

5.3.2.7 Variance Inflation Factor (VIF)

This factor is used determine whether there is serious multicolinearity between the predictors. The VIF value identifies cases of high variance inflation due to complications caused by high multicolinearity. If the VIF value is more than 1, that indicates the multicolinearity exists; however, the multicolinearity may not be serious unless the VIF is less than 5. From the Table 5.5 it is clear that all the VIF values for the predictor variables were more than 1 but less than 5. Therefore, multicolinearity was present between the predictors; however, it might not pose a serious issue.

Table 5.5 SAS Output for Variance Inflation

Variable	**Variance Inflation**
Temperature	1.07447
Water Addition	1.15347
Gas Extraction	1.21482

5.3.2.8 Outliers

These are single data points that affect the trend of the grouped data by pulling it toward its position. The SAS output for checking the outliers are shown in Table 5.6.

Outliers may be X or Y outliers. The X outliers are identified by assessing the diagonal elements of the Hat- matrix (h_{ii}), which are also called leverage values. The cut off point for h_{ii} is 2p/n, where p is the number of parameters in the model and n is the total number of observations. In this MLR model, no X- outlier was observed.

The Y outliers are identified by assessing the studentized or deleted residuals, t_i, and the cut-off value are calculated based on Bonferroni Outlier test at α= 0.1 or 0.05. According to the Bonferroni outlier test, the cut-off points for Y-outliers were $|t_i|>t(1- \alpha/2n, n-p-1)$ = 3.104 and 3.768. No Y-outliers were detected based on cut-off points.

Table 5.6 SAS Output for Checking Outliers

Obs	Residual	RStudent	Hat Diag H	Cov Ratio	DFFITS
1	-1.8916	-1.0369	0.2265	1.4482	-0.7220
2	0.3322	0.1768	0.2208	2.0493	0.1215
3	-0.8475	-0.4275	0.2385	1.7338	-0.2393
4	-2.3123	-1.1237	0.1355	1.0604	-0.4450
5	1.3305	1.0436	0.2709	2.9497	1.4900
6	-4.3512	-2.2148	0.0770	0.3283	-0.6398
7	-2.7474	-1.3663	0.1510	0.8874	-0.5762
8	2.5273	1.7527	0.2394	1.1235	1.8967
9	-0.3137	-0.1552	0.2142	1.7758	-0.0810
10	-2.3204	-1.1381	0.1500	1.0669	-0.4781
11	-0.3967	-0.1876	0.1397	1.6156	-0.0756
12	-0.0659	-0.0304	0.1008	1.5644	-0.0102
13	0.9160	0.4385	0.1538	1.5552	0.1869
14	-2.5422	-1.4610	0.2565	1.0752	-1.0875
15	-0.9773	-0.8868	0.2576	4.4313	-1.5678
16	3.6298	2.1524	0.2274	0.4866	1.5016
17	0.1154	0.0552	0.1588	1.6709	0.0240
18	0.5503	0.2827	0.2693	1.8727	0.1716
19	1.5716	0.7700	0.1761	1.3921	0.3560
20	1.1878	0.5422	0.0647	1.3584	0.1426
21	0.1506	0.0695	0.0975	1.5565	0.0228
22	-0.3945	-0.1800	0.0763	1.5061	-0.0517
23	2.7470	1.3276	0.1054	0.8708	0.4557
24	2.9006	1.3950	0.0889	0.8063	0.4357
25	3.0932	1.4935	0.0844	0.7331	0.4533
26	-1.1521	-0.6178	0.2195	1.8113	-0.4233
27	-1.1355	-0.6621	0.2228	2.0944	-0.5666
28	0.3958	0.2401	0.2767	2.6351	0.2292

5.3.3 Exploring Possible Interaction Terms from plots

Interaction terms arise due to a combined effect of two predictor variables on the response. Three (3) possible interaction terms were considered in this study to explore the interactions between the three predictor variables. However, only a few interactions might be helpful for the model performance, by explaining any of the variabilities in the response that remained unexplained by the preliminary model. To explore the possibility of adding interaction terms, partial regression plots are used. Alternately, the standardized interaction term is plotted against the residuals to detect whether any interaction terms can help the model. For this, the predictors must first be standardized. Standardization is a procedure where the mean is centered by assigning it to zero, and the variance is scaled to one. Standardization helps in understanding a model which has predictors with different scales.

If a linear trend is observed in residual vs. standardized interaction term plot, then that interaction term is considered to be helpful to the MLR model. However, if the points are randomly scattered in the residual vs. standardized interaction plots, then the interaction terms might not be helpful. Figure 5.7 shows the residual plots with standardized residual vs. interaction plots. Based on the figure, none of the interaction terms showed any trend. Therefore, for further confirmation, the t-test was conducted to determine the possible interaction terms.

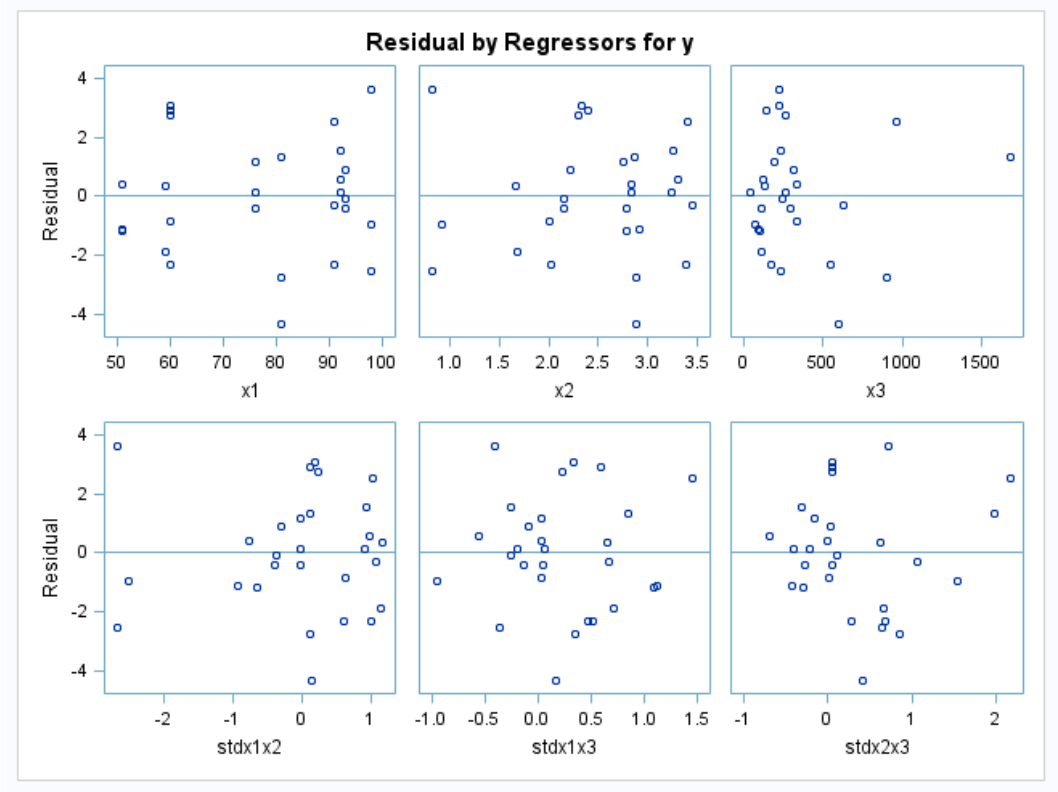

**Note: x1= Temperature, x2= Water Added, X3= Gas Extraction

Figure 5.7 Residual Plots

Table 56 presents the parameter estimates for the MLR model with the added interaction terms. However, the possible interactions terms were not standardized in the table. Table 5.7 presents the parameter estimates of the model with standardized interaction terms.

Based on the results presented in Table 5.8, all three interaction terms were significant at α=0.05 or α=0.10. However, the VIF values are extremely high for all the parameters of the model.

Table 5.7 SAS Output for Checking Possible Interaction Terms

Parameter Estimates						
Variable	**DF**	**Parameter Estimate**	**Standard Error**	**t Value**	**Pr > |t|**	**Variance Inflation**
Intercept	**1**	13.37025	9.65870	1.38	0.1808	0
Temperature (x1)	**1**	-0.04925	0.11243	-0.44	0.6659	19.17828
Water Added (x2)	**1**	-6.37382	3.89739	-1.64	0.1169	48.00356
Gas Extraction (x3)	**1**	0.00134	0.01729	0.08	0.9390	200.18726
x1x2	**1**	0.07195	0.04328	1.66	0.1113	60.98029
x1x3	**1**	0.00013290	0.00024732	0.54	0.5967	297.93360
x2x3	**1**	-0.00608	0.00485	-1.25	0.2243	156.08071

Table 5.8 presents the SAS output after standardizing the interactions terms.

Table 5.8 SAS Output for Checking Possible Interaction Terms

Parameter Estimates						
Variable	**DF**	**Parameter Estimate**	**Standard Error**	**t Value**	**Pr > |t|**	**Variance Inflation**
Intercept	**1**	1.27096	3.09933	0.41	0.6859	0
x1	**1**	0.17350	0.04274	4.06	0.0006	2.77080
x2	**1**	-2.88847	1.07302	-2.69	0.0137	3.63866
x3	**1**	-0.00337	0.00227	-1.49	0.1514	3.43933
stdx1x2	**1**	0.91504	0.55049	1.66	0.1113	1.96555
stdx1x3	**1**	0.77793	1.44770	0.54	0.5967	3.45294
stdx2x3	**1**	-1.62391	1.29704	-1.25	0.2243	4.59238

Based on the results presented in the table, all three interaction terms were significant at α=0.05 or α=0.10. In addition, due to standardization, all the VIF vales decreased substantially and less than 5; hence, this might not be an issue for

multicolinearity. Therefore, based on the t-test, all three interaction terms were considered for model search.

The presence of interaction terms in a model typically induces high multicolinearity, because the interaction terms may be correlated with the original predictors. Hence, it was necessary to check the Pearson's correlation matrix. Table 5.9 presents the Pearson's correlation matrix. If the correlation coefficient (r) had a value greater than 0.7, it meant that the variables were highly correlated and could induce high multicolinearity. The correlation coefficients greater than 0.7 were marked in the table.

Table 5.9 SAS Output for Correlation Analysis with the Added Interaction Terms

Pearson Correlation Coefficients, N = 28							
	Emission	**Temp**	**Water Addition**	**Gas Extraction**	**x1x2**	**x1x3**	**x2x3**
Emission	1.00000	0.51517	-0.45688	-0.45856	-0.12380	-0.38409	-0.49776
Temp	0.51517	1.00000	-0.04401	0.22879	0.46013	0.34109	0.22243
Water Addition	-0.45688	-0.04401	1.00000	0.34242	**0.85716**	0.34506	0.47541
Gas Extraction	-0.45856	0.22879	0.34242	1.00000	0.41884	**0.99037**	**0.98423**
x1x2	-0.12380	0.46013	0.85716	0.41884	1.00000	0.47826	0.53442
x1x3	-0.38409	0.34109	0.34506	**0.99037**	0.47826	1.00000	**0.98141**
x2x3	-0.49776	0.22243	0.47541	**0.98423**	0.53442	**0.98141**	1.00000

**x1x2= Temp x Water Addition; x1x3= Temp x Gas Extraction; x2x3= Water Addition x Gas Extraction

Table 5.10 presents the Pearson's correlation matrix after standardization. If the correlation coefficient (r) had a value greater than 0.7, it meant the variables were highly correlated and could induce high multicolinearity. No values were observed to be more than 0.7 after standardization. Therefore, standardization reduced the multicolinearity.

Table 5.10 SAS Output for Correlation Analysis after Standardization

Pearson Correlation Coefficients, N = 28							
	Emission	**Temp**	**Water Addition**	**Gas Extraction**	**stdx1x2**	**stdx1x3**	**stdx2x3**
Emission	1.00000	0.51517	-0.45688	-0.45856	-0.27890	-0.62022	-0.17814
Temp	0.51517	1.00000	-0.04401	0.22879	-0.21501	-0.52709	0.31170
Water Addition	-0.45688	-0.04401	1.00000	0.34242	0.66308	0.40122	-0.16820
Gas Extraction	-0.45856	0.22879	0.34242	1.00000	0.20221	0.37821	0.69724
stdx1x2	-0.27890	-0.21501	0.66308	0.20221	1.00000	0.43480	-0.08262
stdx1x3	-0.62022	-0.52709	0.40122	0.37821	0.43480	1.00000	0.27914
stdx2x3	-0.17814	0.31170	-0.16820	0.69724	-0.08262	0.27914	1.00000

**x1x2= Temp x Water Addition; x1x3= Temp x Gas Extraction; x2x3= Water Addition x Gas Extraction

5.3.4 MLR Model Search

The MLR model search is the step where potential good models are identified. Parameters which have an insignificant effect on the model are removed in this step. Three methods, backward deletion, best subsets and stepwise regression, were used for the MLR model search. The best MLR model was identified based on the results from all three methods.

Based on the previous analysis, six predictor variables (temperature, water addition, gas extraction, stdx12, stdx1x3 and stdx2x3) were considered for the model search for predicting methane emission from the landfills.

5.3.4.1 Backward Elimination Method for Model Search

Backward elimination method for MLR model search uses an iterative process, where regression is conducted by including all possible variables in the model and the

predictor variables are statistically significant. The SAS output for the iterations using the backward elimination method and summary are shown in Table 5.11 and Table 5.12.

Table 5.11 Backward Elimination Steps

Backward Elimination: Step 0

All Variables Entered: R-Square = 0.7234 and C(p) = 7.0000

Analysis of Variance

Source	DF	Sum of Squares	Mean Square	F Value	Pr > F
Model	6	272.31689	45.38615	9.15	<.0001
Error	21	104.14455	4.95926		
Corrected Total	27	376.46144			

Variable	Parameter Estimate	Standard Error	Type II SS	F Value	Pr > F
Intercept	1.27096	3.09933	0.83396	0.17	0.6859
x1	0.17350	0.04274	81.74145	16.48	0.0006
x2	-2.88847	1.07302	35.93658	7.25	0.0137
x3	-0.00337	0.00227	10.99461	2.22	0.1514
stdx1x2	0.91504	0.55049	13.70282	2.76	0.1113
stdx1x3	0.77793	1.44770	1.43199	0.29	0.5967
stdx2x3	-1.62391	1.29704	7.77375	1.57	0.2243

Bounds on condition number: 4.5924, 119.16

Table 5.11-Continued

Backward Elimination: Step 1

Variable stdx1x3 Removed: R-Square = 0.7196 and C(p) = 5.2888

Analysis of Variance

Source	DF	Sum of Squares	Mean Square	F Value	Pr > F
Model	5	270.88490	54.17698	11.29	<.0001
Error	22	105.57654	4.79893		
Corrected Total	27	376.46144			

Variable	Parameter Estimate	Standard Error	Type II SS	F Value	Pr > F
Intercept	2.03098	2.71284	2.68972	0.56	0.4620
x1	0.15620	0.02764	153.21125	31.93	<.0001
x2	-2.62270	0.93672	37.62012	7.84	0.0104
x3	-0.00346	0.00222	11.63712	2.42	0.1337
stdx1x2	0.93152	0.54067	14.24481	2.97	0.0989
stdx2x3	-1.24746	1.07379	6.47680	1.35	0.2578

Bounds on condition number: 3.4213, 63.486

Table 5.11-Continued

Backward Elimination: Step 2

Variable stdx2x3 Removed: R-Square = 0.7024 and C(p) = 4.5948

Analysis of Variance

Source	DF	Sum of Squares	Mean Square	F Value	Pr > F
Model	4	264.40810	66.10202	13.57	<.0001
Error	23	112.05334	4.87188		
Corrected Total	27	376.46144			

Variable	Parameter Estimate	Standard Error	Type II SS	F Value	Pr > F
Intercept	1.32821	2.66456	1.21053	0.25	0.6229
x1	0.14943	0.02723	146.73894	30.12	<.0001
x2	-2.00696	0.77820	32.40325	6.65	0.0168
x3	-0.00554	0.00134	83.70990	17.18	0.0004
stdx1x2	0.82586	0.53700	11.52264	2.37	0.1377

Bounds on condition number: 1.9482, 24.852

Table 5.11-Continued

Backward Elimination: Step 3

Variable stdx1x2 Removed: R-Square = 0.6717 and C(p) = 4.9182

Analysis of Variance

Source	DF	Sum of Squares	Mean Square	F Value	Pr > F
Model	3	252.88546	84.29515	16.37	<.0001
Error	24	123.57598	5.14900		
Corrected Total	27	376.46144			

Variable	Parameter Estimate	Standard Error	Type II SS	F Value	Pr > F
Intercept	0.18926	2.63136	0.02664	0.01	0.9433
x1	0.13905	0.02712	135.37881	26.29	<.0001
x2	-1.24257	0.61559	20.97888	4.07	0.0548
x3	-0.00547	0.00137	81.85965	15.90	0.0005

Bounds on condition number: 1.2148, 10.328

Table 5.11-Continued

Backward Elimination: Step 4

Variable x2 Removed: R-Square = 0.6160 and C(p) = 7.1484

Analysis of Variance

Source	DF	Sum of Squares	Mean Square	F Value	Pr > F
Model	2	231.90658	115.95329	20.05	<.0001
Error	25	144.55486	5.78219		
Corrected Total	27	376.46144			

Variable	Parameter Estimate	Standard Error	Type II SS	F Value	Pr > F
Intercept	-3.09719	2.19058	11.55869	2.00	0.1697
x1	0.14637	0.02848	152.74612	26.42	<.0001
x3	-0.00648	0.00136	131.99465	22.83	<.0001

Bounds on condition number: 1.0552, 4.221

Table 5.12 Summary of Backward Elimination

Summary of Backward Elimination

Step	Variable Removed	Number Vars In	Partial R-Square	Model R-Square	C(p)	F Value	Pr > F
1	stdx1x3	5	0.0038	0.7196	5.2888	0.29	0.5967
2	stdx2x3	4	0.0172	0.7024	4.5948	1.35	0.2578
3	stdx1x2	3	0.0306	0.6717	4.9182	2.37	0.1377
4	x2	2	0.0557	0.6160	7.1484	4.07	0.0548

Based on the tables presented above, two models were selected as the possible best models, as highlighted in texts (see Table 5.11). Model 1 had 5 variables

(temperature, water addition, gas extraction, stdx1x2, and stdx2x3), and Model 2 had 4 variables (temperature, water addition, gas extraction, and stdx1x2).

5.3.4.2 Stepwise Regression Method for Model Search

The stepwise regression method uses backward elimination and forward selection methods for evaluating the best MLR model. This method also uses an iterative approach, starting with no variables and then adding variables in a step-by-step approach.

The SAS output for the iterations, using the stepwise regression method and summary, are shown in Table 5.13 and Table 5.14.

Table 5.13 Stepwise Regression Method

Stepwise Selection: Step 1

Variable stdx1x3 Entered: R-Square = 0.3847 and C(p) = 22.7097

Analysis of Variance

Source	DF	Sum of Squares	Mean Square	F Value	Pr > F
Model	1	144.81546	144.81546	16.25	0.0004
Error	26	231.64598	8.90946		
Corrected Total	27	376.46144			

Variable	Parameter Estimate	Standard Error	Type II SS	F Value	Pr > F
Intercept	6.93240	0.60932	1153.25742	129.44	<.0001
stdx1x3	-4.21002	1.04425	144.81546	16.25	0.0004

Bounds on condition number: 1, 1
All variables left in the model are significant at the 0.0500 level.

Table 5.14 Summary of Stepwise Regression Method

Summary of Stepwise Selection								
Step	**Variable Entered**	**Variable Removed**	**Number Vars In**	**Partial R-Square**	**Model R-Square**	**C(p)**	**F Value**	**Pr > F**
1	stdx1x3		1	0.3847	0.3847	22.7097	16.25	0.0004

Based on the stepwise regression, only one model was found significant at the 0.05 significance level. Therefore, no model was chosen based on the stepwise regression method.

5.3.4.3 Best Subset Method for MLR Model Search

The best subset method helps to evaluate which predictor variables should be included in the MLR model. This method provides the specified number of best models with one or more variables. In this case, the best subsets method was run several times, starting from one predictor variable until all the predictor variables were included in the model.

Table 5.15 shows the output for the best subset method for MLR model selection.

Table 5.15 SAS Output for Best Subset Method for MLR Model Selection

Number in Model	Adjusted R-Square	R-Square	C(p)	AIC	SBC	Variables in Model
1	**0.3610**	0.3847	22.7097	63.1642	65.82857	stdx1x3
1	**0.2371**	0.2654	31.7642	68.1252	70.78960	x1
2	**0.5853**	0.6160	7.1484	51.9607	55.95734	x1 x3
2	**0.4106**	0.4543	19.4246	61.8020	65.79860	x1 x2
3	**0.6307**	0.6717	4.9182	49.5702	54.89907	x1 x2 x3
3	**0.5970**	0.6418	7.1939	52.0173	57.34611	x1 x2 stdx2x3
4	**0.6506**	0.7024	4.5948	48.8296	55.49060	x1 x2 x3 stdx1x2
4	**0.6345**	0.6886	5.6353	50.0902	56.75125	x1 x2 stdx1x2 stdx2x3
5	**0.6558**	0.7196	5.2888	49.1625	57.15571	x1 x2 x3 stdx1x2 stdx2x3
5	**0.6351**	0.7027	6.5675	50.7958	58.78904	x1 x2 x3 stdx1x2 stdx1x3
6	**0.6443**	0.7234	7.0000	50.7801	60.10554	x1 x2 x3 stdx1x2 stdx1x3 stdx2x3
5	**0.6558**	0.7196	5.2888	49.1625	57.15571	x1 x2 x3 stdx1x2 stdx2x3
4	**0.6506**	0.7024	4.5948	48.8296	55.49060	x1 x2 x3 stdx1x2

The best possible options were selected from the table based on the above stated criteria. The selected two models were similar to the models selected from the backward elimination model.

5.3.5 Best MLR Model Selection

Based on all three methods mentioned above, the selected best MLR models are listed in Table 5.16.

The following criteria were used for selecting the best models:

- R^2 should be high. The coefficient of determination (R^2) is a measure used to describe how well a particular model fits the data. Usually, R^2 never decreases as the number of predictors in the MLR model increase, giving potentially false impression that one should have as many predictors in the model as possible. In practice, the smallest model that yields the highest R^2 is desired.

- Adjusted R^2 should be high. Adjusted coefficients of determination (R^2) penalize the addition of useless variables. Again, in practice, the smallest model with the highest R^2 is desired.

- Mallows C_p value should be small or close to the number of parameters in the model. If it has no bias, or if the model has all the significant parameters included in it, then the C_p value is small; hence, it is used as a criterion for the best MLR model selection.

- Akaike Information Criterion (AIC) or Schwarz Bayesian Criterion (SBC) should be minimized. AIC and SBC are the measures of relative goodness of fit for any MLR model. Hence, AIC and SBC are considered for model selection.

Table 5.16 Selected Models for Best MLR Model Selection

No. of Variables	Variables in Model	R_{adj}^2	R^2	C_p	AIC	SBC
4	**Temperature, Water Addition, Gas Extraction, stdx1x2**	**0.6506**	**0.7024**	**4.5948**	**48.8296**	**55.49060**
5	**Temperature, Water Addition, Gas Extraction, stdx1x2, stdx2x3**	**0.6558**	**0.7196**	**5.2888**	**49.1625**	**57.15571**

Therefore, comparing the two possible models, the model with 4 variables was chosen as the best model.

Table 5.17 presents the parameter estimates for the best model.

Table 5.17 Parameter Estimate for the Selected MLR Model

Parameter Estimates						
Variable	DF	Parameter Estimate	Standard Error	t Value	Pr > |t|	Variance Inflation
Intercept	1	1.32821	2.66456	0.50	0.6229	0
Temperature	1	0.14943	0.02723	5.49	<.0001	1.14487
Water Addition	1	-2.00696	0.77820	-2.58	0.0168	1.94820
Gas Extraction	1	-0.00554	0.00134	-4.15	0.0004	1.21601
stdx1x2	1	0.82586	0.53700	1.54	0.1377	1.90401

The selected MLR model is shown below:

$$E = 1.32821 + 0.1493\ T - 2.0069\ W - 0.00554\ G + 0.82586\ std(T \times W)$$

…… (5.2)

Where,

E = Average CH_4 Emissions (ppm)

T = Temperature (ºF)

W = Water Addition = Total Precipitation (inch) + Total Water/Leachate Addition (inch)

G = Total Gas Extraction (cfm)

std (TxW) = std T x std W = $\left(\frac{T-77.3}{16.7}\right)\left(\frac{W-2.5}{0.9}\right)$

5.3.6 Final MLR Model

The final MLR equation is as follows:

$$E = 18.84246 - 0.07714\ T - 9.0126\ W - 0.00554\ G + 0.09063\ (T \times W)$$

…… (5.3)

The model assumptions were re-verified using SAS analysis output. The verification of the final model is included in Appendix C.

5.3.7 3D Plots Showing the Effect of the Predictor Variables on Emissions

Based on the final MLR model equation developed, interaction plots were developed. The developed MLR model has 4 variables including the response variable (emission); therefore, to plot a 3rd interaction diagram one of the variable has to be assumed as constant.

Section 5.3.7.1 presents the combined effect of water addition and temperature on emission in constant temperatures. Section 5.3.7.2 presents the combined effect of gas recovery and temperature on emissions in constant gas recovery, and section 5.3.7.3 presents the combined effect of gas recovery and water addition on emissions in constant temperatures.

5.3.7.1 Effect of Temperature and Moisture in Constant Gas Recovery

Figure 5.8 through Figure 5.11 presents the 3D plots on the combined effect of temperature and water addition while the total gas extraction rate was assumed to be constant. The total gas extraction was assumed to 350 cfm, 700 cfm, 1500 cfm and 3000 cfm for the Figure 5.8, Figure 5.9, Figure 5.10, and Figure 5.11, respectively.

Based on the plots, when the water addition and gas recovery was constant, the emissions increased with the temperature. In addition, when the temperature and water addition were similar, the emissions decreased with increasing gas recovery. On the other hand, when the gas recovery and the temperature were constant, no change in emissions was observed.

5.3.7.2 Effect of Gas Recovery and Temperature in Constant Water Addition

Figure 5.12 through Figure 5.16 presents the 3D plots on the combined effect of temperature and gas recovery while the total water addition was assumed to be constant.

The total water addition was assumed to be 0.5in, 1.0in, 2.0in, 3.0in and 4.0in for the Figure 5.12, Figure 5.13, Figure 5.14, Figure 5.15, and Figure 5.16 respectively.

Based on the plots, when the temperature and water addition were constant, the emissions decreased with increasing gas recovery. While the gas recovery was constant with a constant waster addition, the emissions were predicted to increase with the temperature. Based on the plots, (from Figure 5.12 through Figure 5.16) at 40°F and 0 cfm gas recovery, the emissions decreased as the water addition increased. On the contrary, at 120°F and 0 cfm gas recovery, the emissions increased as the water addition increased.

5.3.7.3 Effect of Gas Recovery and Water Addition in Constant Temperature

Figure 5.17 through Figure 5.19 presents the 3D plots on the combined effect of water addition and gas recovery while the temperature was assumed to be constant. The temperature was assumed to be 50°F, 70°F and 100°F for the Figure 5.17, Figure 5.18, and Figure 5.19, respectively.

Based on the plots, when gas recovery was constant, the emissions decreased with an increase in water addition (considering temperature was constant). While the temperature and water addition were constant, the emissions decreased due to an increase in gas recovery. Considering all other parameters (i.e. water addition, and gas recovery) were constant, the increase in temperature increased the emissions based on the MLR equation developed.

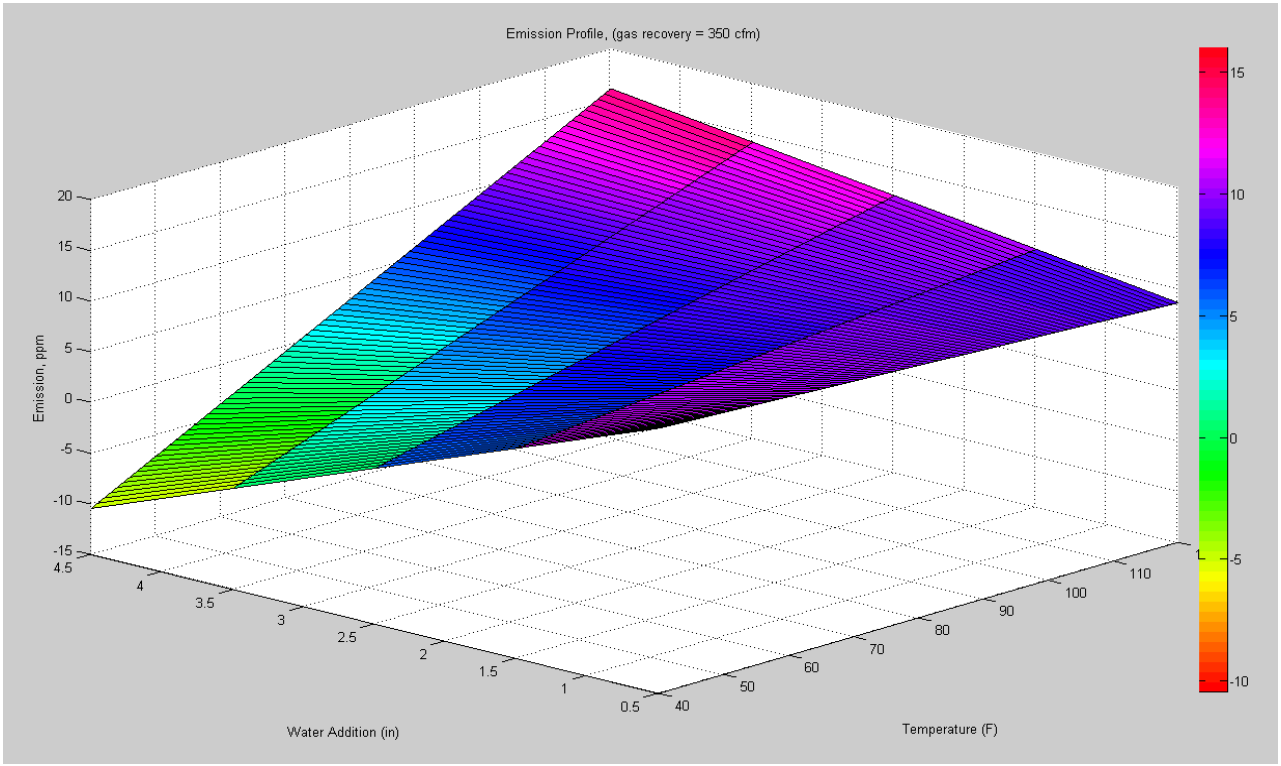

Figure 5.8 3D Plot Showing the Effect of Water Addition and Temperature on Emission with Total Gas Extraction of 350 cfm

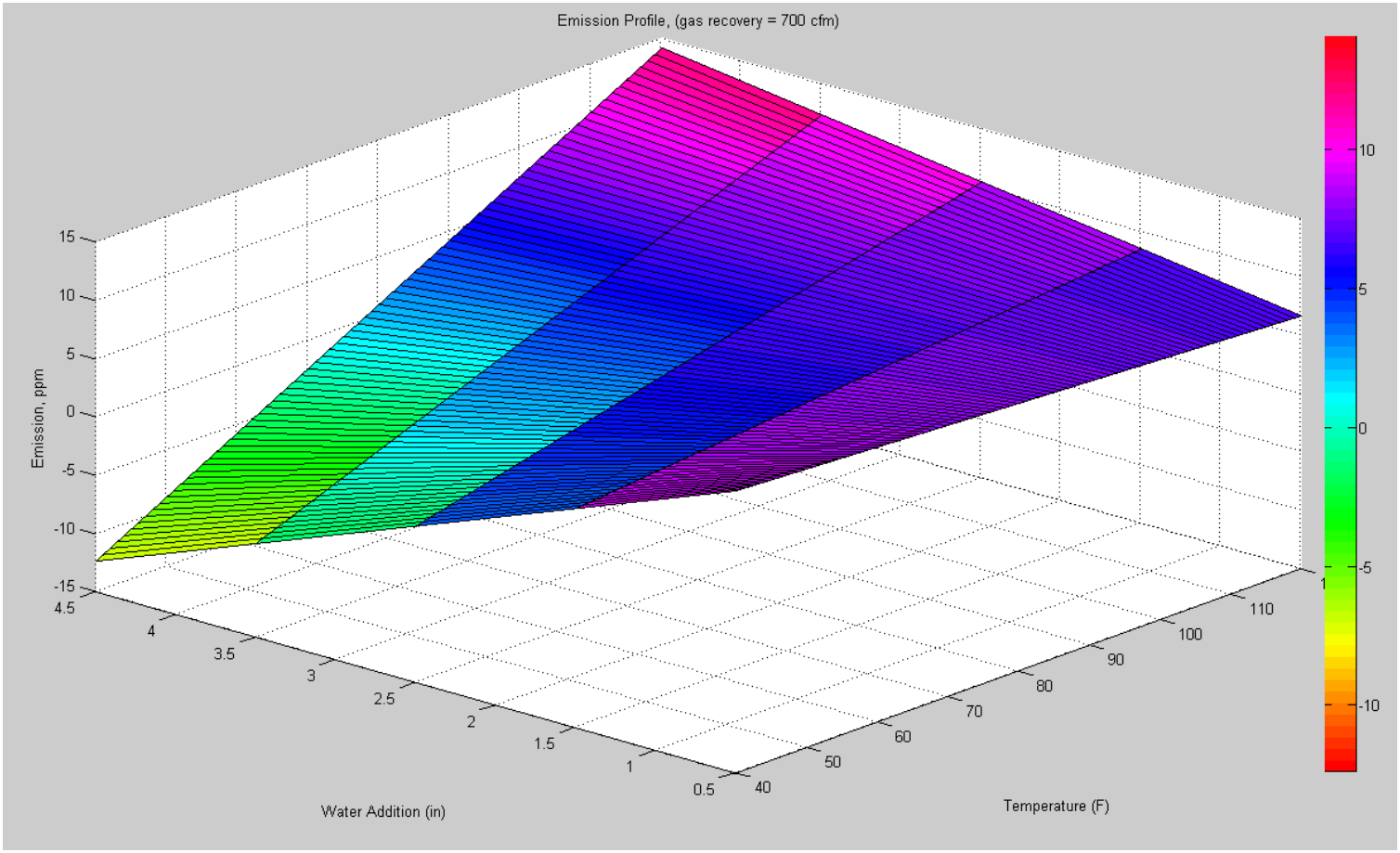

Figure 5.9 3D Plot Showing the Effect of Water Addition and Temperature on Emissions with Total Gas Extraction of 700 cfm

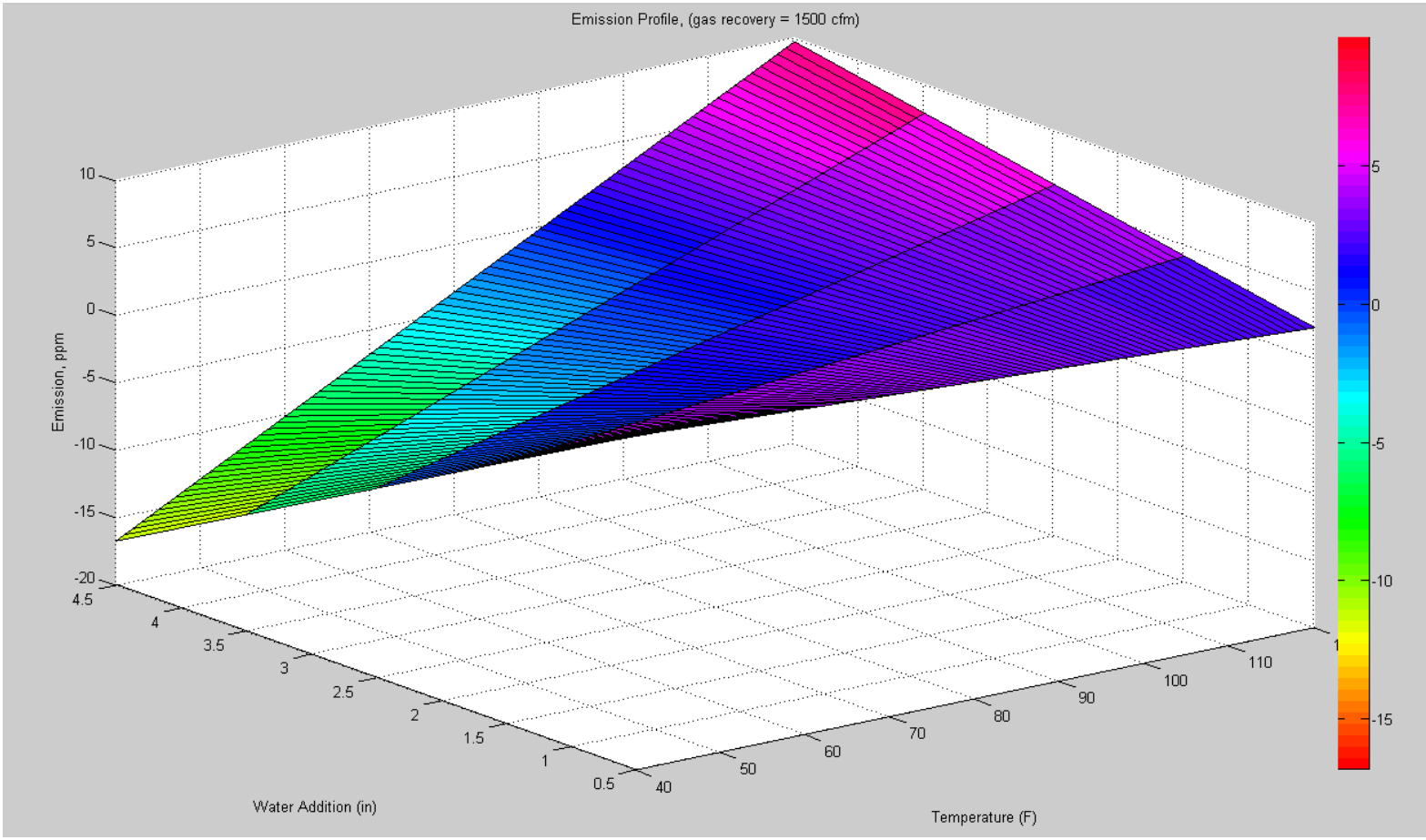

Figure 5.10 3D Plot Showing the Effect of Water Addition and Temperature on Emissions with Total Gas Extraction of 1500 cfm

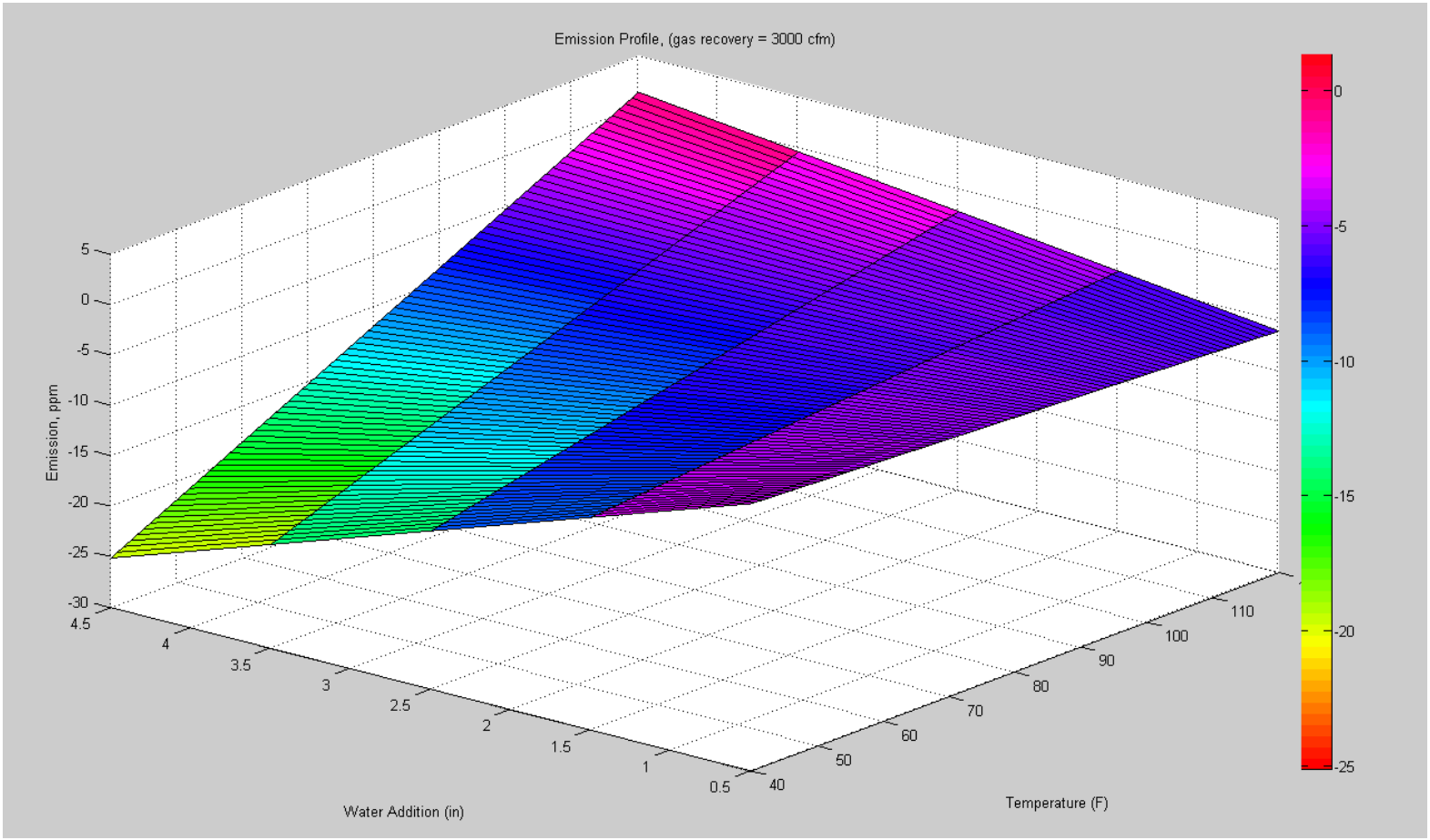

Figure 5.11 3D Plot Showing the Effect of Water Addition and Temperature on Emissions with Total Gas Extraction of 3000 cfm

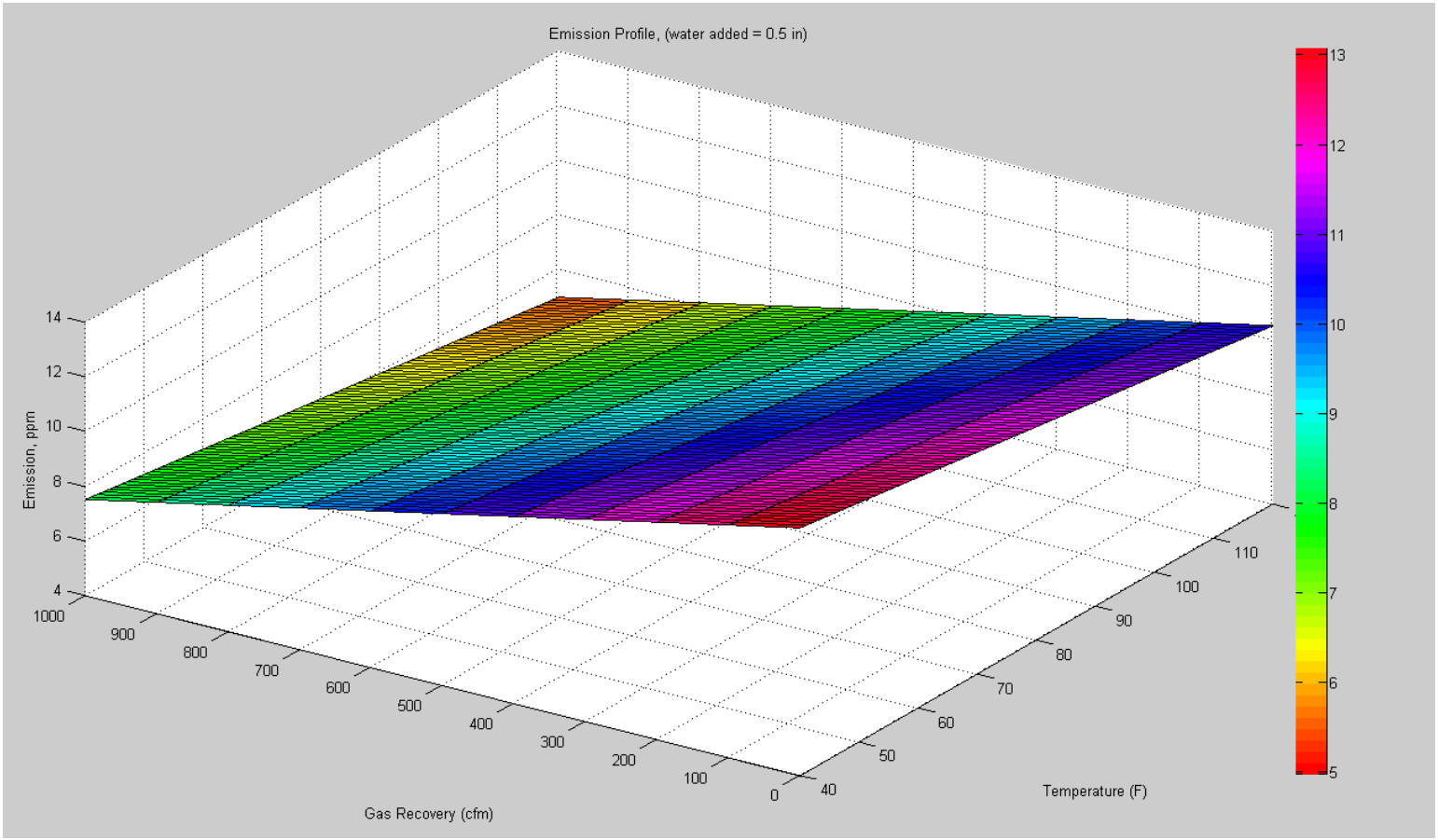

Figure 5.12 3D Plot Showing the Effect of Gas Recovery and Temperature on Emissions at 0.5 in Water Addition

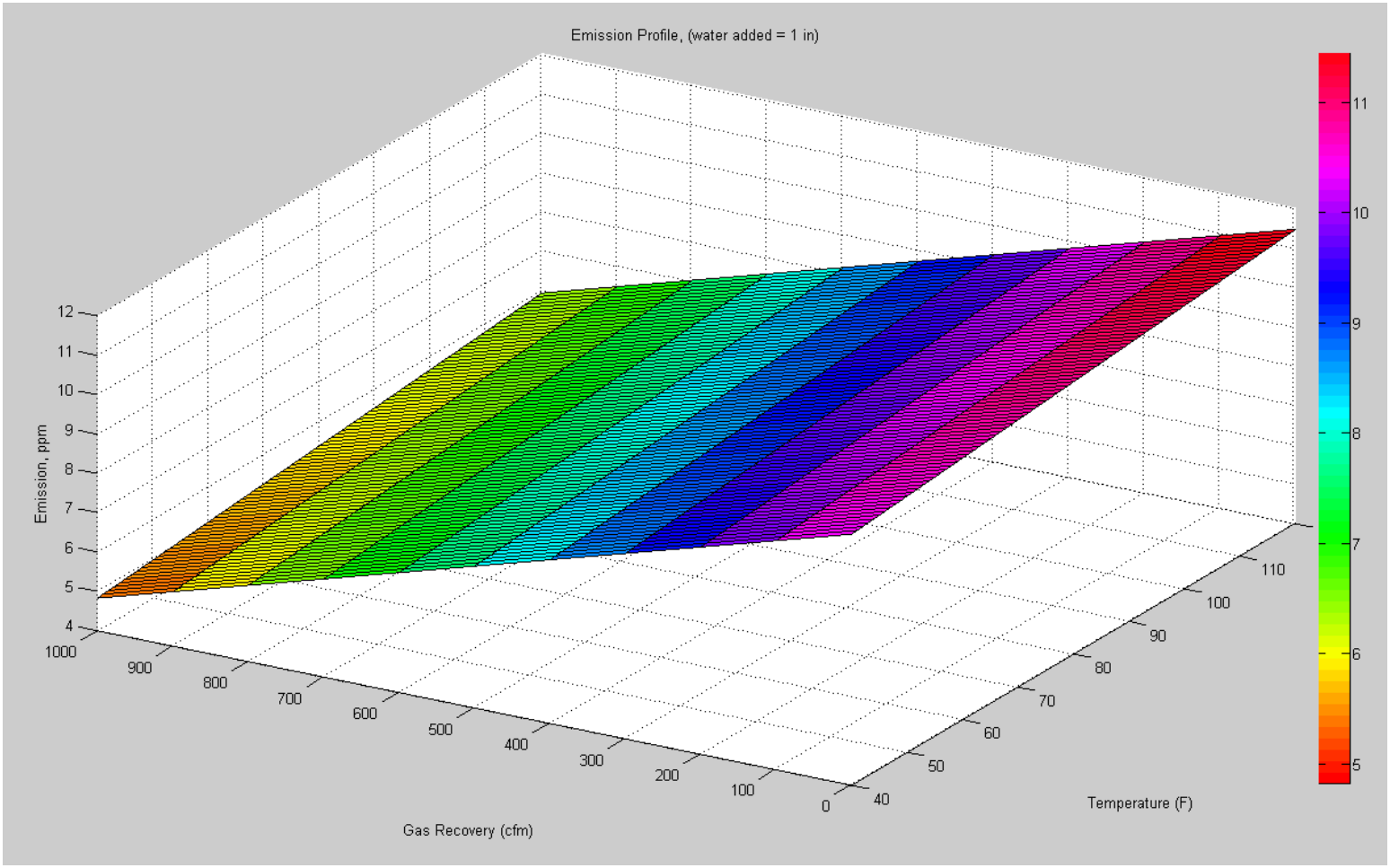

Figure 5.13 3D Plot Showing the Effect of Gas Recovery and Temperature on Emissions at 1.0 in Water Addition

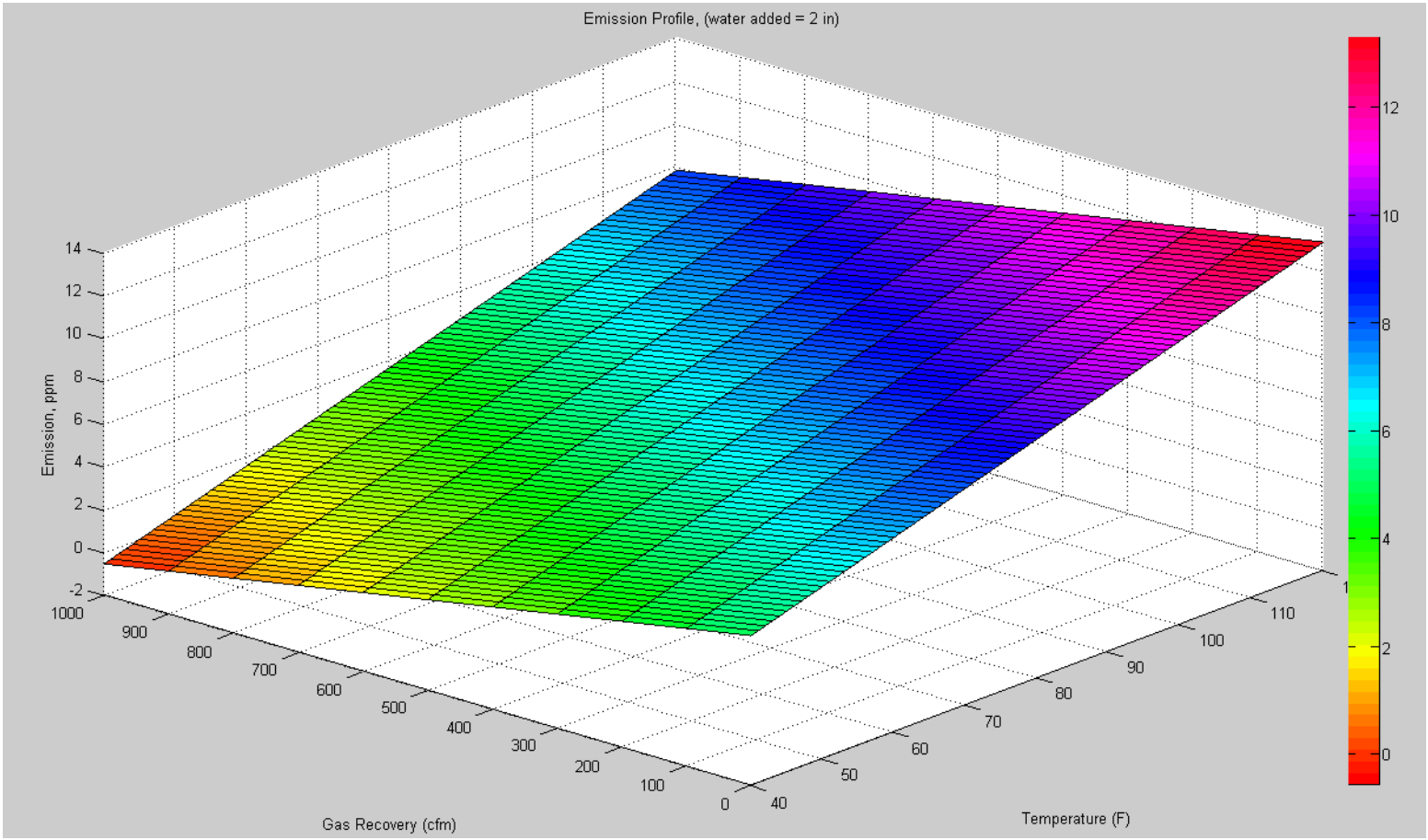

Figure 5.14 3D Plot Showing the Effect of Gas Recovery and Temperature on Emissions at 1.5 in Water Addition

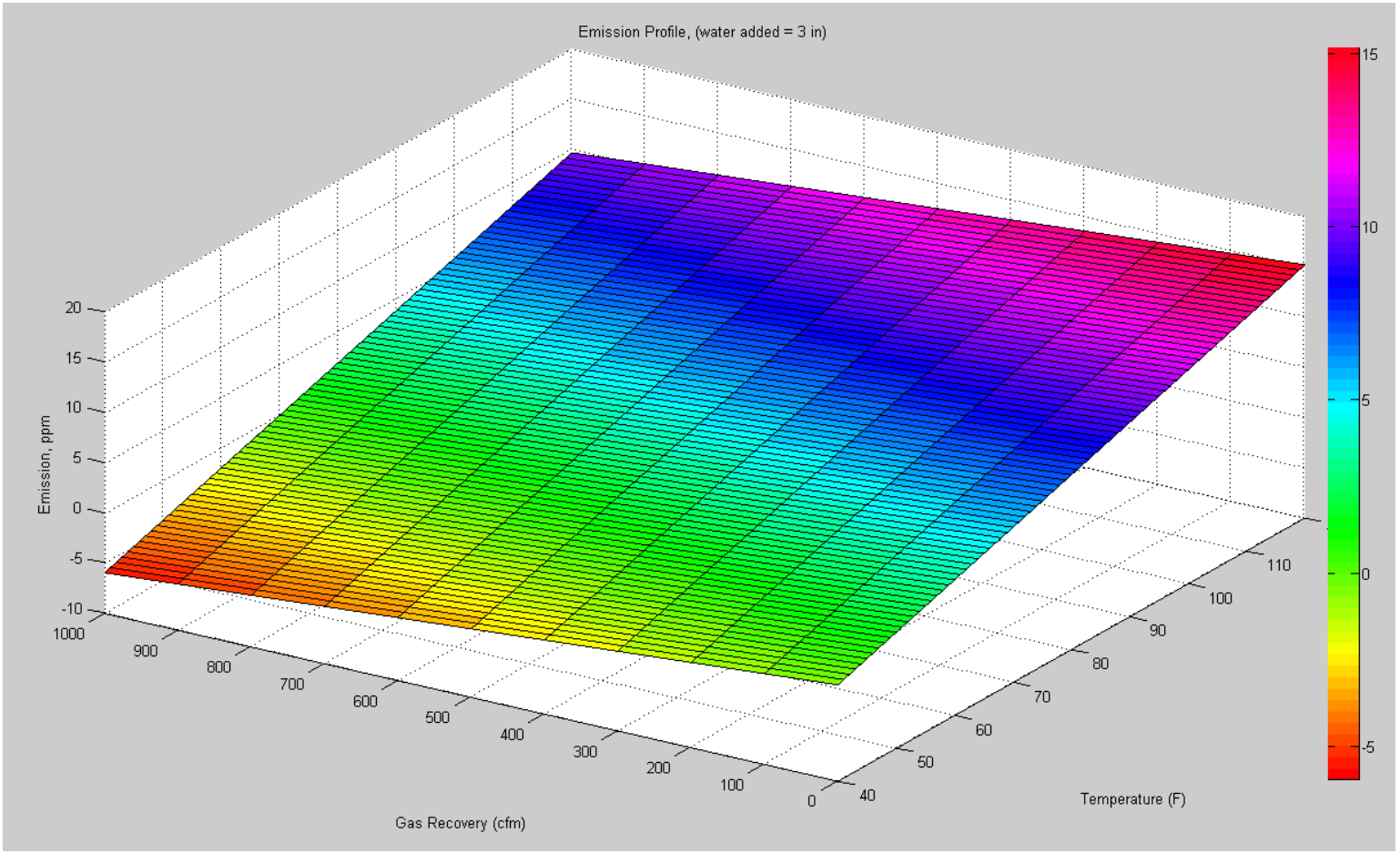

Figure 5.15 3D Plot Showing the Effect of Gas Recovery and Temperature on Emissions at 3.0 in Water Addition

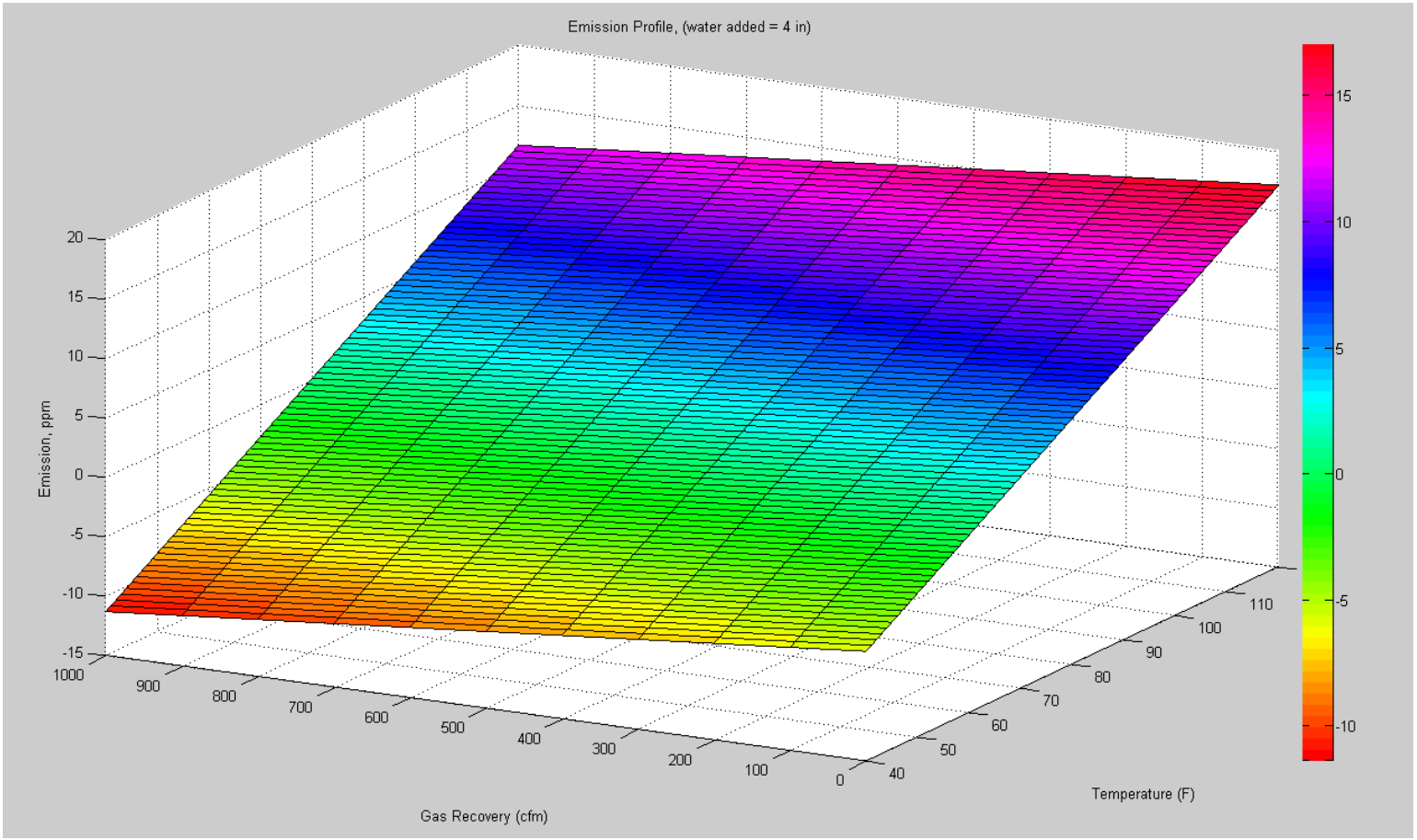

Figure 5.16 3D Plot Showing the Effect of Gas Recovery and Temperature on Emissions at 4.0 in Water Addition

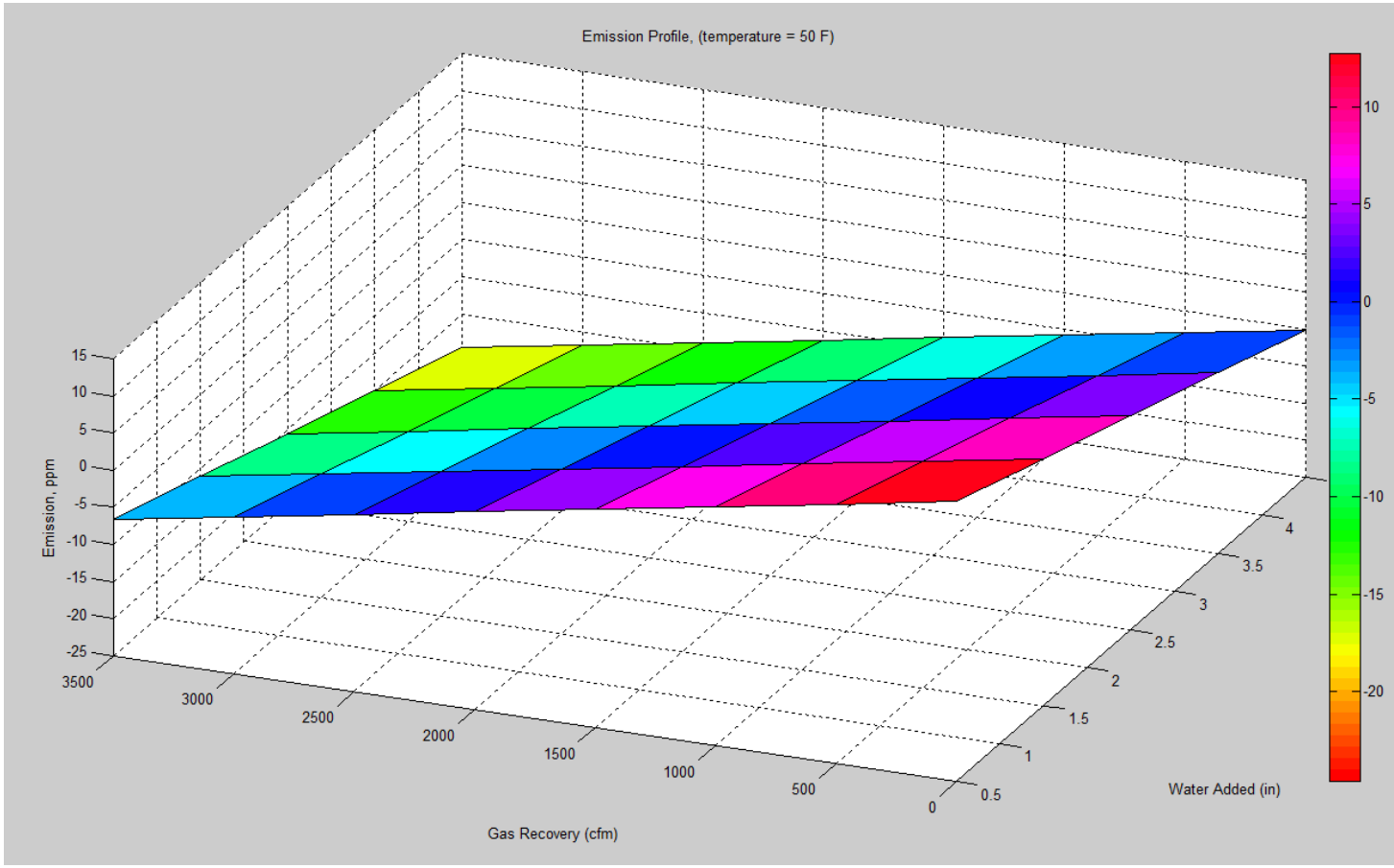

Figure 5.17 3D Plot Showing the Effect of Gas Recovery and Water Addition on Emissions at 50°F

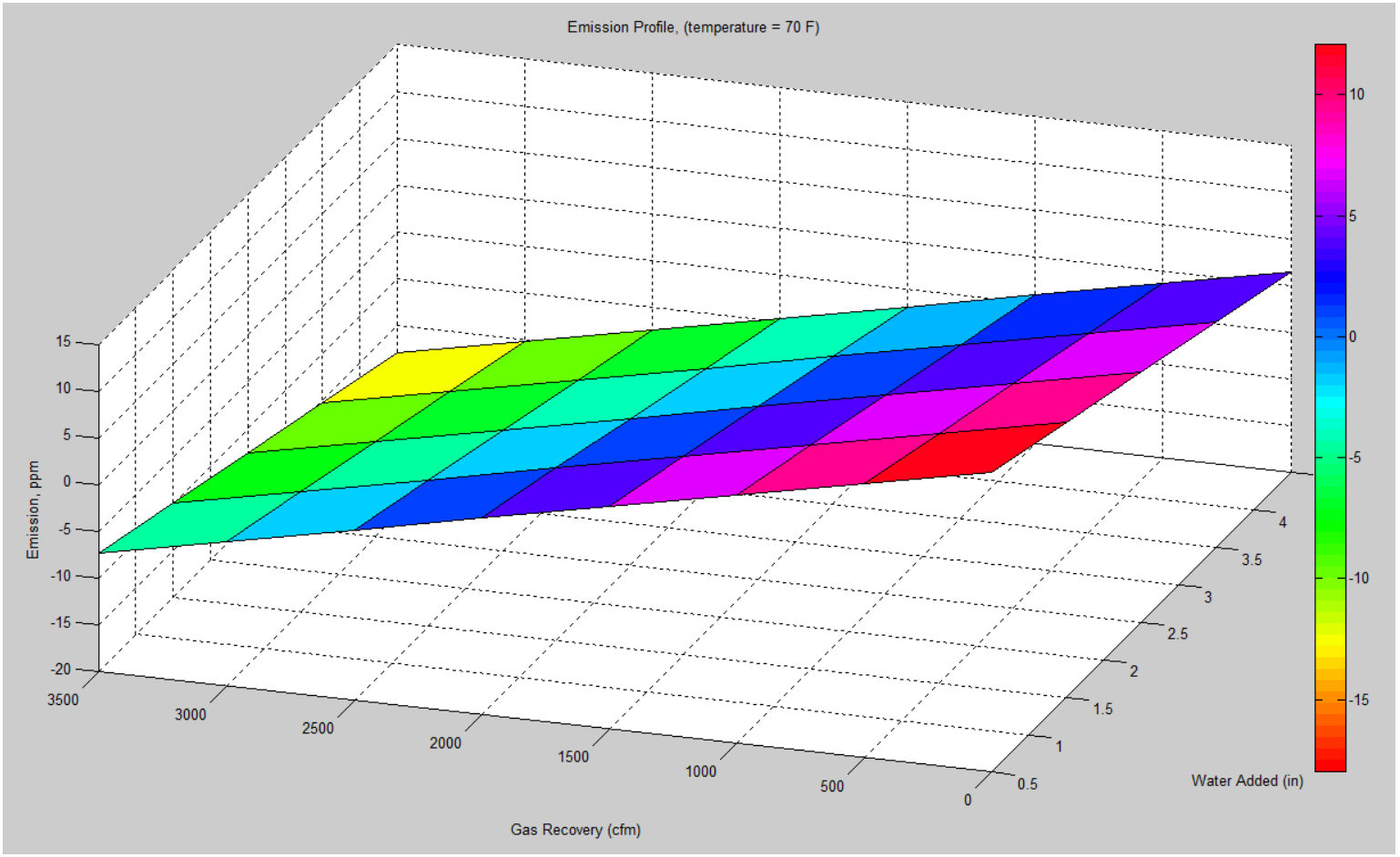

Figure 5.18 3D Plot Showing the Effect of Gas Recovery and Water Addition on Emissions at 70°F

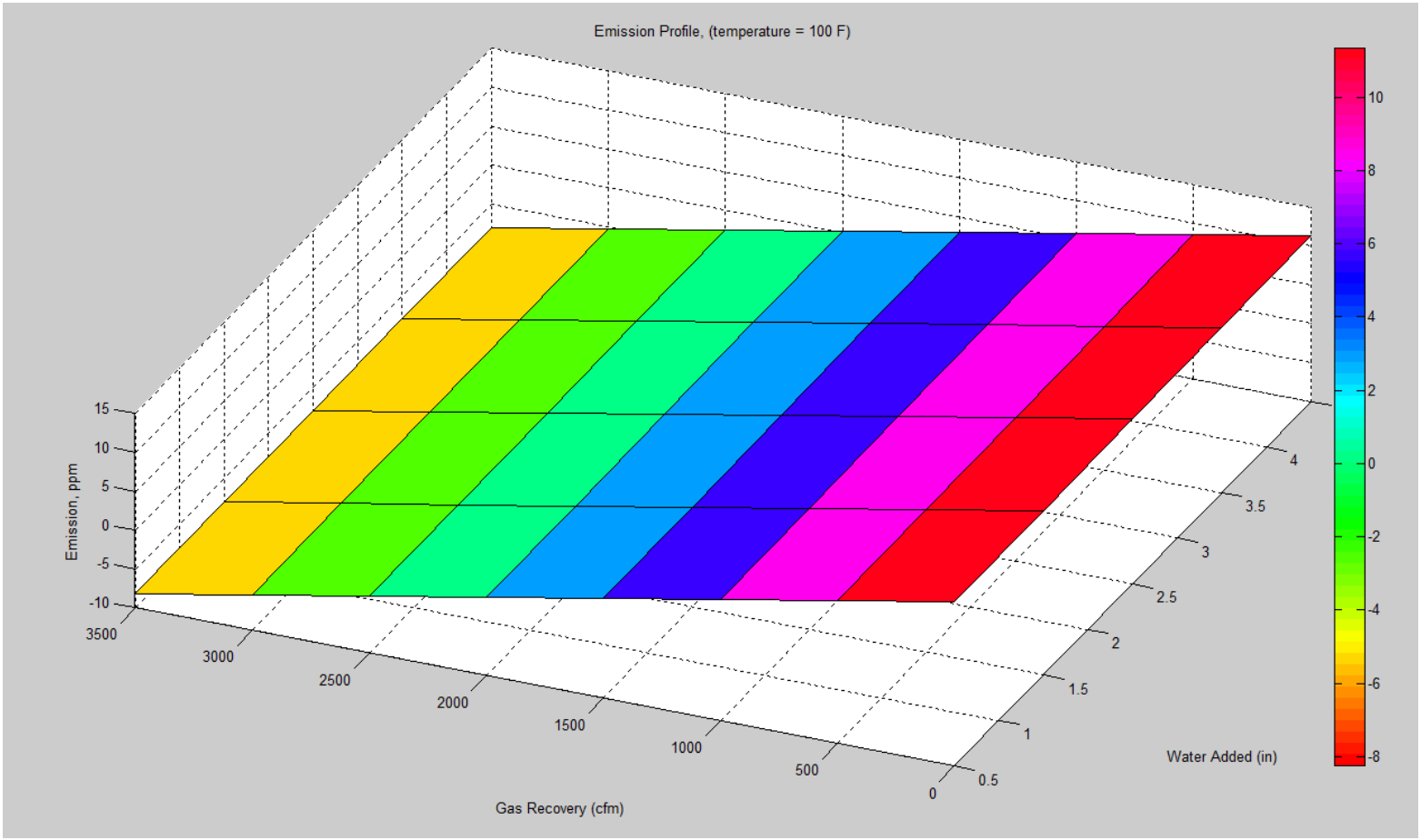

Figure 5.19 3D Plot Showing the Effect of Gas Recovery and Water Addition on Emissions at 100°F

5.3.8 Model Validation

It is required that the developed methane emission model for predicting the overall emission from the landfills be validated to observe the performance of the model. Data from cell 2 (from November and December) and from cell 0 (from September through December) was used to predict the average emissions from the landfill cell. The predicted results were compared with the measured average emissions from the landfills to estimate the variation from model.

The developed MLR equation for estimating methane emissions is:

$$E = 18.84246 - 0.07714T - 9.0126W - 0.00554G + 0.09063 (TxW) \quad \ldots\ldots\ldots\ldots\ldots\ldots\ldots\ldots \quad (5.3)$$

Where,

E = Average CH_4 Emissions (ppm)

T = Temperature (ºF)

W = Water Addition = Total Precipitation (inch) + Total Water/Leachate Addition (inch)

G = Total Gas Extraction (cfm)

Therefore, if the temperature is 50°F, Water addition (precipitation+ Leachate Recirculation = 2.74 in + 0.0966 =2.84 in), and gas recovery 335 cfm,

Predicted Emissions = 18.84246-0.07714 * 50 -9.0126 * 2.86 +0.09063 * (50 * 2.86) = 0.42 ppm.

A summary of comparisons between the predicted emissions from the model and measured emissions from the landfill cell is presented in Table 5.18.

Table 5.18 Summary of Comparison between the Predicted and Measured Methane Emissions

Study Area	Predicted Emissions (ppm)	Measured Emissions (ppm)	Variation
Cell 2	6.90	7.19	-4.22
	7.54	7.67	-1.69
	7.32	7.62	-4.04
Cell 2	1.44	1.31	8.94
	1.00	0.94	6.25
	0.42	0.51	-20.08
Cell 0	1.22	1.10	10.18
	6.56	7.10	-8.31
	5.92	6.30	-6.34
	3.64	2.70	25.91

The comparison between the predicted emissions and the measured emissions indicated that the maximum variation from the predicted emissions from measured emission was 25.91%. However, the average variation from the estimated results was found to be 9.6%, Therefore, we can conclude that the model predicts the average landfill emissions within an average variation of 10%.

Figure 5.20 presents the predicted or estimated emissions from the MLR model with the actual measurement from the field.

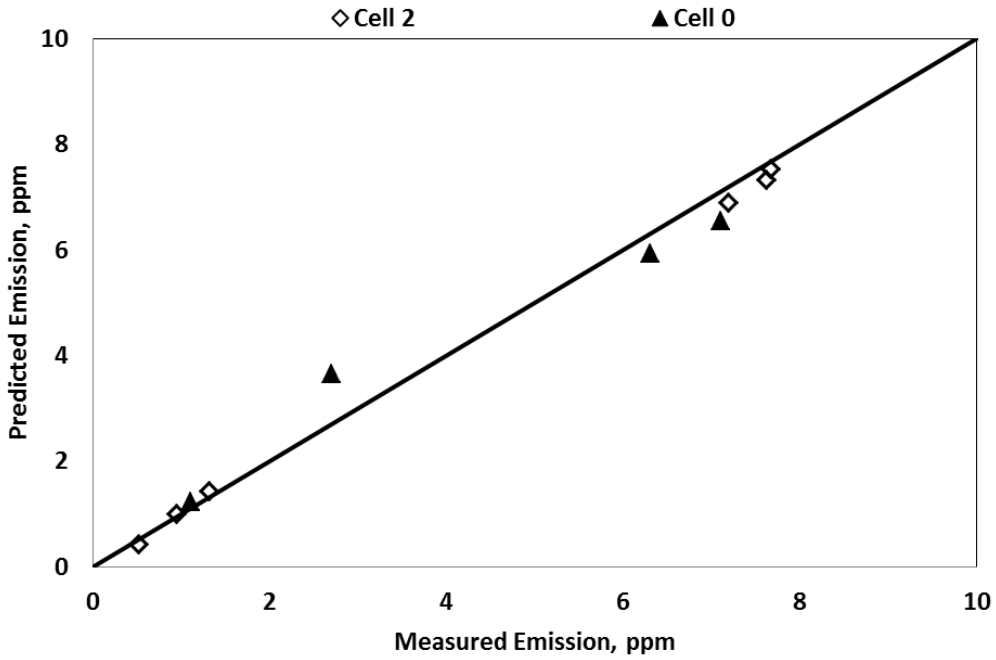

Figure 5.20 Predcieted Methane Emissions with Measured Landfill Emissions

5.3.9 Predicted Emissions Based on the Model

The emissions were estimated for different gas extraction rates for constant temperature and water addition. Figure 5.21 presents the methane emissions vs. the area of the landfill with different gas extraction levels (350 cfm, 700 cfm and 1500 cfm), assuming constant temperature of 100°F and 2.5 in water addition.

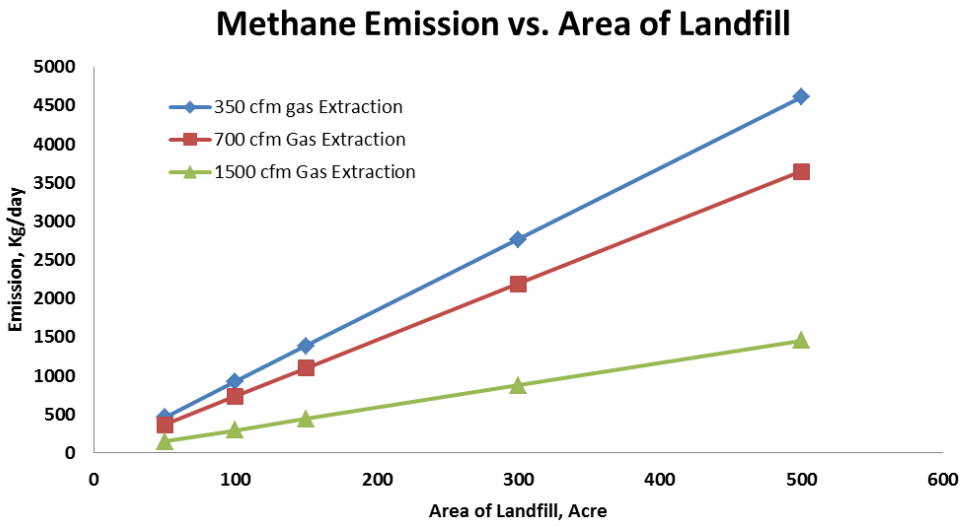

Figure 5.21 Predicted Methane Emission with Measured Landfill Emission

From the figure, the emissions decrease as the gas extraction from the landfill increases. On the other hand, the emissions increase as the area of the landfill increases. Similar trends were also observed for different temperature and water addition.

5.3.10 Uncertainties with the Model

The MLR equation for emission was developed based on the landfill methane emissions measured from the ELR operated cell of the City of Denton landfill for one year. Hence, the model holds the temperature condition between 50°F to 100°F as monitored during the study. Consequently, prediction of emissions beyond this range of temperature would lead to interpolation of data and might be misleading. Similarly for the precipitation, the maximum range was observed up to 3.5 in (including the recirculation) and the predicted emissions beyond that value might lead to higher error in prediction.

In addition, the selected study area was covered with a 2 ft thick intermediate cover. Hence, the prediction of emissions based on the model might also be limited to the

landfills with similar cover system. Therefore, based on the above mentioned conditions the model might provide better predictions in the similar climatological condition and similar cover soils in Texas.

The methane emissions from the landfills varies depending upon the composition of the landfill waste, age of the waste, gas generation capability of the waste, decay rate, presence of moisture within the landfill, landfill cover, and presence of cracks or preferential pathways in the cover. Hence, the variability in the amount of methane emissions induces high uncertainty in the estimation of methane emissions. Similarly, the variation of oxidation capability within the landfill cover might also introduce uncertainty in the model.

Chapter 6

Conclusions and Recommendations

6.1 Introduction

The Based on the field and laboratory investigations conducted, the results can be summarized as:

- Methane emissions from the landfill surface were measured using a portable FID and static flux chamber technique. The portable FID technique was more suitable for this research considering it would provide more elaborate information than the point specific information on surface methane fluxes from the flux chamber method. Therefore, a correlation was developed between the methane concentration and methane emission flux as:

Methane Flux ($gCH_4/m^2/day$) = 0.2443 x Methane Concentration (ppm).

- The measured methane concentration throughout the cell was highly variable, which can be mostly attributed to non-homogeneity of waste and gas generation below the soil cover. In addition, the presence and dynamics of the microbes in the cover soil makes it more complicated and ambiguous.

- Methane concentration was measured from an ELR operated cell (cell 2) as well as a conventional cell (cell 0). Methane concentration for cell 2 varied from 9544.3 ppm to 0 ppm and for cell 0 varied from 0 ppm to 47 ppm for the total investigation period from Dec'12 to Jan'14. The highest methane concentration was observed during the baseline study in cell 2 on December, 2012. However, further monitoring did not show such high methane concentrations on these locations. The high concentration on December during the baseline study on these locations might be attributed to the unusual combination of meteorological combinations of that period.

- Spatial variations from the slope and surface were compared for both cell 0 and cell 2. Based on the results, the concentration from the slopes were higher even with the presence of mulch on the slopes.

- The concentrations were monitored hourly during an 8 hour period every day. Based on the results, the concentrations increased as the temperature increased throughout the day. However, a similar study conducted in the day of gas extraction showed continuous decrease in concentration with time, which was assumed to be the direct impact of gas extraction.

- The monthly/ seasonal variation of methane concentration also asserted the direct effect of climatological factors on emission. The concentration increased as the temperature increased.

- The effects of temperature and precipitation were analyzed on the overall concentration from the landfills. The concentration showed an increasing trend with increase in temperature and decreasing trend with increasing precipitation.

- The effect of an ELR operation near the recirculation pipes showed a lag period between the recirculation and the maximum concentration near the pipe. The concentration near the pipe decreased after 1 day of recirculation, started to increase after 2 days and continued the increase in emission up to 7 days after the recirculation. The concentration decreased after reaching the maximum at the original state before the recirculation. However, the change in concentration was limited to the region near the pipe. No overall change in concentration was observed from the cell due to the recirculation.

- The comparison between the concentration from the conventional and ELR cell showed an overall higher concentration from the ELR cell, which could be attributed to the overall higher gas generation from the ELR cell as well.

- The gas extraction had a direct impact on concentration: the concentration dropped substantially right after the gas extraction from the landfill. However, the gas was extracted once monthly, and comparison with the amount of gas extraction and emission showed that the emission decreased as the gas extraction increased.

- The cover soil is the primary measure used to entrap the methane migration from the landfill. The cover soil also provides the means for methane oxidation with the presence of oxygen within the cover. The overall emission observed from the study was lower than the literature suggests. However, the comparison with the bio-cover results confirmed that the use of mulch on top of the landfill cover had considerable effect on the lower surface methane concentration. In addition, the presence of gas extraction system in both landfill cells was also one of the major reasons of overall lower emissions.

- The methane concentration profile with depth showed the maximum concentration at 2 ft depth near the waste and the concentrations continuously decreased as it reached near the surface. The soil gas profiles provide an understanding on methane oxidation; however, fails to quantify the methane oxidation rate in the cover soil. Therefore, an elaborate set of tests were conducted in controlled temperature and moisture, to evaluate the methane oxidation capacity of the cover.

- Based on the methane oxidation results from the laboratory investigation, the maximum methane oxidation efficiency was observed between 70°F and 85°F for all the soil moisture contents. The oxidation efficiency ranged from 4.68% to 97.26%. In addition, the methane oxidation decreased with increasing moisture. However, with increase in temperature, the oxidation initially increased and then decreased after reaching the peak oxidation rate.

- A methane concentration model was developed using the statistical model considering the effects of temperature, precipitation, leachate recirculation and gas extraction. The model equation is as follows:

Concentration = 18.84246 - 0.07714 Temperature - 9.0126 Water Addition - 0.00554 Gas Extraction + 0.09063 (Temperature x Water Addition)

The developed model was validated and the model showed an excellent agreement between the predicted concentration and the measured concentration from the landfills (average variation 9.6%).

6.2 Limitations of the Study

The study attempts to address the effect of the emerging leachate recirculation practice on the methane concentration. However, the study was limited to only the City of Denton Landfill, Texas. Therefore, the study does not address the geographical/ climatological impact on the study. Moreover, the study was conducted in the landfill cells with intermediate cover systems and only with one type of cover soil. Further study with variations of types of cover, cover soil material and thickness might provide a better understanding of the effect of cover soil on concentration.

6.3 Recommendations for Future Study

The following recommendations are suggested for the future studies:

- Further research is required to evaluate the effect of leachate recirculation from different landfills from the different climatological conditions on emissions.

- Further monitoring of the current study is required to observe the seasonal variations from the landfill and to confirm that similar results are observed from the future monitoring.

- The study was conducted using a portable FID method with the flux chamber method. Further study is required, along with the portable FID method, to compare the results obtained from different methods.

- The current study is limited to a temperature range of 50°F to 100°F. The study does not address the extreme conditions with ice on the landfill surface for several days. Further studies on the extreme landfill conditions are required with the leachate recirculation.

- The study concluded that the gas extraction directly reduces the concentration; however, too much gas extraction leads to oxygen intrusion in the landfill and consequently induces the fire hazard. Therefore, further research is required to determine the optimum gas extraction for maximum reduction in concentration from the landfills.

- The types of cover soil would change the methane oxidation capacity and hence change the methane emission behavior. Further studies are required to monitor the effect of ELR operation with different types of cover, cover soil material and thickness.

- The methane oxidation test was conducted only on the on-site soil materials. Further investigation of methane oxidation on different types of cover soil with controlled temperature and moisture would help to identify a better cover soil for the landfill.

- Further validation of the model is required based on the data sets from different landfills.

Appendix A

Surface Emission Contours for ELR Operated Landfill Cell (cell 2)

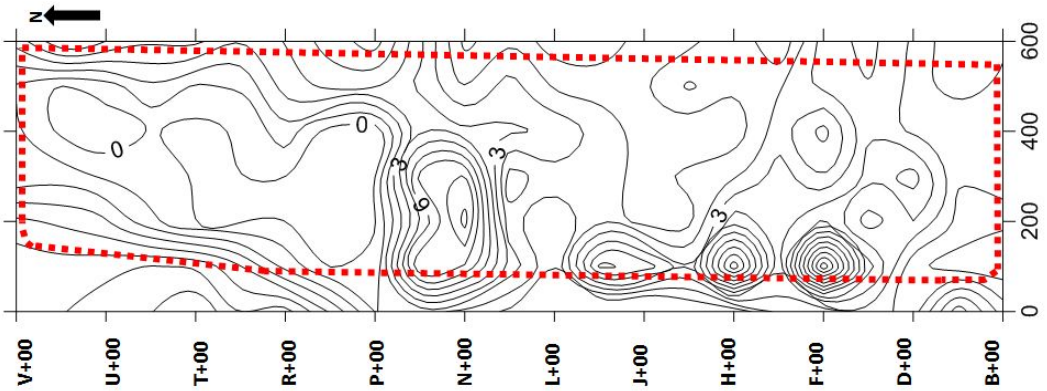

Figure A1: Surface Emission Contour for Cell 2 in February, 2013

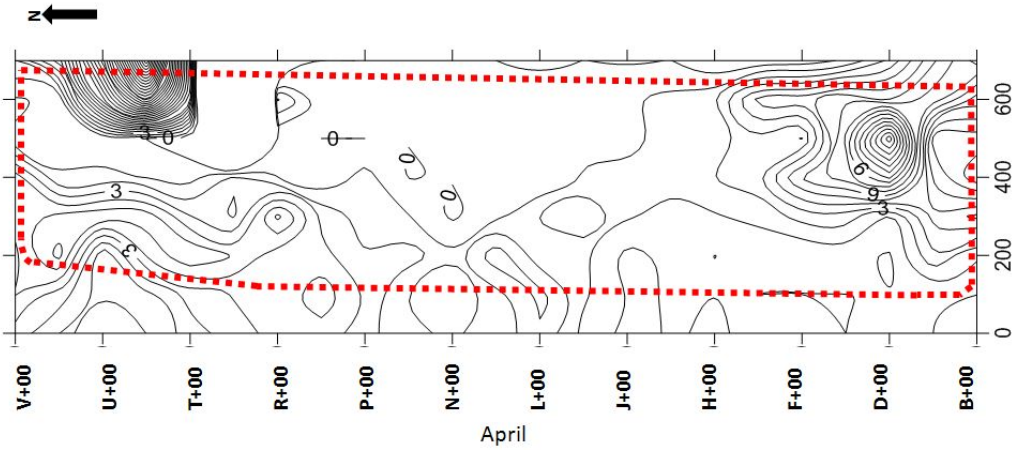

Figure A2: Surface Emission Contour for Cell 2 in April, 2013

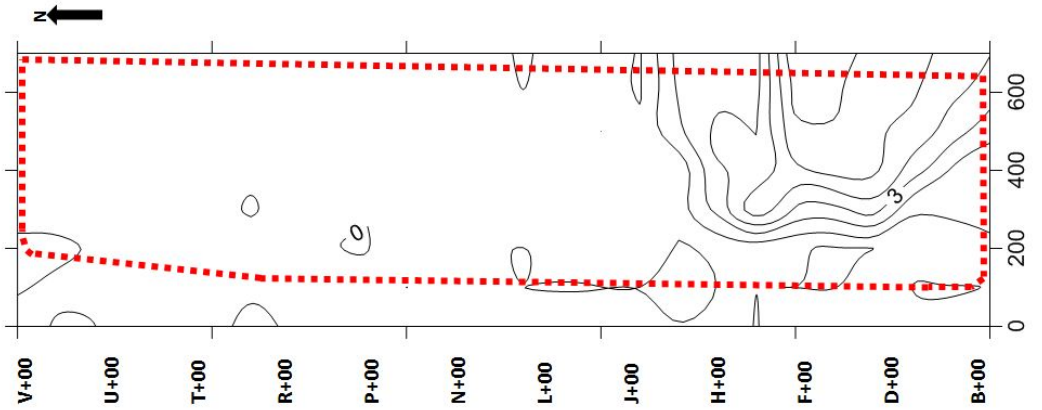

Figure A3: Surface Emission Contour for Cell 2 in May, 2013

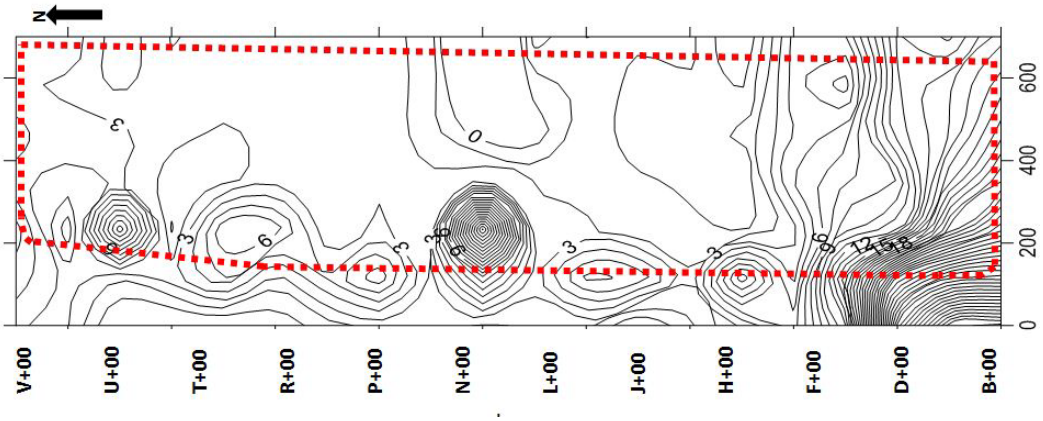

Figure A4: Surface Emission Contour for Cell 2 in June, 2013

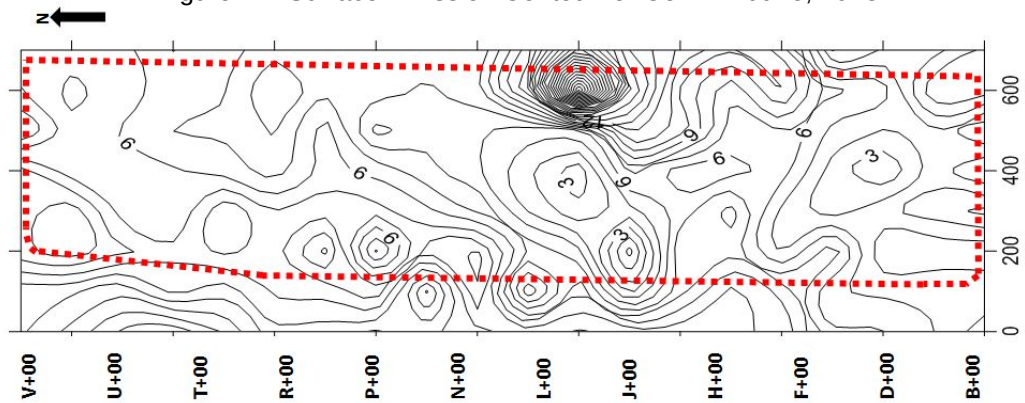

Figure A5: Surface Emission Contour for Cell 2 in July, 2013

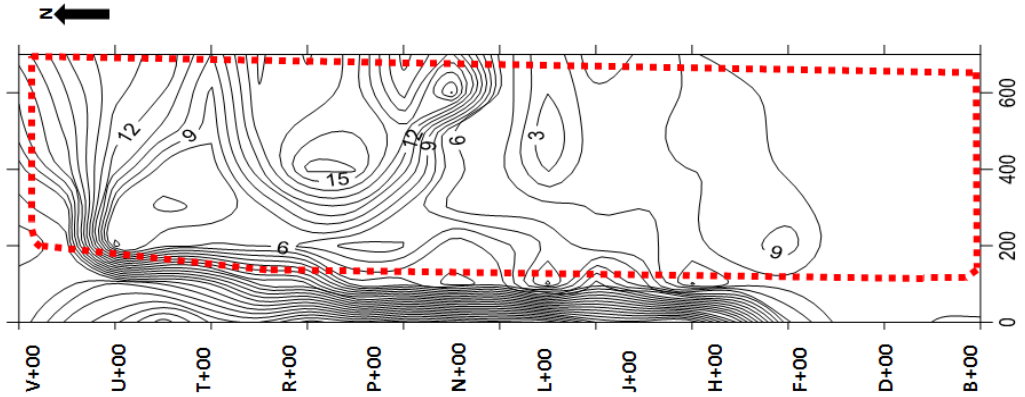

Figure A6: Surface Emission Contour for Cell 2 in August, 2013

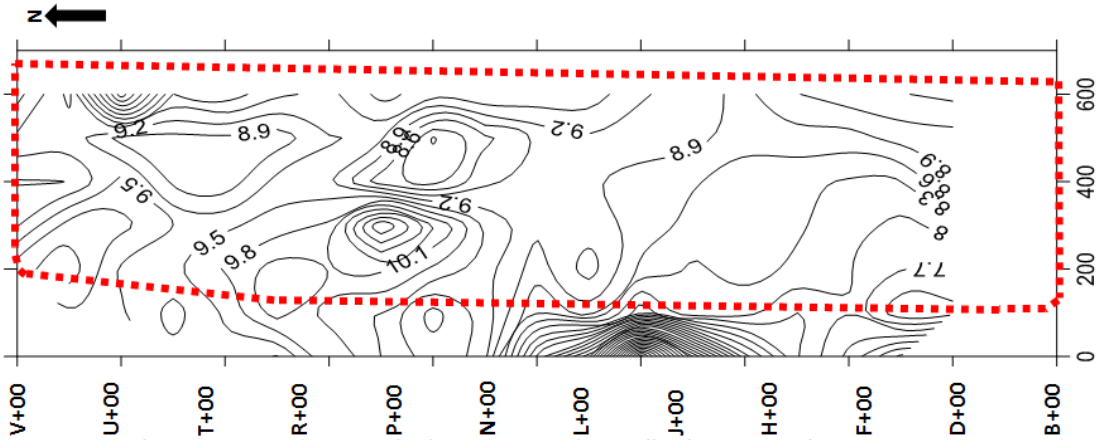

Figure A7: Surface Emission Contour for Cell 2 in September, 2013

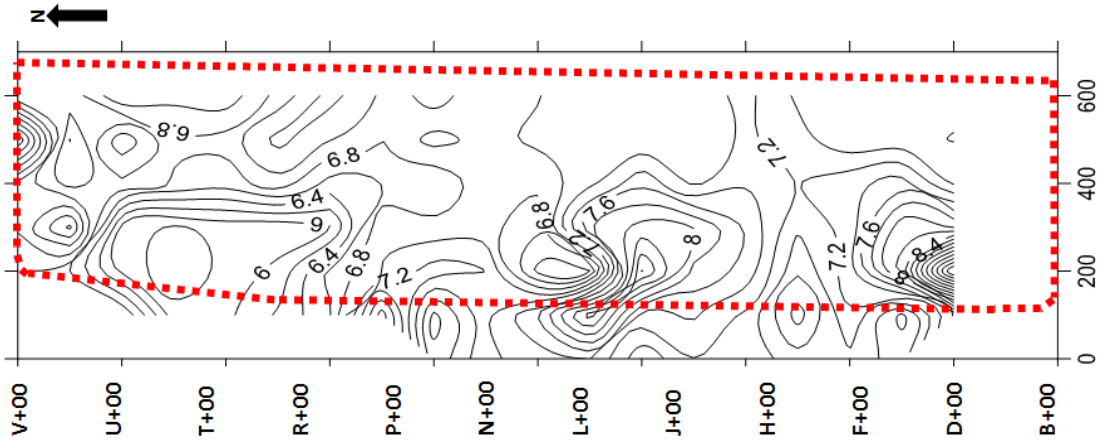

Figure A8: Surface Emission Contour for Cell 2 in October, 2013

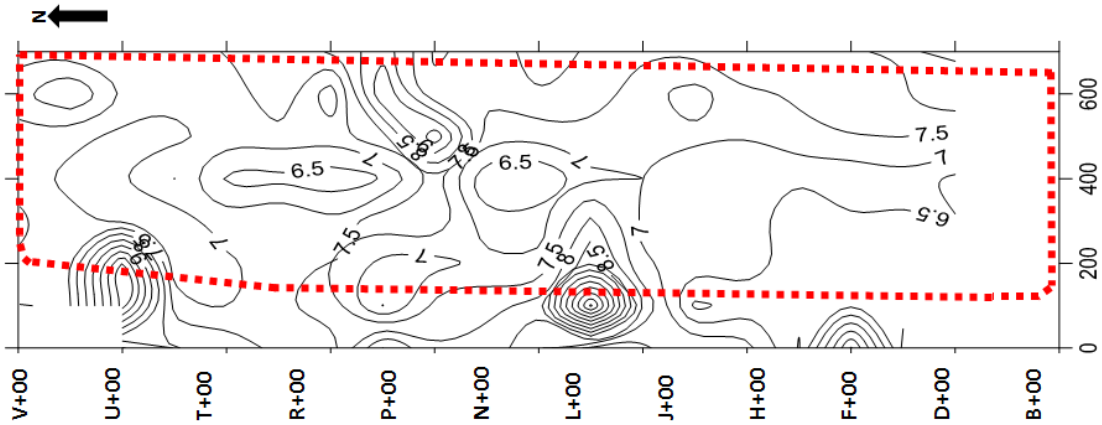

Figure A9: Surface Emission Contour for Cell 2 in November, 2013

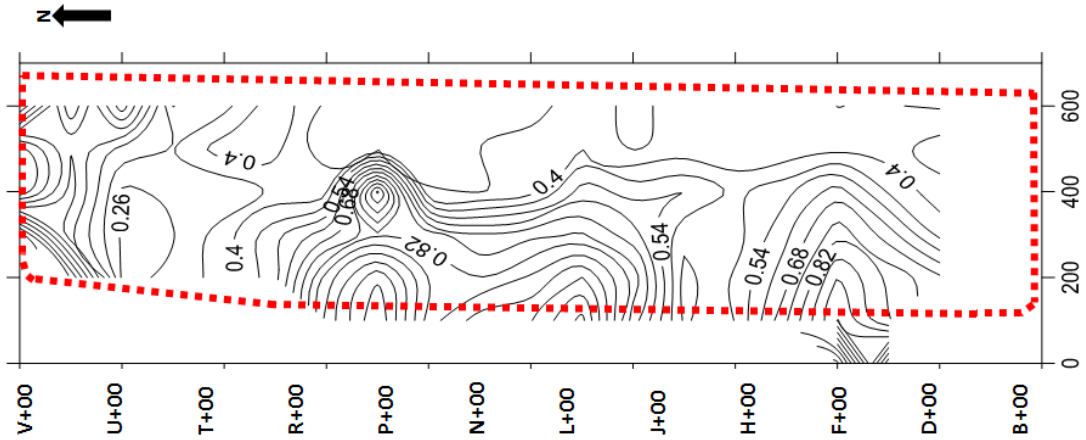

Figure A10: Surface Emission Contour for Cell 2 in December, 2013

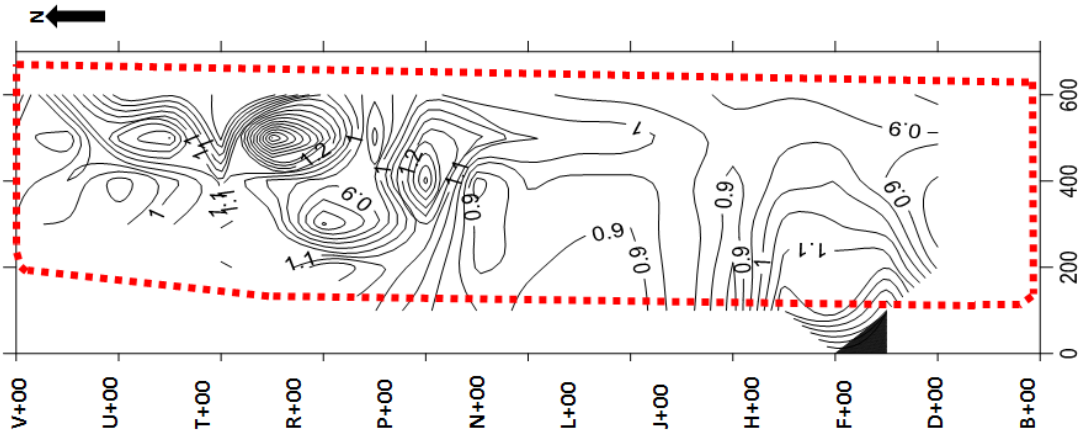

Figure A11: Surface Emission Contour for Cell 2 in January, 2013

Appendix B

Surface Emission Contours for Conventional Landfill Cell (cell 0)

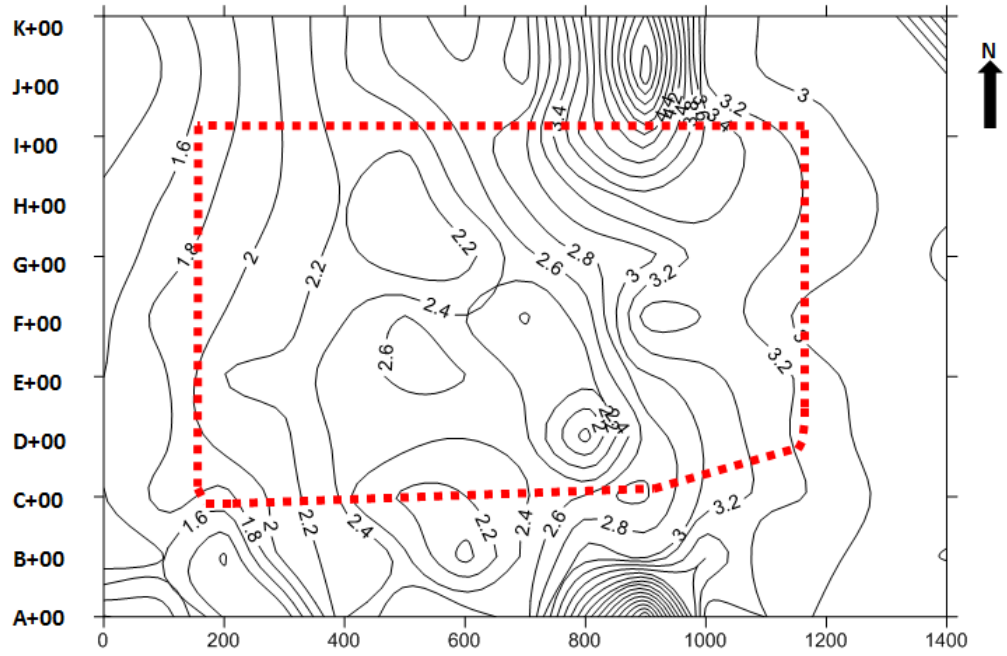

Figure B1: Surface Emission Contour for Cell 0 in August, 2013

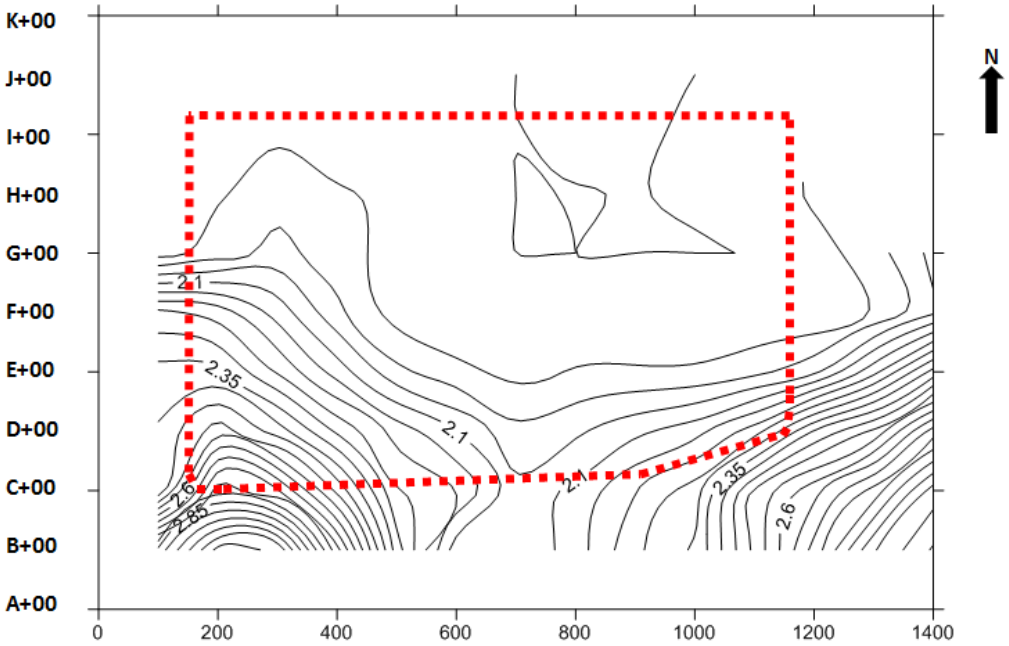

Figure B2: Surface Emission Contour for Cell 0 in September, 2013

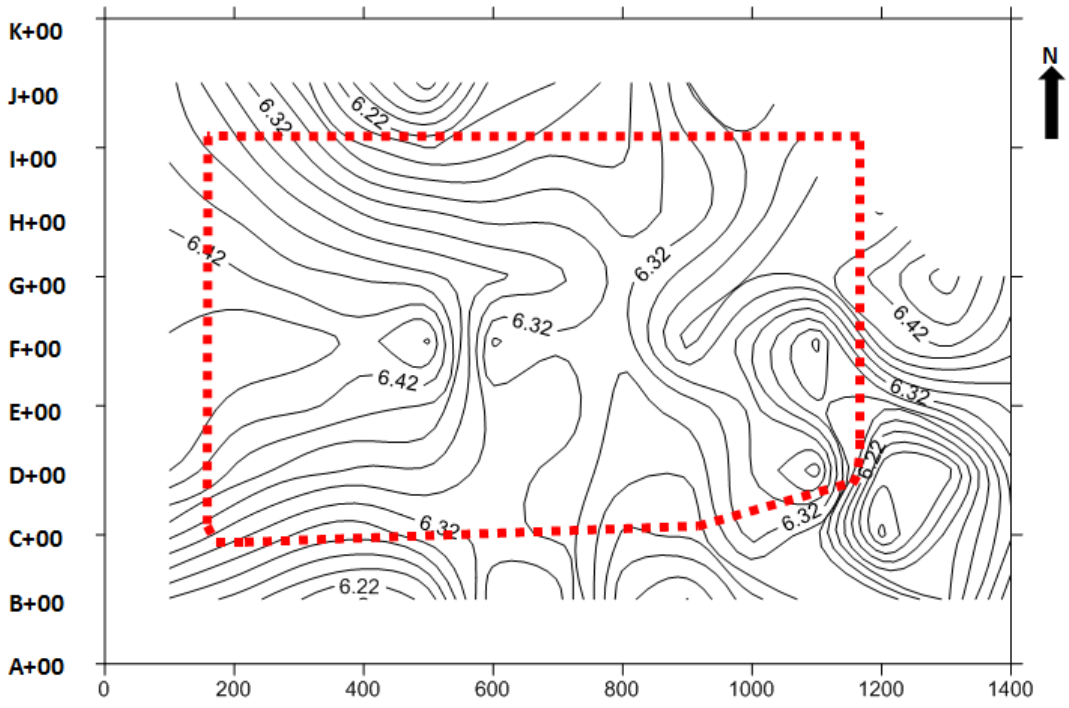

Figure B3: Surface Emission Contour for Cell 0 in October, 2013

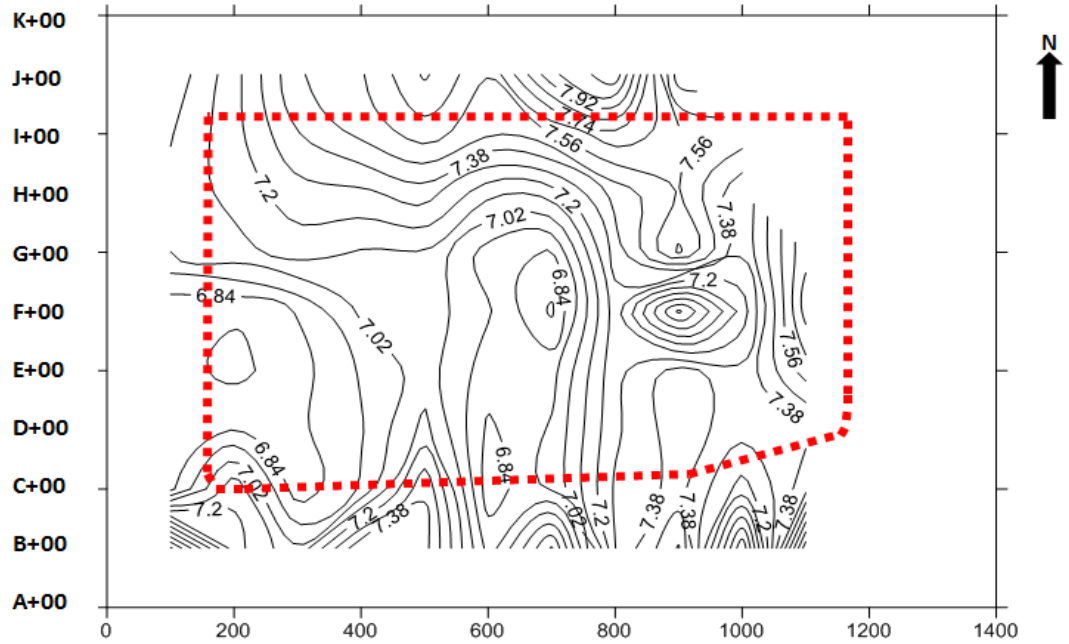

Figure B4: Surface Emission Contour for Cell 0 in November, 2013

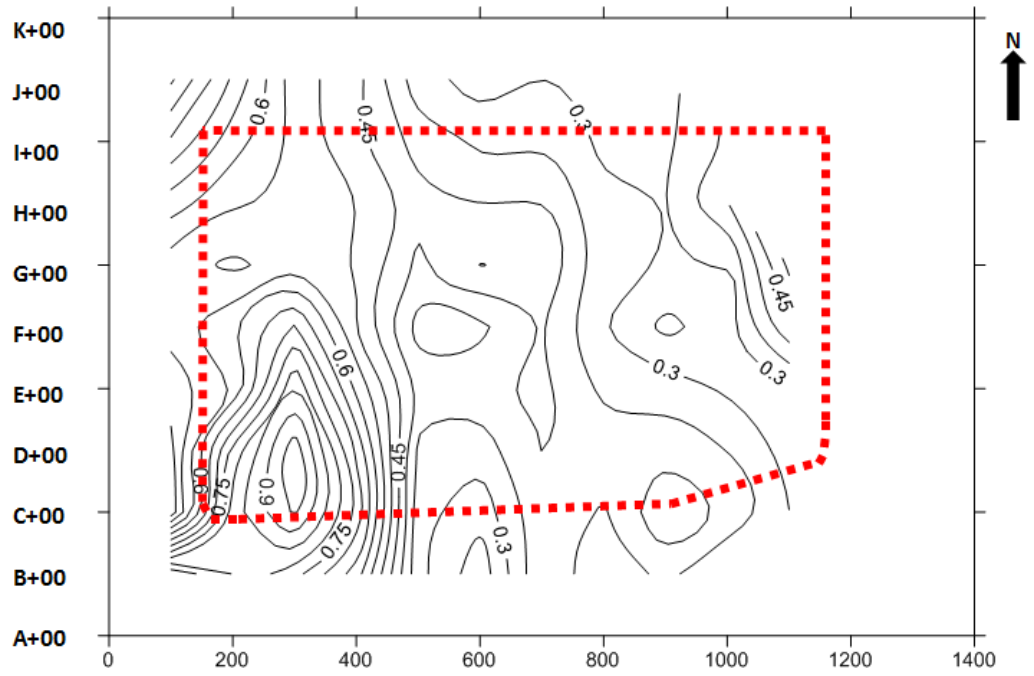

Figure B5: Surface Emission Contour for Cell 0 in December, 2013

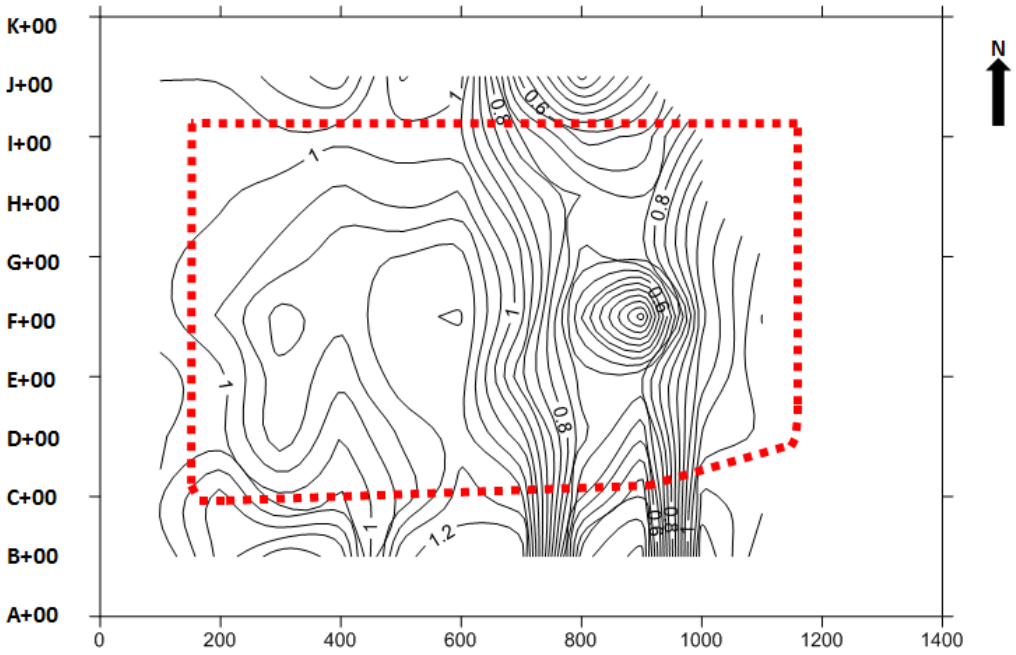

Figure B6: Surface Emission Contour for Cell 0 in January, 2014

Appendix C

Verifying the Model Assumptions for the Developed Model

C1. Checking Assumptions for the MLR Equation

The following assumptions have to satisfy any multiple linear regression (MLR) analysis to verify the model.

5. The model form is reasonable.
6. The residuals have constant variance.
7. The residuals are normally distributed.
8. The residuals are not auto correlated.

These assumptions can be verified by performing residual analysis. Residuals are the error terms or the difference between the predicted value and observed value for the response variable (emission).

C2. MLR Model Form is Reasonable

MLR model form is assumed to be adequate when all the residuals versus predictor plots have no curvature in them. However, the plots (see Figure C1) are pretty scattered for the preliminary model and no curvature was observed in the plots. Therefore, the model form was reasonable.

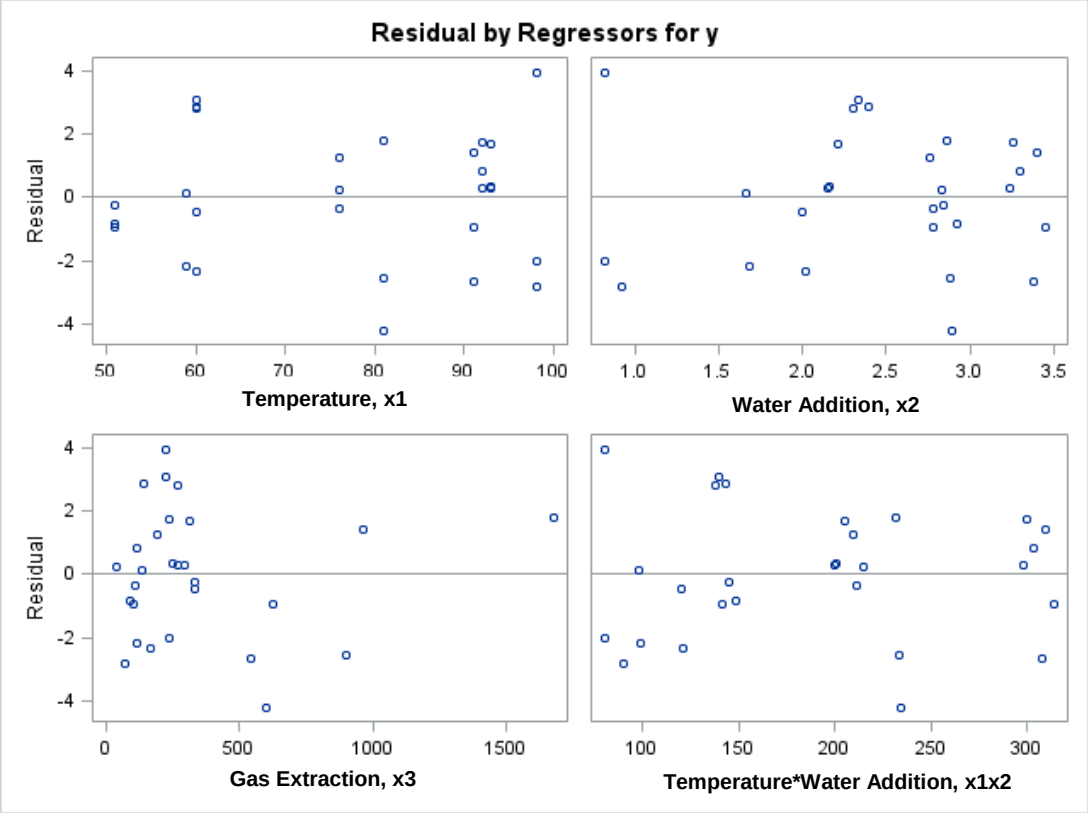

Figure C1: Residual vs. Predictor Plots for the Final Model

C3. Residuals have Constant Variance

MLR model assumes that the errors have constant variance that means when the residuals are plotted against the predicted value of emission, they should be randomly scattered. Presence of funnel shape indicates that variance is not constant and model form is not ok.

Figure C2 presents the residuals vs. predicted emission value for the final model. Based on the plot, no funnel shape was observed which indicated that the residuals had a constant variance in the model. This assumption was further verified using the Modified-Levene test.

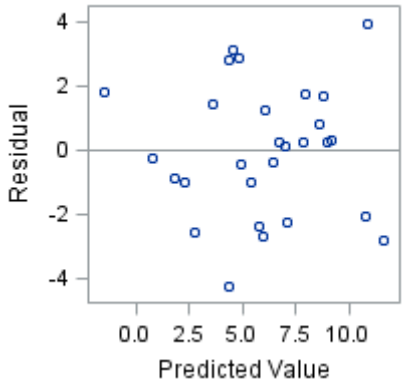

Figure C2: Residual vs. Predicted Emission Value for the Final Model

C4. Residuals are Normally Distributed

The MLR model assumes that the residuals are normally distributed. To check this assumption, residual vs. normal scores were plotted in Figure C3. A linear trend in residuals vs. normal score plot indicates that the residuals are normally distributed. From the figure, the residuals displayed a straight line. Therefore, based on the plot it could be concluded that the normality was satisfied.

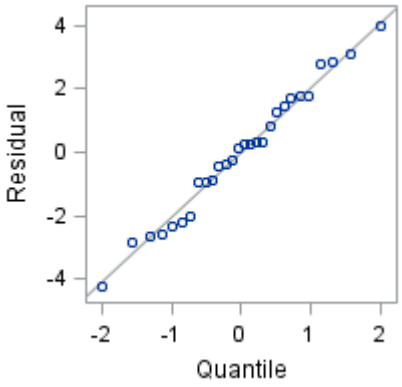

Figure C3: Normal Probability Plot for the Final Model

However, the normality of the preliminary model was further verified using the normality test.

C5. Modified-Levene Test for Checking Constant Variances

This test was performed to detect non constant variance even when there is serious departure from normality. In order to conduct this test, the dataset was divided into two groups based on the fitted values, such that the number of observations in both the groups was approximately equal. In this case, the dividing point was chosen to be E = 5.6. This value was chosen as the dividing value because the numbers of observations in each group were equal to 14. The absolute division (d_{i1}, d_{i2}) of residuals around the medians was calculated for each group. The SAS output for conducting the Modified-Levene test, which uses two sample t-tests, is presented in Table C1.

The following hypotheses are considered for the Modified-Levene Test:

<u>F-test Hypothesis:</u>

H_0: Variances of the two populations (d_1, d_2) are equal.

H_1: Variances of the two populations (d_1, d_2) are not equal.

Considering $\alpha = 0.05$, from the table p value 0.5975> α. Hence, we fail to reject H_0, which means the variances of d_1 and d_2 are equal. Hence, the equal variance output from the t-test was referred for further analysis.

<u>T-test Hypotheses:</u>

H_0: Means of the two populations (d_1, d_2) are equal-hence the constant variance assumption is satisfied.

H_1: Means of the two populations (d_1, d_2) are not equal-hence the constant variance assumption is violated.

From the table p-value = 0.1509>α. Hence, we fail to reject H_0, and the constant variance assumption is satisfied.

Table C1 SAS Output for the Modified-Levene Tests for the Final MLR Model

Obs	group	meand
1	1	2.08794
2	2	1.43008

The TTEST Procedure
Variable: d

group	N	Mean	Std Dev	Std Err	Minimum	Maximum
1	14	2.0879	1.0853	0.2901	0.4793	4.2034
2	14	1.4301	1.2604	0.3369	0.0253	3.8775
Diff (1-2)		0.6579	1.1761	0.4445		

group	Method	Mean	95% CL Mean		Std Dev	95% CL Std Dev	
1		2.0879	1.4613	2.7146	1.0853	0.7868	1.7485
2		1.4301	0.7023	2.1578	1.2604	0.9137	2.0306
Diff (1-2)	**Pooled**	0.6579	-0.2559	1.5716	1.1761	0.9262	1.6118
Diff (1-2)	**Satterthwaite**	0.6579	-0.2569	1.5726			

Method	Variances	DF	t Value	Pr > |t|
Pooled	Equal	26	1.48	0.1509
Satterthwaite	Unequal	25.439	1.48	0.1512

Equality of Variances				
Method	**Num DF**	**Den DF**	**F Value**	**Pr > F**
Folded F	13	13	1.35	0.5975

C6. Test for Normality

For testing normality, the following hypotheses are considered.

H_0: Normality is satisfied.

H_1: Normality is violated.

The SAS output for correlation between residuals and normal scores is shown in Table 5.5. From the table, ρ (e, z) = 0.98807.

Considering α = 0.1, c(α, n) = c (0.1, 28) = 0.969

According to the decision rule, if ρ< c(α, n), then reject H_0.

From Table C2, ρ = 0.98807 > c(α, n) = 0.969 ; hence we fail to reject H_0. In this case, the test was failed to conclude that the normality was violated. Hence, we conclude the normality was satisfied for the preliminary model.

Table C2 SAS Output for Testing Normality for the Final MLR Model

Pearson Correlation Coefficients, N = 28
Prob > |r| under H0: Rho=0

	e	**enrm**
e	1.00000	0.98807
Residual		<.0001
enrm	0.98807	1.00000
Normal Scores	<.0001	

C7. Variance Inflation Factor (VIF)

This factor is used to access if there is serious multicolinearity between the predictors. The VIF value identifies cases of high variance inflation due to complications caused by high multicolinearity. If the VIF value is more than 1, that indicates the multicolinearity exists; however, the multicolinearity may not be serious unless the VIF is

less than 5. From the Table C3 all the VIF values for the predictor variables were more than 1 but less than 5. Therefore, multicolinearity was present between the predictors; however, it might not pose a serious issue.

Table C3 SAS Output for Variance Inflation

Variable	**Variance Inflation**
Temperature (x1)	1.14487
Water Addition (x2)	1.94820
Gas Extraction (x3)	1.21601
Std x1x2	1.90401

C8. Outliers

These are single data points that affect the trend of the grouped data by pulling it toward its position. The SAS output for checking the outliers are shown in Table C4.

Table C4 SAS Output for Checking Outliers

Obs	Residual	RStudent	Hat Diag, H	Cov Ratio	DFFITS
1	-2.1996	-1.1951	0.2917	1.2874	-0.7669
2	0.1189	0.0631	0.3032	1.7906	0.0416
3	-0.4540	-0.2180	0.1470	1.4484	-0.0905
4	-2.3595	-1.1569	0.1336	1.0729	-0.4543
5	1.7943	1.3548	0.6269	2.2422	1.7562
6	-4.2374	-2.1295	0.0624	0.5218	-0.5492
7	-2.5689	-1.2659	0.1326	1.0131	-0.4950
8	1.4375	0.7132	0.1839	1.3651	0.3385
9	-0.9617	-0.4602	0.1343	1.3752	-0.1813
10	-2.6560	-1.3055	0.1244	0.9822	-0.4921
11	0.2886	0.1332	0.0772	1.3480	0.0385
12	0.3337	0.1543	0.0806	1.3510	0.0457
13	1.6774	0.7836	0.0751	1.1767	0.2233
14	-2.0210	-1.0999	0.3007	1.3665	-0.7213
15	-2.8130	-1.5436	0.2773	1.0335	-0.9562
16	3.9570	2.3427	0.3001	0.5860	1.5341
17	0.2797	0.1340	0.1440	1.4530	0.0549
18	0.8377	0.4148	0.1930	1.4885	0.2029
19	1.7501	0.8567	0.1533	1.2518	0.3645
20	1.2332	0.5673	0.0586	1.2337	0.1415
21	0.2313	0.1079	0.0967	1.3789	0.0353
22	-0.3556	-0.1639	0.0748	1.3417	-0.0466
23	2.7994	1.3463	0.0812	0.9149	0.4001
24	2.8633	1.3786	0.0799	0.8969	0.4063
25	3.1018	1.5035	0.0785	0.8311	0.4388
26	-0.9689	-0.4912	0.2278	1.5315	-0.2668
27	-0.8633	-0.4621	0.3080	1.7196	-0.3082
28	-0.2448	-0.1256	0.2533	1.6666	-0.0732

Outliers may be X or Y outliers. The X outliers are identified by assessing the diagonal elements of the Hat- matrix (h_{ii}), which are also called leverage values. The cut off point for h_{ii} is 2p/n, where p is the number of parameters in the model and n is the total number of observations. In this MLR model, no X- outlier was observed.

The Y outliers are identified by assessing the studentized or deleted residuals, t_i, and the cut-off value are calculated based on Bonferroni Outlier test at α= 0.1 or 0.05. According to the Bonferroni outlier test, the cut-off points for Y-outliers were $|t_i| > t(1- \alpha/2n, n-p-1)$ = 3.104 and 3.768. No Y-outliers were detected based on cut-off points.

References

1. Abichou, T., Chanton, J., Powelson, D., Fleiger, J., Escoriaza, S., Lei, Y., & Stern, J. (2006). Methane flux and oxidation at two types of intermediate landfill covers. *Waste Management*, *26*(11), 1305-1312.

2. Abichou, T., Clark, J., Chanton, J., Hater, G., Green, R., Goldsmith, D. & Swan, N. (2012). A new approach to characterize emission contributions from area sources during optical remote sensing technique testing. *Journal of the Air & Waste Management Association*, *62*(12), 1403-1410.

3. Abichou, T., Johnson, T., Mahieu, K., Chanton, J. P., Romdhane, M., Mansouri, I., Fratta, D., Puppala, A.J., & Munhunthan, B. (2010). Developing a design approach to reduce methane emissions from California landfills. In *Proceedings of GeoFlorida 2010: advances in analysis, modeling and design, West Palm Beach, Florida, USA, 20-24 February 2010.* (pp. 2878-2887). American Society of Civil Engineers (ASCE).

4. Abichou, T., Mahieu, K., Yuan, L., Chanton, J., & Hater, G. (2009). Effects of compost biocovers on gas flow and methane oxidation in a landfill cover. *Waste Management*, *29*(5), 1595-1601.

5. Abichou, T., Powelson, D., Chanton, J., Escoriaza, S., & Stern, J. (2006). Characterization of methane flux and oxidation at a solid waste landfill. *Journal of Environmental Engineering*, *132*(2), 220-228.

6. Abichou, T., Yuan, L., & Chanton, J. (2008). Estimating methane emission and oxidation from earthen landfill covers. In *GeoCongress 2008: Geotechnics of Waste Management and Remediation* (pp. 80-87). ASCE.

7. Albanna, M., Fernandes, L., & Warith, M. (2007). Methane oxidation in landfill cover soil; the combined effects of moisture content, nutrient addition, and cover thickness. *Journal of Environmental engineering and Science*, *6*(2), 191-200.

8. Amini., H., & Reinhart. D. R. (2012). Evaluating landfill gas collection efficiency uncertainty. In 15th annual LMOP conference and project expo, Baltimore, MD.

9. Awono, S., Collart, C., Kheffi, A., Fafchamps, R., & Dengis, P. (2005). Flame ionisation detector and linear Kriging method for landfill cap leakage detection. In *Proceedings of the 10th International Waste Management and Landfill Symposium, SARDINIA*.

10. Babilotte, A., Lagier, T., Fiani, E., & Taramini, V. (2010). Fugitive methane emissions from landfills: Field comparison of five methods on a French landfill. *Journal of Environmental Engineering*, *136*(8), 777-784.

11. Barlaz, M. A., Chanton, J. P., & Green, R. B. (2009). Controls on landfill gas collection efficiency: instantaneous and lifetime performance. *Journal of the Air & Waste Management Association*, *59*(12), 1399-1404.

12. Barlaz, M. A., Green, R. B., Chanton, J. P., Goldsmith, C. D., & Hater, G. R. (2004). Evaluation of a biologically active cover for mitigation of landfill gas emissions. *Environmental science & technology*, *38*(18), 4891-4899.

13. Barlaz, M. A., Green, R. B., Chanton, J. P., Goldsmith, C. D., & Hater, G. R. (2004). Evaluation of a biologically active cover for mitigation of landfill gas emissions. *Environmental science & technology*, *38*(18), 4891-4899.

14. Boeckx, P., Cleemput, O. V., & Villaralvo, I. D. A. (1996). Methane emission from a landfill and the methane oxidising capacity of its covering soil. *Soil Biology and Biochemistry*, *28*(10), 1397-1405.

15. Boeckx, P., Van Cleemput, O., & Villaralvo, I. (1997). Methane oxidation in soils with different textures and land use. *Nutrient cycling in Agroecosystems*, *49*(1-3), 91-95.

16. Bogner, J. E., Spokas, K. A., & Burton, E. A. (1997). Kinetics of methane oxidation in a landfill cover soil: temporal variations, a whole-landfill oxidation experiment, and modeling of net CH4 emissions. *Environmental science & technology*, *31*(9), 2504-2514.

17. Bogner, J., & Matthews, E. (2003). Global methane emissions from landfills: new methodology and annual estimates 1980–1996. *Global Biogeochemical Cycles*, *17*(2).

18. Bogner, J., Meadows, M., & Czepiel, P. (1997). Fluxes of methane between landfills and the atmosphere: natural and engineered controls. *Soil Use and Management*, *13*(s4), 268-277.

19. Bogner, J., Spokas, K., Chanton, J., Powelson, D., & Abichou, T. (2005). Modeling landfill methane emissions from biocovers: a combined theoretical-empirical approach. In *Proceedings of the Sardinia '05, international solid and hazardous waste symposium, published by CISA, University of Cagliari, Sardinia*.

20. Börjesson, G., & Svensson, B. H. (1997). Seasonal and diurnal methane emissions from a landfill and their regulation by methane oxidation. *Waste Management & Research*, *15*(1), 33-54.

21. Börjesson, G., Samuelsson, J., & Chanton, J. (2007). Methane oxidation in Swedish landfills quantified with the stable carbon isotope technique in combination with an optical method for emitted methane. *Environmental science & technology*, *41*(19), 6684-6690.

22. Chanton, J. Final Report, May 4, 2011.

23. Chanton, J. P., Abichou, T., Hater, G., Green, R., Bogner, J., Fratta, D., Puppala, A.J., & Munhunthan, B. (2010). Methane oxidation in landfill cover soils. In *Proceedings of GeoFlorida 2010: advances in analysis, modeling and design, West Palm Beach, Florida, USA, 20-24 February 2010.* (pp. 2896-2905). American Society of Civil Engineers (ASCE).

24. Chanton, J. P., Powelson, D. K., Abichou, T., & Hater, G. (2007). Improved field methods to quantify methane oxidation in landfill cover materials using stable carbon isotopes. *Environmental science & technology*, *42*(3), 665-670.

25. Chanton, J. P., Rutkowski, C. M., & Mosher, B. (1999). Quantifying methane oxidation from landfills using stable isotope analysis of downwind plumes. *Environmental science & technology*, *33*(21), 3755-3760.

26. Clark, J. M. (2010). Quantification of Methane Emissions Via the Use of an Optical Remote Sensing Technique in a Landfill Setting.

27. Collart, C., Lebrun, V., Fays, S., Salpéteur, V., Nicolas, J., & Romain, A. C. (2008). Air Monitoring around MSW sanitary landfills in Wallonia: feedback of 10 years field surveys. *Proceedings ORBIT*.

28. Czepiel, P. M., Mosher, B., Crill, P. M., & Harriss, R. C. (1996). Quantifying the effect of oxidation on landfill methane emissions. *Journal of Geophysical Research: Atmospheres (1984–2012)*, *101*(D11), 16721-16729.

29. De Visscher, A., & Van Cleemput, O. (2003). Simulation model for gas diffusion and methane oxidation in landfill cover soils. *Waste Management*, *23*(7), 581-591.

30. De Visscher, A., De Pourcq, I., & Chanton, J. (2004). Isotope fractionation effects by diffusion and methane oxidation in landfill cover soils. *Journal of Geophysical Research: Atmospheres (1984–2012)*, *109*(D18).

31. Durmusoglu, E., Taspinar, F., & Karademir, A. (2010). Health risk assessment of BTEX emissions in the landfill environment. *Journal of hazardous materials*, *176*(1), 870-877.

32. Dwyer, S. F., Reavis, B., & Newman, G. R. E. T. C. H. E. N. (2000). Alternative Landfill Cover Demonstration, FY2000 Annual Data Report. *Sandia Report, in print*.

33. Eklund, B. (1992). Practical guidance for flux chamber measurements of fugitive volatile organic emission rates. *Journal of the Air & Waste Management Association*, *42*(12), 1583-1591.

34. Eklund, B., Anderson, E. P., Walker, B. L., & Burrows, D. B. (1998). Characterization of landfill gas composition at the fresh kills municipal solid-waste landfill. *Environmental Science & Technology*, *32*(15), 2233-2237.

35. Escoriaza, S. C. (2005). Bio-Reactive Landfill Covers: An Inexpensive Approach to Mitigate Methane Emissions.

36. Eun, S. (2004). Hydrogen Sulfide Flux Measurements and Dispersion Modeling from Construction and Demolition (C&D) Debris Landfills (Doctoral dissertation, University of Central Florida Orlando, Florida).

37. Fleiger, J. E. (2006). The effective reduction of methane emissions from landfills using a biocover approach: measuring methane oxidation using static chamber and stable isotope techniques.

38. Gebert, J., & Gröngröft, A. (2006). Performance of a passively vented field-scale biofilter for the microbial oxidation of landfill methane. *Waste Management*, *26*(4), 399-407.

39. Harner, T., Bidleman, T. F., Jantunen, L. M., & Mackay, D. (2001). Soil—air exchange model of persistent pesticides in the United States cotton belt. *Environmental Toxicology and Chemistry*, *20*(7), 1612-1621.

40. Huber-Humer, M., Röder, S., & Lechner, P. (2009). Approaches to assess biocover performance on landfills. *Waste management*, *29*(7), 2092-2104.

41. Huitric, R., & Kong, D. (2006, March). Measuring landfill gas collection efficiency using surface methane concentrations. In *Solid Waste Association of North America (SWANA) 29th Landfill Gas Symposium, St. Petersburg, FL*.

42. Ishigaki, T., Yamada, M., Nagamori, M., Ono, Y., & Inoue, Y. (2005). Estimation of methane emission from whole waste landfill site using correlation between flux and ground temperature. *Environmental geology*, *48*(7), 845-853.

43. Jones, H. A., & Nedwell, D. B. (1993). Methane emission and methane oxidation in land-fill cover soil. *FEMS Microbiology Letters*, *102*(3), 185-195.

44. Jung, Y., Imhoff, P. T., Augenstein, D. C., & Yazdani, R. (2009). Influence of high-permeability layers for enhancing landfill gas capture and reducing fugitive methane emissions from landfills. *Journal of Environmental Engineering*, *135*(3), 138-146.

45. Jung, Y., Imhoff, P. T., Augenstein, D., & Yazdani, R. (2011). Mitigating methane emissions and air intrusion in heterogeneous landfills with a high permeability layer. *Waste management*, *31*(5), 1049-1058.

46. Jung, Y., Imhoff, P., & Finsterle, S. (2011). Estimation of landfill gas generation rate and gas permeability field of refuse using inverse modeling. *Transport in porous media*, *90*(1), 41-58.

47. Kulkarni, H. S. (2012). Optimization of Leachate Recirculation Systems in Bioreactor Landfills.

48. Lebrun, V., Kheffi, A., Gohy, M., Fafchamps, R., Collart, C., & MAQUINAY, J. (2007). Landfill gas (LFG) fugitive emissions on landfill surface–Comparative test of on site analysis devices. In *Proceedings Sardinia*.

49. Lewis, R. G., Folsom, S. D., & Moore, B. (2004). Modified active gas sampling manual. *prepared by HAS Engineers and Scientists for the Florida Department of Environmental Protection*.

50. Lou, X. F., & Nair, J. (2009). The impact of landfilling and composting on greenhouse gas emissions–a review. *Bioresource technology*, *100*(16), 3792-3798.

51. Maciel, F. J., & Jucá, J. F. T. (2011). Evaluation of landfill gas production and emissions in a MSW large-scale Experimental Cell in Brazil. *Waste management*, *31*(5), 966-977.

52. Maurice, C., & Lagerkvist, A. (2003). LFG emission measurements in cold climatic conditions: seasonal variations and methane emissions mitigation.*Cold Regions Science and Technology*, *36*(1), 37-46.

53. Maurice, C., Ettala, M., & Lagerkvist, A. (1999). Effects of leachate irrigation on landfill vegetation and subsequent methane emissions. *Water, air, and soil pollution*, *113*(1-4), 203-216.

54. Merritt, D. A., Hayes, J. M., & Marais, D. J. D. (1995). Carbon isotopic analysis of atmospheric methane by isotope-ratio-monitoring gas chromatography-mass spectrometry. *Journal of Geophysical Research: Atmospheres (1984–2012)*, *100*(D1), 1317-1326.

55. Morales, J. J. (2006). Mitigation of landfill methane emissions from passive vents by use of oxidizing biofilters.

56. Mosher, B. W., Czepiel, P. C., Shorter, J., Allwine, E., Harriss, R. C., Kolb, C., & Lamb, B. (1996). Mitigation of methane emissions at landfill sites in New England, USA. *Energy conversion and management*, *37*(6), 1093-1098.

57. Park, J. W., & Shin, H. C. (2001). Surface emission of landfill gas from solid waste landfill. *Atmospheric Environment*, *35*(20), 3445-3451.

58. Pohland, F. G. (1973). Sanitary landfill stabilization with leachate recycle and residual treatment.

59. Reinhart, D. R., Cooper, D. C., & Walker, B. L. (1992). Flux chamber design and operation for the measurement of municipal solid waste landfill gas emission rates. *Journal of the Air & Waste Management Association*, *42*(8), 1067-1070.

60. Röwer, I. U., Geck, C., Gebert, J., & Pfeiffer, E. M. (2011). Spatial variability of soil gas concentration and methane oxidation capacity in landfill covers. *Waste management*, *31*(5), 926-934.

61. Sadek, S., Ghanimeh, S., & El-Fadel, M. (2007). Predicted performance of clay-barrier landfill covers in arid and semi-arid environments. *Waste management*, *27*(4), 572-583.

62. Samir, S. (2011). Characterizataion and Evaluation of Gas Generation Potential from a Closed Section of a Landfill. M.S. Thesis, The University of Texas at Arlington, Texas, USA.

63. Scheutz, C., Fredenslund, A. M., Nedenskov, J., Samuelsson, J., & Kjeldsen, P. (2011). Gas production, composition and emission at a modern disposal site receiving waste with a low-organic content. *Waste management*, *31*(5), 946-955.

64. Scheutz, C., Kjeldsen, P., Bogner, J. E., De Visscher, A., Gebert, J., Hilger, H. A., Huber-Humer, M., & Spokas, K. (2009). Microbial methane oxidation processes and technologies for mitigation of landfill gas emissions. *Waste Management & Research*, *27*(5), 409-455.

65. Schuetz, C., Bogner, J., Chanton, J., Blake, D., Morcet, M., & Kjeldsen, P. (2003). Comparative oxidation and net emissions of methane and selected non-methane organic compounds in landfill cover soils. *Environmental science & technology*, *37*(22), 5150-5158.

66. Simunek, J., Van Genuchten, M. T., & Sejna, M. (2005). The HYDRUS-1D software package for simulating the one-dimensional movement of water, heat, and multiple solutes in variably-saturated media. *University of California-Riverside Research Reports*, *3*, 1-240.

67. Spokas, K. A., & Bogner, J. E. (2011). Limits and dynamics of methane oxidation in landfill cover soils. *Waste management*, *31*(5), 823-832.

68. Spokas, K., Bogner, J., Chanton, J. P., Morcet, M., Aran, C., Graff, C., ... & Hebe, I. (2006). Methane mass balance at three landfill sites: What is the efficiency of capture by gas collection systems?. *Waste Management*, *26*(5), 516-525.

69. Spokas, K., Graff, C., Morcet, M., & Aran, C. (2003). Implications of the spatial variability of landfill emission rates on geospatial analyses. *Waste Management*, *23*(7), 599-607.

70. Stern, J. C., Chanton, J., Abichou, T., Powelson, D., Yuan, L., Escoriza, S., & Bogner, J. (2007). Use of a biologically active cover to reduce landfill methane emissions and enhance methane oxidation. *Waste Management*, *27*(9), 1248-1258.

71. Tchobanoglous, G., & Kreith, F. (2002). *Handbook of solid waste management* (pp. 1-10). New York: McGraw-Hill.

72. United States Environmental Protection Agency. (1994). Air emissions models for waste and wastewater. Contract no. 68D10118, prepared for office of air quality planning and standards, Research Triangle park, NC.

73. United States Environmental Protection Agency. (2005). Guidance for evaluating landfill gas emissions.

74. United States Environmental Protection Agency. (2008). Methane: sources and emissions.

75. US Environmental Protection Agency, (2005). *Measurement of Fugitive Emissions at a Landfill Practicing Leachate Recirculation and Air Injection*. Office of Research and Development.

76. Wang-Yao, K., Towprayoon, S., Chiemchaisri, C., Gheewala, S. H., & Nopharatana, A. (2006, November). Seasonal variation of landfill methane emission from seven solid waste disposal sites in central Thailand. In *The 2nd Joint International Conference on Sustainable Energy and Environment* (1-4).

77. Weitz, K. A., Thorneloe, S. A., Nishtala, S. R., Yarkosky, S., & Zannes, M. (2002). The impact of municipal solid waste management on greenhouse gas emissions in the United States. *Journal of the Air & Waste Management Association*, *52*(9), 1000-1011.

78. Whalen, S. C., Reeburgh, W. S., & Sandbeck, K. A. (1990). Rapid methane oxidations in a landfill cover soil. *Applied and environmental microbiology*,*56*(11), 3405-3411.

79. Yang, K., Xu, Q., Townsend, T. G., Chadik, P., Bitton, G., & Booth, M. (2006). Hydrogen sulfide generation in simulated construction and demolition debris landfills: Impact of waste composition. *Journal of the Air & Waste Management Association*, *56*(8), 1130-1138.

80. Yuan, L. (2006). Methane emission and oxidation through landfill covers.

81. Zeiss, C. A. (2006). Accelerated methane oxidation cover system to reduce greenhouse gas emissions from MSW landfills in cold, semi-arid regions. *Water, air, and soil pollution*, *176*(1-4), 285-306.

Biographical Information

Sonia Samir was born in Dhaka, Bangladesh on August 18, 1987. She earned her Bachelor's degree in Civil Engineering from Bangladesh University of Engineering and Technology in October, 2009. She enrolled in The University of Texas at Arlington in January, 2010 for her graduate studies and completed her Masters under the supervision of Dr. Sahadat Hossain in August 2011. She continued at the University of Texas at Arlington to pursue a PhD in Civil Engineering. She was awarded the NSF CMMI student participation grant in 2012. She also received the Air and Waste Management Association's (A&WMA) Student Scholarship Award and the TXSWANA Scholarship in 2013. Her poster won third place in the 2nd International Conference on Final Sinks, Espoo, Finland. She was also awarded the Graduate Provost's award in Annual Celebration of Excellence by Students at the University of Texas at Arlington. The author's research interests include municipal solid waste, bioreactor landfills or enhanced leachate recirculation landfills, landfill mining and reclamation, landfill gas and fugitive emission.